Vesicular Trafficking in Osteoblasts

Cecilia M. A. Prêle

A thesis submitted for the degree of

Doctor of Philosophy

in the

University of London

University College London

The Bone and Mineral Centre, Department of Medicine, UCL

5 University Street, London, WC1E 6JJ

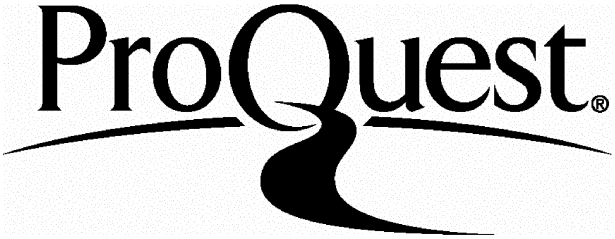

Abstract

Secretion of bone matrix proteins is highly directional. Osteoblasts secrete newly synthesised bone matrix proteins towards the bone surface and away from neighbouring capillaries. The mechanisms responsible for this polarised secretion in osteoblasts have not yet been elucidated.

Using the rat osteosarcoma cell line ROS17/2.8 and primary osteoblast-like cells derived from embryonic rat calvaria, we established that osteoblastic cells express a number of protein components implicated in apical junction complex formation. We therefore propose that osteoblasts may distinguish their apical and basolateral domains through the formation of these intercellular communicating pathways. Subsequently, we identified the expression of the general fusion machinery proteins, α-SNAP and NSF, in osteoblasts and determined v- and t-SNARE expression in these cells, with the particular aim of identifying components of the protein machinery which may be responsible for directing the exit of newly synthesised bone matrix proteins.

We have demonstrated that osteoblastic cells express two splice variants of the v-SNARE VAMP1, rVAMP1B and VAMP1-OB, which localise to the cell cytoplasm in a vesicular manner, partially co-localising with transported matrix proteins, osteocalcin and collagen. Furthermore we identified the expression of synaptotagmins, a large family of specialised v-SNAREs that modulate calcium sensitivity of vesicular trafficking. Thus, osteoblasts may maintain a calcium sensitive exocytosis machinery, possibly under the influence of osteotropic hormones, in addition to their pathway of constitutive exocytosis.

These data provide evidence that directionality of vesicular transport in osteoblasts involves junction complex formation and the SNARE proteins, rVAMP1B and VAMP1-OB.

Declaration

The studies presented in this thesis were performed by the author whilst a member of the Bone and Mineral Centre, Department of Medicine, University College London, UK.

Except where acknowledgement is made, this work is my own and has not been submitted for any other degree in this or any other university or institute of learning.

This thesis is dedicated with

love to my parents.

Acknowledgements

I would like to thank both my supervisors Prof. Mike Horton and Dr. Gudrun Stenbeck for being a constant source of help, support and encouragement throughout the course of this thesis.

A big thank you goes to my colleagues and friends in the Bone and Mineral centre, past and present, for their help and assistance throughout the past 3 years, in particular Steve Nesbitt and Jo Price. My thanks extend to my fellow 'bone buddy' Charlotte Lader.

I would like to thank the members of the Molecular Neuropathology Laboratory at the Imperial Cancer Research Fund (ICRF) for their continuing help, support and scientific discussion. In particular, I would like to thank Dr. Giampetro Schiavo, Shona Osborne and Dr. Judith Herreros for supplying the antibodies crucial to this study and for providing me with neuronal control samples. The crude unfractionated brain tissue preparation, PNS Cortex (post nuclear supernatant), and the crude vesicle containing fraction were prepared and kindly donated by Shona Osborne. PC12 cells and differentiated PC12 cell samples obtained from Judith Herreros.

I thank Prof. Graham Warren, ICRF, for supplying the Golgi marker antibody; GM130 used in the co-localisation studies. Furthermore, I would like to thank Prof. S. Tsuikita and Dr. M. Furuse, Kyoto University, Japan, for kindly donating the occludin (MOC 37) and the ZO-1 (T8-754) antibodies. Antibodies directed against NSF and α-SNAP were obtained fromDr. J. E. Rothman, Memorial Sloane-Kettering Cancer Centre, USA.

My sincere thanks go to Prof. Jane Aubin, University of Toronto, for sharing her valuable knowledge on primary osteoblast-like cell cultures with me. I am extremely grateful to all the members of the Aubin lab for their help and patience during my stay in Toronto.

In addition, I would like to thank the members of the Centre for Cardiovascular and Respiratory Research, in particular Louise, Jenny P., Helen and Olivier, for providing me with some interesting and unforgettable days/nights out. In addition, I would like to thank Dr. Gisela Lindal for kindly donating rat primary cardiac fibroblast samples.

I thank the 29th Streatham Scout group for keeping me sane (or insane). In particular, my sincere thanks go to the Mahers for providing me with a home away from home and especially to Jacks, without whom I would be lost.

A special vote of thanks goes to Steve for his love, support and encouragement.

Finally, I would like to thank the Wellcome Trust for their financial support.

List of Abbreviations

Abs	absorbance
AJ	adherens junction
APS	ammonium persulphate
Asc	ascorbate
ATP	adenosine triphosphate
ATPase	adenosine triphosphatase
AU	arbitrary units
β-GP	beta-glycerophosphate
bp	base pair
BLAST	basic local alignment search tool
BLC	bone lining cell
BMP-2	bone morphogenic protein-2
BSA	bovine serum albumin
BSP	bone sialoprotein
cDNA	complementary deoxyribonucleic acid
Cy5	cyanine
DEPC	diethyl pyrocarbonate
dex	dexamethasone
DMEM	Dulbecco's Modified Earls medium
DMF	N, N-dimethylformamide
DMSO	dimethyl sulphoxide
DNA	deoxyribose nucleic acid
DNase	deoxyribonuclease
dH_2O	distilled water
dNTP	deoxynucleoside triphosphate

ddNTP	dideoxynucleoside triphosphate
DTT	dithiothreitol
ECL	enhanced chemiluminescence
ECM	extracellular matrix
EDTA	ethylenediamine tetracetic acid
ER	endoplasmic reticulum
FCS	foetal calf serum
FITC	fluorescein isothiocyanate
g	relative centrifugal force
GJ	gap junction
h	hour
HRP	horseradish peroxidase
ICRF	Imperial Cancer Research Fund
IF	immunofluorescence
Ig	immunoglobulin
IL-1	Interleukin 1
IPTG	isopropyl-β-D-thiogalactoside
JAM	junction adhesion molecule
kB	kilobase
kDa	kilodalton
LB	Luria-Bertani broth
LP2	lysate pellet fraction 2
MAGUK	membrane associated guanylate kinase
MEM	minimal essential medium
min	minute
mm	millimetre
mRNA	messenger RNA

NCS	newborn calf serum
NEM	N-ethylmaleimide
NGF	Nerve growth factor
NSF	NEM (N-ethylmaleimide) sensitive fusion protein
OB	osteoblast
OC	osteoclast
OCT	orthochlorotoluene
OD	optical density
O/N	overnight
OP	osteoprogenitor
PAGE	polyacrylamide gel electrophoresis
PBS	phosphate buffered saline
PCR	polymerase chain reaction
PFA	paraformaldehyde
PNS cortex	post nuclear supernatant cortex
PS	penicillin and streptomycin
psi	pounds per square inch
PTH	Parathyroid hormone
PTHrP	Parathyroid hormone related protein
PVDF	polyvinylidene difluoride
RACE	rapid amplification cDNA ends
RCOB	rat calvaria derived osteoblastic cells
RH	random hexamer
RNA	ribonucleic acid
RNase	ribonuclease
rpm	rotations per minute
RT	room temperature

RT-PCR	reverse transcription PCR
sec	second
SDS	sodium dodecyl sulfate
SNAP	soluble NSF attachment proteins
SNAP-25	synaptosomal protein of 25 kDa
SNARE	SNAP receptor
SSC	standard saline citrate
SSPE	sodium chloride sodium phosphate EDTA
SSV	small synaptic vesicle
Syt	synaptotagmin
TB	trabecular bone
TE	Tris-EDTA buffer
TEMED	N, N, N', N'-tetramethyl ethylenediamine
TGFβ	Transforming growth factor β
TJ	tight junction
TNF	Tumour necrosis factor
TRITC	tetramethylrhodamine isothiocyanate
Tris	tris (hydroxymethyl)aminoethane
TPE	tris-phosphate EDTA
VAMP	vesicle associated membrane protein/synaptobrevin
v/v	volume per volume
WB	Western Blot
X-gal	5-Bromo-4-chloro-3-indoyl-β-D-galactoside
ZO-1	zonula occludens-1

Table of Contents

Table of Figures

Chapter 1 Introduction

Chapter 2 Materials and Methods

Chapter 3 Primary Osteoblast-Like Cell Culture

Chapter 4 Intercellular Communication between Osteoblasts

Chapter 5 Vesicular Trafficking in Osteoblasts

Chapter 6 Sequence Analysis and Localisation of VAMP1 in Osteoblasts

List of Tables

Chapter 1 Introduction

Chapter 2 Materials and Methods

Chapter 6 Sequence Analysis and Localisation of VAMP1 in Osteoblasts

List of Graphs

Chapter 3 Primary Osteoblast-like Cell Culture

Chapter 1

INTRODUCTION

Chapter 1

INTRODUCTION

1.1 Bone Composition and Structure

Bone is a dynamic and complex living tissue responsible for providing structural support and the mechanical integrity of all vertebrates. In addition to these supportive and protective roles, the skeleton maintains mineral homeostasis within the body.

Structurally, bone is a composite material made of two distinct phases: an organic component comprised of approximately 95 % type I collagen with the remaining 5 % being non-collagenous extracellular matrix proteins (i.e. osteocalcin, osteopontin, osteonectin, bone sialoprotein etc. in addition to proteoglycans). In contrast, the inorganic phase consists of calcium and phosphate in the form of hydroxyapatite ($Ca_{10}(PO_4)_6(OH)_2$); these ions are deposited as crystalline salts on the organic matrix.

Not all bone is identical, with bone of the adult skeleton falling into one of two categories: trabecular (spongy) bone or alternatively cortical (woven) bone. Characteristically, trabecular bone structures form a three dimensional lattice through the perpendicular arrangement of horizontal and vertical trabeculae, resulting in the formation of a highly porous matrix. In contrast, cortical bone is densely packed with collagen fibrils that form concentric lamellae structures (fig.1.1). The structural difference observed in these two bone types is reflected in their respective functions. The three-dimensional structure of the trabeculae houses

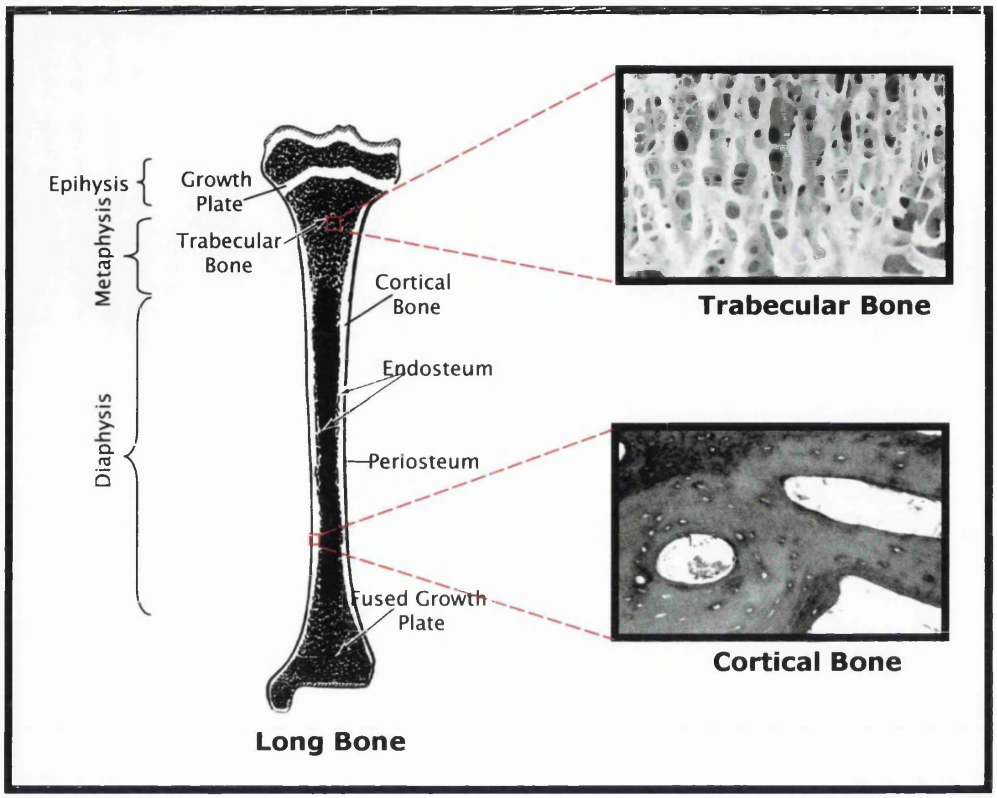

Figure 1.1 Bone Structure.

A schematic representation of bone structure in a long bone (adapted from Baron, 1996; Einhorn, 1996). The growing long bone can be divided into three zones the epiphysis, the midshaft (diaphysis) and the metaphysis. The external portion of the bone is composed of a dense layer of cortical/compact bone while trabecular/spongy bone is found in the internal spaces. Characteristically this porous network is formed by the perpendicular arrangement of thin calcified trabeculae and the resulting internal spaces house the haematopoietic bone marrow. Cortical bone, however, is laid down in a concentric manner forming a lamellar structure.

the bone marrow. In contrast to the metabolic role of trabecular bone, cortical bone contributes to the mechanical and protective functions of bone.

1.2 Bone Cells

The major cellular components of bone are the osteoclasts, osteoblasts, osteocytes and bone lining cells.

1.2.1 Osteoclasts

Osteoclasts are large motile, multinucleated cells derived from haematopoietic stem cells and are primarily involved in the resorption of mineralised bone and the (re)modelling of growing bone.

1.2.2 Osteoblasts

Osteoblasts, which will be discussed in more detail later in section 1.4, are responsible for bone formation.

1.2.3 Bone lining Cells

Bone lining cells are elongated cells of the osteoblast lineage found along the bone surface. Although these cells have the ability to divide, they do not possess a well-developed rough endoplasmic reticulum as observed in osteoblasts, suggesting these cells to be relatively inactive; they do not yet possess the protein synthesis characteristics of mature osteoblasts, hence their alternate name, quiescent osteoblasts.

1.2.4 Osteocytes

Osteocytes represent approximately 20 % of total bone cells. These cells were once osteoblastic in phenotype but have subsequently lost the majority of their metabolic activity and bone formative capacity and have become embedded in mineralised matrix. Even so, they are not isolated and they communicate through an intricate network of cellular processes that penetrate the bone, travelling from the osteocyte lacunae along the canaliculi eventually connecting neighbouring osteocytes with blood vessels.

All three of these cell types: osteoblast, osteocyte and bone lining cells are derived from a common mesenchymal stem cell and define distinct differentiation states of the osteoblast lineage.

1.3 Bone Cell Coupling

Bone is in a constant state of turnover and throughout the skeleton bone is being removed and reformed, modifications and adaptations essential for enabling bone to withstand the mechanical demands placed upon it. Bone turnover is regulated at the cellular level with the bone formation activity of the osteoblasts being tightly coupled to the resorptive actions of the osteoclast. The balance between these two actions is regulated by various systemic factors (i.e. vitamin D, calcitonin and PTH) and local factors (i.e. Interleukin 1 (IL-1), tumour necrosis factor (TNF), transforming growth factor β (TGF-β), etc) which control the rate of bone turnover. Therefore any imbalances in this regulated process may lead to any one of a number of metabolic bone diseases such as osteoporosis or osteopetrosis.

1.3.1 The Remodelling Process

The process of bone remodelling varies slightly between cortical and trabecular bone. Trabecular bone cells are in contact with bone marrow and are therefore likely to be controlled by local osteotropic hormones and cytokines such as IL-1. Cortical bone remodelling, on the other hand, is likely to be controlled by systemic osteotropic hormones such as PTH and vitamin D. Even though the remodelling process in each of these bone types varies, the sequence of events remains the same with adult bone only being replaced at sites of resorption. This process of resorption is tightly controlled and the sequence of events observed in the bone (re)modelling process is described in fig. 1.2.

During the resorptive phase osteoclasts are activated and recruited to the site of resorption, meanwhile, bone lining cells retract and migrate allowing osteoclasts to settle on the bone surface. After attachment osteoclasts form a tight seal around their ruffled border and excavate the bone directly beneath them. After completion of this resorptive phase, these cells either move along the bone surface or detach, known as the reversal phase. At the exposed bone surface, pre-osteoblastic cells are recruited and differentiate into functional osteoblasts that secrete bone matrix. Some of these cells become embedded in the newly deposited matrix as osteocytes. Furthermore, after this formation phase, mononuclear bone lining cells are recruited to cover the new bone surface, the resting phase. All diseases of bone occur as a result of imbalance in this normal cellular remodelling sequence.

Bone formation itself can be divided into three main steps, collagen synthesis and deposition, aggregation of collagen into fibrils and the maturation and mineralisation of the matrix. Mineralisation of the cartilaginous matrix is thought

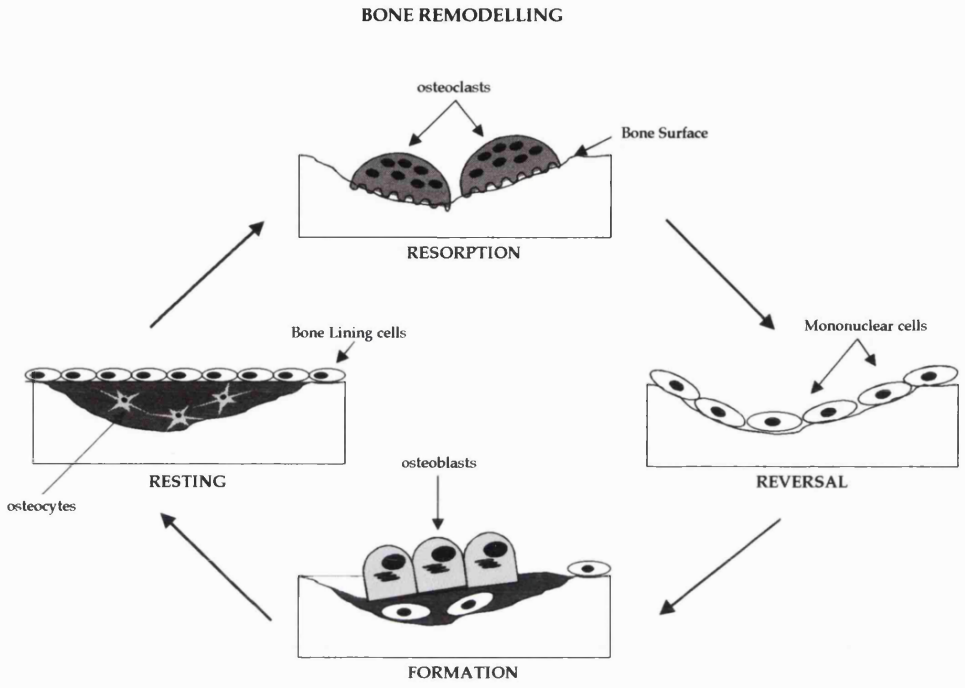

Figure 1.2 A Schematic Representation of Bone Remodelling.

Osteoclast cells are activated and recruited to the site of resorption where they settle on the bone surface forming a tight seal around their ruffled border, the resorption phase. After the bone excavation has been completed these cells either move along the bone surface or detach, the reversal phase. Pre-osteoblast cells are recruited, differentiate into functional osteoblasts and secrete bone matrix at the new bone surface, the formation phase. Subsequently, some of these cells become embedded in the matrix becoming osteocytes. Bone lining cells cover the surface of the newly formed bone during the resting phase.

to occur as a result of the presence of bone matrix proteins that act as mineral nucleators, proteins such as osteocalcin.

1.4 Osteoblasts

Osteoblasts are the key cellular components of bone formation and are responsible for bone matrix secretion. Characteristically, osteoblasts are described as polarised cuboidal basophilic cells with an extensive rough endoplasmic reticulum which is orientated towards the bone surface. Osteoblasts, along with bone lining cells and osteocytes, are derived from multipotential mesenchymal stem cells. These stem cells have the ability to differentiate into a number of different cell types namely, chondrocytes, adipocytes, myoblasts and fibroblasts (Grigoriadis *et al.*, 1988; Owen, 1988; Yamaguchi and Kahn, 1991) (fig. 1.3).

1.4.1 The Osteoblast lineage

Numerous transitory steps leading from mesenchymal stem cells through committed progenitors towards cells expressing the mature osteoblast phenotype have been described. Several key stages identified within this osteoblast lineage define osteoblast maturation: osteoprogenitors, pre-osteoblastic cells, osteoblasts, osteocytes and bone lining cells (fig. 1.4), (Aubin *et al.*, 1993; Hughes and Aubin, 1998). Committed osteoprogenitor cells give rise to the mature osteoblast via pre-osteoblast cell intermediates. In addition, prior to the terminal osteocytic stage, there may be an osteocytic-osteoblast intermediate, which retains the mature osteoblast phenotype even though it has lost the majority of its bone formative capacity. The terminal stage in the osteoblast lineage is the osteocyte (fig 1.4).

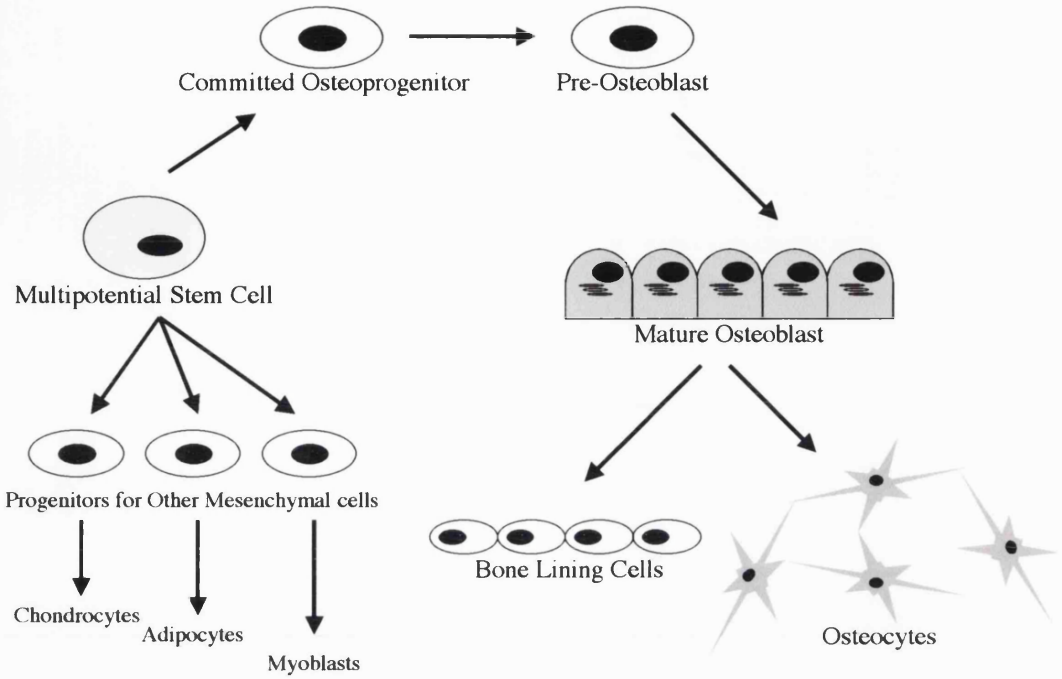

Figure 1.3 Osteoblast Lineage.

Mature osteoblasts are derived from pluripotent mesenchymal stem cells with the ability to differentiate into a number of cell types, such as adipocytes, myoblasts, chondrocytes and fibroblasts. Multipotential stem cells give rise to these different cell types through the formation of restricted monopotential progenitors, such as the osteoprogenitor in the case of the osteoblast lineage. Progression along the osteoblast lineage is thought to be regulated by a number of yet unknown factors ultimately leading to the mature osteoblast phenotype.

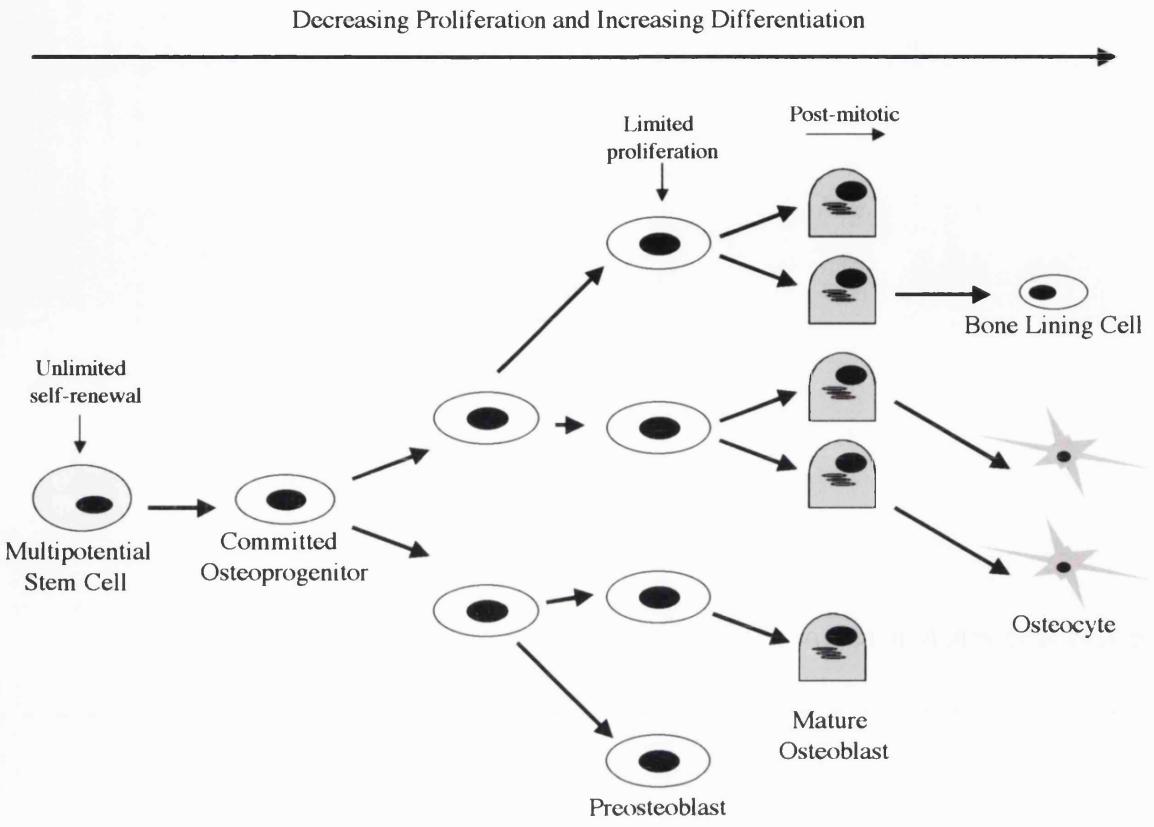

Figure 1.4 Stages of Osteoblast Maturation.

Four stages of osteoblast maturation have been identified to date, osteoprogenitors, pre-osteoblasts, osteoblasts, osteocytes and bone lining cells. With osteocytes representing the terminal differentiation stage of the osteoblast lineage.

This lineage hierarchy suggests that multipotential stem cells give rise to a number of different cell types through the formation of restricted monopotential progenitors (Aubin *et al.*, 1993; Grigoriadis *et al.*, 1988; Hughes and Aubin, 1998; Lian *et al.*, 1999; Reddi, 1995; Yamaguchi and Kahn, 1991).

Osteoprogenitor cells exhibit restricted potential to develop along the osteoblast lineage and this is emphasised by the phenotype of the Cbfa1 knockout mice (Otto *et al.*, 1997; Rodan and Harada, 1997). Although the potential inducers mediating these commitment steps remain largely unknown, there is increasing evidence to suggest that a number of local and systemic factors may play a regulatory role. In particular, glucocorticoids, such as cortisol, which can be mimicked by its synthetic counterpart dexamethasone (dex), in addition to bone morphogenic proteins (BMPs, members of the TGF-β superfamily) (Bellows *et al.*, 1987; Erlebacher *et al.*, 1998; Harada *et al.*, 1991; Mundy *et al.*, 1995; Owen and Friedenstein, 1988; Reddi, 1995).

1.4.2 Osteoblast Maturation

Extensive studies on isolated osteoblast-like cells have indicated that two populations of osteoprogenitor cell exist (Turksen and Aubin, 1991). The first of these is an 'inducible' population, where differentiation along the osteoblastic lineage is dependent upon stimulation by factors such as dex or steroids. The second population represents the constitutive osteoprogenitor cells that will differentiate, *in vitro*, into committed osteoblastic pre-cursors under standard culture conditions (i.e. when supplied with an organic phosphate source such as β-glycerol phosphate (β-GP), L-ascorbate (Asc) and foetal calf serum (FCS).

1.4.3 Osteoblast Phenotype Markers

1.4.3.1 Biochemical Markers

In studying osteoblast cell differentiation a number of biochemical markers have been identified including tissue non-specific alkaline phosphatase and an array of synthesised bone matrix proteins (Bellows *et al.*, 1991; Boskey, 1998; Lian *et al.*, 1999; Marsh *et al.*, 1995; Nagata *et al.*, 1991; Nefussi *et al.*, 1997; Roach, 1994). These markers are expressed at different stages throughout osteoblast development and are currently used to define cells expressing the mature osteoblastic phenotype.

Previous studies have shown the expression of such phenotypic markers to vary depending on the stage of osteoblast differentiation (Bellows *et al.*, 1999; Cowles *et al.*, 1998; Hughes and Aubin, 1998; Malaval *et al.*, 1994). At early stages of the osteoblast lineage, cells are unable to express the 'mature' osteoblastic phenotype i.e. alkaline phosphatase or the ability to respond to PTH (Lian *et al.*, 1999). During these early stages cells express types III and V collagen in addition to type I collagen and fibronectin. At this stage cells, do not express osteocalcin or bone sialoprotein (BSP) (Nefussi *et al.*, 1997). As cells progress towards the mature osteoblastic phenotype there is increased expression of alkaline phosphatase, type I collagen, osteopontin, followed by the synthesis of other bone matrix proteins such as BSP. Osteocalcin is expressed very late in osteoblastic development and is currently used as a terminal differentiation marker, as its expression coincides with the onset of mineralisation (table 1.1) (Lian *et al.*, 1998; Roach, 1994; Rodan, 1992).

	Stem Cells	Early-OP	Late-OP	Pre-OB	OB	Osteocyte	BLC
Alkaline Phosphatase	-	-	-	++	+++	-	-
Osteocalcin	-	-	-	-	+++	+/-?	-
Osteopontin	-	?	+	+	+++	+/-?	-
Osteonectin	-	-	-	+	++	+	-
Bone sialoprotein	-	-	?	+	+++	+/-?	-
Type-I Collagen	+	+	+	+++	+++	+	+
Types III + V Collagen	+	+	+	-	-	-	-
PTH/ PTHrP-R	-	-	-	+	+++	+	?

Table 1.1 Differential Expression of Osteoblast Phenotype Markers.

The expression of osteoblast phenotype markers varies during osteoblast differentiation. OP = osteoprogenitor, OB = osteoblast, BLC = bone lining cell, PTH/PTHrP-R = Parathyroid hormone/parathyroid hormone related protein receptor (Adapted from Aubin *et al.*, 1993; Hughes and Aubin, 1998).

1.4.3.2 Collagenous Proteins

As the major structural component of bone, type I collagen accounts for 90 % of the organic component of bone while the remaining 10 % is formed by non-collagenous proteins (i.e. osteocalcin, matrix-gla-protein, BSP, osteopontin, osteonectin, fibronectin, thrombospondin and small proteoglycans: decorin and biglycan). Type I collagen is essential for the provision of a scaffold onto which matrix can be deposited and is necessary for the induction of osteoblast differentiation (Owen *et al.*, 1990).

1.4.3.3 Non-Collagenous Protein Markers

Tissue non-specific alkaline phosphatase, another important marker of osteoblast differentiation is produced early during differentiation, in comparison to other non-collagenous protein markers (i.e. osteocalcin, osteonectin and bone sialoproteins). Osteonectin and bone sialoproteins are produced and expressed by the osteoblast during bone formation indicating that they may play an important role in mineralisation.

Alkaline Phosphatase

Tissue non-specific alkaline phosphatase expression is widely used as an osteoblast phenotype marker. Alkaline phosphatase is a 160 kDa protein bound to the plasma membrane through a phosphatidyl inositol phospholipid anchor. Alkaline phosphatase is expressed early in comparison to other non-collagenous proteins markers such as osteocalcin, osteonectin, osteopontin and bone sialoprotein (Bellows *et al.*, 1999; Cowles *et al.*, 1998; Lian *et al.*, 1999; Nefussi *et al.*, 1997; Owen *et al.*, 1990). Although, alkaline phosphatase expression is not bone specific, its

expression in osteoblasts, pre-osteoblasts, osteocytes makes it a useful indicator of osteoblastic differentiation (Beck *et al.*, 1998; Bellows *et al.*, 1991). Furthermore, tissue non-specific alkaline phosphatase is expressed in a number of osteosarcoma cell lines but it has also been identified in cartilage, predominately in matrix vesicles (Kirsch *et al.*, 1997; Wuthier, 1986). Therefore, with some caution, alkaline phosphatase expression can be used to follow cell development from pre-osteoblast to mature osteoblast with an increase in alkaline phosphatase expression representing a shift in an osteoblastic cell population towards a more differentiated state.

It has been suggested that alkaline phosphatase may play a crucial role in matrix mineralisation although its specific role has yet to be determined (Bellows *et al.*, 1991; Boskey, 1992; Boskey, 1998; Fedde *et al.*, 1999; Hunter *et al.*, 1996). Bellows *et al.*, 1991, have demonstrated that inhibition of alkaline phosphatase expression through treatment with levamisole leads to the blocking of mineralisation *in vitro*, further supporting the hypothesis that alkaline phosphatase expression is essential for mineralisation. However, subsequent studies revealed that the progression of mineralisation remained unaffected by lemamisole treatment, implicating alkaline phosphatase at the initiation phases of mineralisation (Bellows *et al.*, 1991).

Osteocalcin

Osteocalcin (bone gla-protein), a bone specific matrix protein containing gamma carboxylated glutamic acid residues, is expressed by differentiated osteoblastic cells. Although the specific function of osteocalcin remains unclear, it has been suggested that this protein may play a major role in calcium hydroxyapatite binding (Boskey, 1992). However, in contrast, recent observations in osteocalcin

deficient mice have revealed that the absence of osteocalcin results in an increase in bone density as compared to normal mice (Ducy *et al.*, 1996). These findings suggest that osteocalcin may be a negative regulator of bone formation. In addition to its expression in osteoblastic cells, osteocalcin expression has been reported in human osteocytes, further strengthening the argument that osteocalcin is an osteoblastic phenotype marker expressed late in the osteoblast lineage. For these reasons osteocalcin has proven to be a valuable protein marker for both the osteoblastic phenotype and for bone turnover.

Osteopontin

Osteopontin is a phosphorylated glycoprotein, which localises to the mineralisation front and has been shown to promote the attachment and spreading of the rat osteosarcoma cell line, ROS17/2.8 (cited by Noda *et al.*, 1988). Although osteopontin is expressed by the osteoblast, and at varying degrees by cells at different stages throughout the osteoblast lineage, expression is not restricted to bone tissue.

1.5 Bone Growth

Intramembranous ossification and endochondrial ossification are the two processes mediating bone growth. Bone growth and development in the flat bones of the skull, scapula and mandible is mediated by intramembranous ossification, whilst endochondrial ossification is responsible for bone development in the long bones. In contrast to the direct mineralisation of a collagenous matrix observed in intramembranous ossification, longitudinal bone growth requires the formation of a cartilaginous matrix 'model' that is subsequently replaced by bone.

1.5.1 Intramembranous Ossification

In intramembranous ossification cells of the mesenchymal origin proliferate and differentiate directly into pre-osteoblasts and subsequently into osteoblasts. These cells form bone matrix characteristic of woven bone, more specifically, collagen bundles are deposited in discrete patches with limited organisation. As the process of bone formation progresses a large number of osteocytes are found embedded within the mineralised matrix.

1.5.2 Endochondrial Ossification

Occurring in long bones, endochondrial ossification is characterised by the formation of a cartilaginous matrix that will be ultimately replaced by bone. Mesenchymal stem cells proliferate and differentiate into pre-chondroblasts and then chondroblasts in a manner similar to the osteoblasts. Similar to the osteocyte, chondroblasts also become embedded in their own matrix, chondrocytes; however, these cells retain their ability to proliferate. Chondrocytes organise themselves into regular columns in the growth plate of long bones; these cells enlarge and become hypertrophic towards the latter stages of growth (i.e. the chondrocytes furthest from the region of growth) and ultimately undergo apoptosis. This hypertrophic region becomes highly vascularised with blood vessels containing the haematopoietic bone marrow. The cartilaginous matrix is progressively calcified through the nucleation of mineral containing extracellular matrix vesicles (ECMs). Calcified cartilage is resorbed by the osteoclast allowing further vascularisation of the cartilaginous matrix. Osteoblasts are then recruited and deposit bone matrix on the remaining cartilage template.

1.6 Mineralisation

Bone mineral is comprised of calcium hydroxyapatite a compound rich in calcium and phosphate ions and, in addition, contains 'impurities' such as carbonate, magnesium and acid phosphate. Using the existing collagenous matrix as a scaffold, bone mineral is deposited as discrete packages in defect sites within this matrix. The crystalline structures become larger, due to the addition of ions or further aggregation of existing crystals, and more perfect (i.e. less impurities) as the bone matures.

Mineralisation has been studied extensively *in vitro* using a variety of cell models. Both primary osteoblast-like cells derived from either day 21 embryonic rat calvaria or alternatively from adult rat bone marrow stromal cell cultures, have been used to determine osteoblast differentiation and mineralisation *in vitro*. Although the exact mechanisms meditating mineralisation remain unclear, presently two models of mineralisation exist; one favours mineralisation through the formation and crystallisation of matrix vesicles and a second involves the direct mineralisation of the collagenous extracellular matrix.

1.6.1 Matrix vesicle mediated Mineralisation

Recently, it has been suggested that bone mineral may form in the protective environment of membrane bound vesicular bodies known as extracellular matrix vesicles (ECM) (Boskey, 1992; Boskey *et al.*, 1992a; Boskey *et al.*, 1992c; Johnson *et al.*, 1989; Wuthier, 1986). ECM vesicles, originally identified in calcifying cartilage and mineralising turkey tendons, are released from chondrocytes and facilitate initial mineral deposition through the accumulation of calcium and phosphate ions. Further characterisation has shown these vesicles to be rich in alkaline phosphatase,

a potential nucleator of crystallisation. Subsequently, it has been suggested that osteoblasts also have the ability to mineralise matrix through the formation and deposition of mineral as discrete membrane bound packets; however, the potential role of these ECM vesicles in an osteoblast mediated mineralisation process remains disputed. In addition to providing a protective environment, thus optimising the conditions required for the nucleation and crystallisation of calcium and phosphate ions, these matrix vesicles contain an array of molecules known to degrade potential inhibitors of mineralisation (i.e. ATP, pyrophosphate and proteoglycans).

1.6.2 Mineralisation of the Collagen Scaffold

Collagen synthesis is essential for bone formation as mineral is deposited onto an existing collagenous extracellular matrix template. Non-collagenous proteins appear to play a major role in aiding the mineralisation process by taking on a number of crucial roles. During mineralisation the concentration of osteopontin is bi-phasic, with osteopontin concentration being high at initial stages and low at the later stages of mineralisation. This observation implies that osteopontin may, in addition to its role in bone cell attachment, act as an initiator of mineralisation. Furthermore, osteocalcin and osteonectin have been implicated in the regulation of mineralisation.

1.6.3 *In vitro* Models of Mineralisation

Differentiation and progression of cells along the osteoblast cell lineage, in addition to osteoblast cell function, have been investigated *in vitro* using cellular models of mineralisation. A number of routinely used primary osteoblast cell cultures are derived from embryonic rat/mouse calvaria long bones or bone marrow. These isolated osteoblastic cell populations can be stimulated, using a variety of factors, to

form and mineralise nodules *in vitro*. Alternatively, explant cultures, based on the ability of cells to migrate from a fragment of bone, have been used to isolate osteoblastic cells. Notably the cells isolated from these cultures retain the ability to proliferate and form colonies of clonal cell populations. In addition to these primary osteoblast-like cell cultures, the mouse cell line, MC3T3-E1, which was derived from embryonic mouse calvaria is the only cell line identified to date that has the ability to form and mineralise nodules *in vitro*.

1.6.3.1 Osteoblastic cells derived from embryonic rat/mouse Calvaria

Embryonic calvaria are commonly used as a source of osteoblast-like cell populations, particularly since cells isolated from these preparations predominately express the mature osteoblastic phenotype. This is partly due to the developmental stage of the calvarium and is assisted by the fact that cells of the calvaria are actively making new bone. In addition, sequential collagenase digestion of calvaria results in the isolation of an osteoblast enriched cell population away from the fibroblastic cell population also present within the skull bones.

There are, of course, advantages and disadvantages of using this system. Firstly the cell population obtained is heterogeneous and the number of cells obtained varies from preparation to preparation. Culture conditions and culture duration have a direct effect on nodule formation and mineralisation. Furthermore, these cells are phenotypically unstable when cultured for long periods and, therefore, cells have to be used at the lowest possible passage number.

1.6.3.2 Culture Conditions

Culture conditions have a direct effect on mineralisation observed *in vitro*. Studies investigating the effect of specific culture conditions on osteoblastic cell differentiation and mineralisation *in vitro* have revealed the following factors to be essential for mineralisation: ascorbic acid (Asc), β-glycerophosphate (β-GP) and dexamethasone (dex). Although limited nodule formation and mineralisation may be observed without these factors, they are required for optimal nodule formation and mineralisation *in vitro* (discussed in more detail in Chapter 3).

Ascorbic Acid

In addition to stimulating cell proliferation when added during the logarithmic growth phase, ascorbic acid (Asc) has a stimulatory effect on the expression of the osteoblastic differentiation markers, osteocalcin and tissue non-specific alkaline phosphatase (Harada *et al.*, 1991; Malaval *et al.*, 1994; Xiao *et al.*, 1997). Asc is important for collagen synthesis and is a co-factor for peptidyl hydroxylase and lysine hydroxylase, enzymes responsible for proline hydroxylation and, hence, the stability of the collagen triple helix (Chambers and Laurent, 1997; Gronowicz and Raisz, 1996). Furthermore, Asc promotes collagen maturation and extracellular matrix deposition (Franceschi *et al.*, 1994; Harada *et al.*, 1991; Quarles *et al.*, 1992). The action of Asc is mediated through its direct action on matrix deposition (Franceschi *et al.*, 1994).

Isolated osteoblastic cell populations are heterogeneous. Thus, optimising culture conditions to favour cells of the osteoblast lineage enhances the overall cell yield. Moreover, osteoblasts are derived from mesenchymal stem cells which have the potential to differentiate into a number of cell type such as fibroblasts, myoblasts,

chondroblasts or adipocytes (Grigoriadis *et al.*, 1988; Yamaguchi and Kahn, 1991); these are also present within the calvarial osteoblast cell populations. Therefore, culture selection is crucial for the establishment of a predominately osteoblastic cell population and Asc has been shown to be essential for the production of mineralised nodules in long term primary osteoblast-like cell cultures (Bellows *et al.*, 1986; Quarles *et al.*, 1992).

Dexamethasone

Osteoblasts contain classical glucocorticoid receptors, indicating that glucocorticoids may have a direct effect on osteoblast cell function. Glucocorticoids have been shown to exert both anabolic and catabolic effects on bone, depending on the cellular model and the specific glucocorticoid concentration used. Physiological concentrations, 10^{-8} M, of glucocorticoids enhance the activity of hormones and growth factors leading to an increase in osteoblast cell differentiation and bone formation. Glucocorticoids are used widely *in vivo* as anti-immflamatory agents, with pro-longed treatment resulting in an increase in bone loss, glucocorticoid-induced osteoporosis. In contrast, synthetic glucocorticoids, such as dexamethasone (dex), which are used *in vitro* are reported to have a stimulatory effect on mineralisation, enhancing nodule formation and mineralisation in both rat bone marrow stromal cell cultures and in rat calvaria derived osteoblast cell cultures.

In rat calvaria derived osteoblastic cell cultures, 10^{-8} M dex increases the proliferative capacity of osteoprogenitor cells resulting in an increase in the number and size of bone nodules observed *in vitro* (Bellows and Aubin, 1989; Bellows *et al.*, 1987; Bellows *et al.*, 1986). *In vitro* studies using rat bone marrow derived cell

cultures have revealed dex treatment to be important for the establishment of the osteoblastic phenotype, with untreated cells remaining fibroblastic. Mouse derived osteoblastic cells, however, differ in their glucocorticoid requirements with physiological concentrations of dex having no effect (or an inhibitory effect) on the mineralising mouse cell line, MC3T3-E1, suggesting that glucocorticoids exert complex effects on osteoblastic cell cultures.

The differential effect of glucocorticoids on osteoblasts observed *in vivo* and *in vitro* imply that these compounds can exert complex effects on osteoblast cell function. Delany and colleagues (Delany *et al.*, 1994) have suggested that glucocorticoids act directly on osteoblastic cells through the up- or down-regulation of osteoblast gene expression, or indirectly by altering the expression of osteoblast growth factors.

β-Glycerophosphate

The incorporation of an organic phosphate source into primary osteoblast-like cell cultures is essential for mineralisation. β-GP is cleaved by the action of specific phosphatases, releasing inorganic phosphate that is subsequently deposited on the surface of the forming bone nodule. β-GP treatment does not, though, alter the mRNA expression levels of bone matrix proteins such as type I collagen, osteopontin, osteocalcin or tissue non-specific alkaline phosphatase. However, in long term bone nodule formation and mineralisation cultures, alkaline phosphatase and type I collagen mRNA expression levels decline with osteopontin, bone sialoprotein and osteocalcin mRNA levels remaining elevated throughout the time course (Chung *et al.*, 1992; Gronowicz and Raisz, 1996).

The incorporation of an organic phosphate source into primary osteoblast-like cell cultures induces *in vitro* calcification; however, the mechanism by which β-GP

exerts this effect remains debated (Gronowicz and Raisz, 1996). Boskey and co-workers have demonstrated that mineral crystals formed through β-GP (10 mM) induced mineralisation resulted in the formation of more perfect mineral crystals, i.e. containing less impurities, than those formed in cultures treated with inorganic phosphate (Boskey *et al.*, 1992b).

1.7 Intercellular Communication

The ability of osteoblasts to form intercellular communication channels, gap junctions (GJ), through the hexameric association of connexin molecules has been well documented but it remains unclear whether or not these cells have the ability to form tighter associations through adherens junction (AJ) or tight junction formation (TJ). TJ and AJ junction formation has been characterised extensively in epithelial cell models and demonstrates the ability of these cells to establish and maintain a polarised state.

Cell polarisation is of particular interest within osteoblasts since these cells are responsible for the polarised secretion or transport of bone matrix proteins. It has been suggested that osteoblasts may come together in an 'epithelial type manner' (Yamaguchi *et al.*, 1995) which may actively aid the mineralisation process by allowing osteoblasts to deposit matrix as part of a concerted effort. Previous studies have identified the presence of TJ in freeze fracture samples of odontoblasts, during early stages of dentinogenesis (Arana-Chavez and Katchburian, 1997; Calle, 1985). Odontoblasts are derived from mesenchymal stem cells and are similar to osteoblasts, in that they are the cells responsible for synthesising and secreting the organic component of dentine. Dentine is a calcified connective tissue with a

composition and mode of formation similar to bone (Butler, 1995; Butler *et al.*, 1997). Odontoblasts differ from osteoblasts in that they are exposed to a different microenvironment and synthesise dentine specific matrix proteins (Butler *et al.*, 1997). TJ formation, however, within an osteoblastic cell monolayer has not yet been investigated in bone.

1.7.1 Intercellular Communicating Pathways

Three main types of intercellular junctions have been described: tight junctions (TJ), adherens junctions (AJ) and gap junctions (GJ). In epithelial cells, a commonly used cellular model of vectorial transport, the cell is divided into distinct apical and basolateral domains by the presence of TJs located towards the most apical surface of the cell. To date a variety of protein components associated with these apical junction complexes have been identified (table 1.2).

These proteins include the peripheral membrane proteins ZO-1 (Balda and Matter, 1998; Itoh *et al.*, 1991; Van Itallie and Anderson, 1997), ZO-2, ZO-3 (members of the guanylate kinase homologue family)(Itoh, Morita *et al.* 1999) and an array of cytoplasmic proteins such as cingulin, 7H6 and symplekin. Furthermore, a number of proteins associated with cytoskeletal attachment have been identified and localised to the AJ; α, β, and γ-catenins, α-actinin and vinculin (for review see Van Itallie and Anderson 1997). Although possible interactions of these proteins have been investigated (fig. 1.5), the mechanism by which these proteins interact, regulating barrier and fence functions have yet to be determined.

Tight Junction Associated Proteins

	Molecular Weight	Reference
Transmembrane Proteins		
Occludin*	65 kDa	(Furuse *et al.*, 1993; Muresan *et al.*, 2000)
Claudin	23 kDa	(Furuse *et al.*, 1998a; Morita *et al.*, 1999a)
JAM	40 kDa	(Ebnet *et al.*, 2000; Martin-Padura *et al.*, 1998)
Cytoplasmic Proteins		
ZO-1	220 kDa	(Balda and Anderson, 1993; Itoh *et al.*, 1993; Stevenson *et al.*, 1986; Willott *et al.*, 1993)
ZO-2	160 kDa	(Beatch *et al.*, 1996; Gumbiner *et al.*, 1991; Itoh *et al.*, 1999b; Jesaitis and Goodenough, 1994)
ZO-3	130 kDa	(Haskins *et al.*, 1998)
Cingulin	155 kDa	(Citi *et al.*, 1988; Cordenonsi *et al.*, 1999)
Symplekin	150 kDa	(Keon *et al.*, 1996; Mitic and Anderson, 1998)
AF-6*	180-195 kDa	(Ebnet *et al.*, 2000; Mandai *et al.*, 1997; Yamamoto *et al.*, 1997; Yamamoto *et al.*, 1999)
19B1	220 kDa	(Merzdorf and Goodenough, 1997)

Table 1.2 Tight Junction Associated Proteins. (adapted from Citi and Cordenonsi, 1998) Tight junction associated proteins and their apparent molecular weights. The differences observed in the apparent molecular size of these proteins are due either to tissue specific or species-specific variations or may in part be due to protein phosphorylation. (JAM = Junction Adhesion Molecule). For review see (Anderson and Van Itallie, 1999; Balda and Matter, 1998; Citi and Cordenonsi, 1998; Gumbiner, 1987). (* In addition a number of isoforms have been identified)

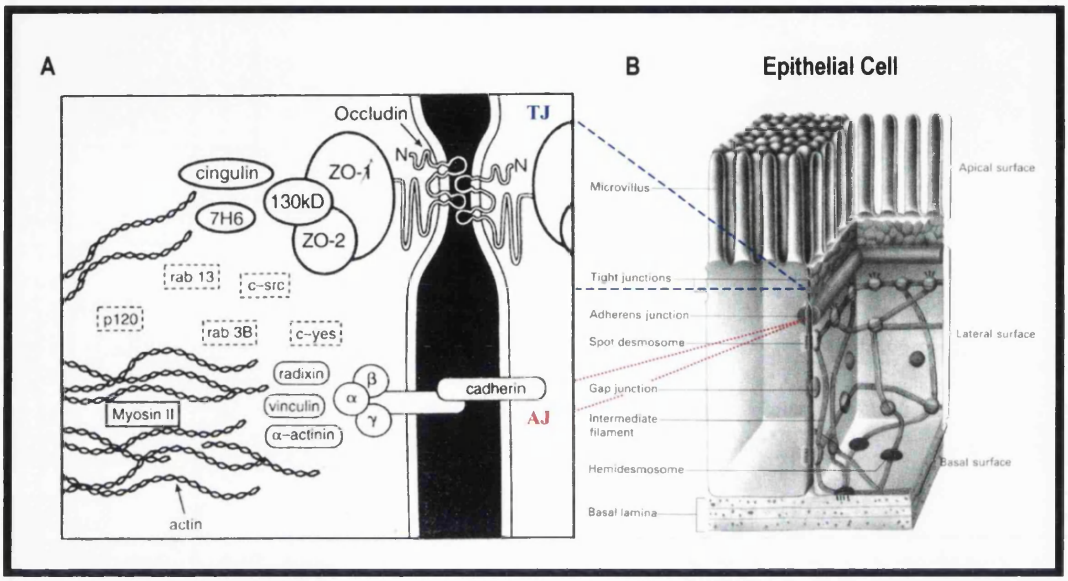

Figure 1.5 Intercellular Communication in Polarised Epithelial Cells.

Three types of intercellular communicating pathways have been identified in epithelial cells: TJ, AJ and GJ. TJ and AJ form towards the apical cell surface and are collectively referred to as the apical junction complex, whilst GJ formation is observed at the lateral surfaces between adjacent cells. Molecular dissection of these junction complexes has revealed the presence of the transmembrane protein occludin, ZO-1 (localising to the TJ of epithelial cells and the AJ in non-epithelial cells), ZO-2, ZO-3 (130 kDa protein), cadherins, α-, β- and γ-catenins, α-actinin, cingulin, 7H6 and vinculin. *In this model*, TJ formation is achieved via the homotypic interactions of occludin molecules and their interactions with ZO-1/ZO-2 and the p130 protein, now known as ZO-3. In contrast, AJ formation is achieved through the homophilic association of calcium dependent cell surface glycoproteins, cadherins.

1.7.2 Tight Junctions

Tight junctions have been shown to be crucial for the development of cell surface polarity within epithelial cells and also for the establishment and maintenance of a semi-permeable diffusion barrier.

1.7.2.1 Tight Junction Associated Proteins

Occludin

Until recently, occludin, a ~65 kDa peripheral membrane protein with 4 transmembrane spanning domains (Furuse *et al.*, 1994; Furuse *et al.*, 1993), was generally accepted as being the integral membrane protein required for TJ formation. However, studies characterising junction formation in occludin knockout embryonic stem cells (Saitou *et al.*, 1998) have demonstrated that occludin is not solely responsible for TJ formation and that occludin, in fact, has more of a functional role rather than a structural one.

Subsequent studies of the structural architecture of TJ, focusing in particular on TJ fibril formation, have re-affirmed these observations (Hirase *et al.*, 1997; Mitic *et al.*, 1999; Tsukita and Furuse, 1999) and in 1998 Furuse and co-workers, identified a further, novel TJ associated multi-gene family, the claudins (Furuse *et al.*, 1998a; Furuse *et al.*, 1998b; Morita *et al.*, 1999a).

Claudins

Claudins are a growing family of proteins and have molecular weights of approximately 23 kDa. They show structural similarity to occludin (i.e. they contain 4 transmembrane spanning domains), but there is no sequence similarity

between these molecules (fig 1.6) (Furuse *et al.*, 1998a). Recent evidence suggests claudins, rather than occludin, to be essential for TJ formation (Furuse *et al.*, 1998a; Furuse *et al.*, 1998b). It would appear that TJ formation and claudin association could have a similar level of complexity to the connexins in GJ formation with at least 20 members of the family described and each with differing tissue distribution (table 1.3).

L-fibroblasts do not normally have the ability to form TJ. Upon transfection with occludin or claudin, however, TJs have been identified between these cells. Specifically, occludin has been shown to localise to the newly formed TJ strands in a punctate manner. Claudins, though, create longer TJ fibrils, strengthening the argument that claudins rather than occludin are the leading players in formation of TJ strands (Furuse *et al.*, 1998a; Tsukita and Furuse, 1999).

The Membrane Associated Guanylate Kinase (MAGUK) Superfamily

The identification of the claudin family of membrane associated proteins and their role in TJ formation has recently led to a re-evaluation of the protein-protein interactions in TJ (for review see Mitic *et al.*, 2000) (fig. 1.7). ZO-1, zonula occludens 1, is a member of a family of highly related cytoplasmic proteins, MAGUKs, and is thought to be crucial for the stability of the TJ. Members of this family are characterised by the presence of one or more PDZ domains (postsynaptic protein-95/discs large/zonula occludens-1, PSD-95/DLG/ZO-1; PDZ), a src homology (SH-3) domain and an enzymatically inactive guanylate kinase-like domain (GUK) (Itoh *et al.*, 1999b; Mitic *et al.*, 2000; Willott *et al.*, 1993).

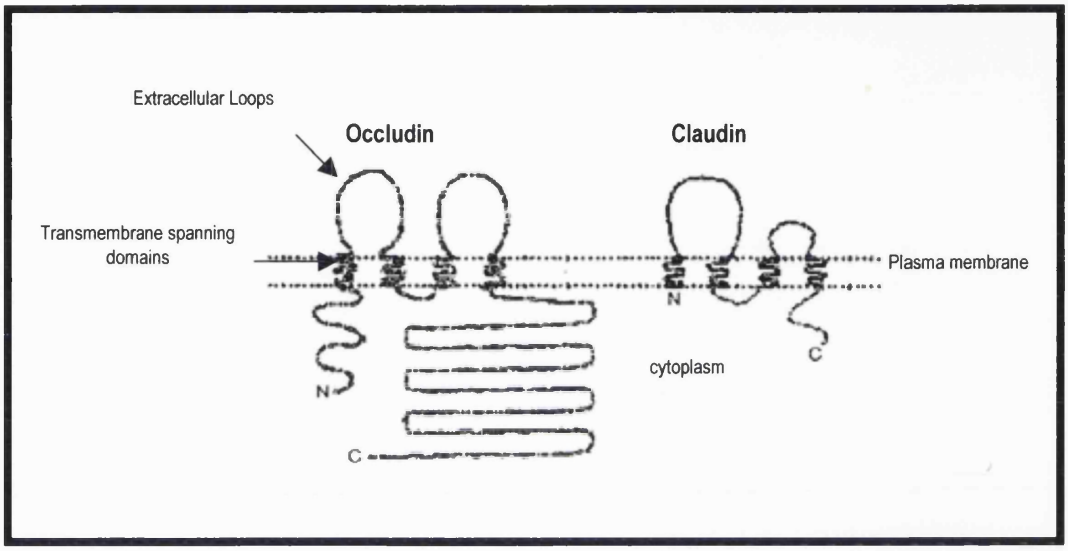

Figure 1.6 Occludin and Claudins are Key Tight Junction protein Components.

Recent investigations have revealed that occludin is not solely responsible for TJ formation or its barrier and fence functions. Furuse and co-workers have identified a novel multigene family of proteins, claudins, and shown them to localise to TJ. Although there is no sequence homology between these two proteins, hydrophobicity plots have revealed structural similarities. Similar to occludin, claudins have four transmembrane spanning domains, 2 extracellular loops with both the N and C termini located on the cytoplasmic surface. Compared to occludin, claudin contains a shorter N terminal domain and second extracellular loop in addition to a shorter C terminal domain.

Claudin Isoform	Tissue Distribution	References
Claudin 1	Li/L:/K/T/H	(Furuse *et al.*, 1998a; Furuse *et al.*, 1998b)
Claudin 2	Li/K	(Furuse *et al.*, 1998a; Furuse *et al.*, 1998b)
Claudin 3/RVP1	L/Li/K/T	(Morita *et al.*, 1999a; Peacock *et al.*, 1997)
Claudin 4/CPE-R	L/K/B	(Katahira *et al.*, 1997; Morita *et al.*, 1999a)
Claudin 5/TMVCF	H/B/Sp/L/Li/SM/K/T	(Morita *et al.*, 1999a; Morita *et al.*, 1999c)
Claudin 6	K (not in adult tissues)	(Morita *et al.*, 1999a)
Claudin 7	Li/L/K/T	(Morita *et al.*, 1999a)
Claudin 8	L/K/T	(Morita *et al.*, 1999a)
Claudin 9	?	(Mitic *et al.*, 2000)
Claudin 10	L/K	(Mitic *et al.*, 2000)
Claudin 11/OSP	B/T	(Mitic *et al.*, 2000; Morita *et al.*, 1999b)
Claudin 12	?	(Mitic *et al.*, 2000)
Claudin 13	?	(Mitic *et al.*, 2000)
Claudin 14	L	(Mitic *et al.*, 2000)
Claudin 15	K	(Mitic *et al.*, 2000)
Claudin 16	L/K	(Mitic *et al.*, 2000)
Claudin 17	?	(Mitic *et al.*, 2000)
Claudin 18	?	(Mitic *et al.*, 2000)
Claudin 20	?	(Mitic *et al.*, 2000)

Table 1.3 The Claudin Multigene Family .

The Claudin Family of TJ associated proteins is a growing family with over 20 family members identified to date, based on sequence identity and structural similarities. Table 1.3 describes the claudin family and their specific tissue distributions. Claudins 1 and 2 are the most closely related family members, showing ~47 % sequence identity at the amino acid level. (RVP1 = rat ventral prostate protein 1, CPE-R = *Clostridium perfringens* enterotoxin receptor, TMVCF = transmembrane protein deleted invelo-cardio-facial syndrome, OSP = oligodendrocyte-specific protein). B = brain, H = heart, K = kidney, Li = liver, L = Lung, Sp = spleen, SM = skeletal muscle, T = testis. For a review of the claudin multigene family see (Mitic *et al.*, 2000; Morita *et al.*, 1999a).

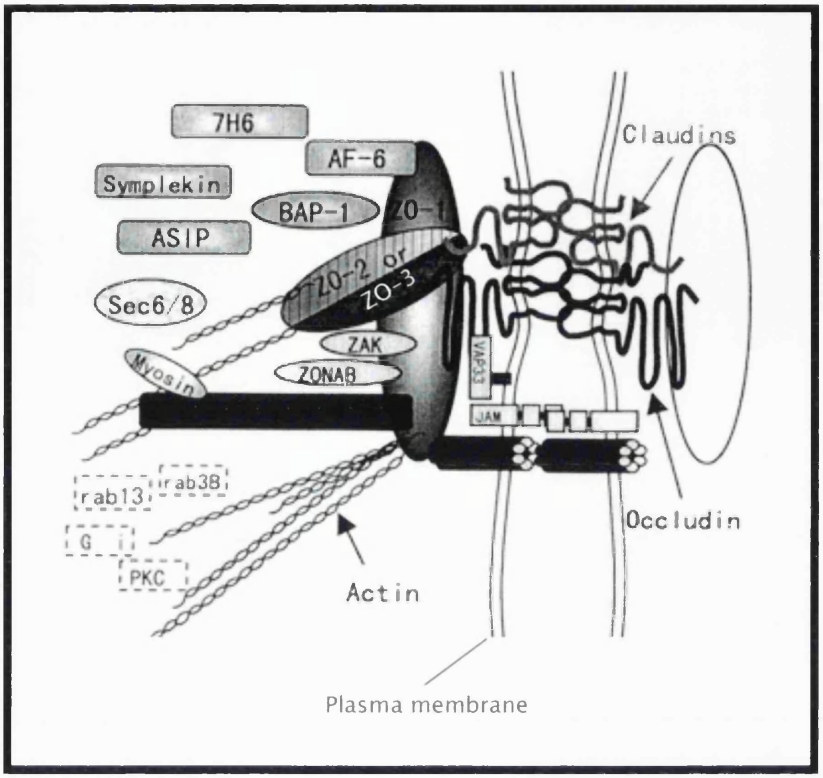

Figure 1.7 Revised Protein-Protein Interactions at the Tight Junction.

ZO-1 interacts with the C terminal 255 amino acids of occludin and with claudins. In addition, ZO-1 interacts with an array of cytoplasmic proteins; ZO-2, ZO-3, actin, AF-6, although the exact mechanisms mediating these protein-protein interactions remain unclear (adapted from Mitic *et al.*, 2000).

Interestingly, ZO-1 not only localises to the TJ plaque but localises also to the AJs in the absence of a TJ, suggesting that ZO-1 is a transient junction protein (Rajasekaran *et al.*, 1996). Recent investigations into ZO-1 function have demonstrated that ZO-1 is crucial for TJ formation; ZO-1 is implicated in the recruitment of occludin to the TJ (Mitic *et al.*, 1999). Furthermore, these latest findings propose that the formation of an AJ is a prerequisite for TJ formation (Mitic *et al.*, 1999). In addition to its interaction with the cytoplasmic proteins ZO-2, ZO-3 and AF-6 (Wittchen *et al.*, 1999; Yamamoto *et al.*, 1997), ZO-1 interacts with the C-terminal 255 amino acids of occludin (Furuse *et al.*, 1994; Mitic *et al.*, 1999). Furthermore, ZO-1 is also believed to interact directly with members of the claudin familiy (Itoh *et al.*, 1999a); members of the claudin family contain PDZ-binding motifs at their carboxyl terminal (Itoh *et al.*, 1999a).

1.7.3 Adherens Junctions

Adherens junctions are thought to form the structural and adhesive support of the epithelial cell monolayer. AJs are characterised by the presence of calcium dependent cell surface glycoproteins, cadherins, which associate via homophilic interactions creating cell-cell adhesion specificity. Additionally, an array of cytoplasmic proteins associated with cytoskeletal attachment and cell signalling have been identified at the AJ (table 1.4) (Tsukita, 1989). Of these proteins, α- and β- catenins, vinculin and α-actinin have all been shown to associate with the actin cytoskeleton and localise at the sites of cellular interaction in both epithelial and non-epithelial cells. These cytoskeletal interactions are thought to stabilise the junctional complex.

Adherens Junction Associated Proteins

	Molecular Weight	Reference
Transmembrane Proteins		
E-Cadherin	80 – 84 kDa	(Geiger *et al.*, 1990; Hay *et al.*, 2000; Suzuki, 1996; Yap *et al.*, 1997; Yonemura *et al.*, 1995)
Cadherins (N,E,P,R)	80 kDa	(Ferrari *et al.*, 2000; Geiger *et al.*, 1990; Hay *et al.*, 2000; Nose *et al.*, 1987; Suzuki, 1996; Yap *et al.*, 1997; Yonemura *et al.*, 1995)
Cytoplasmic Proteins		
ZO-1	220 kDa	(Balda and Anderson, 1993; Itoh *et al.*, 1997; Itoh *et al.*, 1993; Itoh *et al.*, 1991; Stevenson *et al.*, 1986; Willott *et al.*, 1993)
Cytoskeletal Attachment Proteins		
α-Catenin	102 kDa	(Aberle *et al.*, 1996; Rudiger, 1998)
β-Catenin	92 kDa	(Aberle *et al.*, 1996; Birchmeier *et al.*, 1993; Orsulic and Peifer, 1996)
γ-Catenin/plakoglobin	83 kDa	(Aberle *et al.*, 1996; Franke *et al.*, 1987; Lewis *et al.*, 1997)
α-Actinin	100 kDa	(Craig and Pardo, 1979; Drenckhahn and Franz, 1986)
vinculin		(Rudiger, 1998; Weiss *et al.*, 1998)

Table 1.4 Proteins associated with Adherens Junction Formation.

AJ associated proteins and their respective molecular weights. Differences observed in the apparent molecular weights of these proteins are due either to species or tissue specific variation or due to protein phosphorylation (for review on AJ components see Aberle *et al.*, 1996; Geiger *et al.*, 1987; Yap *et al.*, 1997).

1.7.3.1 Adherens Junction Associated Proteins

Cadherins and Catenins

Approximately 30 members of the cadherin family have been identified to date, all of which show differential tissue distributions: for example, E-cadherin (embryo and epithelia), P-cadherin (placenta, skin, epithelium and endothelium) (Nose *et al.*, 1987), N-cadherin (neuronal and mesodermal tissues) and L-CAM (liver) (Herrenknecht, 1996; Nollet *et al.*, 2000). Characteristically, cadherins mediate cell to cell adhesion by means of homotypic interaction with cadherin molecules on neighbouring cells. Structurally, classical cadherins contain a large N-terminal extracellular domain, a single transmembrane spanning domain and a C-terminal cytoplasmic tail.

The adhesive function of cadherins is dependent upon their physical association with catenins, a group of intracellular proteins that link cadherin to the actin cytoskeleton. α-, β-, γ-Catenins form a stable complex with cadherin by binding to its cytoplasmic domain. More specifically, catenins interact with the terminal 72 amino acids of the cytoplasmic domain of cadherins. β- or γ-Catenin can bind to cadherins during protein synthesis, whilst α-catenin associates with the complex once it reaches the plasma membrane, thus, linking the cadherin-catenin complex to the actin cytoskeleton (Aberle *et al.*, 1996; Herrenknecht, 1996; Yap *et al.*, 1997). β- and γ-Catenins are, however, mutually exclusive and cannot exist in the same cadherin-catenin complex.

Interestingly, catenins show homology to other cytoskeletal attachment proteins. α-Catenin is related to vinculin (Herrenknecht *et al.*, 1991), whilst β-catenin is

related to the desmosome associated protein, plakoglobin (Herrenknecht, 1996). Vinculin is a cytoskeletal protein associated with cell-cell or cell-matrix interactions and is involved in the transmembrane linkage of integrins to the actin cytoskeleton. β-Catenin shows homology to the central portion of plakoglobin which contains multiple internal repeats of 42 amino acids (*arm* motif), originally identified in Drosophila *armadillo* protein, a protein involved in embryonic pattern formation. *Armadillo* forms a complex with DE-cadherin and drosophilla α-E-catenin (Oda *et al.*, 1993). The function of *arm* motifs remains largely unknown; however, phosphorylation-induced junctional disassembly specifically targets catenins, implicating these proteins in signal transduction pathways (Aberle *et al.*, 1996; Orsulic and Peifer, 1996; Yap *et al.*, 1997).

1.7.3.2 Cadherin Expression by Osteoblastic Cells

Osteoblasts have been shown to express an array of cadherin molecules and it was hypothesised that the cell to cell adhesion mediated by these molecules may be required for osteoblast differentiation (Cheng *et al.*, 1998; Ferrari *et al.*, 2000; Hay *et al.*, 2000). Specifically, murine osteoblastic cells have been shown to express N-cadherin, cadherin-11, cadherin-4, OB-cadherin and E-cadherin (Babich and Foti, 1994; Luegmayr *et al.*, 2000; Okazaki *et al.*, 1994).

Cadherin expression in osteoblastic cells is developmentally regulated by a number of factors, such as parathyroid hormone (PTH) and calcium (Babich and Foti, 1994). These factors are responsible for regulating both cadherin function and cellular localisation. Although bone morphogenic protein-2 (BMP-2) induces osteogenic differentiation, the expression of multiple cadherins and the formation of cadherin mediated cell to cell adhesion in human osteoblasts has been shown to be crucial for this BMP-2 mediated effect (Cheng *et al.*, 1998).

1.7.4 Gap Junctions

Gap junctions (GJ) are aqueous intercellular channels that form in both epithelial and non-epithelial cells. They are formed through the hexameric association of the connexin molecules and direct intercellular signalling in the form of ions and secondary metabolites, through a network of aqueous channels, towards the neighbouring cell (Bruzzone *et al.*, 1996a; Bruzzone *et al.*, 1996b). Channels are formed through the homotypic association of the connexin molecules that create junctions with varying molecular size, permeability and ionic strength selectivity (Koval *et al.*, 1995; Kumar, 1999; Nicholson *et al.*, 2000; Steinberg *et al.*, 1994).

Investigations into GJ communication in osteoblasts have revealed that these cells express connexin-43, 45 and 46 (Donahue *et al.*, 2000; Koval *et al.*, 1997; Schirrmacher *et al.*, 1992). Furthermore, connexin-43 and 45 mediated cell to cell communication has been shown to be required for the expression of the mature osteoblastic phenotype (Lecanda *et al.*, 1998). A morphological study of intercellular communicating junctions during osteocytic differentiation and in osteoblastic cells has revealed that osteoblasts are interconnected by both GJs and AJs (Doty, 1981; Palumbo *et al.*, 1990).

1.8 Vesicular Trafficking

Both the secretory and endocytic pathways are composed of a number of membrane bound compartments. Intracellular communication between these compartments is mediated by vesicles that bud from the starting compartment (i.e. the trans-Golgi network) and subsequently fuse with the membrane of a more distal compartment (i.e. the plasma membrane). The molecular mechanisms underlying vesicle transport are highly regulated and specific. In constitutive exocytosis,

common to all eukaryotic cells, these vesicles fuse with the plasma membrane shortly after their formation. Vesicle accumulation, however, is observed within exocrine, endocrine and neuronal cells where fusion events do not occur spontaneously and require an appropriate signal (i.e. calcium influx) to trigger membrane fusion. Recently, biochemical and genetic dissection of this regulated exocytic pathway has provided us with valuable insight into the molecular mechanisms contributing to the specificity of vesicular trafficking.

Using a cell free system, reconstitution of individual steps of both the biosynthetic and endocytic transport pathways has led to the molecular characterisation of these intracellular processes (Rothman, 1994; Rothman and Orci, 1992).

Rothman and co-workers revealed that transport between the isolated Golgi cisternae could be reconstituted by incubating the membranes with cytosol and ATP (Balch *et al.*, 1984; Fries and Rothman, 1980). Upon treatment with NEM, vesicle accumulation was observed on the acceptor membranes, indicating that an NEM-sensitive fusion protein (NSF) is required for membrane fusion. Moreover, transport vesicle fusion was restored in the presence of cytosol, thus identifying NSF as a cytosolic protein. Further studies have revealed that NSF attaches to the membrane via cytoplasmic proteins, soluble NSF attachment proteins (SNAPs). Through the identification of these SNAP proteins, their integral membrane receptors, SNAREs, were identified leading to the identification of the SNARE complex. Ultimately these finding have led to the formation of a hypothesis, the SNARE hypothesis, which remains a general model for the specificity of all membrane fusion events.

1.8.1 The General Fusion Machinery Proteins – NSF and SNAP

As discussed above, a number of soluble proteins required for small synaptic vesicle (SSV) docking and fusion have been identified. The first of these soluble proteins was the so-called N-ethylmaleimide sensitive factor (NSF), an ATPase involved in a variety of intracellular transport pathways. NSF binds to its membrane receptors via another soluble protein SNAP (soluble NSF attachment protein) (Rothman, 1994; Sollner *et al.*, 1993a; Sollner and Rothman, 1996; Whiteheart *et al.*, 1992). In addition to being essential for membrane fusion, SNAPs and NSF are conserved peripheral membrane proteins implicated in the recycling of SNARE receptors (Burgoyne and Morgan, 1998; Morgan, 1995; Sollner *et al.*, 1993a). Several isoforms of SNAP have been identified namely: α-, β- and γ-SNAP. β-SNAP has an almost exclusive neuronal tissue distribution whilst α-SNAP is described as being the ubiquitously expressed SNAP isoform. γ-SNAP is a more distantly related SNAP isoform (Stenbeck, 1998; Whiteheart *et al.*, 1993; Woodman, 1997).

1.8.1.1 N-ethylmaleimide Sensitive Factor (NSF)

NSF is an ATPase that has been shown to be essential for membrane fusion events. Comprised of six identical 76 kDa subunits, NSF was first identified because of its ability to restore intercisternal Golgi transport after NEM treatment in a cell free system (Rothman, 1994; Rothman and Orci, 1992) (Wilson *et al.*, 1989). The identification of the yeast homologue of NSF, SEC18 (Eakle *et al.*, 1988), and the ability of SEC18 to replace its mammalian counterpart, NSF, in a cell free system demonstrates the evolutionary conservation of this protein (Rothman, 1994; Steel *et al.*, 1999). Moreover, NSF activity has been shown to be required at every step of

the secretory pathway and takes part in a variety of different fusion events (Burgoyne and Morgan, 1998).

1.8.2 The SNARE Hypothesis

The identification of integral membrane SNAP receptors, SNAREs, and their specific interactions led to formation of the current model of vesicle transport, the SNARE hypothesis. The SNARE hypothesis proposes that specificity of targeting and fusion events is mediated by a number of small integral membrane proteins (SNAREs, soluble NSF attachment protein receptors) that are specific for either the vesicle membrane (v-SNAREs) or for the target membrane (t-SNAREs). The interaction of the two cognate SNAREs forms the highly stable SNARE complex which acts as a receptor for the general fusion machinery proteins, α-SNAP and NSF (Hohl *et al.*, 1998; Sollner *et al.*, 1993a; Sollner *et al.*, 1993b; Sollner and Rothman, 1996). In the original SNARE hypothesis, fusion was triggered by NSF mediated SNARE complex disassembly. However, more recent evidence proposes a NSF-independent fusion mechanism (Nichols *et al.*, 1997; Weber *et al.*, 2000) and Weber and co-workers suggest that SNARE proteins themselves are capable of mediating membrane fusion. In the updated SNARE hypothesis, the interaction of a v-SNARE with its cognate t-SNARE brings the two membranes into close proximity allowing the actual fusion event to occur (fig 1.8) (Rothman, 1994; Sollner *et al.*, 1993a; Sollner *et al.*, 1993b; Sollner and Rothman, 1996).

The identification of large families of v- and t-SNAREs in both yeast and mammalian cells has emphasised the generality of the SNARE mediated vesicle fusion. Additionally, the specific localisation of different v- and t- SNAREs to distinct compartments of the secretory and endocytic pathways implicate SNARE

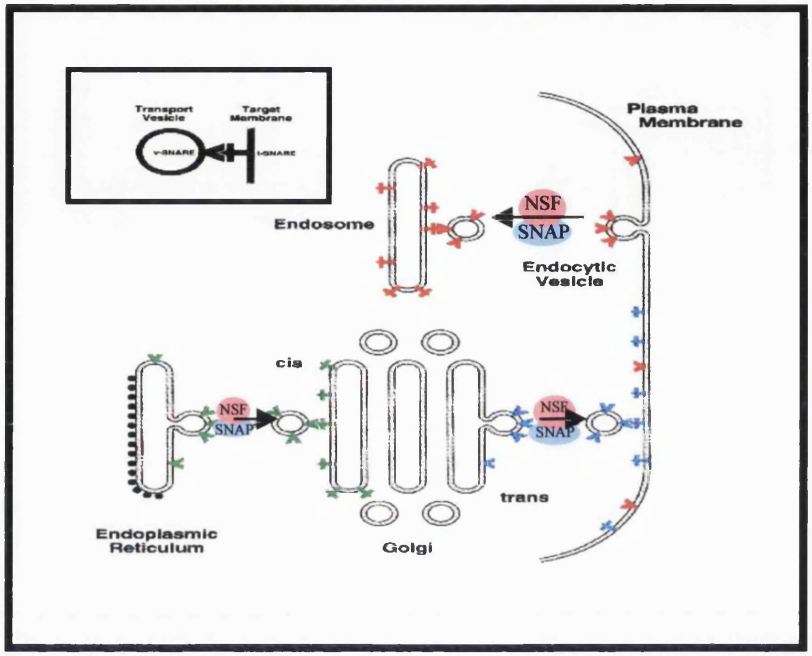

Figure 1.8 The SNARE Hypothesis. (adapted from Rothman, 1994)

According to the SNARE hypothesis specific targeting of transport vesicles to target membrane is achieved by a population of membrane bound proteins localising to both the vesicle (v-SNARE) and target (t-SNARE) membranes (Rothman, 1994; Sollner *et al.*, 1993a; Sollner *et al.*, 1993b; Sollner and Rothman, 1996). The cognate interaction of these v-/t-SNAREs governs specificity within membrane fusion whilst providing a scaffold for the general fusion machinery proteins α-SNAP and NSF to bind, resulting in the formation of the 20S fusion particle responsible for catalysing fusion. Furthermore, these proteins have been identified as the key protein components common to all intracellular fusion events.

proteins in the provision of specificity within membrane targeting and fusion.

The SNARE hypothesis assumes that all eukaryotic cells contain families of v- and t-SNAREs, therefore, to validate this hypothesis, a number of studies using tetanus and botulinum neurotoxins were performed. Clostridial neurotoxins are potent inhibitors of neurotransmitter release, and Montecucco and colleagues have demonstrated that these toxins specifically cleave v-SNAREs; for example tetanus toxin cleaves VAMP (Schiavo *et al.*, 1992). Further investigations demonstrated that VAMP is also cleaved by botulinum neurotoxins-B, D, F, G (BoNt/B, D, F, G) (Schiavo *et al.*, 1992; Schiavo *et al.*, 1994; Schiavo *et al.*, 1993b). Similarly, BoNt/A and E specifically cleave SNAP-25 (Blasi *et al.*, 1993a; Schiavo *et al.*, 1993a), BoNt/C cleaves syntaxin (Blasi *et al.*, 1993b; Schiavo *et al.*, 1995), while cellubrevin is cleaved by BoNt/D and F (for review see Schiavo *et al.*, 2000). The selective cleavage of SNARE proteins with neurotoxins has provided direct evidence that these proteins participate in neurotransmitter release, thus validating the SNARE hypothesis (for review see Huttner, 1993; Montecucco *et al.*, 1996; Schiavo *et al.*, 2000).

1.8.3 SNAP Protein Receptors (SNAREs)

The characterisation of synaptic vesicle trafficking has led to the identification of a number of prototypic SNARE proteins. Two SNARE proteins localising to the plasma membrane, syntaxin and synaptosomal associated protein of 25 kDa (SNAP-25), and the vesicle associated membrane protein (VAMP) interact to form a highly stable core complex (fig. 1.9) (Hohl *et al.*, 1998; Rossi *et al.*, 1997; Rothman, 1994).

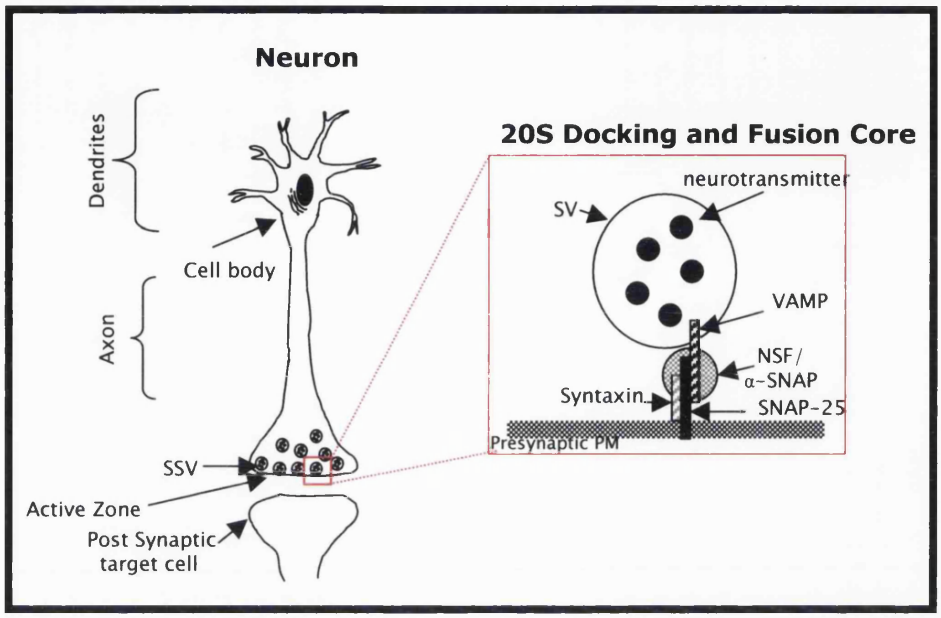

Figure 1.9 The 20S Docking and Fusion Complex.

Characterisation of neurotransmitter release has led to the identification of key SNARE proteins. Of particular interest are the interactions of target membrane SNARE proteins syntaxin, SNAP-25, with the vesicle associated membrane protein, VAMP. These proteins interact via their coiled-coil regions forming a highly stable core complex which in turn acts as a receptor its functional ligands α-SNAP and NSF.

Rothman and colleagues proposed the terms v-SNARE and t-SNARE to describe the localisation of these proteins to vesicle and target membranes respectively. Recent investigations into vesicular trafficking in non-neuronal cells have led to the identification of a number of novel SNARE proteins which show homology to existing VAMP, syntaxin or synaptotagmin family members (Advani *et al.*, 1998).

These SNARE proteins have been suggested to interact through the formation of heteromeric α-helical coiled-coils which are based on the presence of repeated heptad motifs within their sequence (Chapman *et al.*, 1994; Harbury, 1998; Terrian and White, 1997). SNAP-25 contributes two helical segments to a coiled-coil structure while syntaxin and VAMP each contribute one (Chapman *et al.*, 1994; Montal, 1999). The coiled-coil has been implicated in the tethering of target membranes, facilitating the formation of the SNARE complex (Clague, 1999). In addition, this coiled coil structure contributes to the stability of the fusion core complex.

1.8.4 Vesicle Associated Membrane Protein (VAMP)

VAMP is a 13 kDa protein localised to small synaptic vesicles (SSVs), dense core granules and synaptic-like vesicles in a variety of cell types. Although ten different isoforms of VAMP have been identified on the basis of structural and sequence similarities, only three isoforms have been extensively characterised: VAMP1, VAMP2 and Cellubrevin (Chilcote *et al.*, 1995; McMahon *et al.*, 1993). These VAMP isoforms have been identified in a number of vertebrate tissues, both neuronal and non-neuronal, though, their distribution varies. VAMP1 and VAMP2, originally identified in brain (Elferink *et al.*, 1989; Trimble *et al.*, 1990), were later shown to be

widely distributed in non-neuronal rat tissues (table 1.5) (Ralston *et al.*, 1994; Rossetto *et al.*, 1996).

1.8.4.1 VAMP Structure

VAMP is a type II membrane protein. Structurally, VAMP is composed of a proline rich amino terminus divergent between isoforms, a conserved central region containing the coiled-coil segment with specific neurotoxin cleavage sites, and a single transmembrane spanning domain (Trimble, 1993; Trimble *et al.*, 1988). The majority of this protein is cytoplasmic with only a short and poorly conserved intra-vesicular C-terminal domain (fig1.10) (Berglund *et al.*, 1999; Isenmann *et al.*, 1998; Mandic *et al.*, 1997; Trimble, 1993). The coiled-coil region is responsible for the interaction of VAMP with its cognate t-SNAREs, syntaxin 1 and SNAP-25. The VAMP molecule is encoded by five exons, I-V, exons I-IV being responsible for its cytoplasmic and transmembrane spanning domains, whilst exon V encodes the short C-terminal intra-vesicular portion.

1.8.4.2 VAMP Isoforms

Although VAMP was initially identified and localised in neuronal tissues it was recently demonstrated that VAMP1 and 2 have a wider tissue distribution (table. 1.5) (Mandic *et al.*, 1997; Rossetto *et al.*, 1996). Furthermore, a number of novel VAMP isoforms, VAMPs 4 (Steegmaier *et al.*, 1999), 5 (Zeng *et al.*, 1998), 7 (toxin insensitive VAMP, TI-VAMP) (Advani *et al.*, 1999; Coco *et al.*, 1999), and VAMP8 (endobrevin)(Advani *et al.*, 1998; Prekeris *et al.*, 1999; Wong *et al.*, 1998b) have been identified in non-neuronal tissues. Additionally, a growing number of VAMP1 mRNA splice variants have been identified in non-neuronal tissues.

Rat Tissue	VAMP1	VAMP2	Cellubrevin
Brain	+	+	+
Spinal cord	+	+	ND
Kidney	+	+	+
Adrenal Gland	+	+	ND
Heart	+	+	+
Spleen	+	ND	+
Liver	+	ND	+

Table 1.5 Rat Tissue Distribution of VAMP Isoforms.

In addition to their differential and complementary distribution patterns in the brain, VAMP1 and VAMP2 are differentially expressed in rat tissues: rat spinal cord, kidney, adrenal gland and heart tissue. ND = not determined.

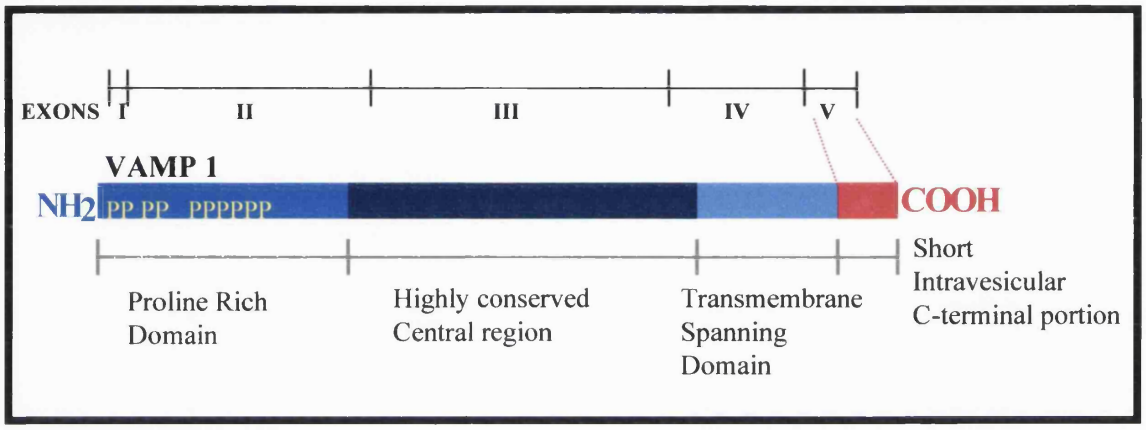

Figure 1.10 A Schematic Representation of the VAMP1 Structure.

VAMP1 is encoded by 5 exons and contains three major domains: an amino terminal portion that contains a proline rich region and has been shown to vary between isotypes (blue), followed by a highly conserved central region containing specific cleavage sites of neurotoxins (dark blue) and a hydrophobic transmembrane spanning domain (light blue). In addition to this large cytoplasmic portion, VAMP1 contains a short intravesicular carboxyl terminal segment (red) (Trimble *et al.*, 1988).

1.8.4.3 VAMP1 Splice Variants

An increasing number of VAMP1 splice variants have been identified (Berglund *et al.*, 1999; Isenmann *et al.*, 1998; Mandic *et al.*, 1997). As products of alternative splicing between exons IV and V, these proteins characteristically contain altered C-terminal residues. Recent data by Isenmann and co-workers (1998) has suggested that these differential C-terminal residues are responsible for the targeting of these proteins to specific sub-cellular compartments of the secretory pathway.

1.8.4.3.1 Localisation of Exons I-V in the rat VAMP1 Coding Region

Characterisation of the humanVAMP1 (hVAMP1) gene has revealed the location of exon boundaries in the cDNA transcript; however, specific sites in rat VAMP1 (rVAMP1) have not yet been fully elucidated. A comparison made between the hVAMP1 coding region (353 bp) and the rVAMP1 coding sequence revealed that rVAMP1 shows ~93 % homology to hVAMP1. In addition, and similar to hVAMP1, exons were located at the following sites on the rVAMP1 coding region: exon I, is encoded by base pairs 33-34, exon II, 34-161, exon III, 161-320, exon IV, 320-372, exon V, 372-386 (fig. 1.11).

1.8.4.3.2 Sequence Analysis of VAMP1 Splice Variants

Sequence analysis reveals that the first identified neuronal rat VAMP1A (rVAMP1A) isoform has a C-terminal sequence YIFT (Trimble *et al.*, 1988); furthermore, this isoform localises exclusively to synaptic vesicles. In contrast, hVAMP1B, the first VAMP1 splice variant to be identified, contains the positively charged RRD C-terminal residues (fig. 1.12) which are responsible for targeting this

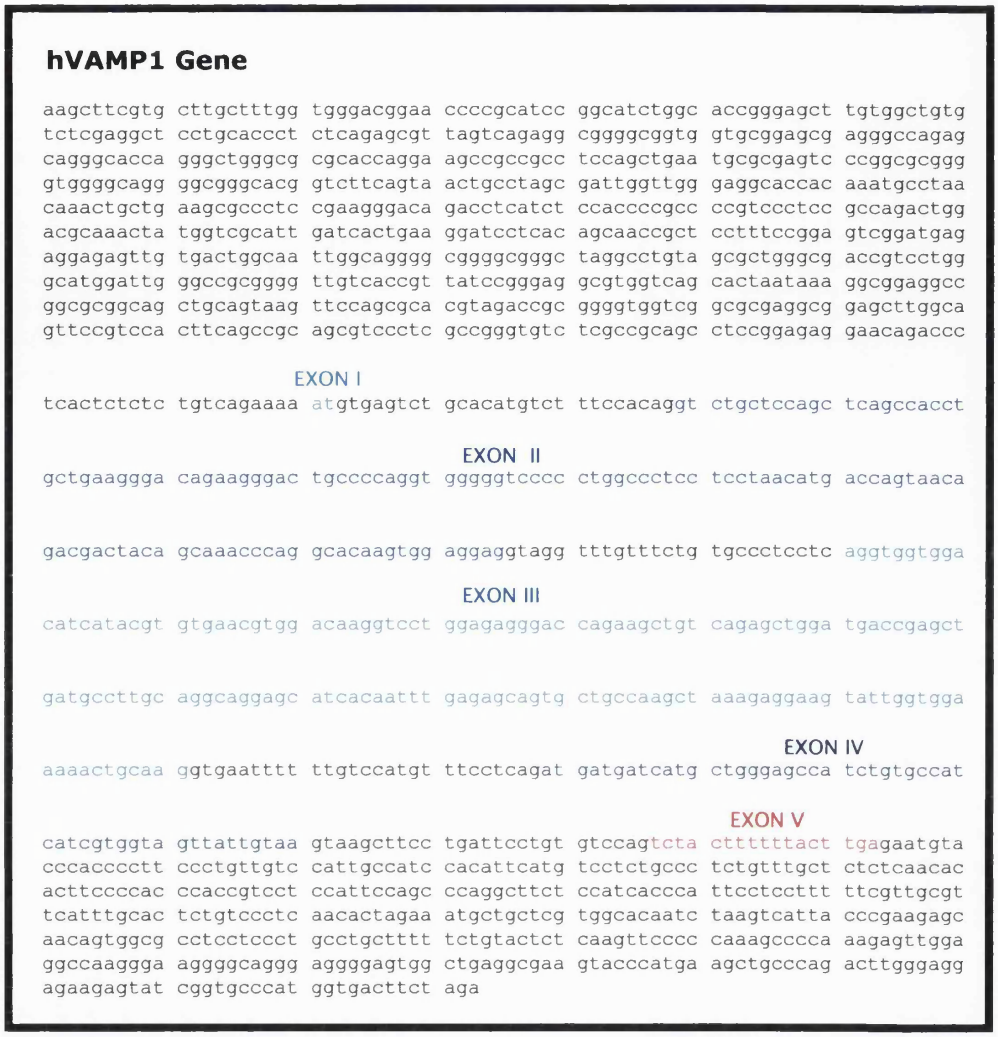

Figure 1.11 Localisation of VAMP1 encoding Exons I-V within the Human VAMP1 Gene. The location of exons I-V in rVAMP1 cDNA have been estimated by comparison of rVAMP1 with the hVAMP1 cDNA transcript. Specifically, Exon I, encoded by a 2 bp sequence located between bps 33 and 34 of the full length VAMP1 cDNA sequence. Similarly, exon II coding sequence is located between bps 34-161, exon III, bps 161-320, exon IV, bps 320-372 and exon V, bps 372-386. Exons I-IV are responsible for encoding the N-terminal and cytoplasmic domains while exon V encodes the highly variable C-terminal intra-vesicular portion of the VAMP1 protein.

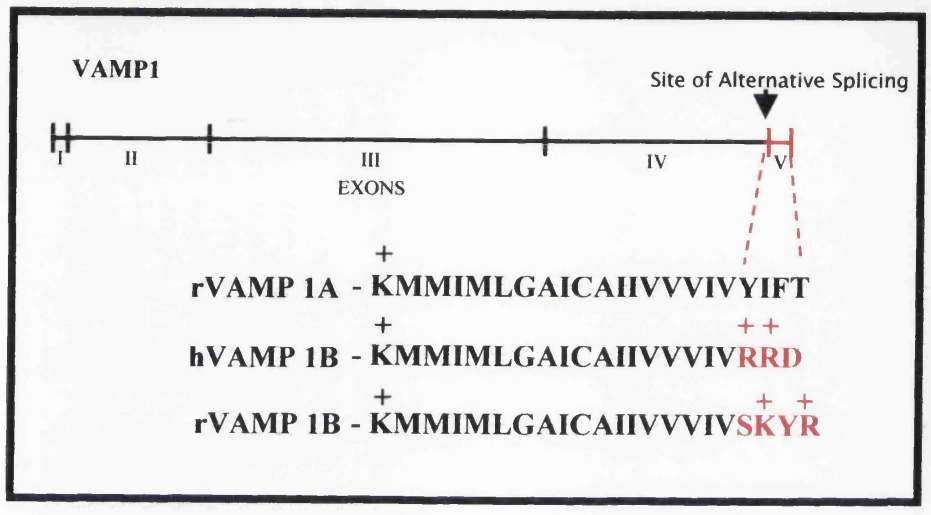

Figure 1.12 VAMP1 Splice Variants.

VAMP1 splice variants result from alternative splicing between exons IV and V of the VAMP1 cDNA transcript, creating an altered carboxyl terminal amino acid sequence (red). Human and rat splice variants, hVAMP1B and rVAMP1B, have been identified. Both, rVAMP1 B and hVAMP1B contain positively charged C-terminal residues, which, in the case of hVAMP1B, are responsible for its targeting to the mitochondria. Although it has been proposed that rVAMP1B may also be targeted to the mitochondria, its specific localisation has yet to be determined.

protein to the mitochondria of transfected human endothelial cells (Isenmann *et al.*, 1998). In addition, hVAMP1B is expressed in fibroblasts and neutrophils.

In 1997, Mandic and co-workers identified a rat isoform of the VAMP1B splice variant, rVAMP1B. Similar to hVAMP1B, rVAMP1B has been shown to contain a positively charged C-terminal residue sequence, SKYR (fig. 1.12) and shortened membrane anchor. Consequently, it has been suggested that rVAMP1B may also be targeted to the mitochondria, although, specific co-localisation of rVAMP1B to mitochondria has not yet been determined. In addition to the VAMP1B splice variants described above (fig. 1.12), Berglund and co-workers (1999) have investigated further the highly variable C-terminal portion of VAMP1 and identified four additional VAMP1 splice variants, VAMP1C to F. Similar to VAMP1B, sequence variations occur at the extreme C-terminus portion of the VAMP1 cDNA transcripts and are a direct result of alternative splicing between exons IV and V, with exons I-IV remaining conserved. Moreover, VAMP1C to F splice variants are widely expressed (i.e. brain, kidney, peripheral blood mononuclear cells, eosinophils and neutrophils).

The apparent abundance of these VAMP family members in non-neuronal tissues suggests a universal role of VAMP in vesicle targeting and fusion (Berglund *et al.*, 1999).

1.8.5 Synaptosomal Associated Protein of 25 kDa (SNAP-25)

SNAP-25, a palmitoylated protein identified in the neuronal system (Oyler *et al.*, 1989; Zhao *et al.*, 1994; Vogel and Roche, 1999), is required for axonal growth during neuronal development and in nerve terminal plasticity in the mature nervous

system. SNAP-25 is expressed as two developmentally regulated isoforms: SNAP-25 a/b (Hodel, 1998; Vogel and Roche, 1999). Both the amino terminal and carboxyl terminal domains of this protein are highly conserved and form intermolecular coiled-coils. Encoded by eight exons, SNAP-25a and SNAP-25b isoforms are a result of alternative splicing at exon 5, which leads to a difference in the cysteine containing 9 amino acid motif responsible for palmitoylation (Bark, 1993; Bark and Wilson, 1994). SNAP-23, the ubiquitously expressed homologue of SNAP-25 shows approximately 60 % sequence identity to SNAP-25 (Ravichandran *et al.*, 1996; Wong *et al.*, 1997). SNAP-23, however, has shorter coiled-coil forming domains and is believed to mediate constitutive exocytosis through its interaction with the ubiquitously expressed isoforms of syntaxin and VAMP.

1.8.6 Syntaxin

A 35 kDa target SNARE, syntaxin, identified on the basis of its interaction with the calcium sensitive v-SNARE, synaptotagmin (p65), has proved to be one of the key SNARE proteins implicated in regulated exocytosis (Bennett *et al.*, 1992). Syntaxin is a typical type II membrane protein with a cytosolic N-terminal domain followed by a single transmembrane spanning domain (Bennett *et al.*, 1992; Bennett *et al.*, 1993). Syntaxins interact in a calcium-dependent manner with some isoforms of the synaptotagmin family of SSV associated proteins (Clague, 1999; Hayashi *et al.*, 1995; Hazzard *et al.*, 1999; Hohl *et al.*, 1998; McMahon and Sudhof, 1995; Rossi *et al.*, 1997).

1.8.6.1 The Syntaxin Family of t-SNAREs

Syntaxins are a large and growing t-SNARE family with approximately 18 isoforms identified to date. These isoforms have been shown to localise to a number of specific intracellular compartments (summarised in table 1.6) with syntaxin 1 (HPC1) being the best characterised isoform.

1.8.7 Synaptotagmins

Synaptotagmins are a family of targeting v-SNAREs, some of whom have been implicated in calcium regulated exocytosis (Brose *et al.*, 1992; Osborne *et al.*, 1999; Schiavo *et al.*, 1998; Sudhof and Rizo, 1996). In addition to their role as calcium sensors in neuroexocytosis, these proteins have also been implicated in general regulated secretion (Martinez *et al.*, 2000). Characteristically these proteins contain an intravesicular amino terminus, a single transmembrane domain and a cytoplasmic domain containing two repeat domains that are homologous to the C2 regulator domains of protein kinase C (fig. 1.13) (Perin *et al.*, 1991a; Perin *et al.*, 1991b). These C2 domains, termed C2A and C2B, are implicated in the calcium-regulated interactions of synaptotagmins with membrane phospholipids and syntaxins (Chapman *et al.*, 1995; Duncan *et al.*, 2000; Sutton *et al.*, 1995; Zhang *et al.*, 1998).

Extensive studies have revealed that these proteins are widely distributed in both nervous tissue and in a number of non-neuronal tissues (Kwon *et al.*, 1996; Schiavo *et al.*, 1998). Furthermore, the characteristic C2 binding domains of synaptotagmin have been identified in a variety of proteins with differing functions. These include phospholipases, lipid kinases and rab-specific GTPase activating proteins (Newton, 1995; Wang *et al.*, 2000; Williams and Katan, 1996; Wymann and Pirola, 1998).

Syntaxin Isoform	Tissue Expression	Subcellular Location	Reference
Syntaxin 1 a	B/N/Lu	PM/SG	(Bennett *et al.*, 1993; Brimhall *et al.*, 1999; Tagaya *et al.*, 1995)
Syntaxin 1 b	B	PM	(Bennett *et al.*, 1993)
Syntaxin 2*	K/Li	PM/E	(Fujita *et al.*, 1998; Quinones *et al.*, 1999)
Syntaxin 3*	K/Li/N	PM/SG	(Fujita *et al.*, 1998; Ibaraki *et al.*, 1995)
Syntaxin 4	ubq	PM	(Fujita *et al.*, 1998)
Syntaxin 5	N	ER/G	(Advani *et al.*, 1998; Dascher *et al.*, 1994; Ravichandran and Roche, 1997; Rowe *et al.*, 1998)
Syntaxin 6	ubq	TGN/E	(Bock *et al.*, 1997; Bock *et al.*, 1996)
Syntaxin 7	B/N	E/L	(Nakamura *et al.*, 2000; Prekeris *et al.*, 1999; Wang *et al.*, 1997; Wong *et al.*, 1998a)
Syntaxin 8	ubq	ER/E/G	(Prekeris *et al.*, 1999; Steegmaier *et al.*, 1998)
Syntaxin 9	N	?	
Syntaxin 10	H/SM/P	TGN	(Tang *et al.*, 1998c)
Syntaxin 11	H/Pl/N	TGN/E	(Advani *et al.*, 1998; Tang *et al.*, 1998a; Valdez *et al.*, 1999)
Syntaxin 12	B/Lu/K (ubq?)	E	(Tang *et al.*, 1998d)
Syntaxin 13	B	E/PM	(Advani *et al.*, 1998; Hirling *et al.*, 2000)
Syntaxin 14	?	?	EST Database
Syntaxin 15	?	?	EST Database
Syntaxin 16*	N	G/ER	(Simonsen *et al.*, 1998; Tang *et al.*, 1998b)
Syntaxin 17	?	ER	(Steegmaier *et al.*, 2000)
Syntaxin 18	Ubq	ER/G	(Hatsuzawa *et al.*, 2000)

Table 1.6 The Syntaxin Family of t-SNAREs.

B = brain, H = heart, K = kidney (Mandon *et al.*, 1997), Li = liver (Fujita *et al.*, 1998), Lu = lung, N = neutrophils (Martin-Martin *et al.*, 1999), P = pancreas, Pl = placenta, SM = skeletal muscle (Sumitani *et al.*, 1995). E = endosome, ER = endoplasmic reticulum, G = Golgi, L= lysosome, PM = plasma membrane SG = secretory granule, TGN = trans-Golgi network. (* In addition, a number of splice variants have been identified).

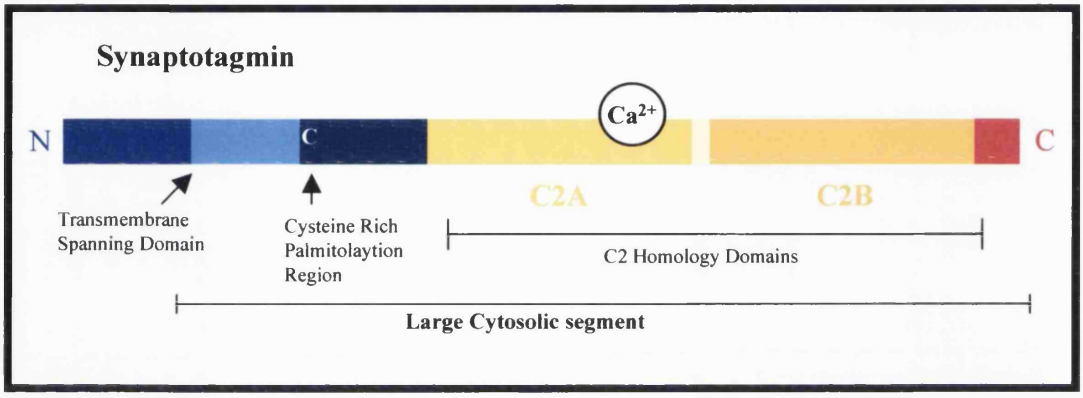

Figure 1.13 The Structure of Synaptotagmin.

The synaptotagmin proteins contain an intravesicular amino terminus, a single transmembrane domain and a cytoplasmic domain containing two repeat domains that are homologous to the C2 regulator domain of protein kinase C. Although the cytoplasmic domain of Synaptotagmin is highly conserved, variations occur in the C2 binding domains of the protein.

1.8.7.1 Synaptotagmin Isoforms

To date, approximately 12 different synaptotagmin genes have been identified, each isoform having its own tissue specific distribution (table 1.7). Although high homology is observed in the cytoplasmic portions of these proteins, differences are found in the C2A and C2B domains, suggesting distinct functions for these two domains (Schiavo *et al.*, 1998; Sugita and Sudhof, 2000; Zhang *et al.*, 1998). The role of synaptotagmins in regulated exocytosis has been extensively studied in neuroexocytosis. Blocking synaptotagmin in PC12 cells leads to the inhibition of neurotransmitter release, further implicating synaptotagmins in the highly regulated exocytic processes of neurons. In addition, these proteins have been shown to interact with a number of membrane-associated proteins, in particular the t-SNARE, syntaxin 1 (Bennett *et al.*, 1992; Chapman *et al.*, 1995).

1.8.8 The Rab Family of GTP-Binding Proteins

As discussed previously, a number of soluble factors are required for vesicular trafficking. The rab family of proteins, small GTP binding proteins, which are members of the Ras superfamily, have been implicated in the regulation of vesicle fusion (Chavrier and Goud, 1999; Clague, 1999; Darchen and Goud, 2000; Jahn and Sudhof, 1999). There have been approximately 30 Rab family members identified to date, all of which localise to specific intracellular membrane compartments: Rab3 is localised to the synaptic vesicle whilst rab5 is present on early endosomes and is implicated in the regulation of early endosome fusion and vesicle formation (Woodman, 1998). In addition, a number of Rab homologues have been identified in yeast, some of which have been shown to interact with VAMP homologues, implicating VAMP/Rab interaction at two stages of the yeast secretory pathway.

Synaptotagmin Isoform (Syt)	Tissue Distribution	Homology to Syt I (%)	Ca^{2+} Dependent C2A binding PS	Syntaxin 1	C2B binding - PI
Syt I	B	-	+	+	+
Syt II	B	81.4	+	-	-
Syt III	Ubiquitous	34.5	+	+	+
Syt IV	Ubiquitous	39.2	-	+	+
Syt V	B	41.3	+	-	-
Syt VI	Ubiquitous	40.7	-	+	+
Syt VII	Ubiquitous	46.7	+	?	?
Syt VIII	Ubiquitous	45.3	-	+	+
Syt IX	Ubiquitous	62.6	?	+	+
Syt X	B	39.5	?	-	-
Syt XI	B	39.6	-	+	+
Syt B/K	B/kidney	38.7	?	-	-

Table 1.7 Synaptotagmin Isoforms: Tissue Distribution, Sequence Identity to Syt I and C2A/C2B specific binding. Of the 12 synaptotagmin isoforms, Syt I and II are the most closely related, with Syt II showing 81 % sequence homology to Syt I. C2A domains confer calcium dependent/independent binding of phosphatidyl serine (PS) and syntaxin I whilst the C2B domain is responsible for the binding of phospholipids, PI = phosphoinositide. (B = Brain).

In addition, Rab3 and VAMP interactions have been observed on synaptic vesicles (Darchen and Goud, 2000).

The nature of this VAMP/Rab interaction remains unclear; however, its presence in both the mammalian and the yeast secretory pathways suggest that it may form part of a conserved machinery localised to the vesicle membrane.

Although there is an ongoing debate as to the exact function of SNAREs in vesicular transport, it is clear that they are crucial to vesicle docking and fusion events. This has been exemplified by the inability of cells with neurotoxin cleaved VAMP molecules, to mediate neurotransmitter release. The specialised mechanisms responsible for the secretion of neurotransmitters are likely to have evolved from the trafficking machinery responsible for mediating delivery of vesicles from Golgi to plasma membrane.

1.8.9 In summary

Although it is generally accepted that osteoblastic cells are polarised and deposit bone matrix proteins specifically onto the bone surface, away from neighbouring cells and capillaries, the precise mechanisms mediating cell polarity and the molecular mechanisms underlying the directionality of protein transport remain somewhat elusive. Further investigation into the molecular mechanisms mediating vectorial transport in osteoblasts is, therefore, crucial to understanding osteoblast cell function.

1.9 Aims of this thesis

The main objective of this thesis is to investigate the molecular mechanisms mediating vesicular transport within bone cells. In particular, emphasis is placed on establishing the molecular mechanisms used by osteoblasts to establish and maintain cell polarity and to achieve directed protein transport (fig. 1.14).

Osteoblasts are polarised cells that organise themselves into a monolayer lining the bone surface. It has been suggested that these cells come together in a so-called epithelial type manner; therefore, we hypothesise that osteoblasts may use a molecular machinery similar to epithelial cells to achieve and maintain cell polarity.

Furthermore, we hypothesise that directed protein transport within these cells may be facilitated by the presence of a number of membrane bound vesicular intermediates. We suggest that osteoblastic cells may achieve direct bone matrix protein secretion through the formation of membrane bound intermediates, directed and targeted to the specific site of deposition through a SNARE mediated mechanism.

1.10 Specific Layout of This Thesis

Chapter 3 – Primary Osteoblast-like Cell Culture:

In attempt to understand the mechanisms mediating bone matrix protein secretion in osteoblasts, an *in vitro* model of nodule formation and mineralisation was established. Chapter 3 discusses the optimisation of these primary osteoblast-like cell cultures and the culture conditions required to maximise the osteoblastic cell

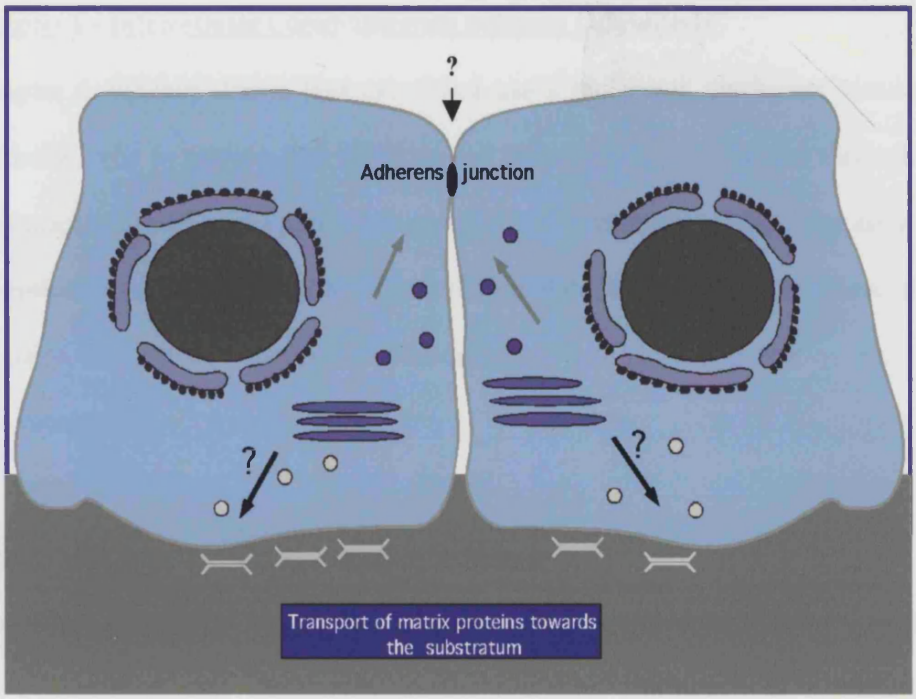

Figure 1.14 Vesicular Trafficking in Osteoblasts.

Osteoblasts align themselves along the bone surface in an epithelial-like monolayer. This thesis tests the hypothesis that osteoblasts may use a molecular mechanism similar to epithelial cells in order to achieve directed bone matrix protein secretion. Furthermore, protein components of the molecular machinery responsible for vectorial transport within osteoblasts were investigated.

content of an isolated cell population and hence its ability to form and mineralise three-dimensional nodule structures *in vitro*.

Chapter 4 – Intercellular Communication between Osteoblasts

Chapter 4, the hypothesis that osteoblast use a molecular machinery similar to epithelial cells to achieve and maintain cell polarity was investigated through the characterisation of apical junctional complexes in osteoblastic cells. The ability of an epithelial cell model, MDCK cells, to differentiate between apical and basolateral domains through the formation of intercellular communicating pathways was used as a comparison.

Chapter 5 – Vesicular Trafficking in Osteoblasts

Recently a number of key proteins implicated in regulated neuroexocytosis have been identified and implicated in the secretory pathways of a variety of non-neuronal tissues. Therefore, it is possible that these proteins may play a role in directed protein transport in osteoblasts. The nature of these proteins was addressed in osteoblastic cells.

Chapter 6 – Analysis and Localisation of VAMP1 in Osteoblasts

The identification of VAMP1 in osteoblasts implied a role in the directionality of bone matrix protein secretion. We identified the presence of a targeting v-SNARE, VAMP1, in these cells. In this chapter, I investigate further the VAMP1 isoform expressed in osteoblastic cells and attempt to localise this protein to specific sub-cellular compartments within the cell.

Chapter 2

MATERIALS AND METHODS

Chapter 2

MATERIALS AND METHODS

2.1 Materials - Buffers and Media Composition

2.1.1 Standard Buffers:

Acrylamide/Bis solution:	37.5:1 acrylamide/bis solution (Anachem, UK).
Blocking buffer:	5 % dry Milk, fat-free (Fluka,UK) in PBS Tween
PBS Tween:	0.05 % Tween 20 (Sigma, UK) in PBS
Phosphate Buffered Saline (PBS):	140 mM NaCl, 1.8 mM KH_2PO_4, 2.7 mM KCl, 8 mM Na_2HPO_4
SDS loading buffer (5x):	520 mM SDS, 500 mM DTT, 0.05 % bromophenol blue, 50 % glycerol, 312.5 mM Tris
SDS Running buffer:	250 mM Tris base, 190 mM glycine, 17 mM SDS
Stripping buffer:	100 mM 2-mercaptoethanol, 2 % SDS, 62.5 mM Tris pH 6.7
Transfer Buffer:	192 mM glycine, 25 mM Tris (pH 8.3), and 10 % methanol (added just prior to use) stored at 4 °C

2.1.2 Staining Solutions

Alkaline phosphatase staining:	0.27 mM Napthol AS-MX phosphate (Sigma, UK) 0.4 % N,N-dimethylformamide, 0.1 M Tris pH 8.3, 2.33 M Fast Red TR salt (Sigma, UK) in dH_2O (filtered prior to use, Whatman No. 1)
Coomassie Blue:	0.1 % coomassie brilliant blue, 30 % methanol, 40 % acetic acid in dH_2O
Destain solution:	30 % methanol, 10 % acetic acid in dH_2O
Methylene Blue staining solution:	0.4 % methylene blue, 500 mM sodium acetate pH 5.2
Ponceau S staining solution (10x):	2 % Ponceau S, 30 % trichloroacetic acid in dH_2O
van Gieson staining solution:	45.5 % saturated picric acid solution, 0.08 % acid fuchsin solution in dH_2O.

2.1.3 Buffers and Media for Cell Culture

Cell Freezing Media:	10 % DMSO (dimethyl sulphoxide), 90 % FCS in α-MEM, made immediately prior to use and pre-chilled on ice (Gibco, Life Technologies, Paisley, UK)
Digestion Buffer:	690 U/ml collagenase (Sigma, UK), 16 mM D-sorbitol, 6 µg/ml chondrotin sulphate (Fluka Biochemica) and 9.7 U/ml DNase (Sigma, UK) in Krebs II A buffer

Krebs II A Buffer:	111.2 mM NaCl, 21.3 mM Tris base, 13 mM glucose, 5.4 mM KCl, 1.3 mM $MgCl_2$ to pH 7.4 followed by the addition of 0.5 mM $ZnCl_2$, sterile filtered (0.2 µM filter) and stored at 4 °C
Penicillin/Streptomycin (PS):	100 U/ml penicillin and 100 µg/ml streptomycin in PBS (Gibco Life Technologies, Paisley, UK)
Trypsin/EDTA:	0.25 % Trypsin, 1 mM EDTA in Hanks balanced salt solution without calcium or magnesium (Gibco Life Technologies, Paisley, UK)

2.1.4 Cell Fixation Buffers

10 % Neutral Formalin Buffer:	1 % formalin, 113 mM Na_2HPO_4, 20 mM $NaH_2PO_4.H_2O$ in dH_2O
4 % PFA:	4 % paraformaldehyde pH 7.4 in PBS

2.1.5 Immunofluorescence Buffers

Saponin Permeabilisation Buffer:	0.5 % BSA, 0.1 % saponin, 0.02 % sodium azide in PBS
Triton Permeabilisation Buffer:	20 mM Hepes, 300 mM sucrose, 50 mM NaCl, 3 mM MgCl2, 0.5 % Triton X-100, 0.05 % sodium azide in dH_2O, pH 7.0

Wash Buffer:	5 % newborn calf serum (Gibco, Life Technologies, Paisley, UK), 0.02 % sodium azide in PBS

2.1.6 Molecular Biology Buffers

DEPC water:	0.05 % v/v diethyl pyrocarbonate in dH_2O (treated for 24 h before autoclaving)
Denhart's solution (50x):	1 % Ficoll 400 (Pharmacia, UK), 1 % polyvinylpyrrolidone, 1 % BSA, Fraction V (Sigma, UK) in dH_2O sterile filtered (0.2 µM filter)
DNA Ligase buffer (10x):	300 mM Tris-HCl pH 7.5, 100 mM $MgCl_2$, 100 mM DTT, 10 mM ATP (Promega, UK)
DNA loading buffer (10x):	20 % Ficoll, 0.1 M EDTA pH 8.0, 0.25 % xylene cylanole, 0.25 % Orange G in dH_2O
Elution Buffer:	5 mM Tris pH 7.5, (Oligotex protocol, Qiagen, UK)
First Strand synthesis buffer (5x):	250 mM Tris pH 8.3, 375 mM KCl, 15 mM $MgCl_2$ (Gibco, Life Technologies, Paisley, UK)
MOPS buffer (10x):	200 mM MOPS (3-N-morpholino-propane sulphonic acid), 10 mM EDTA pH 8.0, 80 mM sodium acetate in dH_2O, pH 7.0
Oligotex resin:	10 % (w/v) suspension of Oligotex particles in 10 mM Tris pH 7.5, 500 mM NaCl, 1 mM EDTA, 0.1 % SDS, 0.1 % NaN_3 (Oligotex protocol, Qiagen, UK)

OW2 Wash buffer: 10 mM Tris pH 7.5, 150 mM NaCl, 1 mM EDTA (Oligotex protocol, Qiagen, UK)

PCR Nucleotide Mix: Premixed 10 mM deoxynucleotide solution, dATP, dTTP, dCTP, and dGTP at 10 mM each in water pH 8.0 (Boehringer Mannheim)

PCR Reaction buffer: 50 mM KCl, 10 mM Tris-HCl pH 9.0, 0.1 % Triton X-100, Magnesium free (Promega).

Pre-hybridisation solution: 5x SSPE, 1x Denhardts solution, 0.1 % SDS, 20 μg/ml salmon sperm DNA (denatured for 5 min at 95 °C)

RNA Gel Running buffer (5x): 0.1 M MOPS, 40 mM sodium acetate, 5 mM EDTA in DEPC-treated H_2O

RNA Loading buffer: 50 % formamide, 6.1 % formaldehyde, 1x MOPS in DEPC treated H_2O

SSC (20x): 3 M NaCl, 0.3 M sodium citrate, pH 7.4

SSPE (20x): 3 M NaCl, 200 mM $NaH_2PO_4.H_2O$, 20 mM EDTA (pH 8.0) in d H_2O, pH 7.4 (sterilised by autoclaving)

TE Buffer: 10 mM Tris pH 8.0, 1 mM EDTA

Tris Phosphate EDTA buffer (TPE, 10x): 90 mM Tris, 2 mM EDTA (pH8.0), 13 mM phosphoric acid

DNA Purification Buffers- (Qiagen Protocols)

Buffer EB (Elution Buffer): 10 mM Tris pH 8.5

Buffer P1 (Resuspension Buffer):	50 mM Tris pH 8.0, 10 mM EDTA, 100 µg/ml RNase A (stored at 4 °C)
Buffer P2 (Lysis Buffer):	200 mM NaOH, 0.1 % SDS
Buffer PB:	> 25 % guanidine hydrochloride, < 40 % Isopropanol (Proprietary information, QIAquick gel extraction protocol and QIAprep spin miniprep protocol, Qiagen, UK)
Buffer PE:	Ethanol and Tris based solution, (Proprietary Information, QIAquick gel extraction protocol and QIAprep spin miniprep protocol, Qiagen, UK)
Buffer QG:	> 25 % guanidine isothiocyanate, (Proprietary information, QIAquick gel extraction protocol, Qiagen, UK)
Buffer N3 (Neutralisation Buffer):	< 25 % acetic acid, > 25 % guanidine hydrochloride, (Proprietary information, QIAprep spin miniprep protocol, Qiagen, UK)

2.1.7 Bacterial Media

Ampicillin (1000x):	100 mg/ml stock in water (used at a final concentration of 100 µg/ml) sterile filtered (0.2 µM filter)
IPTG:	1 M isopropyl-B-D-thiogalactopyranoside in dH_2O, stored at –20 °C
Lauria-Bertani Medium (LB):	10 g/L bacto-tryptone, 5 g/L bacto-yeast

	extract, 10 g/L NaCl in dH_2O pH 7.0 with NaOH, autoclaved at 120 °C for 20 min
LB Agar Plates:	LB Medium, 15 g/L bacto-agar
SOC Medium:	20 g/L bacto-tryptone, 5 g/L bacto-yeast extract, 0.5 g/L NaCl, 2.5 mM KCl, to pH 7.0 with NaOH, 10 mM $MgCl_2$ and 20 mM glucose were added prior to use
X-gal:	4 % X-Gal, (5-bromo-4-chloro-3-indolyl-B-D-Galactoside) in DMF (N, N-dimethylformamide) stored at –20 °C

2.2 Methods

2.2.1 Cell Culture

All nodule forming cultures were carried out in medium containing batch tested, heat inactivated FCS from Gibco, Life Technologies, Paisley, UK. Cells were grown in a humidified incubator with 5 % CO_2 /95 % air. Temperature was maintained at 37 °C.

2.2.1.1 Isolation of Primary Osteoblast-like Cells

Primary osteoblast-like cells were isolated from day 21 embryonic rat (Wistar) calvaria using sequential collagenase digestion. Two pregnant Wistar strain rats were sacrificed by cervical dislocation and calvaria isolated from rat pups. Approximately 25 calvaria were cut severally and the resulting calvarial fragments incubated in 4 ml of digestion buffer at 37 °C with gentle shaking. After 10 min the enzyme solution containing the released cells was collected and combined with an

equal volume of FCS (Gibco Life Technologies, Paisley, UK). Fresh enzyme mix was added to the remaining calvaria, which were incubated for a further 10 min (x2), followed by two 20 min incubations. Cells obtained from these five sequential digestions were labelled populations I – V, plated into individual T-75 mm^2 tissue culture flasks containing α-MEM, 15 % FCS, 100 U/ml penicillin, 100 μg/ml streptomycin solution and 25 μg/ml gentamicin and incubated O/N at 37 °C in a humidified atmosphere consisting of 95 % air and 5 % CO_2. Following O/N settling, cell fractions II through to V were trypsinised (section 2.2.16), pooled (fraction I, a predominantly fibroblastic cell population was discarded) and total cell number estimated using a haematocytometer. Subsequently, cells were plated into 35 mm wells at a density of $3x10^4$ cells/well for either total RNA extraction or whole cell extraction. Alternatively, cells were plated directly onto serum coated 19 mm glass coverslips for immunocytochemistry at a cell density of $1x10^4$ cells per well (fig. 2.1).

2.2.1.2 Primary Nodule forming Cultures

Cells were maintained in culture for 22 days in standard medium (α-MEM, 15 % FCS, 100 U/ml penicillin/100 μg/ml streptomycin and 25 μg/ml gentamicin) supplemented with 50 μg/ml L-ascorbate, +/- 10^{-8} M dexamethasone (Fluka, Biochemica, UK) and 10 mM β-glycerophosphate (Fluka, UK). Media was changed after the first 24 h and then every three days. Nodule formation and mineralisation was examined at different time points using histological staining methods, whilst protein expression and mRNA levels of specific protein components were determined using immunocytochemistry, Western blotting, RT-PCR and Northern blotting techniques.

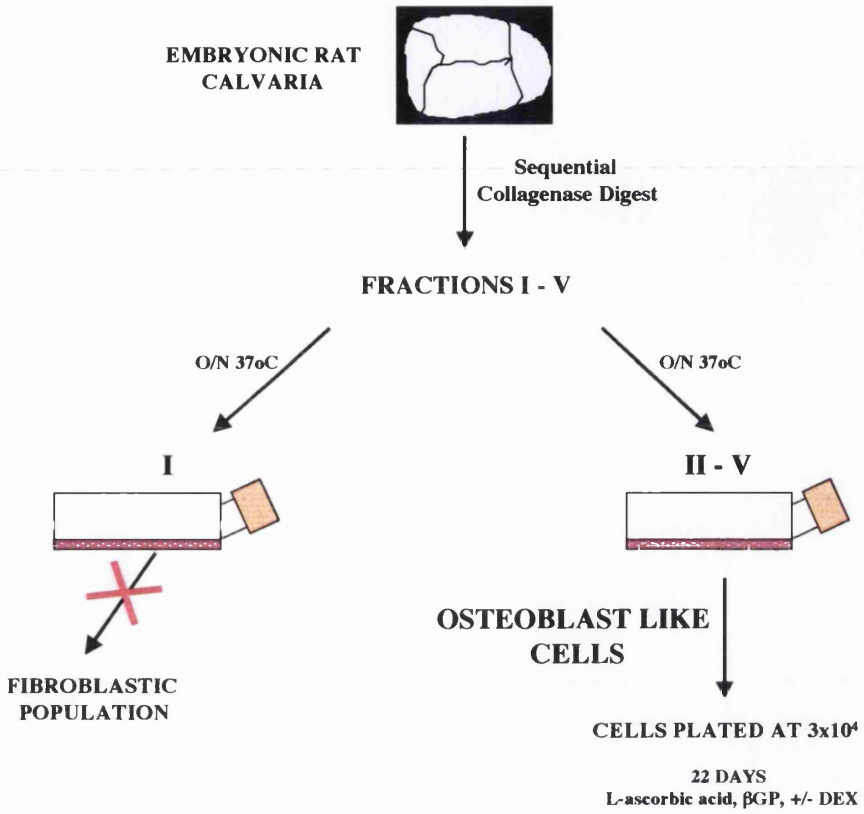

Figure 2.1 Primary Osteoblast Cell Isolation.

Osteoblastic cells were isolated from day 21 embryonic rat calvaria. Calvaria were cleaned to remove connective tissue and blood vessels and subsequently subjected to sequential collagenase digestion. Isolated cell populations I-V were harvested by centrifugation, plated into individual T-75 culture flasks and incubated O/N at 37 °C. After an initial 24 h incubation period cells were recovered and fractions II through to V pooled. Fraction I, a predominately fibroblastic cell population was discarded. Osteoblast-like cells were plated onto serum coated glass coverslips at a cell density of 1 x 10^4 cells per 19 mm coverslip, directly into T-25 flask (7.5 x 10^4 cells) or onto 35 mm wells at 3 x 10^4 cells. After an initial 24 h incubation period in standard culture conditions cells were treated with Asc, β-GP with or without 10^{-8} M dex. Cells were maintained in culture for 22 days.

2.2.1.3 Culture of ROS17/2.8 Cells

The rat osteosarcoma cell line, ROS 17/2.8, were grown in DMEM (Gibco Life Technologies, Paisley, UK) containing glutamax (L-alanyl-L-glutamine) supplemented with 5 % FCS, 100 U/ml penicillin/100 µg/ml streptomycin. Confluent cells were harvested by trypsinisation and either split and returned to culture or plated on serum coated glass coverslips at a density of 5 x 10^4 cells/19 mm coverslip and grown to confluence. Subsequently, cells were fixed in 4 % PFA pH 7.4 and stored at 4 °C until required.

2.2.1.4 MDCK Cells

Madine Darby Canine Kidney cells were grown to confluence in DMEM (Gibco Life Technologies, Paisley, UK) supplemented with 4 mM L-glutamine, 10 % FCS, 100 U/ml penicillin/100 µg/ml streptomycin. Cells were plated on serum coated 19 mm glass coverslips at a density of 7.5 x 10^4 cells/19 mm coverslip and grown to confluence. Subsequently, cells were fixed in 4 % PFA pH 7.4 and stored at 4 °C until required.

2.2.1.5 MC3T3 Cells

MC3T3 cells were grown as described by Francheschi et al, 1994. Cells harvested by trypsinisation and centrifugation were plated onto 35 mm wells at a density of 3x10^4 cells/well for total RNA extraction or whole cell extraction into SDS lysis buffer for protein analysis. Alternatively, cells were plated directly onto glass coverslips for immunocytochemical analysis at a density of 1x10^4 cells per well. Cells were allowed to settle O/N under standard culture conditions (α-MEM, 10 % FCS, 100 U/ml penicillin/100 µg/ml streptomycin). Following this initial

settlement period, cells were treated with 50 μg/ml L-ascorbate (Fluka, Biochemica) and 10 mM β-glycerophosphate (Fluka) to stimulate cell proliferation, differentiation and nodule formation. Cells were cultured up to 25 days and samples taken at different time points throughout this time course for characterisation and analysis (see chapter 3).

2.2.1.6 Trypsinisation of Adherent Cells

Trypsin/EDTA solution was thawed and warmed to RT. Culture medium was aspirated and adherent cells washed once in PBS. Trypsin/EDTA solution was added to the flask (5 ml/ T-75 cm flask) and the flask returned to the incubator for 5 min. Gentle tapping dislodged cells and an equal volume of medium containing 10 % FCS was added to inactivate trypsin. Cells were harvested at RT by centrifugation at 1000 rpm (140 g) for 5 min in a Beckman GS-6R swing bucket bench-top centrifuge. Cells were both counted and plated at the required density for immunocytochemistry (method 2.2.3) or passaged and returned to culture. Alternatively, cell stocks were frozen as described in section 2.2.1.7.

2.2.1.7 Freezing and Storage of Cells

Cells were harvested as described in section 2.2.1.6 and cell number estimated using a haematocytometer. Cells were pelleted at RT by centrifugation at 1000 rpm (140 g) for 5 min in a Beckman GS-6R swing bucket bench-top centrifuge and pellets resuspended in freezing media (pre-chilled on ice). Approximately 2 x 10^6 cells/ml were aliquoted into cryo-vials (Nunc, UK). Cryo-vials containing the cell suspensions were placed in a 'Nalgene cryo 1 °C freezing container' containing 250 ml of isopropyl alcohol and placed at –80 °C. This system freezes the cells at a

rate of –1 °C/min. After 4 h (or O/N) cells were transferred to liquid nitrogen for long term storage.

2.2.1.8 Thawing of Frozen Cells

Cells stored under liquid nitrogen were thawed at 37 °C for 2 min. Thawed cells were diluted into 5 ml of culture medium containing 10 % FCS, 100 U/ml penicillin/100 µg/ml streptomycin and cultured in T-25 cm^2 tissue culture flask until they reached confluence (2-3 days). Cells were passaged and expanded into a T-75 cm^2 tissue culture flask and then cultured as normal.

2.2.2 Immunocytochemistry

ROS 17/2.8 cells and MDCK cells were plated onto serum coated glass coverslips at a density of $5x10^4$ cells per 19 mm coverslips and cultured under the conditions described above. Confluent/ sub-confluent cells were washed once in PBS and subsequently fixed in 4 % paraformaldehyde (pH 7.4) for 5 min on ice. Fixed cells were washed 3 times in PBS and stored in PBS at 4 °C until required. Similarly, primary osteoblast-like cells and MC3T3 cells were plated at a density of $1x10^4$ cells/19 mm glass coverslip. These cells were grown under the culture conditions required for nodule formation and mineralisation (described above 2.2.1.2), and cells fixed at different time points during nodule formation and mineralisation.

For VAMP1 expression cells, were simultaneously permeabilised and blocked in saponin permeabilisation buffer for 30 min at RT, prior to incubation with primary antibody. For junctional protein expression, cells were permabilised in a Triton

based permeabilisation buffer for 5 min on ice. Subsequently, cells were washed 3x in PBS and blocked in wash buffer for 30 min at RT.

Following a one hour blocking step with either wash buffer or saponin buffer, cells were incubated with primary antibodies at the appropriate concentration (see tables 2.1, 2.2 and 2.3) for 1 h at RT. The antibody solution was discarded and cells were washed 3x and incubated in either wash buffer or saponin buffer at RT for 30 min. FITC and TRITC conjugated secondary antibody was prepared at a 1:40 dilution into either wash buffer or saponin buffer. Alternatively, Cy5 secondary antibody was prepared at a dilution of 1:100. Secondary antibodies used varied, depending on the species that the primary antibody was raised in. Either swine anti rabbit, goat anti rabbit, rabbit anti mouse or goat anti mouse were used. Simultaneous staining for F-actin using rhodamine conjugated phalloidin (Molecular probes) was performed. 1 U/ml of rhodamine conjugated phalloidin was added to the secondary antibody solution prior to the incubation at RT for 30 min. As previously described, samples were consequently subjected to a serial washing steps. Glass coverslips were mounted either in a Mowiol based immunomount containing anti-fade or in glycerol antifade (Citifluor, UK) and analysed using confocal scanning laser microscopy.

2.2.3 Confocal Laser Scanning Microscopy

Confocal microscopy was carried out using a Leica TCS NT (Leica, Germany) system with a 750 mW Omnichrome crypton-argon laser. Cells were mounted either in PBS antifade or glycerol antifade (Citifluor, UK); frozen tissue sections were mounted in Mowiol based immunomount with antifade and viewed by standard fluorescence microscopy. Objectives used varied depending on the

samples observed (x16, x40 oil immersion or x63 water immersion). Background staining was accounted for using Ig negative controls. Images were collected for FITC, TRITC and Cy5 fluorochromes with BF 530/30 nm, BP 600/30 nm and LP 665 nm filters respectively. Images were collected on either the X-Y (horizontal plane) or the lateral Z-X plane and displayed as single, dual or triple fluorescence images.

2.2.4 Western Blot Analysis

2.2.4.1 Preparation of Samples for Western Blot Analysis

Cells were grown to confluence. Adherent cells were washed with PBS and dislodged by cell scraping. Cells were harvested at RT by centrifugation at 1,200 rpm (195 g) for 5 min in a Beckman GS-6R swing bucket bench-top centrifuge. The resulting cell pellet was resuspended in PBS and cell number estimated using a haematocytometer.

Cells were collected by further centrifugation at 1,200 rpm (195 g) for 5 min at RT and resuspended in the appropriate amount of SDS loading buffer required to give a final cell concentration of 50,000 cells or 100,000 cells per 10 µl. Samples were incubated for 5 min at 96 °C prior to loading on a reducing SDS-PAGE. Approximately $5x10^4$ or $1x10^5$ cells were loaded per lane, unless otherwise stated, and proteins were resolved by electrophoresis for 1 h at 40 mA. The molecular weights of the bands were assessed by comparison with pre-stained low molecular weight protein markers (New England, BioLabs).

2.2.4.2 SDS PAGE

Gel plates were assembled in accordance with the Mini-Protean II electrophoresis instruction manual (BioRad, UK). The degree of separation depends on the concentration of polyacrylamide used and the amount of cross-linking. The amount of SDS that binds to a denatured polypeptide is in direct proportion to its molecular weight, hence SDS-polypeptide complexes migrate in accordance to protein size.

A number of separating gels, containing different concentrations of bis-acrylamide (BioRad, UK) were used depending on the size of the protein of interest: 15 %, 10 % and 7.5 %. For example, a 15 % separating gel requires a solution with a final concentration of 15 % acrylamide/bis solution (Anachem, UK), 375 mM Tris HCl pH 8.8, 0.1 % SDS, 0.04 % TEMED (BioRad, UK) and 0.1 % ammonium persulphate (APS). TEMED, N,N,N',N'-tetramethylethylenediamine, accelerates polymerisation and was added along with APS immediately prior to the gel being poured. After polymerisation at RT for 30 min, a standard 5 % stacking gel was poured (5 % acrylamide/bis solution, 125 mM Tris HCl pH 6.8, 0.1 % SDS, 0.1 % APS and 0.1 % TEMED). The stacking gel was poured directly onto the surface of the polymerised separating gel and a teflon comb inserted into the stacking gel solution.

Following polymerisation, the gel was mounted on the mini gel electrophoresis apparatus (Mini-Protean II electrophoresis system, BioRad, UK) and 1x SDS running buffer (see section 2.1.1 for composition) added to the top and bottom reservoirs. Samples in SDS loading buffer were prepared by heating them to 96 °C for 5 min to denature the proteins. Denatured protein samples were loaded and the gels were run at 20 mA, initially, until proteins reached the bottom of the stacking

gel and at 40 mA for a further 1 h or until the bromophenol blue front reached the bottom of the separating gel. The gel apparatus was disassembled and gels were either stained with coomassie blue or washed and blotted onto nitrocellulose/PVDF membranes for western blot analysis.

2.2.4.3 Visualisation of Proteins Resolved by SDS PAGE

Coomassie Blue Staining

Proteins resolved on SDS polyacrylamide gels were visualised by staining with coomassie brilliant blue. Coomassie solution was heated briefly in the microwave prior to use and the gel stained for 20 min at RT. The stained gel was washed repeatedly in destain. Gels were dried in a BioRad drying oven in accordance with the manufacturers published guidelines.

2.2.4.4 Immunoblotting of Resolved Protein Samples

Following SDS-PAGE, resolved proteins were blotted either onto nitrocellulose or PVDF membranes at 100 V for 60 min using the BioRad mini gel blotting system. Membranes were rinsed in dH_2O and equilibrated in transfer buffer prior to transfer. After the transfer, membranes were rinsed in dH_2O, incubated with 1x Ponceau S reversible staining solution and the resulting protein distribution was recorded. Membranes were washed twice in PBS/Tween 20 and blocked in blocking buffer containing 0.02 % sodium azide O/N at 4 °C (or alternatively for 1 h at RT). After this initial blocking step membranes were probed with the required primary antibody, diluted in blocking buffer, for either 2 h at RT or at 4 °C O/N (for primary antibody concentrations see tables 2.1, 2.2, 2.3). Prior to incubation with a

Junction Protein Screen		Source	Concentration IF	WB
Claudin 1 (71-7800)	pc	Zymed, Cambridge, Bioscience, UK	20 µg/ml	2 µg/ml
Claudin 2 (51-6100)	pc	Zymed, Cambridge, Bioscience, UK	3 µg/ml	2 µg/ml
Occludin (71-1500)	pc	Zymed, Cambridge, Bioscience, UK	10 µg/ml	1 µg/ml
Occludin (MOC37)	mc	Tsukita, Furuse *et al*, Kyoto University, Japan	Neat, tissue culture supernatant*	
ZO-1 (33-9100)	mc	Zymed, Cambridge, Bioscience, UK	20 µg/ml	2 µg/ml
ZO-1 (T8-754)	mc	Tsukita, Furuse *et al*, Kyoto University, Japan	Neat, tissue culture supernatant*	
ZO-1 (61-7300)	pc	Zymed, Cambridge, Bioscience, UK	-	0.5 µg/ml
Pan-Cadherin (C3678)	pc	Sigma, Immunochemicals, UK	1:100	1:250
E-Cadherin (DECMA 1)	pc	Sigma, Immunochemicals, UK	1:100	1:500
P-Cadherin (13-5800)	mc	Zymed, Cambridge Bioscience, UK	1:500	1:1000
N-Cadherin (C2542)	mc	Sigma, Immunochemicals, UK	1:50	1:100
Plakoglobin (PG5.1)	mc	Progen, UK	-	1:10
α-Catenin	pc	Sigma Immunochemicals, UK	1:800	1:2000
β-Catenin	pc	Sigma Immunochemicals, UK	1:100	1:1000
α-actinin (A5044)	mc	Sigma, Immunochemicals, UK	1.3 µg/ml	0.65 µg/ml
Vinculin (v-9131)	mc	Sigma, Immunochemicals, UK	1:400	1:100

Table 2.1 Junctional Protein Screen.

Antibodies used throughout this study for western blotting (WB), immunocytochemistry (IF). * Neat tissue culture supernatants were not used for western blot analysis. Antibodies are either expressed as a final concentration of µg/ml used or as a working dilution. (pc=polyclonal, mc=monoclonal).

SNARE Protein Screen		Source	Concentration IF	Concentration WB
VAMP1	pc	G. Schiavo, ICRF, London	3 µg/ml	2 µg/ml
VAMP1 (affinity purified)	pc	G. Schiavo, ICRF, London	1:200	1:250
VAMP1	mc	Synaptic Systems, GmbH, Germany	1:250	1:500
VAMP	pc	Synaptic Systems, GmbH, Germany	1:250	1:500
VAMP2	pc	G. Schiavo, ICRF, London	1:200	1:500
Synaptotagmin I	mc	Zymed, Cambridge, Bioscience, UK	10 µg/ml	1 µg/ml
Synaptotagmin II	pc	S. Osborne, G. Schiavo, ICRF, London	1:10	1:100
Synaptotagmin IV	pc	S. Osborne, G. Schiavo, ICRF, London	20 µg/ml	2 µg/ml
Synaptotagmin X	pc	S. Osborne, G. Schiavo, ICRF, London	-	1:100
Synaptotagmin B/K	pc	S. Osborne, G. Schiavo, ICRF, London	-	0.5 µg/ml
SNAP 25	pc	G. Schiavo, ICRF, London	1:100	1:250
Syntaxin 1 (HPC1)	mc	Transduction Laboratories, UK	25 µg/ml	1 µg/ml
Syntaxin 4	mc	Transduction Laboratories, UK	0.5 µg/ml	0.25 µg/ml
Syntaxin 6 (S55420)	mc	Transduction Laboratories, UK	-	0.05µg/ml
Fusion Proteins				
NSF (6E6)	mc	J. Rothman, Sloane and Kettering, USA	1:100	-
NSF	pc	J. Rothman, Sloane and Kettering, USA	-	1:100
α-SNAP	pc	J. Rothman, Sloane and Kettering, USA	1:250	1:1000

Table 2.2 SNARE Protein and General Fusion Machinery Protein Screen.

Antiobodies used throughout this study for western blotting (WB), immunocytochemistry (IF). Antibodies are either expressed as a final concentration of µg/ml used or as a working dilution. (pc=polyclonal, mc=monoclonal).

Osteoblastic Markers and other proteins		Source	Concentration IF	WB
Alkaline phosphatase	mc	J. Aubin, University of Toronto, Canada	1:500	-
Osteocalcin	pc	K. Leuven, Belgium	1:250	1:500
Osteopontin	mc	Sigma, Immunochemicals, UK	1:500	-
Collagen Type I (C2456)	mc	Sigma, Immunochemicals, UK	1:1000	-
GM130 (golgi marker)	mc	G. Warren, ICRF, London	1:100	-
ER	mc	R. Pepperkok, ICRF, London	1:10	-
GAPDH	mc	Chemicon, UK	-	1:200

Table 2.3 General Antibodies.

Secondary antibodies used varied depending on the host species of the primary antibody used and its species reactivity. Antibody concentration is expressed as a working dilution. (pc=polyclonal, mc=monoclonal). FITC and TRITC labelled secondary antibodies were obtained from DAKO, Cambridgeshire, UK while Cy5 labelled antibodies were obtained from Amersham, UK. FITC and TRITC conjugated secondary antibodies were used at a dilution of 1:40 while Cy5 conjugated secondary antibodies were used at 10 μg/ml. For western Blot analysis HRP conjugated secondary antibodies were obtained from BioRad, UK and used at a working dilution of 1:3000.

horse-radish peroxidase (HRP) conjugated secondary antibody (goat-anti-rabbit for polyclonal antibodies or goat-anti-mouse for monoclonal antibodies, BioRad, UK) the blots were serially washed in PBS/Tween 20. Secondary antibody was diluted 1/3000 into blocking buffer without sodium azide and the samples incubated for 1 h at RT. Washing was repeated and blots developed using the ECL or ECL+ detection systems (Amersham, UK).

2.2.4.5 Immunoblotting onto PVDF membranes

Proteins were blotted onto PVDF membranes as described in section 2.2.4.4 with one modification. Prior to blotting, PVDF membranes were incubated for 5 min in methanol before equilibration in transfer buffer.

2.2.4.6 ECL Detection Systems for Nitrocellulose Membranes

Bound peroxidase activity was detected using an ECL detection system kit. ECL kits are based on the oxidation of diacylhydrazide lumiol to an acridinium ester by the combined action of HRP and peroxide. Equal volumes of reagents 1 and 2 were mixed and the membrane incubated for 1 min. Excess reagent was removed before developing. Blots were covered in saran wrap and exposed to Kodak Bio-Max films (Sigma, UK) for varying time periods (usually between 30 sec to 3 min).

2.2.4.7 ECL+ Detection Systems for PVDF Membranes

Reagents were incubated at RT prior to use. Detection solutions A and B were mixed at a ratio of 40:1 as described in Amersham ECL+ detection protocol. PVDF membranes were washed and incubated with the mixed detection solution for

5 min at RT. Excess reagent was removed and blots were wrapped in saran wrap and subsequently exposed to Kodak, BioMax film (Sigma, UK) for varying time periods, ranging from 1 sec to 1 min.

2.2.4.8 Stripping of Western Blots

Following an incubation of 30 min at 50 °C in stripping buffer, membranes were washed 2x 10 min in PBS/Tween to remove the denaturing conditions. Prior to immunodetection with primary antibody blots were blocked in 5 % milk in PBS/Tween for 30 min at RT, or alternatively for 10 min at RT after heating the blocking solution.

2.2.5 Northern Blot Analysis

2.2.5.1 Total RNA Extraction

Prior to isolation of RNA all equipment was rinsed with DEPC-treated water. All reagents used were of molecular biology grade.

Cells were grown to confluence and total RNA extracted in accordance with the TRIzol protocol (Gibco Life Technologies, Paisley, UK). TRIzol is a mono-phasic solution of phenol and guanidine isothiocyanate, which maintains the integrity of the RNA during cells lysis (Chomczynski and Sacchi, 1987). The addition of chloroform and subsequent centrifugation separates the solution into an aqueous and organic phase. The RNA remains in the aqueous phase. The DNA and proteins are localised to the interphase and organic phases respectively.

Adherent cells were harvested by addition of 1 ml of RT TRIzol/ 10 cm^2. The resulting TRIzol suspensions were aliquoted into RNase free 1 ml microfuge tubes, snap frozen in liquid nitrogen and stored at -80 °C until required.

Frozen TRIzol cell suspension aliquots were thawed and incubated for 5 min at RT. To each ml of cell suspension 0.2 ml of chloroform was added, tubes were inverted to mix their contents and incubated at RT for a further 3 min. Samples were centrifuged at 13,000 rpm (16,060 g) for 15 min at 4 °C in a Heraeus Fresco Biofuge (Sorvall Heraeus, Kendro Laboratory Products, UK) and the upper aqueous phase retained. Total RNA was prepared as follows. 0.5 ml of isopropanol was added and samples incubated at RT for 10 min. The precipitated RNA product was recovered by centrifugation at 13,000 rpm (16,060 g) for 10 min at 4 °C, and the resulting RNA pellet washed in 75 % ethanol. Following a final centrifugation at 7,500 rpm (1600 g) for 5 min at 4 °C (Heraeus, fresco Biofuge), the RNA pellet was air dried at RT and resuspended in 30 µl of RNase free DEPC treated water. Finally, the total RNA solution was incubated at 55 °C for 10 min. Total RNA concentration was estimated using GeneQuant (Pharmacia Biotech, Cambridge, UK) or a Beckman spectrophotometer and stored at –80 °C until required. RNA quality was assessed by resolving ~ 1µg of total RNA on a 1.5 % TPE agarose gel.

2.2.5.2 Estimation of RNA concentration

The estimated RNA concentration was based on the assumption that 40 µg of total RNA in 1 ml gives an $OD_{260nm} = 1$. Using 5 µl of isolated RNA in a capillary tube, RNA concentration was estimated using GeneQuant (Pharmacia Biotech). The spectrophotometer was blanked with DEPC treated water or TE buffer and the absorbance of each sample read at both 260 nm and 280 nm. The quality of RNA

sample was calculated by comparing the ODs obtained at the two wavelengths; 260 nm reflects the nucleotide content while 280 nm describes the protein content of the sample. A ratio of between 1.8 and 2 reflects good quality uncontaminated RNA. Further to checking RNA quality spectrophotomerically, RNA was visualised by resolving ~ 1 µg of RNA sample on a 1 % TPE agarose gel containing 5 µg/ml ethidium bromide.

2.2.5.3 Agarose Gel Preparation and Electrophoresis

A 1 % denaturing formamide gel was prepared by the addition of 1 g of agarose into 86 ml of DEPC-treated water with 10 ml of 10x MOPS buffer. Heating the solution briefly in the microwave dissolved the agarose. The agarose solution was allowed to cool to approximately 50 °C and 19.4 ml of 37 % formaldehyde was added (final concentration of 7.2 % formaldehyde). The gel was poured into a gel casting tray and allowed to polymerise at RT for 30 min. Following polymerisation the gel was transferred to a BioRad Mini-SUB DNA tank and submerged in 1x MOPS running buffer. After an initial denaturation step at 65 °C samples were loaded at a concentration of 10 µg per lane and resolved at 100 V for 1 h 30 min. Subsequently, the gel was washed for 20 min in DEPC-treated water to remove any remaining formaldehyde and the RNA transferred to nylon membranes, either by O/N capillary transfer or under constant pressure using the Biometra Vacu-blot system at 100 psi for 3-4 h. The integrity of the RNA on the blot was assessed using methylene blue staining and comparison with the 5 µg of loaded RNA ladder.

2.2.5.4 Capillary Transfer of RNA

A tray containing 20x SSC transfer buffer was set up containing a support plate and a glass plate to form a bridge. A sheet of 3 mm Whatman filter paper soaked in 20x SSC transfer buffer was used as a wick with a second piece of filter paper placed on top. Care was taken to avoid air bubbles underneath both sheets of filter paper. The gel was washed and equilibrated in 20x SSC transfer buffer then placed open well side down on the wick and bubbles removed by rolling a sterile pipette over the surface of the gel. A sheet of nylon membrane (Hybond-N, Amersham), cut slightly larger than the gel itself, was placed on top of the gel followed by several sheets of 3 mm Whatman filter paper (all cut to size). Finally a stack of absorbent paper towels were placed on top and a glass plate to distribute the weight placed on top. RNA was left to transfer at RT O/N.

2.2.5.5 RNA Transfer Using Vacu-Blot

Alternatively, RNA was transferred using the Biometra Vacu-Blot system. The Vacu-Blot apparatus was set up as per manufacturer's instructions. The vacuum pump was connected directly to the Vacu-Blot. The filter plate holder was placed in the collecting tank and the porous filter plate placed on top. Two sheets of 3 mm Whatman filter paper pre-soaked in 20x SSC transfer buffer were placed on top. Nylon membrane (Hybond-N, Amersham, UK) was cut to size and placed on top (after equilibration in 20x SSC transfer buffer). To eliminate bubbles, a sterile pipette was rolled across the membrane. A wet rubber mat, with the centre cut out slightly smaller than the size of the agarose gel), was placed on top. The gel was placed on the hole in the rubber mat leaving ~ 5 mm boundary of gel on each side of the rubber mat. Finally, the coverplate with buffer reservoir was placed on top and held in place using clips. A small amount of 20x SSC transfer buffer was

added, to hold the gel in place and the vacuum applied (~ 100 psi). The reservoir was topped up with 20x SSC transfer buffer and the RNA transfer carried out at a constant pressure (100 psi) for 4 h.

2.2.5.6 Methylene Blue Staining

To check both the integrity of the RNA and efficiency of transfer and loading, the nylon membrane was washed for 10 min in 0.5 % acetic acid, incubated for 10 min in methylene blue staining solution followed by a final 10 min wash in distilled water.

2.2.5.7 Fixing of RNA Blot

The membrane was washed in 2x SSC and RNA immobilised by drying the membrane at 80 °C for 5 min (sandwiched between two sheets of 3 mm Whatman filter paper) followed by UV cross-linking in a Stratalinker UV Crosslinker 2400, (Stratagene, UK) using autocrosslink mode, 120,000 microjoules for approximately 30 sec.

2.2.5.8 Preparation of ^{32}P labelled DNA probe

Radioactively labelled probes were prepared from DNA samples obtained from PCR products. The DNA fragments were purified from 1.5 % TPE agarose gels using the Qiagen QIAquick spin column gel extraction protocol (described in section 2.2.9). The DNA concentration was estimated and the DNA fragments labelled with [$\alpha^{32}P$] dCTP in accordance with the Amersham multiprime labelling kit. This kit uses random sequence hexanucleotides to prime DNA synthesis on a denatured template DNA at numerous sites along its length creating probes of

different fragment size. Furthermore, the same site of template DNA can be copied more than once by DNA synthesis primed by other random hexanucleotides thus maximising the amount of labelled probe generated.

Briefly, 25 ng of gel purified DNA was resuspended in 8 µl of DEPC treated water. Following denaturation at 65 °C for 10 min, 25 ng of cDNA was combined with the following reagents; 4 µl of each dNTP (dATP, dTTP, dGTP, 10 mM), 5 µl of 10x reaction buffer, 5 µl of BSA/primer solution and water (final reaction volume 50 µl). 5 µl of [α^{32}P] dCTP was added along with 2 µl of enzyme (1 U/µl Klenow fragment DNA polymerase I) and the reaction incubated at 37 °C for 45 min.

2.2.5.9 Purification of Labelled cDNA probe

Labelled probes were purified by gel filtration using ProbeQuant G-50 Micro columns (Amersham, UK). ProbeQuant Sephadex G-50 filters trap the unincorporated labelled nucleotides, thus separating them from the labelled DNA probe.

The resin was resuspended by vortexing the column and centrifugation at 800 g for 1 min. Following this centrifugation step the 50 µl reaction volume containing the radioactively labelled probe was slowly applied to the column and the column placed in a 1.5 ml tube and centrifuged at 800 g for 2 min. The purified probe was collected in the support tube.

2.2.5.10 Probing of Northern Blot

The RNA blot was pre-hybridised in pre-hybridisation solution for 1 h at 65 °C. The pre-hybridisation solution was discarded and between 7 and 10 ml of fresh pre-hybridisation solution added to the hybridisation tube. Both the purified probe and 20 µg/ml salmon sperm DNA were incubated for 5 min at 95 °C and subsequently added to the hybridisation tube. Hybridisation was performed at 65 °C O/N, rotating.

Subsequently, the radioactive probe was removed and the membrane washed 2x 5 min in 2x SSPE/0.1 % SDS to remove any unbound probe. A second more stringent wash in 1x SSPE/0.1 % SDS for 15 min at 65 °C was performed. The labelled membrane was wrapped in saran wrap and exposed on a phosphoimager screen for 3 h at RT. Radioactively labelled RNA/DNA hybrids were visualised using a phosphoimager (FLA 3000G, Fuji Films Ltd, Tokyo, Japan) and Aida 2.0 (Raytest, UK) and Image Reader FLA 3000 (Fuji Films Ltd, Tokyo, Japan) analysis packages.

2.2.6 Reverse Transcription – Polymerase Chain Reaction (RT-PCR)

Reverse transcription PCR was carried out on RNA samples, using both random hexamer (RH) and oligo dT primers (dT) (Pharmacia, UK)), in accordance with the Superscript II Reverse transcriptase protocol (Gibco Life Technologies, Paisley, UK). Superscript II RNase H reverse transcriptase was used to synthesis the first strand of cDNA. Briefly, ~ 5 µg of total RNA was combined with 1.25 µM RH or dT primers in 12 µl of dH_2O, heated to 70 °C for 10 min then chilled on ice. Following a brief centrifugation, 4 µl of 5 x first strand synthesis buffer, 2 µl of 0.1 M DTT and 1 µl of 10 mM dNTP mix (Boehringer Mannheim), were added to the primer/cDNA

mix (total reaction volume of 20 µl). Contents of the tubes were mixed and incubated at 42 °C for 2 min prior to the addition of 200 units (1 µl) of Superscript II reverse transcriptase. Following a further 50 min incubation at 42 °C the reaction was inactivated by incubation at 70 °C for 15 min. Complementary RNA template was removed upon treatment with RNase H (Gibco Life Technologies, Paisley, UK). 2 units (1 µl) of *E.coli* RNase H was added to each reaction and incubated at 37 °C for 20 min. The resulting single stranded cDNA product was diluted to 250 µl by the addition of 230 µl of TE buffer, oligo dT and RH samples were pooled, aliquoted and cDNA stored at -20 °C until required. Approximately 2.5 µl of oligo dT/RH transcribed, single stranded cDNA was used per 50 µl PCR reaction volume.

2.2.7 Polymerase Chain Reaction (PCR)

PCR was performed using 2.5 µl of the diluted single stranded cDNA product per 50 µl PCR amplification reaction. Other PCR reaction components: 0.25 µM of each gene specific primers, 1x PCR reaction buffer in the presence of 1.5 mM $MgCl_2$. The cDNA and gene specific primers (primer sequences are shown in tables 2.4, 2.5 and 2.6) were combined in a final sample volume of 10 µl (dH_2O) and overlayed with molecular biology grade mineral oil (Sigma, UK). A mastermix consisting of PCR reaction buffer, $MgCl_2$ and Taq Polymerase (Promega, UK) was prepared and 40 µl of mastermix added to each reaction tube after the initial denaturation step.

Primer	Sequence (5′-3′)	T_m (°C)
Junction Proteins		
5′ Claudin 1/2	GYTGGKGMCARCATYGTGAC	58
3′ Claudin 1/2	CAGGARMAGSAAAGKAKGAC	48
5′ Claudin 3	CAACTGCGTACAAGATGAGACGG	68
3′ Claudin 3	GCGTGGCGTCTGTAACCATCTG	70
5′ Claudin 4	ATGGCGTCTATGGGACTACAG	64
3′ Claudin 4	TCTGCCCGGAAGCCACCATAG	68
5′ Claudin 8	GTATGAGGCATGCCAACATCAGA	68
3′ Claudin 8	CTGTTGCTCCTTTCAGTACAACAA	68
5′ Occludin	CACTATGAAACCGACTACACGAC	68
3′ Occludin	CCGTCTGTCATAGTCTCCCAC	66

Table 2.4 Primer Sequences used for RT-PCR analysis of Junction Protein Components.

An estimate of primer melting temperature (T_m) was calculated as: $T_m \cong 4\,(G+C) + 2(A+T)$.

Primer	Sequence (5′ – 3′)	T_m (°C)
VAMP1 Screen		
VAMP1 5′ a	ATGTCTGCTCCMGCTCAGCCAC	74
VAMP1 3′a	AGCTTGGCAGCACTKSTYTC	64
$VAMP1B_{nt}$	CTCCATCAAGGAACATCCTTG	62
VAMP1B.	CAGTGCCTCAGCGATACTTACTTA	70
VAMP1-OB	CAGAGTCTAGTGGAGACCTTC	64
VAMP1 3′ RACE reaction		
R_T	CCAGTGAGCAGAGTGACGAGGACTCGAGCTCAA GCTTTTTTTTTTTTTTTT	126
R_O	CCAGTGAGCAGAGTGACG	58
R_1	GAGGACTCGAGCTCAAGC	58
VAM 3′	AGGCAGGAGCGTCAGTGTTTGAGA	74

Table 2.5 VAMP1 Primer Sequences.

VAMP1 and VAMP1 3′RACE reaction primer sequences. An estimate of primer melting temperature (T_m) was calculated as: $T_m \cong 4\,(G+C) + 2(A+T)$.

Primer	Sequence (5′-3′)	T_m (°C)
5′ Alkaline Phosphatase	CAACTCATTTGTGCCAGAGAA	60
3′ Alkaline Phosphatase	TCAACTCATACTGCATGTCCC	62
5′ Osteocalcin	ATGAGGACCCTCTCTCTGCT	62
3′ Osteocalcin (rat)	CCCTAAACGGTGGTGCCATA	62
3′ Osteocalcin (mouse)	AATAGTGATACCGTAGATGCG	60
5′ Osteopontin	ATGAGACTGGCAGTGGTTTGC	62
3′ Osteopontin	CTTTAATTGACCTCAGAAGATGAA	64
5′ β-Actin	TGTATGCCTCTGGTCGTACCAC	68
3′ β-Actin	ACAGAGTACTTGCGCTCAGGAG	68

Table 2.6 General Primer Sequences.

Primer sequences used for the amplification of osteoblast phenotype markers and for the amplification of β-Actin control. An estimate of primer melting temperature (T_m) was calculated as: $T_m \cong 4\,(G+C) + 2(A+T)$.

PCR conditions vary depending on the specific melting temperatures (T_m) of the gene specific primers used. Using manual 'hot start' PCR typical PCR conditions were as follows: 94 °C for 5 min (to denature samples), 72 °C for 3 min (for the addition of mastermix which was heated for 1 min at 94 °C prior to its addition), 94 °C for 1 min, 58 °C for 1 min (annealing temperature varied depending on the T_m of the gene specific primer used), 72 °C for 1 min x35 cycles (unless otherwise stated). A final extension step of 72 °C for 10 min was followed by a 4 °C soak (held at 4 °C until required). Resulting PCR products were resolved and analysed on a 1.5 % TPE agarose gel, and their respective sizes estimated by comparison with 1 kB DNA ladder, 1 kB plus DNA ladder (Gibco, Life Technologies, Paisley, UK) or 100 bp ladder (BioRad, UK).

2.2.8 3′ Rapid Amplification of cDNA ends (RACE) Reaction

RACE reaction, rapid amplification of cDNA ends, was used to amplify partial cDNA ends between a known point and either the 3′ or 5′ end of the particular cDNA transcript (fig. 2.2).

2.2.8.1 Poly A^+ mRNA Isolation from Total RNA

The majority of eukaryotic mRNAs end in a homopolymer of 20-250 adenosine nucleotides, the poly A tail, thus allowing mRNA to be separated from a pool of total cellular RNA. Separation is achieved by hybridising the polyadenylated tails of the mRNA molecules to oligo dT primers immobilised on a solid matrix. RNA lacking a poly A tail will fail to bind and will be removed. Hybridisation of the poly A tail to the oligo dT primers requires a high salt concentration, therefore

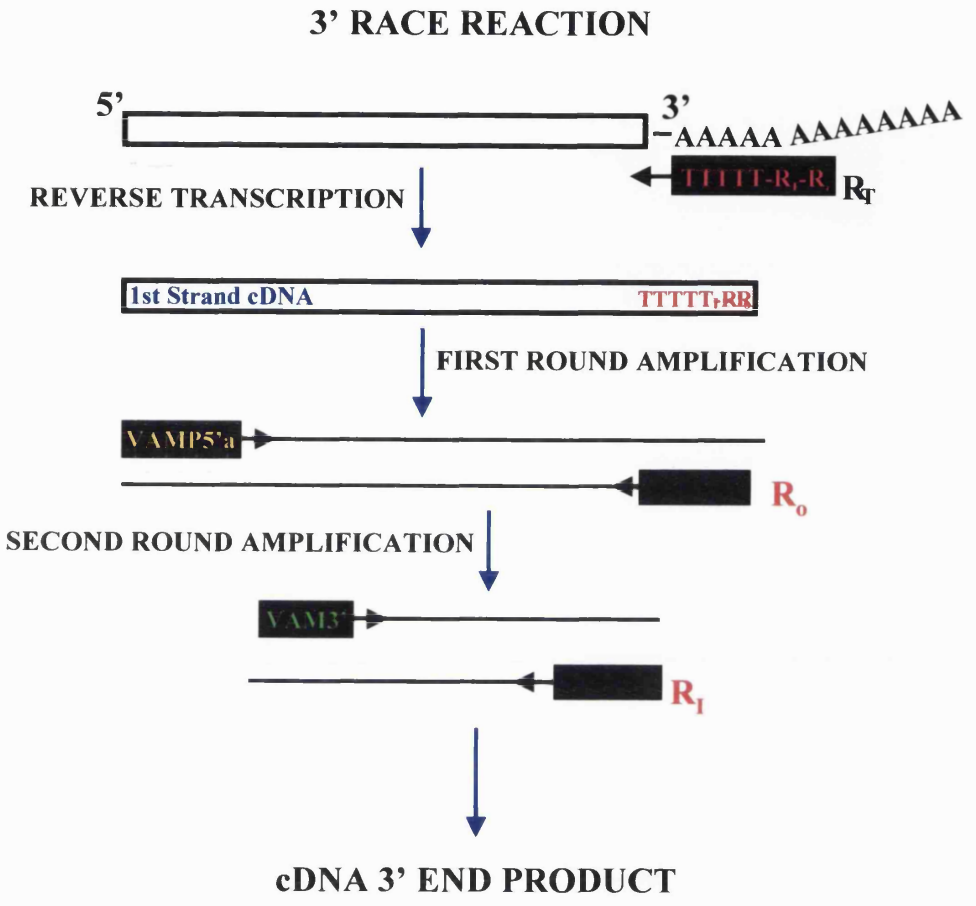

Figure 2.2 A schematic representation of 3′ Rapid Amplification of cDNA Ends.

For 3′ end amplification of mRNA, mRNA was reverse transcribed using a hybrid R_T primer containing 17 oligo dTs followed by a 35 base oligonucleotide sequence (containing the anchor primers, R_o and R_I). The resulting cDNA was amplified using the gene specific primer VAMP1 5′a (table 2.5) and the external anchor primer R_o. Nested PCR was performed on the product using a second gene specific primer VAM3′ RACE and the internal anchor primer R_I.

bound mRNA can be eluted by lowering the ionic strength and destabilising the oligo dT/poly A hybrids.

Initially total RNA was isolated from ROS cells in culture (TRIzol protocol, Gibco Life Technologies, Paisley, UK) and poly A^+ mRNA isolated in accordance with the oligotex protocol (Qiagen, UK). In brief, 40 µg of total RNA was diluted in DEPC treated water and combined with 15 µl of pre-heated (37 °C) oligotex resin. Samples were initially incubated at 65 °C for 3 min and then at RT for 10 min. Following centrifugation at 13,000 rpm (Biofuge Fresco, Heraeus) for 2 min the supernatant was collected and applied to the spin column and centrifuged at 13,000 rpm for 1 min. The column was washed twice in OW2 wash buffer and the bound RNA eluted using 20 µl of elution buffer preheated to 70 °C. Poly A^+ RNA was precipitated on ice for 30 min in 0.3 M ammonium acetate (pH 5.2) and 2.5 volumes of ice cold ethanol and the resulting RNA pellet collected by centrifugation at 13,000 rpm at 4 °C. The pellet was washed in 70 % ethanol and the RNA pellet was resuspended in DEPC treated water, stored at -80 °C until required.

2.2.8.2 Reverse Transcription Reaction

1 µg of poly A^+ RNA was incubated at 80 °C for 3 min, transferred to ice and added to the reverse transcription reaction components: 0.1 µM R_T primer, 4 µl of 5x first strand synthesis buffer, 1 µl of 10 mM dNTP mix, 2 µl of 0.1 M DTT and 0.25 µl (10 U) of RNasin and 1 µl (200 U) of Superscript II reverse transcriptase (Gibco, Life Technologies, Paisley, UK). Samples were incubated at RT for 5 min, 60 min at 42 °C and 10 min at 50 °C. A further incubation at 70 °C for 15 min inactivated the reverse transcriptase. RNase H (1.5 U) was added and the samples incubated at

37 °C for 20 min to destroy the remaining RNA template. The reaction mix was diluted to a final volume of 500 µl in TE buffer, pH 7.5.

2.2.8.3 First Round Amplification of cDNA

3' RACE reaction (rapid amplification of cDNA ends) was performed on either poly A^+ mRNA (Oligotex Protocol, Qiagen, UK) or total RNA (TRIzol protocol, Gibco, Life Technologies, Paisley, UK) isolated from osteoblastic cell cultures. Reverse transcription was performed using Superscript II reverse transcriptase (Gibco, Life Technologies, Paisley, UK) and a hybrid oligo dT primer (R_o) containing 17 dTs followed by a 35 base oligonucleotide sequence containing the anchor primers R_o and R_I (Table 2.4). Following first strand synthesis, single stranded cDNA was used as a template for amplification of the VAMP1 transcript which was amplified using the gene specific primer VAMP1 5'a, located at the extreme N-terminal portion of the VAMP1 molecule and the external anchor primer R_o. A second gene specific primer VAM3', located further downstream of VAMP1 5'a, was used along with the internal anchor primer R_I to amplify the specific 3' cDNA product.

First round amplification: 5 µl of diluted single stranded cDNA product, 25 pmoles of the gene specific primer, VAMP1 5'a and the anchor primer R_o, in PCR reaction buffer with 2.5 U of Taq polymerase/50 µl reaction volume. PCR conditions were as follows; 98 °C for 5 min, 75 °C for 3 min, 54 °C for 2 min, 72 °C for 40 min followed by 94 °C for 1 min, 54 °C for 1 min, 72 °C for 3 min (30 cycles), 72 °C for 10 min. PCR reactions were carried out in a Perkin Elmer Cetus 480 DNA thermal cycler.

2.2.8.4 Second Round Amplification

Second round amplification, using nested primers R_I and the gene specific primer VAM3', was set up as described previously for first round amplification. PCR conditions were as follows: 98 °C for 5 min, 75 °C for 3 min, 54 °C for 2 min followed by 94 °C for 1 min, 54 °C for 1 min, 72 °C for 3 min (30 cycles), 72 °C for 10 min. The resulting PCR products were resolved by agarose gel electrophoresis (1.2 % TPE agarose gel), and the cDNA product size estimated by comparison with 100 bp DNA ladder or 1 kB plus DNA ladder (BioRad, UK). The resulting VAMP1 3' end cDNA transcript was purified using QIAquick gel extraction kit (Qiagen, UK) (section 2.2.9). Purified cDNA product was ligated into pGEM-T vector and transformed into competent *Escherichia coli* JM109 cells using the heat shock method (section 2.2.12.2). Following subcloning and plasmid purification the amplified VAMP1 cDNA transcripts were sequenced using ABI Prism Dye terminator sequencing (sections 2.2.13, 2.2.15 and 2.2.16).

2.2.9 DNA Purification from Agarose Gels

Amplified PCR products were resolved on a 1.5 % TPE agarose gel containing 50 µg of ethidium bromide, for 40 min at 80 V and visualised by UV (~ 365 nm). Bands were excised using a clean scalpel and PCR products purified from the gel using the QIAquick gel extraction kit (Qiagen, UK).

Briefly, the excised bands were weighed and the agarose melted by incubation at 50 °C for 10 min in 3 volumes of extraction buffer QG (assuming 100 mg to be ~ 100 µl). Buffer QG solubilises the agarose slice and optimises the conditions required for DNA binding to the silica membrane of the spin column. After solubilisation of the agarose gel slice, 1 volume of isopropanol was added and the

resulting DNA solution applied to the spin column and centrifuged at 13,000 rpm (16,060 g) for 1 min at 4 °C in a Heraeus Fresco Biofuge (Sorvall Heraeus, Kendro Laboratory Products, UK). To ensure complete removal of agarose the spin column was flushed with 0.5 ml of buffer QG, centrifuged for a further 1 min and subsequently washed with 0.75 ml of ethanol containing buffer PE. Following centrifugation, for 1 min in the first instance and a further 1 min to dry the column, the DNA was eluted using 30 µl buffer EB, allowed to stand for 1 min at RT and centrifuged at 13,000 rpm for 1 min. The concentration of the purified DNA product was estimated either using GeneQuant (Pharmacia) or by comparison with 500 ng of λ Hin*d*III digest (New England Biolabs, UK) resolved on a 1.5 % TPE agarose gel. DNA was stored at – 20 °C until required.

2.2.10 TA Cloning into Promega pGEM-T or pGEM-T Easy vectors

DNA obtained from gel purified PCR products were ligated into pGEM-T vector (Promega, UK). Assuming a 1:1 molar ratio of insert DNA to vector DNA, the amount of insert required was calculated as follows:

$$\frac{\text{ng Vector} \times \text{Kb size of Insert}}{\text{Kb size of vector}} = \text{ng Insert required}$$

50 ng of vector and variable amounts of insert (depending on insert size) were incubated with 1 Weiss U/µl of T_4 DNA ligase in ligase buffer. The 10 µl reaction was incubated at 16 °C O/N. The resulting ligated product was transformed into competent cells such as *E.coli* JM109 (as described in method 2.2.11) and transformants selected using IPTG/X-gal blue/white selection.

2.2.11 Transformation of Ligation Mix into *Escherischia coli* JM109 cells

The ligated DNA/vector product was transformed into competent *E.coli* cells using either high efficiency transformation by electroporation or alternatively the heat shock method.

2.2.11.1 High Efficiency Transformation by Electroporation

Electrocompetent *E.coli* JM109 cells were acquired from Promega, UK or stocks prepared as follows. 1 litre of LB broth was inoculated with 1:100 volume of an O/N culture and cells grown at 37 °C with vigorous shaking until they obtained an OD_{600nm} of 0.6 (mid log-phase). Flasks were chilled on ice and cells harvested by centrifugation in a cold rotor at 4000 g for 15 min. The resulting bacterial pellet was resuspended in 1 litre of ice cold water and centrifuged for a further 15 min. Pellets were washed in 500 ml of ice cold water. The resulting bacterial pellet was resuspended in 20 ml of ice cold 10 % glycerol and centrifugation steps repeated. Finally the cells were resuspended in 2 ml of ice cold 10 % glycerol aliquoted and stored at - 70 °C.

Prior to transformation, competent cells were thawed gently on ice. The following components were combined: 50 µl of electro-competent cells were added to 2 µl of ligation mix, mixed and left on ice for 1 min. The mixture was transferred to pre-chilled electroporation cuvettes. Electroporation apparatus (BioRad) settings: 2.5 kV, 25 µF and the pulse controller set to 200 Ω. After the pulse was applied (~ 4.4 msec) 1 ml of SOC medium was added to each sample and gently mixed. The samples were transferred to sterile tubes and incubated at 37 °C for 45 min with shaking prior to inoculation onto IPTG/X-gal treated LB/ampicillin (100 µg/ml)

agar plates. Plates were incubated O/N at 37 °C and transformants selected for by X-gal/IPTG (blue/white) selection (see section 2.2.11.3).

2.2.11.2 Transformation using Heat Shock

High efficiency competent *E.coli* JM109 cells (Promega) were thawed and 50 µl added to 2 µl of the PCR product/Vector ligation. Samples were incubated on ice for 20 min, then 45 sec at 42 °C and incubated on ice for a further 2 min. 1 ml of SOC medium was added to each transformation sample and mixed. Cells were incubated at 37 °C for 1 h with shaking and then plated onto X-gal/IPTG treated LB/ampicillin agar plates (100 µg/ml). Plates were incubated O/N at 37 °C and transformants selected using X-gal/IPTG (blue/white) selection.

2.2.11.3 X-gal/IPTG (blue/white) Selection

Both pGEM-T and p-GEM-T Easy vectors (Promega, UK) carry a short segment of *E.coli* DNA that contains the regulatory sequence and coding sequence for the first 146 amino acids of the β-galactosidase gene (*lac* Z) (fig. 2.3). The polycloning site is embedded within this coding region. The presence of the multiple cloning site within the lac Z coding region does not however, affect the reading frame and thus an enzymatically active β-galactosidase protein can be formed. Lac^+ bacteria can be easily identified because they form blue colonies in the presence of X-gal. Insertion of foreign DNA into this site however, disrupts this gene preventing β-galactosidase synthesis. Therefore bacteria containing the recombinant plasmids form white colonies.

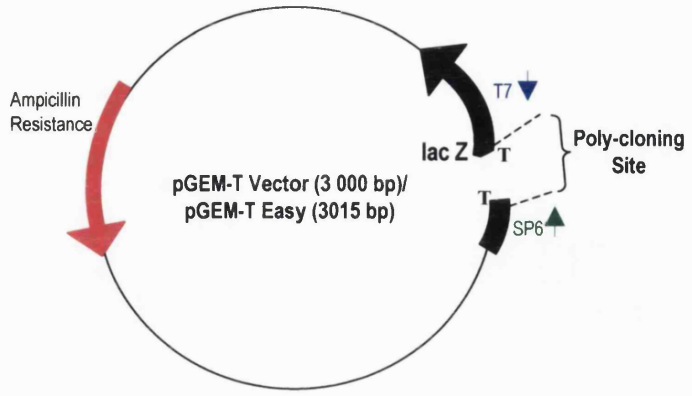

pGEM-T Vector

T7 Transcription Start

```
5'...TGTAA TACGA CTCAC TATAG GGCGA ATTGG GCCCG ACGTC GCATG CTCCC GGCCG
3'..ACATT ATGCT GAGTG ATATC CCGCT TAACC CGGGC TGCAG CGTAC GAGGG CCGGC
```

T7 Promoter Apa I

```
CCATG GCCGC GGGATT (INSERT) ATCAC TAGTG CGGCC GCCTG CAGGT CGACC ATATG
GGTAC CGGCG CCCTA    TTAGTG ATCAC GCCGG CGGAC GTCCA GCTGG TATAC
```

Spe I SP6 Transcription Start

```
GGAGA GCTCC CAACG CGTTG GATGC ATAGC TTGAG TATTC TATAG TGTCA CCTAA AT...3'
CCTCT CGAGG GTTGC GCAAC CTACG TATCG AACTC ATAAG ATATC ACAGT GGATT TA...5'
```

SP6 Promoter

pGEM-T-Easy Vector

T7 Transcription Start

```
5'...TGTAA TACGA CTCAC TATAG GGCGA ATTGG GCCCG ACGTC GCATG CTCCC GGCCG CCATG
3'..ACATT ATGCT GAGTG ATATC CCGCT TAACC CGGGC TGCAG CGTAC GAGGG CCGGC GGTAC
```

T7 Promoter

```
GCGGC CGCGG GAATT CGATT (INSERT) ATCAC TAGTG AATTC GCGGC CGCCT GCAGG TCGAC
CGCCG GCGCC CTTAA GCTA    TTAGTG ATCAC TTAAG CGCCG GCGGA CGTCC AGCTG
```

EcoR I EcoR I SP6 Transcription Start

```
CATAT GGGA GAGCT CCCAA CGCGT TGGAT GCATA GCTTG AGTAT TCTAT AGTGT CACCT AAAT...3'
GTATA CCCT CTCGA GGGTT GCGCA ACCTA CGTAT GGAAC TCATA AGATA TCACA GTGGA TTTA...5'
```

SP6 Promoter

Figure 2.3 p-GEM-T and p-GEM-T easy Cloning Vectors.

pGEM-T and pGEM-T easy cloning vectors contain specific restriction enzyme sites located in the multiple cloning site regions flanking the cloned insert. Digestion results in the linearisation of the vector and the release of the intact insert. The T7 and Sp6 promoter regions are also located within these flanking regions.

LB/ampicillin (100 µg/ml) agar plates were treated with 40 µl of X-gal solution (20 mg/ml) and 4 µl of IPTG solution (200 mg/ml). The X-gal and IPTG solutions were spread over the surface of the plates and the plates dried at 37 °C. Following inoculation with the transformation culture, the agar plates were incubated at 37 °C O/N. Subsequently, plates were removed from the incubator and stored at 4 °C to facilitate blue/white screening.

2.2.12 Isolation of Recombinant Plasmids

A single bacterial colony was inoculated into 5 ml of LB/ampicillin broth and grown to saturation overnight at 37 °C with vigorous shaking. 2 ml of bacterial cells were harvested by centrifugation at 5,000 rpm for 2 min at 4 °C in a benchtop centrifuge. The resulting bacterial cell pellet was resuspended in 250 µl of buffer P1 (Qiagen QIAprep, miniprep, protocol), and lysed with an equal volume of cell lysis buffer (P2) and mixed gently. The addition of 350 µl of buffer N3 neutralised the reaction and the reactants were centrifuged at 13,000 rpm for 10 min. The supernatants were collected and applied to the spin columns. Following an initial centrifugation for 1 min at 13,000 rpm, 4 °C, columns containing bound plasmid DNA were washed sequentially with 0.5 ml buffer PB, 0.75 ml of PE buffer and centrifuged for 1 min at 13,000 rpm, 4 °C. Following a final 1 min centrifuge to dry the column, plasmid DNA was eluted in 50 µl of EB elution buffer.

2.2.12.1 Restriction Endonuclease Digestion

Subcloned transformants were assessed for the presence of insert using restriction enzyme digestion. pGEM-T and pGEM-T easy vectors (Promega, UK) contain

multiple cloning sites with unique restriction sites (fig. 2.3). Therefore, samples were either digested with EcoRI (pGEM-T easy) or with NcoI and ApaI (pGEM-T). These enzymes each have specific restriction sites located on the plasmid regions flanking the cloned insert (fig. 2.3). Restriction digests were carried out in a total reaction volume of 10 µl under the standard conditions: 2.5 µl of purified plasmid DNA, 1 µl of the appropriate 10x reaction buffer (New England Biolabs, UK or Promega, UK), 1 µl (~10 U) of each restriction endonuclease and samples incubated at 37 °C for 1 h. Digestion products were resolved on a 1.5 % TPE agarose gel (~45 min at 80 V). The approximate molecular weights of the bands were estimated by comparison with 100 bp or 1kB DNA plus ladder (BioRad, UK).

2.2.13 Glycerol Stocks

A single bacterial colony was inoculated into 5 ml of LB broth containing 100 µg/ml ampicillin and grown O/N at 37 °C with vigorous shaking. An 850 µl aliquot of the bacterial suspension was placed into a 1 ml cryo-vial (Nunc, Gibco, Life Technologies, Paisley, UK) along with 150 µl of sterile glycerol (pre-chilled on ice). Samples were vortexed, immediately snap frozen in liquid nitrogen and subsequently transferred to –80 °C for long term storage.

2.2.14 Sequencing

Sequencing was performed using the ABI PRISM dye-terminator cycle sequencing ready reaction kit (Perkin Elmer, UK). This dye-terminator sequencing method utilises four dideoxynucleoside triphosphates (ddATP, ddTTP, ddCTP and ddGTP), each tagged with a different fluorescent dye thus the growing chain of DNA is simultaneously terminated and labelled with the dye corresponding to the

terminating base. Dideoxynucleosides triphosphates resemble deoxynucleoside triphosphates (dNTPs) except that they lack a 3'-OH group. They can add to a growing chain during polymerisation, but they cannot be added onto and therefore serve as chain terminators.

2.2.14.1 PCR Cycling and DNA Precipitation

Recombinant plasmids were sequenced using the Perkin Elmer ABI PRISM dye terminator cycle sequencing ready reaction kit. Double stranded plasmid DNA (ds DNA) was prepared as described in section 2.2.13. Approximately 1 µl (~ 1 µg) of ds DNA template was added to 3.2 pmol of sequencing primers either T7 or Sp6 (see fig. 2.3 for the forward and reverse primer sequences). In addition 8 µl of pre-prepared sequence mix (ddATP, ddCTP, ddGTP, ddTTP dye terminators in Tris pH 9, $MgCl_2$, thermal stable pyrophosphatase and AmpliTaq DNA polymerase, FS (Fast sequencing, Perkin Elmer, UK), giving a final reaction volume of 20 µl.

The cycling conditions were as follows: 96 °C for 30 sec, 50 °C for 15 sec, 60 °C for 4 min (x 25 cycles) followed by a final 4 °C soak cycle.

2.2.14.2 Purification of PCR Extension Products

Dye terminators were removed by ethanol precipitation. Using the entire PCR cycling product (20 µl), DNA was precipitated as follows by adding 2 µl of 3 M sodium acetate pH 4.6 and 50 µl of 95 % ethanol. Samples were vortexed, placed on ice for 10 min and precipitated DNA collected by centrifugation at 13,000 rpm, 4 °C for 30 min. The ethanol solution was aspirated and the DNA pellet washed in 70 %

ethanol (13,000 rpm, 4 °C for 15 min). Finally the pellet was dried in a vacuum centrifuge and samples resuspended and loaded onto a sequencing gel.

2.2.15 Sequence Analysis

Sequence analysis was performed using EditView and Sequence Navigator analysis packages (ABI PRISM, Perkin Elmer). The sequences obtained were compared to existing cDNA sequences in the database using the BLAST (basic local alignment search tool) search tool.

2.2.16 Histochemical Staining

2.2.16.1 Alkaline Phosphatase Staining

Alkaline phosphatase expression was determined in osteoblastic cell lines and in primary nodule forming cells at a variety of time points during the nodule formation and mineralisation process (between days 3-22). Cells were either fixed in neutral formalin buffer (10 % formalin, 113 mM Na_2HPO_4, 29 mM $NaH_2PO_4.H_2O$ in water) on ice for 15 min or at RT for 5 min in 4 % paraformaldehyde. Cells were incubated for 45 min at RT with alkaline phosphatase staining solution (see section 2.1.2). Napthol AS-MX phosphate acts as a substrate for alkaline phosphatase; as a result of phosphatase activity Napthol AS-MX is released and reacts with the fast red TR salt, forming an insoluble pink precipitate at sites of phosphatase activity.

2.2.15.2 von Kossa Staining for Mineral deposits

von Kossa staining was used to demonstrate the extent of mineralisation in nodule forming and mineralising primary osteoblastic-cell cultures (2.2.1.2). Cells were initially stained for alkaline phosphatase activity as described above. Alkaline

phosphatase positive cultures were washed in distilled water and stained with 2.5 % silver nitrate solution for 30 min at RT in the dark. Post incubation, cells were exposed to daylight and subsequently, washed in distilled water to remove any remaining silver nitrate. Stained cell cultures were washed in tap water for 1 h rinsed and air dried. Mineral appears dark brown/black due to deposition of silver grains.

2.2.16.3 van Gieson Stain for Collagen

Cells were incubated with van Gieson staining solution for 3 min at RT. Van Gieson solution was removed and cells dehydrated through sequential washes with ethanol (70 %, 95 %, and 100 %), for approximately 30 sec each. Collagen stains red.

2.2.17 Immunohistochemistry

2.2.17.1 Preparation of Frozen Sections

Calvaria were dissected from either 3 day old Sprague Dawley rat pups or day 21 embryonic rats (Wistar strain). Samples of embryonic rat calvaria, with skin and brain intact, were dissected and stored at -80 °C until required. Femurs were also dissected, with skin and muscle intact, and embedded in OCT (orthochlorotoluene) embedding medium (BDH, UK). OCT embedded samples were frozen on dry ice and transferred to liquid nitrogen.

Calvaria and femur sections were collected on electrostatically charged superfrost microscope slides (BDH, UK) and kept at a constant temperature of -20 °C throughout the process. Serial sections of 7 μm were collected on a Cryostat (Bright

Instruments, UK). Sections were analysed using both histochemical staining and immunohistochemistry.

2.2.17.2 Histochemical staining of Calvarial/Femur sections

Sections were thawed very briefly at RT, so as not to dry them and immediately fixed in 4 % PFA at 4 °C for 20 min. Subsequently, sections were washed 1x in PBS followed by 3x in distilled water. Alkaline phosphatase staining was carried out as previously described in section 2.2.17.1. Following Alkaline phosphatase staining sections were stained briefly with a 1 in 5 dilution of hematoxylin (Sigma, UK), sections were carefully rinsed 3x in dH_2O and dried at RT. Tissue sections were mounted in immunomount (Shandon, Pittsburgh, USA) and allowed to dry O/N.

2.2.17.3 Immunohistochemical Staining

Unfixed tissue sections were thawed and fixed for 5 min at RT in 3.7 % formaldehyde. Following serial washing steps in PBS (3x 5 min), sections were permeabilised in methanol, 5 min at – 20 °C, washed in PBS and incubated for 60 min at RT in BSA blocking buffer (containing 3 % BSA in PBS). BSA blocking buffer was denatured at 80 °C for 2 min and filtered prior to use. Primary antibodies (tables 2.2, 2.3 and 2.4) were diluted in 3 % BSA/PBS and tissue sections incubated with the appropriate antibody for 45 min at 37 °C. Tissue sections were subsequently washed in PBS (3x 5 min washes at RT). Secondary antibodies were diluted 1:40 into 3 % BSA/PBS and tissue sections incubated with the antibody for 30 min at 37 °C. Following three final washing steps in PBS (5 min each), immunostained tissue sections were mounted in immunomount (Shandon, Pittsburgh, USA) and immuno-reactivity visualised by either confocal laser scanning microscopy or fluorescent microscopy using a Zeiss microscope.

Chapter 3

PRIMARY OSTEOBLAST-LIKE CELL CULTURE

Chapter 3

PRIMARY OSTEOBLAST-LIKE CELL CULTURE

3.1 Aim

The aim of this part of the thesis was to isolate an enriched population of osteoblast-like cells, expressing the mature osteoblastic phenotype, and to subsequently stimulate these cells to first form nodules and then to mineralise these nodular structures *in vitro*. This would be used as a 'functional' osteoblastic model of mineralisation for later studies. In addition, these studies optimised nodule formation and mineralisation in the murine osteoblastic cell line, MC3T3-E1, establishing them as a more readily available model of *in vitro* mineralisation.

3.2 Introduction

3.2.1 Osteoblasts

Osteoblasts are the cells present on the bone surface at sites of bone matrix deposition and are responsible for bone formation. Osteoblasts are post-proliferative, cuboidal cells and are identified by their ability to express high levels of tissue non-specific alkaline phosphatase along with a number of osteoblast phenotype-specific phenotype markers (see Chapter 1, table 1.1).

Cells of the osteoblast lineage are derived from multi-potential mesenchymal stem cells. Progenitor cell populations, present in the isolated cell population, have the potential to progress along a number of pathways, namely the adipogenic (Beresford *et al.*, 1992), fibroblastic or myoblastic pathways (Grigoriadis *et al.*, 1988).

The proportion of each of these cell types within an isolated cell population, together with the selective culture conditions used, determines the number of osteoblastic colonies, and hence the number of nodules, formed in culture.

3.2.2 Biochemical Markers

Osteoblast differentiation and cell lineage studies have led to the identification of a number of osteoblastic cell phenotype markers, such as tissue non-specific alkaline phosphatase, type I collagen, osteopontin and osteocalcin expression. These markers are used to define cells expressing the mature osteoblastic phenotype and are expressed at different stages of osteoblast development (see Chapter 1, table 1.1). Although alkaline phosphatase expression is not bone specific, it is used as an indicator for osteoblastic differentiation. An increase in alkaline phosphatase expression is thought to indicate a shift in an osteoblastic population towards a more differentiated state. Additionally, the synthesis of bone matrix proteins is used to identify the different stages of osteoblast differentiation. 90 % of synthesised bone matrix comprises collagen (predominantly type I), whilst the other 10 % is formed from a range of non-collagenous protein components including osteocalcin, BSP, osteopontin, osteonectin, fibronectin, thrombospondin and small proteoglycans such as decorin and biglycan.

Previous studies have shown the expression of such phenotypic markers varies depending on the stage of osteoblast differentiation. At early stages of osteoblast differentiation, cells express types III and V collagen in addition to type I collagen and fibronectin. These cells, however, do not express osteocalcin or BSP. When pre-osteoblasts are differentiating into mature osteoblasts, they express increasing amounts of alkaline phosphatase, type I collagen and osteopontin, followed by the

synthesis of other bone matrix proteins such as BSP. Osteocalcin is expressed very late in the osteoblast development and is currently used as a terminal differentiation marker, as its expression coincides with the onset of mineralisation.

3.2.3 Osteoblast-Like Cell Cultures – An *in vitro* model of Mineralisation

As discussed previously, section 1.6.3, primary osteoblast-like cell cultures isolated from either embryonic rat calvaria, rat bone marrow or explant cultures can be stimulated with L-ascorbate (Asc), β-glycerophosphate (β-GP) and dexamethasone (dex) to mineralise *in vitro*, thus providing an *in vitro* model of mineralisation.

3.3 Results

3.3.1 Osteoblast-like cells in Long Term Nodule Culture

As discussed previously (Chapter 1, section 1.6.3), primary osteoblast-like cell cultures are commonly used *in vitro* as cellular models of nodule formation and mineralisation. Cells isolated from embryonic rat calvaria provide a source of cells that express predominately the osteoblastic phenotype. In isolated cell populations, cultured under the conditions described in sections 2.2.1.1 and 2.2.1.2, cell proliferation occurs between days 0 to 5 (day 0 is the day on which the cells are harvested and plated). Typically, cells at day 3 are in the proliferative phase while cells at day 6 of culture have taken on the cubodial morphology of confluent osteoblast-like cells (figs. 3.1 A and B). In some areas cells have started to condense, initiating the formation of a nodular structure (fig. 3.1 B). However, three-dimensional nodular structures were not obvious until day 9 (fig. 3.1 C).

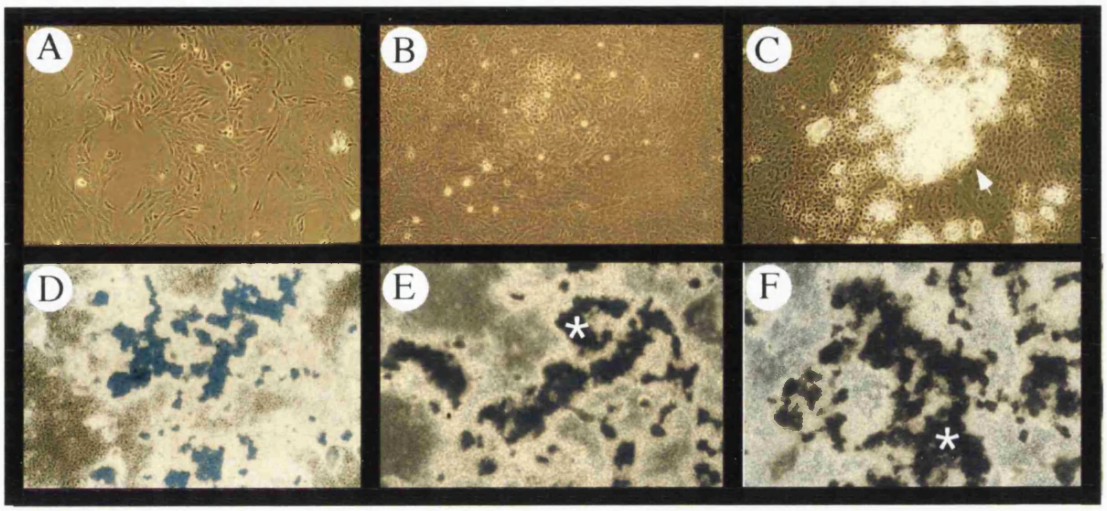

Figure 3.1 Primary Osteoblast-like Cells in Culture.

A-F show primary osteoblast-like cells at various stages throughout nodule formation and mineralisation process. A and B, days 3 and 6 cells are in the proliferative phase and cells that have become confluent with a cubodial morphology. C, day 9 cells have condensed and started to form nodules (shown by the white arrow). By day 15, D, some nodules are mineralised. Mineral deposits (as indicated by *) are more numerous in these cultures around days 19 and 22 (E and F).

Mineralisation of the matrix was first detected at day 15 (fig. 3.1 D) and increased progressively during the culture period. Heavy mineralisation of these cultures was observed by day 22 (fig. 3.1 F).

Cells in the monolayer part of the culture are confluent and retain their cubodial morphology, whilst cells at the base of the nodule form multilayers. Mineral deposits are detected as dark opaque structures sitting directly on the top of the nodules (see figure 3.2). Characterisation of nodular structures by Bharagava *et al.* (1988) has shown these structures to resemble woven bone.

3.3.2 Characterisation of Primary Osteoblast-like Cell Cultures

Alkaline phosphatase expression, a key marker for the osteoblastic phenotype, was used to assess the osteoblast-like component of primary cells isolated from embryonic rat calvaria and to determine the optimal conditions required for nodule formation and mineralisation. As described previously, sequential digestion of rat calvaria releases an osteoblast enriched but heterogeneous population of cells. Cells can be driven along the osteoblast lineage upon treatment with Asc, β-GP and dex.

Alkaline phosphatase expression was determined using the histochemical staining method described in section 2.2.16.1, on cell cultures at different stages of nodule formation and mineralisation (see figure 3.3).

A-F represent cells taken from days 3, 6, 9, 15, 19, and 22 of primary nodule forming cultures. Alkaline phosphatase expression increases between the proliferative

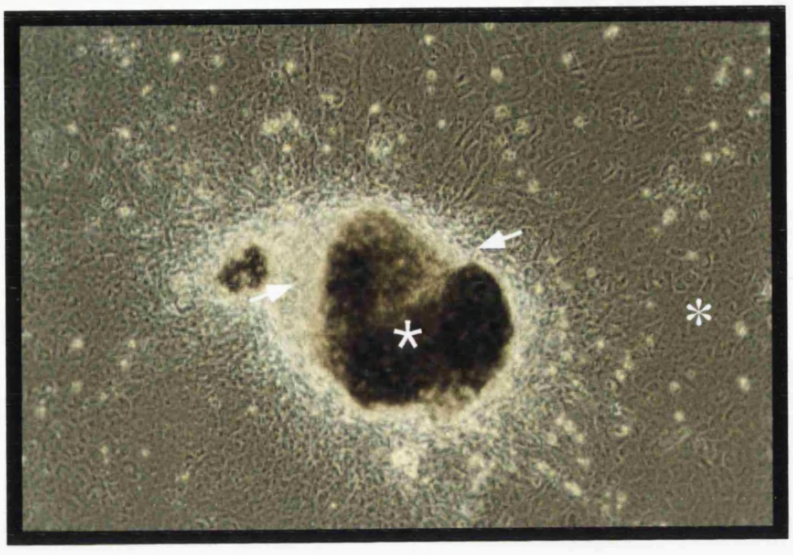

Figure 3.2 Mineralised Nodule.

Mineralised nodules were formed by cells isolated from day 21 embryonic rat calvaria and cultured for 22 days, in the presence of Asc, β-GP and dex. Cells in the monolayer appear cuboidal (*) while cells located towards the base of the nodule were condensed into multilayers (→). Mineral deposits are seen on the top of the nodule structures (*).

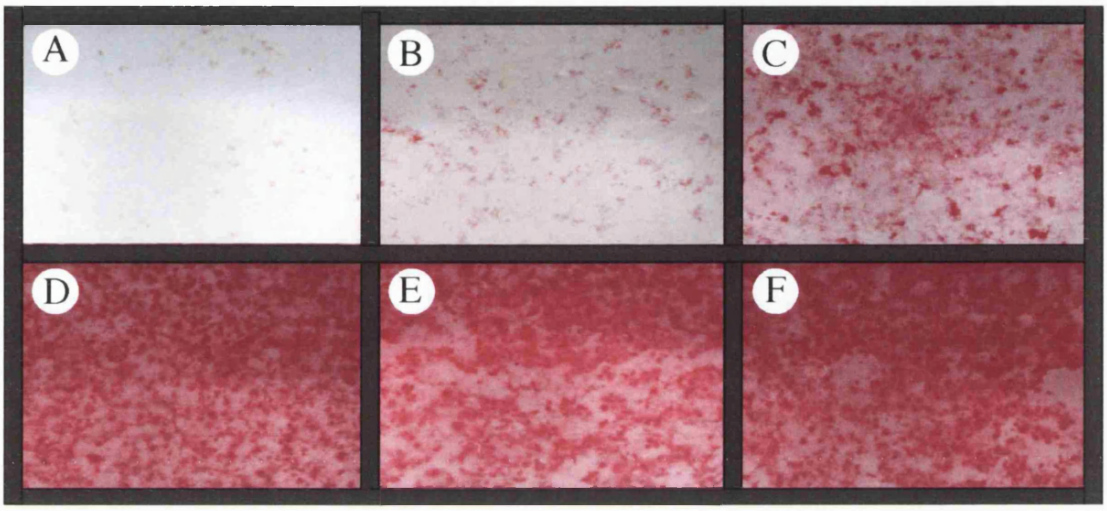

Figure 3.3 Alkaline Phosphatase expression in Primary Nodule forming Osteoblast-like cell culture. A to F, represent days 3, 6, 9, 15, 19 and 22 of a nodule forming and mineralising culture. Alkaline phosphatase expression increased between the proliferative phase (days 3 to 6, A and B) and the differentiation stage (day 9, C) and was maintained at high expression levels throughout the remainder of the culture time course, indicating that these cells are predominately osteoblastic in phenotype.

stage, days 3 to 6 (fig. 3.3 A and B), and the differentiation stage, day 9 onwards (fig. 3.3 C). Alkaline phosphatase expression is maintained at these levels throughout the mineralisation stage days 15 through to day 22 (fig. 3.3 D to F). These results are in accordance with data published by Bellows *et al.* (1986) and suggest that these isolated cells are predominately osteoblastic in phenotype. Treatment of cultures with Asc during the logarithmic growth phase increases cell proliferation and the expression of osteoblast associated protein markers such as alkaline phosphatase and osteocalcin in post confluent cells (Bellows *et al.*, 1987).

3.3.3 Optimisation of Nodule formation in Primary Osteoblast-Like cell culture

Bellows and co-workers have demonstrated that dex, a synthetic glucocorticoid, has a stimulatory effect on *in vitro* nodule formation and mineralisation in rat derived primary osteoblast cultures. In addition, they have previously shown that concentrations of 10^{-8} M dex are comparable to physiological concentrations of naturally occurring glucocorticoids such as cortisol. Primary cell cultures vary from preparation to preparation, and here I have attempted to optimise nodule formation and mineralisation in rat derived osteoblast-like cell cultures by optimising the culture conditions required. Throughout this part of the study alkaline phosphatase expression is used as a marker for the mature osteoblastic phenotype.

3.3.3.1 The Effect of Dexamethasone on Alkaline Phosphatase in Osteoblasts

Alkaline phosphatase expression was assessed at different times during primary osteoblast-like cell culture. Keeping the cell plating density constant, i.e. at $3x10^4$ cells per 35 mm well of a 6 well tissue culture plate, cells were cultured in the

presence of Asc, β-GP and under a range of dex concentrations, ranging from 10^{-5} M to 10^{-10} M.

As a control, a population of cells were cultured in the absence of dex. Alkaline phosphatase expression was assessed histochemically at different time points throughout these cultures. Using the NIH Image programme, a value for the intensity of alkaline phosphatase staining was obtained. A mean for each sample set (n=3) was calculated and the significance of the results was determined using Anova, see graph 3.1.

Graph 3.1, demonstrates a dose dependent effect of dex on alkaline phosphatase expression. Decreased expression of alkaline phosphatase was observed in cell cultures exposed to concentrations of dex higher than 10^{-8} M. There was little effect observed on cells cultured in the presence of dex at concentrations lower than 10^{-8} M dex, suggesting that alkaline phosphatase protein expression levels are optimal at these concentrations.

Subsequent experiments were performed in the presence of 10^{-8} M dex, since nodule formation increased in dex treated cultures, as compared to those untreated. In addition, a concentration of 10^{-8} M dex is comparable with previously published results and reflects the physiological concentration of naturally occurring glucocortiocoids (Bellows *et al.*, 1987; Bellows *et al.*, 1986).

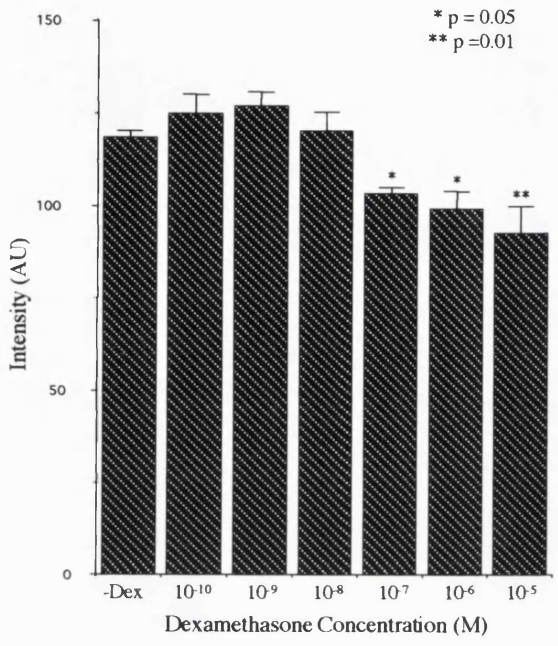

Graph 3.1 Effect of Dexamethasone Concentration on Alkaline Phosphatase Expression. Cells were plated at a density of $3x10^4$ cells per 35 mm well and cultured in the presence of Asc, β-GP and a variety of dex concentrations. Alkaline phosphatase expression decreased significantly at concentrations higher than 10^{-8} M dex, compared to the – dex control cultures. Alkaline phosphatase expression in these cultures is optimal for dex concentrations between 10^{-10} M and 10^{-8} M.

3.3.3.2 The Effect of Cell Plating Density on Alkaline Phosphatase Expression

Alkaline phosphatase expression and nodule formation have previously been shown to depend on the initial cell plating density (Bellows and Aubin, 1989). To optimise nodule formation and mineralisation in primary osteoblast-like cell cultures, the effect of cell plating density on alkaline phosphatase expression was investigated.

Using a variety of plating densities (500, $1x10^3$, $1x10^4$, $2x10^4$, $3x10^4$ and $4x10^4$), cells were plated and cultured in the presence of Asc, β-GP and in the presence or absence of 10^{-8} M dex (as determined above). The intensity of alkaline phosphatase was measured as described above, with n=3, (graph 3.2).

Alkaline phosphatase expression on day 22 of the culture was lower in cultures initially plated at lower cell densities (500 or 1000 cells per 35 mm well). At low cell numbers, the proliferative phase is prolonged and as a result cells take longer to reach confluence and thus nodule formation and mineralisation is delayed in these cultures. At the higher plating densities of $1x10^4$ to $4x10^4$ cells per 35 mm well, alkaline phosphastase expression increased with little difference detected in the intensity of alkaline phosphatase staining between these cultures. Dex treatment had little or no effect on the alkaline phosphatase expression levels of cell plated at high cell density, indicating that dex has no effect on the proliferative capacity of these cells nor on their progression along the osteoblast lineage. Cultures treated with or without dex do, however, follow a similar trend, suggesting that a minimum cell plating density of $1x10^4$ cells per 35 mm well is required to optimise alkaline phosphatase expression and thus the osteoblastic content and nodule forming abilities of these cultures. Although a cell plating density of $4x10^4$ cells per 35 mm has a similar effect on alkaline phosphatase expression, subsequent cultures

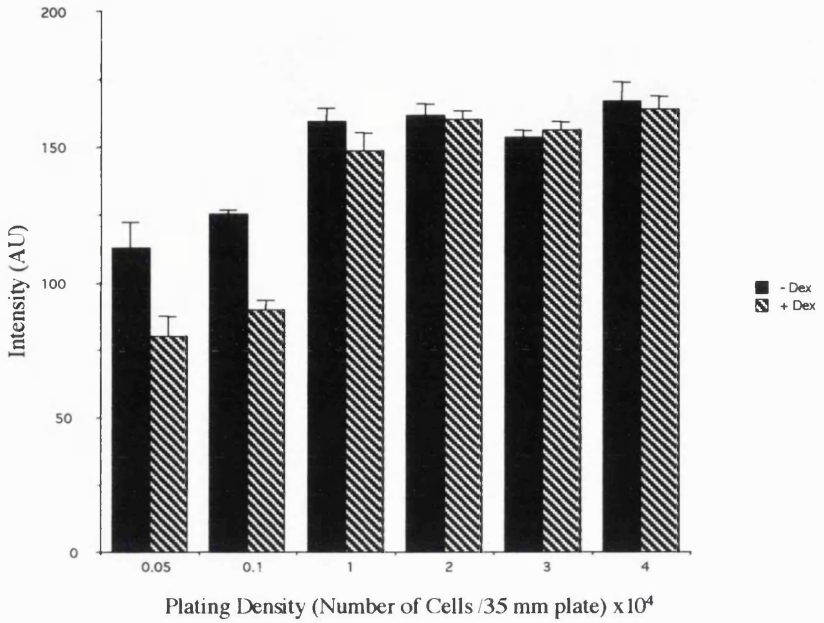

Graph 3.2 Effect of Cell Plating Density On Alkaline Phosphatase Expression.

Cells were cultured for 22 days in the presence of Asc, β-GP, + or - 10^{-8} M dex. Alkaline phosphatase expression was lower in cells plated at the very low cell densities of 500 or 1000 cells per 35 mm well, whilst a 1.5 fold increase in alkaline phosphatase expression was observed in cells plated at densities above $1x10^4$ cells per 35 mm well. Cells treated without dex follow a similar trend, suggesting that a plating density between $1x10^4$ and $3x10^4$ is required to give optimal alkaline phosphatase expression in these cells.

were plated at $3x10^4$ cells per 35 mm, maximising the number of experiments that could be carried out from an isolated cell population whilst providing results comparable with published data.

3.3.3.3 Alkaline Phosphatase Expression in Nodule Forming Cell Cultures

Cells were cultured under the conditions optimised above, sections 3.3.3.1 and 3.3.3.2, and alkaline phosphatase expression assessed at a variety of time points over the duration of the culture, in an attempt to determine the culture duration required for optimal nodule formation and mineralisation.

Cells were cultured for 22 days and alkaline phosphatase expression determined at days 3, 6, 9, 16, 19 and 22 of nodule forming culture. Samples with cells cultured in the absence of dex were used as a control (graph 3.3).

These results demonstrate that culture duration has a direct effect on alkaline phosphatase expression. In the earlier stages of culture, the proliferative phase days 3-9, alkaline phosphatase expression increased in a linear fashion. By days 16 to 22 alkaline phosphatase expression had reached its maximum and levelled off. Control cultures, cultured in the absence of dex, follow a similar trend, suggesting that a culture duration of at least 19 days is required for maximum alkaline phosphatase expression.

The ability of cells to express alkaline phosphatase, a marker for the mature osteoblastic phenotype, determines the osteoblastic content of these isolated cell populations. However, alkaline phosphatase expression does not assess the ability of these cells to deposit matrix proteins. Therefore, van Gieson staining was

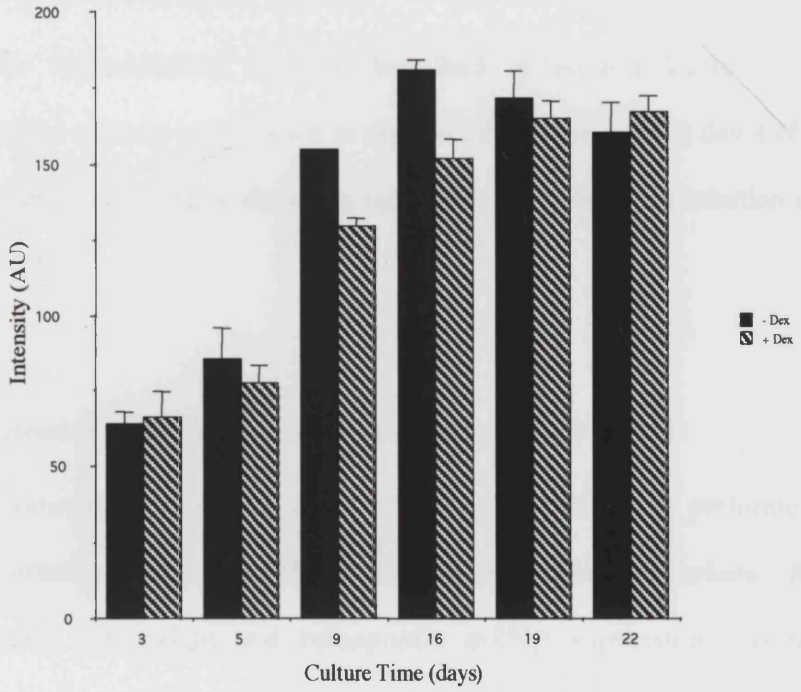

Graph 3.3 Alkaline Phosphatase Expression During Nodule Formation and Mineralisation. Cells were cultured using the optimised conditions of 10^{-8} M dex and a cell plating density of $3x10^4$ cells/35 mm well. Alkaline phosphatase expression increased during the proliferative and initial differentiation phases, between days 3 to 16, and levelled off towards the terminal mineralisation stage at days 19-22.

performed and used to assess the ability of these cells to deposit a collagenous matrix.

3.3.4 van Gieson Staining for Collagen

Using the histochemical method described in section 2.2.16.3, primary osteoblast-like cultures were shown to express collagen as early as day 4 of nodule forming cultures. Collagen, shown in red, had a cytoplasmic distribution in these cells, (fig. 3.4).

3.3.5 Expression of Osteoblast Phenotype Markers using RT-PCR

Reverse Transcription-Polymerase Chain Reaction (RT-PCR) was performed using primers directed against a number of osteoblast phenotypic markers. Alkaline phosphatase, osteocalcin and osteopontin mRNA expression was used to demonstrate that primary cells, isolated from day 21 embryonic rat calvaria and cultured in the presence of Asc and dex, exhibit the phenotypic characteristics associated with the mature osteoblast (see fig. 3.5).

β-GP was not used in these cultures because the deposition of mineral in these cultures, especially towards the final time point of day 22 when the cultures become heavily mineralised, made it difficult to extract RNA efficiently. Total RNA was isolated from cells at day 4, 7, 12, 17 and 20 of nodule forming culture and cDNA synthesised using superscript II RTase.

Similar to results discussed previously for alkaline phosphatase staining, RT-PCR revealed an increase in alkaline phosphatase mRNA levels during the proliferative and differentiation phases (days 4 to 12). Osteocalcin mRNA was not detected at

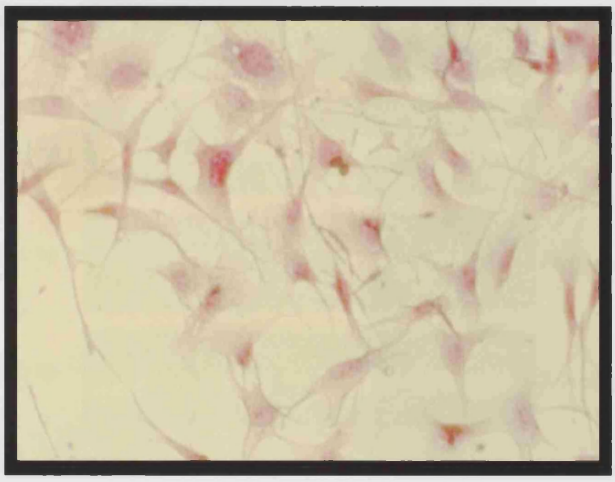

Figure 3.4 Van Gieson Staining for Collagen in Primary Osteoblastic cells.

Collagen expression was detected as early as day 4 in primary nodule forming cell cultures, cultured in the presence of Asc and dex. Collagen staining, shown in red, has a cytoplasmic distribution in these cells.

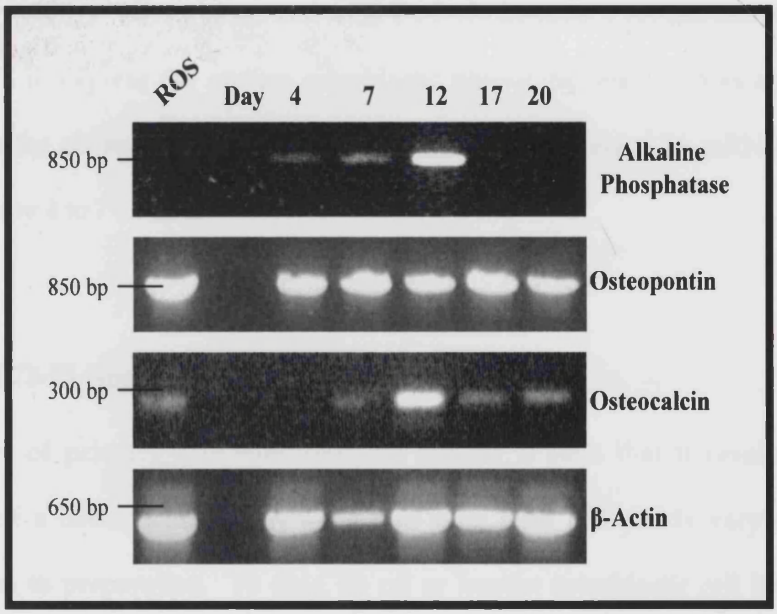

Figure 3.5 mRNA Expression of Osteoblast Phenotype Markers using RT-PCR.

mRNA levels of key osteoblastic markers, osteopontin, alkaline phosphatase and osteocalcin were determined in primary osteoblast-like cells from nodule forming cultures using RT-PCR. cDNA was synthesised from RNA harvested from days 4, 7, 12, 17 and 20 of nodule forming cultures. ROS 17/2.8 cell cDNA was used as a positive control for cells expressing a mature osteoblastic phenotype.

day 4 of these cultures but was expressed throughout the differentiation and condensation phases of these cultures (days 7, 12, 17 and 20). Osteopontin mRNA levels remained constant throughout the time course, from day 4 onwards, as did β-actin mRNA levels. (β-Actin was used as control for the PCR conditions used and the cDNA quality). cDNA generated from ROS 17/2.8 cells, a rat osteosarcoma cell line known to express the mature osteoblastic phenotype, was used as a positive control for the expression of osteoblastic markers and expressed an mRNA profile similar to day 4 to 7 cultures.

3.3.6 MC3T3-E1 Nodule Forming Cell Cultures

The nature of primary osteoblast-like cell culture is such that it results in the isolation of a heterogeneous population of cells with cell yields varying from preparation to preparation. To date, no rat or human osteoblastic cell lines have been identified with the ability to form and mineralise nodules *in vitro*. The rat osteosarcoma cell line, ROS 17/2.8, expresses a mature osteoblastic phenotype at both the mRNA and protein level. Furthermore, these cells have the ability to deposit a collagenous matrix *in vitro*; however, these cells are unable to mineralise this matrix. MC3T3-E1, a cell line derived from murine calvarial cells, is the only cell line identified to date that has the ability to form and mineralise nodules *in vitro*. Cultures of MC3T3-E1 resulting in nodule formation and mineralisation were established, providing a readily available and comparative model of *in vitro* nodule formation and mineralisation. Whilst the conditions required for MC3T3-E1 nodule forming and mineralising cell cultures have been well established (Chung *et al.*, 1992; Franceschi *et al.*, 1994; Quarles *et al.*, 1992; Sudo *et al.*, 1983), these studies allowed us to optimise MC3T3-E1 cell culture, nodule formation and mineralisation in our hands.

Similar to primary osteoblast-like cells isolated from day 21 embryonic rat calvaria, MC3T3-E1 cells show a time dependent and sequential expression of osteoblastic characteristics. Glucocorticoids such as dex have been shown to have little or no effect on nodule formation and mineralisation in these cells. MC3T3-E1 cells, described as being immature osteoblasts, require treatment with Asc and β-GP to stimulate osteoblast differentiation. ROS cells were used as a control for cells expressing the mature osteoblastic phenotype.

3.3.6.1 MC3T3 Nodule Formation

MC3T3 cells were plated at a cell density of $3x10^4$ cells per 35 mm well and cultured under the standard conditions required for nodule formation and mineralisation, i.e. in the presence of Asc and β-GP for 25 days.

Cell proliferation occurs between day 0 and 6 in these cultures, but varies depending on the cell plating density used. Day 0 samples are taken from cells passaged and plated at the same time as cells used for nodule culture, but which were allowed to grow to confluence under standard culture conditions, i.e. without additions. Typically, cells at days 0 to 6 (figs. 3.6 A and B) were in the proliferation phase, while at days 10 to 15 cells had started to condense at sites of nodule formation (figs. 3.6 C and D). It was not until days 20 to 25 (figs. 3.6 E and F), however, that mineralisation was detected in these cultures. The number of nodules observed in MC3T3-E1 cell cultures were less numerous than those detected in rat calvaria derived osteoblast-like cell cultures, RCOBs. In addition, mineralisation of nodules formed by MC3T3 cells occurred quite late on in the time course (fig. 3.6), at days 20 to 25. At day 25 (fig. 3.6 F), some of these nodules were mineralised, mineral deposits being indicated (*).

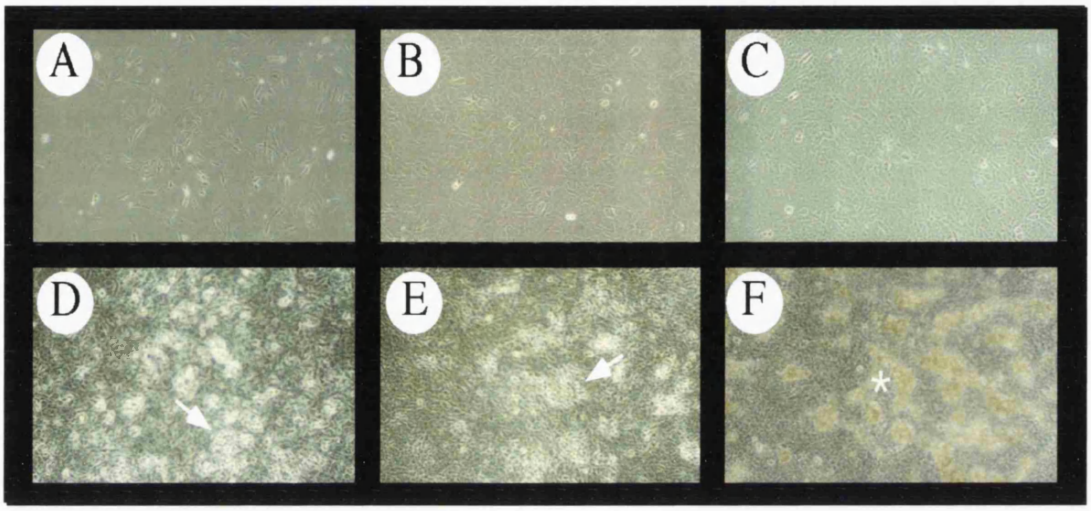

Figure 3.6 MC3T3-E1 Cells in Nodule Forming Culture.

A-F show MC3T3 cells at various stages throughout nodule formation and mineralisation. At days 0 and 6, A and B, cells are in the proliferative phase. At days 12 and 15, C and D, cells are confluent and have a typical cuboidal morphology. Areas of cell condensation were detected at sites of nodule formation at days 15 and 20, D and E (→) with mineral deposits detected at day 25, F (*).

3.3.7 Characterisation of MC3T3 Cell Culture

Histochemical staining revealed that MC3T3-E1 nodule forming cultures expressed the osteoblast phenotype markers, alkaline phosphatase and collagen, as determined using van Gieson staining (section 2.2.16.3), at varying degrees throughout the culture period.

3.3.7.1 Alkaline Phosphatase Expression in MC3T3 Cell Cultures

MC3T3-E1 cells characteristically represent an immature population of osteoblastic cells; therefore, alkaline phosphatase protein was undetectable during the early stages of cell culture at days 6 and 9 (fig, 3.7 A and B). However, as these cells differentiate and become more 'osteoblastic' in phenotype, towards the latter stages of the culture (days 15, 20 and 25, figs. 3.7 C to E), alkaline phosphatase protein levels increased (fig. 3.7).

3.3.7.2 van Gieson Staining for Collagen in MC3T3 Cell Cultures

Similarly, the intensity of van Gieson staining for collagen, shown in red, increased from the early time points of the culture (days 0 to 9, fig. 3.8 A to C), i.e. reflecting the progression of these cell cultures from the proliferative phase to a confluent and differentiated state. As these cells differentiate towards the mature osteoblastic phenotype, they have the ability to deposit matrix (fig. 3.8) and mineralise it (fig. 3.6).

These results demonstrate that under the appropriate culture conditions MC3T3-E1 cells have the ability to differentiate into cells expressing the mature osteoblastic phenotype.

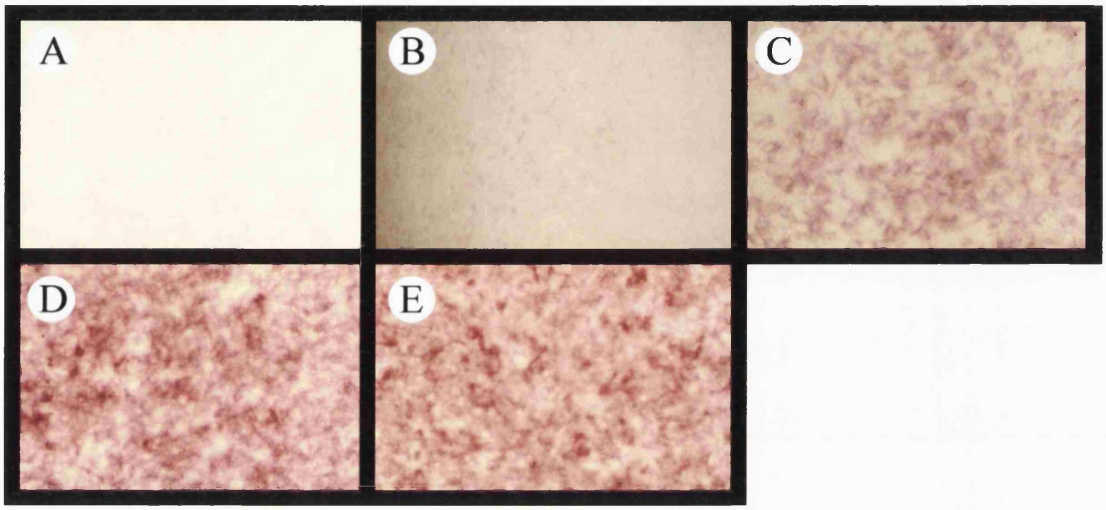

Figure 3.7 Alkaline Phosphatase Expression in MC3T3 nodule Cultures.

Alkaline phosphatase expression was undetected at early stages of these nodule forming cultures, reflecting the immature nature of these osteoblast-like cells. Following the initial cell proliferation phase, days 0 to 6 (A and B), alkaline phosphatase expression was detected at day 9, C, the differentiation phase, and increased in the latter stages of the culture, days 15, 20 and 25 (D to F).

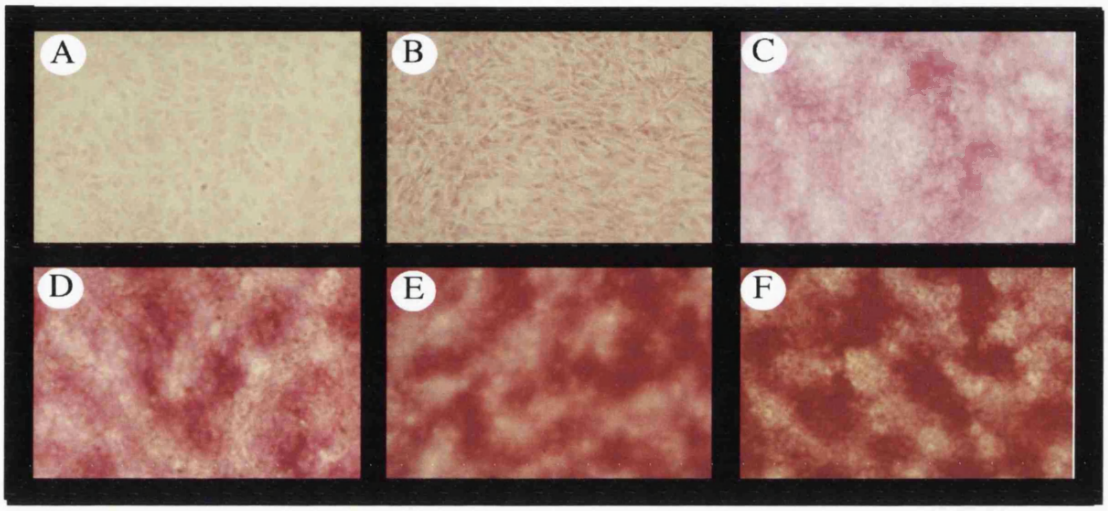

Figure 3.8 van Gieson Staining For Collagen in MC3T3 cell Cultures.

Low levels of collagen protein expression, shown in red, were detected at the earlier stages of cell proliferation and condensation, days 6 and 9 (A and B). Staining intensified at the more differentiated culture stages at days 12 and 15, C and D. However, it was not until the terminal differentiation phase, indicated by mineralisation, that high expression levels of collagen, due to matrix deposition, were detected. (days 20 and 25, E and F).

3.3.7.3 RT-PCR Analysis of Osteoblast Phenotype Markers in MC3T3 Cultures

RT-PCR was used to determine the expression of the osteoblast phenotype markers, alkaline phosphatase, osteocalcin and osteopontin in MC3T3-E1 cell cultures, to examine if these cells express the mature osteoblastic phenotype during nodule formation and mineralisation *in vitro*. Primers were designed specifically directed against mouse alkaline phosphatase, osteocalcin and osteopontin cDNA (see Chapter 2, table 2.6). Representative PCR products obtained using cDNA derived from MC3T3-E1 cells at days 6, 12, 15, 20 and 25 of nodule forming cultures were resolved by agarose gel electrophoresis (fig 3.9), and compared with control PCR analysis of MC3T3-E1 cells; cells plated at day 0 and grown to confluence without treatment. The quality of the cDNA was checked using β-actin PCR amplification.

Unlike the data obtained for protein expression levels of alkaline phosphatase, mRNA levels increased from day 6 to 12 and then remained the same throughout the remainder of the time course. Similarly, osteopontin mRNA remains at the same expression level throughout proliferative, differentiation and mineralisation stages. Osteocalcin mRNA was expressed at all the time points studied.

3.4 Discussion

3.4.1 Primary Osteoblastic Cell Cultures

Primary cell cultures derived from embryonic rat calvaria (RCOB) are widely used to assess osteoblast cell differentiation and function (Aubin *et al.*, 1993; Hughes and Aubin, 1998; Owen *et al.*, 1990; Reddi, 1995). In addition, cells isolated from rat

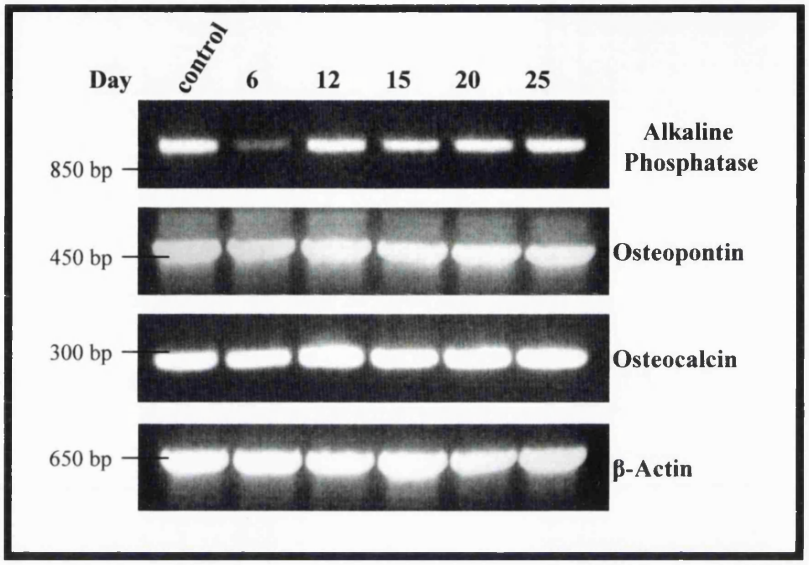

Figure 3.9 mRNA Expression of Osteoblast Phenotype Markers in MC3T3 Nodule Forming Cultures using RT-PCR. Representative PCR products obtained using cDNA derived from days 6, 12, 15, 20 and 25 of MC3T3-E1 nodule forming cultures were resolved by agarose gel electrophoresis. PCR analysis was also performed on a control sample of MC3T3-E1 cells, harvested at day 0 and grown to confluence without treatment with Asc or β-GP. The cDNA quality was checked using β-actin PCR amplification.

calvaria and from rat bone marrow (RBM) are commonly used as models of *in vitro* nodule formation and mineralisation (Bellows *et al.*, 1987; Bellows *et al.*, 1986).

The rat calvarial cell culture system was favoured over rat bone marrow stromal cell culture for several reasons. Cell populations isolated from rat calvaria and rat bone marrow both contain a heterogeneous population of cells consisting of osteoprogenitor cells at different stages of differentiation, as well as containing a sub-population of cells expressing the mature osteoblast phenotype. Rat bone marrow derived cells, RBMs, however, contain a higher proportion of progenitor cells (Bellows *et al.*, 1990). Although, these cells form nodules and mineralise *in vitro*, they divide more slowly and hence take longer to reach confluence. Additionally, the nodules formed in RBM cultures have been shown to be fewer in number and smaller in size than those observed in RCOB cultures.

Cells isolated from donor tissues such as embryonic rat calvaria have been shown to be phenotypically unstable when cultured for long periods of time (Wada *et al.*, 1998); therefore, cells were used at passage 1 in these studies. In an attempt to assess the osteoblastic content of the isolated cell population, and to confirm that these cells retain their osteoblastic phenotype during nodule formation and mineralisation, cells were characterised at various time points throughout a 22 day culture period.

In addition to the phenotypic instability of RCOB cells, the accessibility and number of cells isolated in any one cell preparation is limited. Cell yields vary from preparation to preparation. Therefore, in order to obtain sufficient cell yields for the nodule forming cultures, two litters of Wistar rat embryos were used per preparation. Cell yields obtained from enzymatic digestion of Wistar strain

embryonic rat calvaria proved to be greater than those obtained with Sprague Dawley rats. Furthermore, rat calvaria derived cell populations isolated from embryonic Wistar rat calvaria are better characterised.

As previously discussed, treatment of cell cultures with Asc and β-GP is crucial for *in vitro* nodule formation and mineralisation. Asc is required for cell proliferation and matrix production, whilst β-GP provides the phosphate source required for mineralisation (see Chapter 1, 1.6.3.2). Other contributing factors that may determine the number of nodules formed and the extent of mineralisation observed in this culture system are serum batch and duration of culture. These have been accounted for through serum batch testing and using a minimum culture duration time of 22 days (Beck *et al.*, 1998).

3.4.1.1 Optimisation and Characterisation of RCOBs

In this study alkaline phosphatase protein expression levels were estimated as intensity of staining (AU) and used to optimise the culture conditions required for maximum osteoblast cell number and, subsequently, the level of nodule formation and mineralisation observed *in vitro*. The majority of the isolated cells expressed alkaline phosphatase at increasing levels throughout the proliferative phase and at constant high levels through to the terminal differentiation phases, indicating that the proportion of alkaline phosphatase positive cells in these cultures increases with time (fig. 3.3). This observation implies that the proportion of differentiated osteoblastic cells increases with culture duration.

Using RT-PCR, the expression of the osteoblast phenotype markers alkaline phosphatase, osteocalcin and osteopontin were assessed at the mRNA level (fig.

3.5). Alkaline phosphatase was observed at days 4, 7 and 12 in primary osteoblastic cell cultures; however, mRNA levels of alkaline phosphatase were below the limit of detection at days 17 or 20. Similarly, alkaline phosphatase mRNA was not detected in ROS 17/2.8 cells. In view of the high levels of alkaline phosphatase protein expression, detected using histochemical staining (fig. 3.3), these observations were surprising. The effect observed on alkaline phosphatase mRNA levels could be attributed to β-GP treatment. Gerstenfeld and co-workers have reported a decline in both collagen mRNA levels and alkaline phosphatase mRNA levels in long term cultures supplemented with β-GP (cited by Gronowicz and Raisz, 1996).

In contrast to the relatively stable levels of osteopontin mRNA observed, low levels of osteocalcin mRNA were detected at days 7, 12, 17 and 20 of RCOB cultures and in ROS 17/2.8 cells. The undetectable levels of osteocalcin during the early proliferative phase, day 4, is not particularly surprising since at this stage both the proportion of cells expressing the mature osteoblastic phenotype and total cell numbers are low. In theory, as the culture progresses and cells acquire the mature osteoblastic phenotype, the mRNA levels of osteocalcin would be expected to increase, coinciding with *in vitro* mineralisation. The results obtained, however, do not show this. This suggests that either the PCR conditions used to detect osteocalcin mRNA levels were sub-optimal or that the intracellular turnover of osteocalcin mRNA *in vitro* is relatively high. The latter assumes that osteocalcin is a stable protein that does not need to be rapidly replenished in this *in vitro* system. In an attempt to investigate osteocalcin mRNA levels in RCOB cultures during nodule formation and mineralisation, the PCR conditions would need further optimisation, perhaps by increasing the number of cycles or the cDNA concentration.

Alternatively, a more quantitative analysis could be performed using Northern blot analysis.

Although these RT-PCR results are not quantitative, the presence of osteocalcin mRNA in RCOB cultures indicates that they have the potential to express osteocalcin. Taken together with the high levels of alkaline phosphatase protein expression and osteopontin mRNA levels, these results show that RCOBs are predominately osteoblastic in phenotype and demonstrate an ability to retain the osteoblast phenotype during the process of nodule formation and mineralisation.

In an attempt to demonstrate the ability of these cells to synthesis matrix, RCOBs were histochemically stained for collagen using van Gieson staining. Intracellular expression of collagen was observed in cells taken from day 4 of primary osteoblastic cell culture. The absence of van Gieson staining in the surrounding extracellular matrix was expected, since at day 4 these cells are in the proliferative phase and matrix deposition occurs towards the later stages of cell differentiation. Although collagen/matrix protein expression was detected at low levels in the cell cytoplasm, indicative of collagen or matrix synthesis, non-specific trapping of van Gieson stain was observed in the cell nucleus. One possible explanation for this nuclear staining could be that cell fixation and/or staining techniques were not optimal for this histochemical staining method. Therefore, this finding must be interpreted with some caution; van Gieson stain may be binding non-specifically to other matrix proteins localised to the cell nucleus. In order to confirm the expression and localisation of type I collagen in these cells, immunocytochemistry could be performed using specific antibodies. Alternatively, type I collagen mRNA levels could be assessed using Northern Blot analysis, bearing in mind that a decline in type I collagen mRNA levels has been previously described in nodule

forming and mineralising cell cultures treated with β-GP (Gronowicz and Raisz, 1996).

Alkaline phosphatase staining has convincingly, shown the sequential and time dependent expression of the osteoblast phenotype during nodule formation and mineralisation as previously reported by Nefussi *et al.*, (1997). In addition, these studies have confirmed that factors such as dex concentration, cell plating density and culture duration contribute to both the number of nodules formed and the level of mineralisation observed *in vitro*, complementing findings previously published by others (Bellows *et al.*, 1987; Bellows *et al.*, 1991). These studies have optimised the culture conditions required for *in vitro* nodule formation and mineralisation: cell plating density of 3×10^4 cells/35 mm well and treatment of primary rat calvaria cell cultures with the synthetic glucocorticoid dex at 10^{-8} M.

Primary cell culture provides a reliable model of nodule formation and mineralisation. However, as discussed above, cell preparation and isolation and the long-term nature of the nodule forming cultures means that the cells are not readily accessible. Taking into account the problems of cell number, accessibility and phenotypic instability of primary cells, we investigated the possibility of using a cell line equivalent model that could be easily accessed, was phenotypically stable and that would provide data that was comparable to primary cell data already obtained.

3.4.1.2 Optimisation and Characterisation of MC3T3-E1 Cultures

MC3T3-E1 cells, a cell line derived from mouse calvaria cells, is the only cell line available to date that has been shown to form and mineralise nodules *in vitro*

(Quarles *et al.*, 1992; Sudo *et al.*, 1983; Zhou *et al.*, 1995). Although these cells express an immature osteoblastic phenotype, they can be stimulated to express the mature osteoblastic phenotype upon treatment with Asc and β-GP.

Alkaline phosphatase expression was assessed in MC3T3-E1 cells grown in culture for 25 days (Beck *et al.*, 1998). Unlike in primary osteoblast-like cells, alkaline phosphatase expression is very low at initial plating stages and during the early stages of cell proliferation. Cells are immature at these stages and proliferate, but do not express detectable levels of alkaline phosphatase until they become confluent and more differentiated. However, as these cell cultures progressed to form nodules and mineralise, high levels of alkaline phosphatase protein expression were detected (fig. 3.7). RT-PCR analysis revealed that these cells express alkaline phosphatase mRNA throughout nodule formation and mineralisation. Interestingly, lower levels of alkaline phosphatase mRNA were detected during the proliferative phase at day 6. At this early stage both cell number and the proportion of cells expressing the mature osteoblastic phenotype is low. Although alkaline phosphatase mRNA levels cannot be used to gauge protein expression, they do indicate the potential of MC3T3-E1 cells to express alkaline phosphatase at the protein level. Similarly, osteopontin and osteocalcin mRNA was detected throughout nodule formation and mineralisation, once again demonstrating that these cells contain the information required to synthesis osteoblastic matrix proteins. The constant mRNA levels observed during nodule formation and mineralisation demonstrate that MC3T3-E1 cells retain the ability to express these proteins throughout these processes, suggesting that they have the potential to retain an osteoblastic phenotype throughout the culture duration.

Van Gieson staining, observed during nodule formation and mineralisation, demonstrated the ability of MC3T3-E1 cells to actively deposit a collagenous matrix *in vitro*. Compared to the low levels of van Gieson staining observed during the early stages of these cultures (fig. 3.8, day 9), an increase in collagen was observed in the later stages of cell differentiation (days 12 to 15) and mineralisation (days 20 to 25).

Although MC3T3-E1 cells form mineralised nodules, morphologically these nodular structures differ from those observed in RCOB cultures. MC3T3-E1 cells form flatter nodules than those observed with RCOB (Xiao *et al.*, 1997; Zhou *et al.*, 1995). Furthermore, Bellows *et al* (1987) have reported that dex treatment has little or no effect on nodule formation in these cells. In view of these differences, and possible species variation, the question remains as to whether or not this murine model of *in vitro* mineralisation can truly be used as a comparative model for rat calvaria primary osteoblastic cultures. However, the limitations of primary osteoblastic cell cultures and the unique ability of this permanent cell line to mineralise *in vitro* renders MC3T3-E1 as a viable model of nodule formation and mineralisation.

3.5 Summary

- A population of osteoblast-like cells, characteristically osteoblastic in phenotype, have been isolated.
- Optimal conditions for cell proliferation, differentiation and *in vitro* nodule formation and mineralisation have been determined.
- MC3T3-E1 cells have been stimulated to form nodules and to deposit mineral *in vitro*.

Two 'functional' *in vitro* models of nodule formation and mineralisation, comparable to mineralisation *in vivo* have been established. These cultures are used in subsequent chapters to assess intercellular communicating pathways in osteoblasts during nodule formation and mineralisation. In addition, these cultures are used to investigate the molecular mechanisms mediating directed bone matrix protein secretion of functional osteoblasts.

Chapter 4

INTERCELLULAR COMMUNICATION BETWEEN OSTEOBLASTS

Chapter 4

INTERCELLULAR COMMUNICATION BETWEEN OSTEOBLASTS

4.1 Introduction

The mechanisms by which osteoblasts achieve regulated and directed bone matrix protein secretion are not clearly understood. Osteoblasts form intercellular junctions and it has been suggested that the presence of such communicating pathways may be responsible for the co-ordination of these cells into an epithelial type monolayer (Yamaguchi *et al.*, 1995), which may in turn play an important role in the establishment and maintenance of cell polarity. Intercellular communication may also aid the mineralisation process by enabling osteoblasts to deposit matrix as part of a concerted effort, maximising their efficiency. The presence of gap junction (GJ) communication has been well documented in osteoblastic cells (Bruzzone *et al.*, 1996a; Doty, 1981; Schirrmacher *et al.*, 1992; Yamaguchi *et al.*, 1995; Ziambaras *et al.*, 1998). This study establishes that in addition to GJ formation, osteoblastic cells have the potential to form apical junctional complexes.

4.1.1 Intercellular Communication in ROS 17/2.8 Cells

Osteoblasts form GJ through the association of connexin molecules but it remains unclear as to whether or not these cells form tighter membrane associations.

In a morphological study of intercellular junction complexes during osteocyte differentiation, Palumbo *et al.* (1990) identified that, in addition to GJ, osteoblastic cells contain structures with the morphological characteristics of adherens junctions

(AJ). The ability of these cells to form apical junctional complexes, such as AJ, suggested that they may be able to establish distinct apical and basolateral domains and hence cell polarity.

Recent investigations into osteoblastic cell polarity with the differentially targeted enveloped viruses, Influenza virus haemagglutinin (HA) and vesicular somatitis virus glycoprotein (VSV-G), indicate that the bone attachment membrane of osteoblasts is the apical surface whilst the bone marrow facing surface membrane is basolateral in nature (Ilvesaro *et al.*, 1999).

4.1.2 MDCK Cells – A model of Intercellular Communication

Epithelial cells are divided into apical and basolateral domains by the presence of junctional complexes (for review see Anderson and Van Itallie, 1995; Balda and Matter, 1998). Molecular dissection of intercellular communicating pathways in Madine Derby Canine Kidney epithelial cells (MDCK) has led to the identification of the protein components required for TJ and AJ complex formation (Balda and Matter, 1998; Citi and Cordenonsi, 1998; Citi *et al.*, 1988; Furuse *et al.*, 1998a; Furuse *et al.*, 1993; Haskins *et al.*, 1998; Itoh *et al.*, 1993; Itoh *et al.*, 1991; Stevenson *et al.*, 1986). MDCK cells form both AJs and apical TJs. The presence of these junction complexes have been shown to be crucial for the establishment and maintenance of cellular polarity and the provision of a semi-permeable diffusion barrier within the epithelial cell monolayer (Anderson and Van Itallie, 1995; Balda and Matter, 1998). In addition, these junction complexes add to the structural and adhesive support of the epithelial cell monolayer. The establishment of such intercellular pathways is crucial to epithelial cell function. Characteristically, MDCK cells provide an

accessible and well characterised model of *in vitro* junction formation and were used throughout this study as a positive control of junction protein expression.

4.1.3 Formation of Intercellular Junctions – Protein Components

Through the biochemical dissection of the junction complexes, a number of key proteins implicated in apical junction complex formation have been identified and characterised. ZO-1, zonula Occludens 1, was the first of these proteins to be identified and localised to the TJ plaque (Stevenson *et al.*, 1986). A cytoplasmic protein that mediates protein-protein interactions, ZO-1 was also found in the AJ (Itoh *et al.*, 1997; Itoh *et al.*, 1993; Itoh *et al.*, 1991), suggesting that ZO-1 may transiently localise to AJ in the absence of TJ formation. Furthermore, this strengthens the hypothesis that junction complexes form in a sequential manner; i.e. first AJ are formed, followed by TJ (Mitic *et al.*, 1999).

Following the identification of ZO-1, occludin, an integral membrane protein, was localised to the TJ (Furuse *et al.*, 1993). Until recently, occludin was regarded as the key TJ protein component crucial for the formation and maintenance of the TJ. However, in 1998, Furuse and co-workers identified a novel multi-gene family, the claudins which were also detected in TJ. Transfection of claudin into TJ deficient L-fibroblasts led to the conclusion that claudins, rather than occludin, mediate TJ formation (Anderson and Van Itallie, 1999; Furuse *et al.*, 1998a; Furuse *et al.*, 1998b; Tsukita and Furuse, 1999). These findings have added a further level of complexity to the process of TJ formation. In addition to these membrane associated proteins, a number of cytoplasmic proteins implicated in protein-protein interactions and cytoskeletal attachment have been identified at apical junction complexes. These proteins include α-, β- and γ-catenin, ZO-2, ZO-3, α-actinin, vinculin, AF-6 and

cingulin, (Itoh *et al.*, 1999a; Itoh *et al.*, 1999b; Rudiger, 1998; Weiss *et al.*, 1998; Yamamoto *et al.*, 1997) which localise to sites of cellular contact in both epithelial and non-epithelial cells (Yonemura *et al.*, 1995).

Due to the limited availability of antibodies directed against these junction complex protein components, only the expression of key proteins (occludin, claudin, ZO-1, α-, β-, and γ-catenin, α-actinin and vinculin) were investigated in osteoblastic cells.

4.2 Aims

The aim of this study was to investigate and characterise junction formation in osteoblasts and to investigate the possibility that osteoblastic cells use a molecular machinery similar to epithelial cells to achieve and maintain cell polarity and, thus, achieve directed protein transport.

4.3 Results

4.3.1 Junction Protein Expression in Osteoblastic cells – Western Blot Analysis

Using Western blot analysis, the expression of proteins associated with apical junction complex formation was determined on total cell extracts of ROS 17/2.8 and primary osteoblastic cells derived from embryonic rat calvaria (RCOBs), grown in monolayer before being harvested.

Western blot analysis revealed the expression of cadherins, proteins implicated in AJ formation, in both osteoblastic cells, ROS 17/2.8 and RCOBs (fig. 4.1 A). Initially the expression of cadherins in these cells was assessed using a broad-spectrum pan-cadherin antibody. Further investigation showed that N- and P-cadherins were expressed in both ROS 17/2.8 and RCOB cells. Osteoblastic cells also express the TJ and AJ associated protein, ZO-1 (fig. 4.1 A). However, the expression of occludin, a key TJ protein component, could not be addressed in ROS 17/2.8 cells, RCOBs or in MDCK cells using this method, as the available antibody failed to work using Western blotting. Furthermore, immunohistochemical staining of occludin on sections of rat kidney and rat liver have demonstrated that the occludin (MOC37) antibody does not cross-react with rat, despite wider species reactivity (data not shown).

These studies also demonstrated that osteoblastic cells express an array of cytoplasmic proteins associated with cytoskeletal attachment to the plasma membrane. These proteins have been localised to the AJ plaque (fig. 4.1 B) in other cell types. Of these proteins, osteoblastic cells express α- and β-catenins, proteins known to interact directly with the cadherins and ZO-1. Furthermore, these cells express the actin cytoskeleton attachment proteins, vinculin and α-actinin.

Having identified a number of proteins involved in apical junction complex formation in osteoblastic cells, the specific localisation of these proteins within ROS 17/2.8 cells and RCOBs was investigated using immunocytochemistry and confocal laser scanning microscopy. In addition, the localisation of these junction-associated proteins was determined on the epithelial cell line, MDCK.

Figure 4.1 Junction Protein Expression on Osteoblastic Cells.

Western blot analysis revealed that osteoblastic cells express a number of key protein components implicated in apical junction formation. Both ROS 17/2.8 cells and primary osteoblastic cells (RCOBs) express an array of cadherin molecules and ZO-1 (A), in addition to several of the cytoplasmic proteins associated with adherens junction formation, α- and β-catenin, α-actinin and vinculin (B). MDCK cells were used as a positive control for junction protein expression.

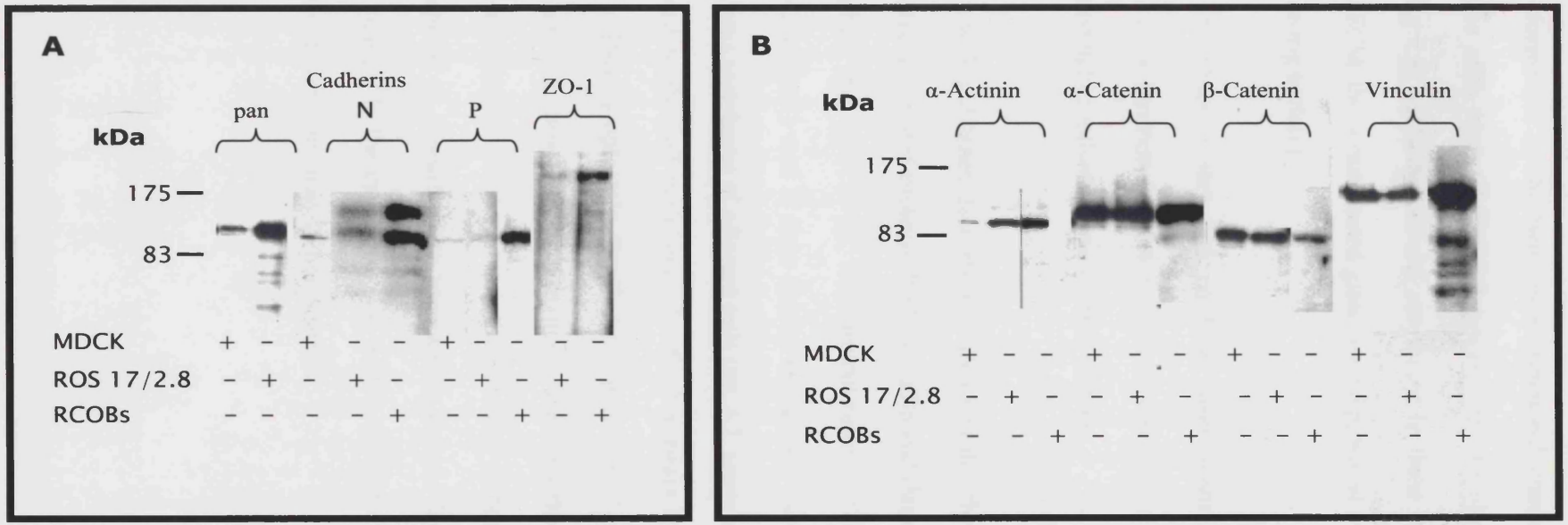
A
Cadherins
pan
N
P
ZO-1
kDa
175
83
MDCK + − + − − + − − − −
ROS 17/2.8 − + − + − − + − + −
RCOBs − − − − + − − + − +
B
kDa
α-Actinin
α-Catenin
β-Catenin
Vinculin
175
83
MDCK + − − + − − + − − + − −
ROS 17/2.8 − + − − + − − + − − + −
RCOBs − − + − − + − − + − − +

4.3.2 Apical Junction Protein Expression in MDCK Cells

Anatomically, these cells are divided into distinct apical and basolateral domains through the formation of the two apical junctional complexes, AJ and TJ; in addition, these cells form GJ, located towards the basolateral membrane (see Chapter 1, fig. 1.5). (The basolateral membrane in these cells is the membrane closest to the ECM, the serum coated glass coverslip, whilst the apical membrane is the medium-facing surface).

Using immunocytochemistry and confocal laser scanning microscopy, the expression of these junction-associated proteins were characterised in MDCK cells that had formed tight confluent monolayers in culture.

In accordance with published data, these studies revealed that MDCK cells express the tight junction associated proteins ZO-1, occludin and claudin 1 which localise to the cell periphery (fig. 4.2 A to C). In confluent cultures, these proteins, with the exception of claudins 1 and 2, were almost exclusively localised to contact sites along the plasma membrane of adjacent cells (fig. 4.2, arrowhead *). In addition to being localised to the cell periphery, claudin 1 appears to have a cytoplasmic distribution. This cytoplasmic distribution of claudin 1 could either indicate non-specific antibody binding or, alternatively, indicates that a sub-population of claudin 1 resides in the cytoplasm with the potential of being re-localised to the plasma membrane as a result of an appropriate signal. In these cells claudin 2 localises exclusively to the cytoplasm (fig. 4.2 D) and not the plasma membrane, suggesting that this staining may be non-specific.

Figure 4.2 Junction Protein Expression on MDCK Cells.

The expression of TJ associated proteins (A to D) and AJ associated proteins (E to K) was determined in confluent MDCK cells using immunocytochemistry and confocal laser scanning microscopy. TJ proteins ZO-1, occludin and claudin 1 were localised to the cell periphery (A to C, arrowhead *); however, localisation of claudin 2 to specific cell to cell contact sites was not detected (D). Furthermore, and in keeping with previously published data, the expression of cadherins (F), in particular E-cadherin (E), along with the cytoplasmic proteins α-, β- and γ-catenins, α-actinin and vinculin localised to the cell periphery, concentrating at sites of cell to cell contact (G to K). In addition, vinculin localised to focal contacts on the basolateral surface of the cell (L, →). (arrowhead * = cell to cell contacts, → = focal contacts).

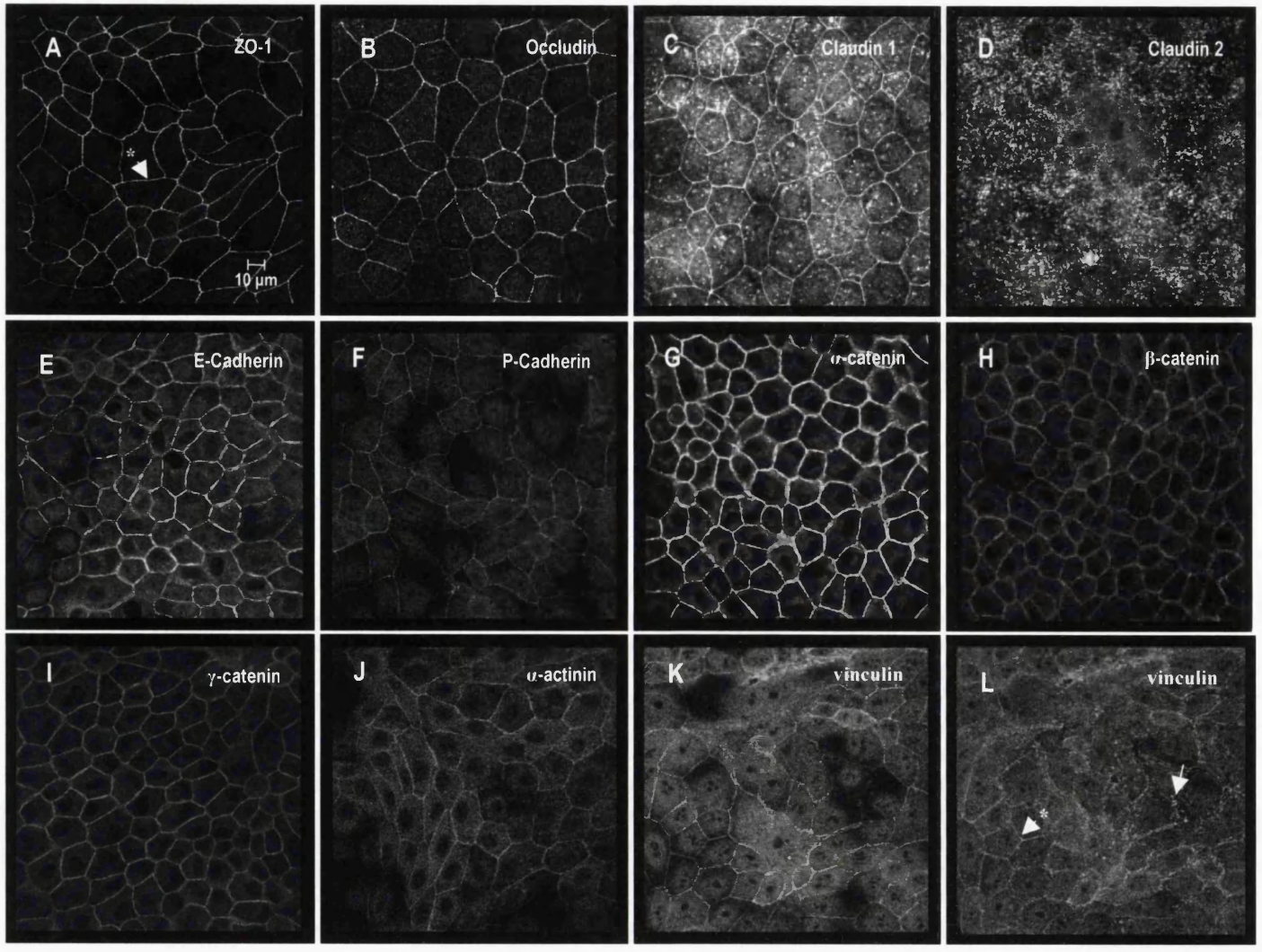
A
ZO-1
10 µm
B
Occludin
C
Claudin 1
D
Claudin 2
E
E-Cadherin
F
P-Cadherin
G
α-catenin
H
β-catenin
I
γ-catenin
J
α-actinin
K
vinculin
L
vinculin

In addition to the above mentioned TJ associated proteins, a number of key AJ associated proteins were detected in MDCK cells. Cadherins were identified using a broad-spectrum pan-cadherin antibody (fig. 4.2 F). E-cadherin was expressed along the sites of cell to cell contact (fig. 4.2 E). These proteins were also expressed to a lesser extent within the cell cytoplasm.

In addition, MDCK cells express a number of cytoplasmic proteins associated with cytoskeletal attachment namely, α-, β-, γ-catenins, α-actinin and vinculin (fig. 4.2 G to K) which localised to the plasma membrane in confluent cell cultures concentrated at sites of cell to cell contact. The presence of such an abundant cytoplasmic pool of these proteins is not surprising, particularly since these cytoskeletal attachment proteins are implicated not only in junctional complex formation, function and stability but also play a crucial role in cell signalling mechanisms. For example, vinculin expression was also detected in focal contacts on the basolateral surface of these cells (fig. 4.2 L, →). Vinculin is associated with focal adhesions, points of close contact between the cell membrane and the extracellular matrix (ECM) (Burridge *et al.*, 1988). These focal contacts have a complex structure and involve integrin-mediated attachment, thus facilitating the transmission of signals from ECM to the cytoplasm through ECM linkage to the cytoskeleton.

Having established the optimal conditions for immunocytochemistry, junction protein expression was assessed in the osteoblastic cell line, ROS 17/2.8.

4.3.3 ROS 17/2.8 Cells Express Key Protein Components of Adherens Junctions

ROS 17/2.8 cells were cultured on serum coated glass coverslips and grown to confluence. Although these cells did not form tight confluent monolayers, as previously observed for MDCK cell cultures, junction protein localisation was assessed in areas of highest cell density within these cultures. The expression and localisation of key junction protein components were assessed using immunocytochemistry and revealed that, although osteoblastic cells express proteins associated with the formation of AJs, there is an apparent absence of proteins associated with TJ formation.

Specifically, ROS 17/2.8 cells express ZO-1, cadherin, α-catenin, α-actinin and vinculin (fig. 4.3). ZO-1 localised to the cell periphery with additional immuno-reactivity detected within the cell cytoplasm (fig. 4.3 A, arrowhead *). The TJ associated proteins occludin, claudin 1 and claudin 2 were not detected using this method (fig. 4.3 B to D). Although these cells failed to express E-cadherin (fig. 4.3 E), cadherin expression was detected using a broad-spectrum pan-cadherin antibody (fig. 4.3 F), and localised to the cell periphery, in particular at sites of cell to cell contact and within the cell cytoplasm (fig. 4.3 F, arrowhead *). In areas of sub-confluence, cadherin localisation was restricted to sites of intercellular contact (fig. 4.3 F →). Similarly, α-catenin, α- actinin and vinculin were localised to the plasma membrane (fig. 4.3 G, I and J, arrowhead *) and the cytoplasm within these osteoblastic cells.

Vinculin was also localised to focal contacts towards the apical surface of osteoblastic cells (fig. 4.3 K, →).

Figure 4.3 Junction Protein Expression on Osteoblastic Cells.

Using immunocytochemistry and confocal laser scanning microscopy, the expression and localisation of TJ associated proteins (A to D) and AJ associated proteins (E to K) were determined in ROS 17/2.8 cells. ZO-1 was localised to the cell periphery, concentrated specifically towards sites of cell to cell contact (A, arrowhead *). The expression of other key TJ associated protein markers, such as occludin, claudin 1 and claudin 2 were not detected (B to D). Cadherins were detected using a broad-spectrum pan-cadherin antibody (F), but osteoblasts failed to express E-cadherin (E). Osteoblastic cells expressed the cytoplasmic proteins, α-catenin, α-actinin and vinculin; these proteins localised to the cell periphery concentrating at sites of cell to cell contact (G, I and J, arrowhead *). In addition, vinculin localised to focal contacts on the basolateral surface of the cell (K, →). Although the cytoplasmic protein β-catenin was detected in osteoblastic cells using Western blot analysis, it was not detected using immunocytochemistry. (arrowhead * = cell to cell contacts, → = focal contacts).

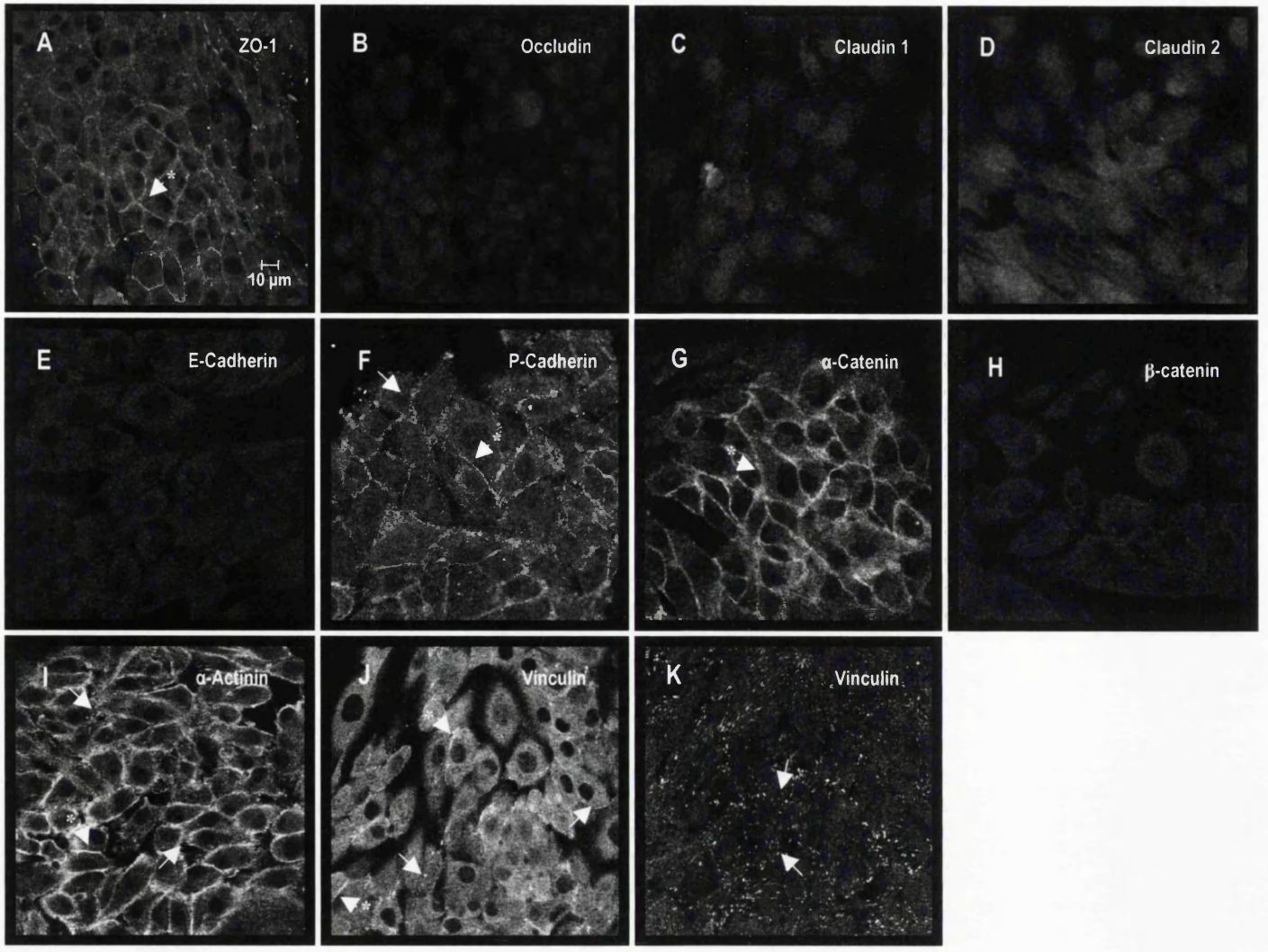
A
ZO-1
10 µm
B
Occludin
C
Claudin 1
D
Claudin 2
E
E-Cadherin
F
P-Cadherin
G
α-Catenin
H
β-catenin
I
α-Actinin
J
Vinculin
K
Vinculin

Although an apparent abundance of β-catenin was detected in osteoblastic cells using Western blot analysis, β-catenin expression was not detected in these cells using immunocytochemistry (fig. 4.3 H).

These data provide evidence that osteoblastic cells express the protein components required for AJ formation. However, in an attempt to understand more fully the expression and distribution of junction associated proteins in relation to cell to matrix interactions, ROS 17/2.8 cells and primary rat calvaria derived osteoblast-like cells (RCOBs) were cultured on a variety of substrates and the localisation of ZO-1 was examined.

4.3.4 ZO-1 Expression in Osteoblastic Cells is Dependent on the Adhesion Substrate

These experiments revealed localisation of ZO-1 in osteoblastic cells to be dependent upon the substrate onto which the cells are cultured. Cells were cultured on either foetal calf serum (FCS), osteopontin or fibrillar collagen coated glass coverslips, or directly onto dentine slices (fig. 4.4).

4.3.4.1 FCS coated glass coverslips

In both ROS 17/2.8 and RCOBs grown on FCS coated glass coverslips, ZO-1 expression was localised to the cell periphery, specifically concentrating at sites of cell to cell contact (fig. 4.4 A and E, arrowhead *). In RCOBs, however, ZO-1 appears to have a more punctate, focal distribution (fig. 4.4 A, →). In ROS 17/2.8 cells the ZO-1 appears to have a linear distribution at sites of cell to cell contact (fig. 4.4 E, arrowhead *).

Figure 4.4 Localisation of ZO-1 is dependent on the substrate onto which Osteoblast-like cells are plated.

ZO-1 localised to the plasma membrane in a linear fashion, concentrated at the sites of cell to cell contact (C and F, arrowhead *) whereas in other conditions staining was more punctate (A, B and D, →). The specific localisation of ZO-1 in ROS 17/2.8 cells remained less affected by the substrate upon which they were plated whilst RCOBs localised ZO-1 to the plasma membrane when coated on FCS (A, arrowhead *) or osteopontin (C, arrowhead *). In contrast, when cultured on dentine (B) or fibrillar collagen (D) these cell express ZO-1 in a more punctate manner at sites of cell to cell contact (B and D →). ZO-1 was expressed in ROS 17/2.8 cells concentrated to the plasma membrane of adjacent cells with areas of sub confluent cells expressing the protein in a punctate manner (→). (arrowhead * = cell to cell contacts, → = focal contacts).

FCS
Dentine
Osteopontin
Fibrillar Collagen
RCOBs
ROS 17/2.5
A
B
C
D
E
F
G
ZO-1
10 µm

4.3.4.2 Dentine

In RCOBs cultured on dentine slices, ZO-1 distribution appears to be localised exclusively to focal adhesions (fig. 4.4 B, →), whilst ROS 17/2.8 cells expressed ZO-1 in a linear distribution localised particularly at sites of cell to cell contact (fig. 4.4 F, arrowhead *).

4.3.4.3 Osteopontin

Unlike the expression patterns of ZO-1 observed on RCOBs cultured on either FCS coated glass coverslips or dentine, ZO-1 is expressed in a more linear fashion in cells plated on osteopontin (fig. 4.4 C, arrowhead *); ZO-1 immuno-reactivity was also detected at points of focal contacts (fig. 4.4 C, →). There was only limited expression of ZO-1 in ROS 17/2.8 cells and this was localised to the plasma membrane towards sites of cell to cell contact (fig. 4.4 G, arrowhead *).

4.3.4.4 Fibrillar Collagen

Although ZO-1 expression was detected on RCOBs, these cells did not appear to grow well on fibrillar collagen and did not form confluent monolayers. ZO-1 was expressed in a punctate manner towards sites of cell to cell contact (fig. 4.4 D, →). ZO-1 expression was not determined on ROS 17/2.8 cells cultured on collagen coated glass coverslips because these cells did not grow well on this substrate. These cells rounded up and detached.

These investigations highlighted that ZO-1 localisation to the plasma membrane is dependent on the substrate on which the cells were cultured. Although ZO-1 was expressed at varying degrees under all conditions, maximal ZO-1 expression was

observed on cells plated and cultured on either dentine slices or on osteopontin coated glass coverslips. It would, however, appear that plating osteoblastic cells onto serum coated glass coverslips does not drastically alter ZO-1 expression and subsequent experiments used cells that were cultured on either serum coated glass coverslips or on dentine slices.

4.3.5 ZO-1 Expression is Apparently Up-regulated by Dexamethasone

Briefly, ROS 17/2.8 cells were plated on serum coated glass coverslips and cultured either in the presence of dex, Asc or a combination of dex, Asc and β-GP (fig. 4.5). In untreated ROS cells ZO-1 localised to the plasma membrane in a linear fashion, concentrated at points of cell to cell contact. In areas where the cells are sub-confluent, ZO-1 immuno-reactivity had a focal type distribution at the cell periphery (fig. 4.5 A, →). A similar localisation of ZO-1 was observed in both Asc treated and in dex, Asc and β-GP treated cultures (fig. 4.5 C-D, →). Interestingly, an apparent increase in ZO-1 expression was observed in cells cultured in the presence of dex; here, whilst ZO-1 localised to the sites of cell to cell contact it also showed a wider distribution throughout the cell cytoplasm (fig. 4.5 B, arrowhead *). Although these results are not quantitative, they imply that ZO-1 expression in osteoblasts is up-regulated by glucocorticoids.

4.3.6 Localisation of Junction Proteins on Primary Osteoblast-like Cells

Western blot analysis has identified that primary osteoblast-like cells expressed a number of proteins associated with AJ formation (fig. 4.1). Using immunocytochemistry and confocal laser scanning microscopy, AJ-associated proteins were localised in RCOBs cultured on dentine slices.

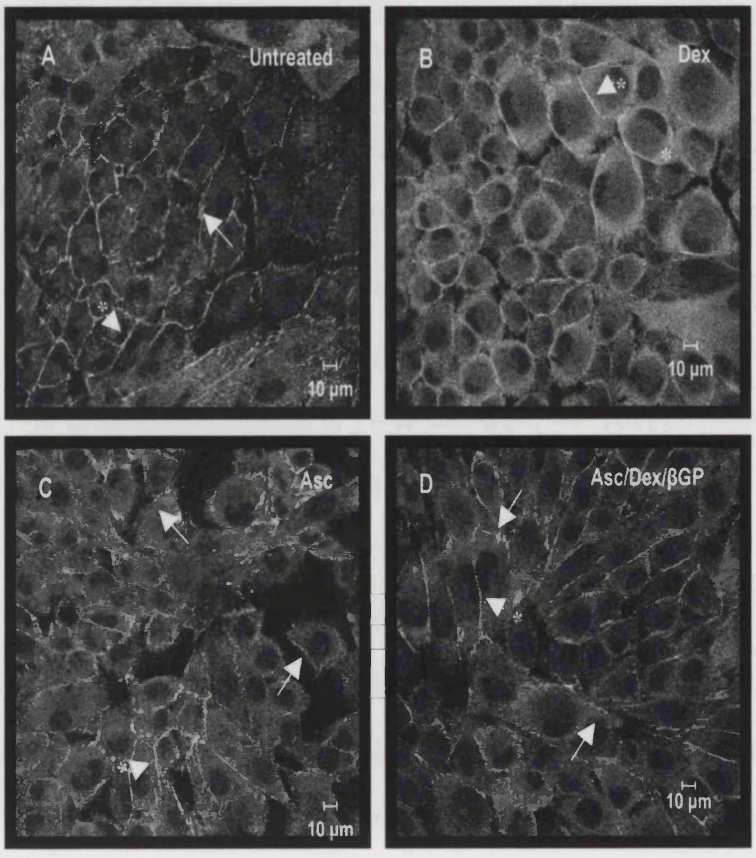

Figure 4.5 ZO-1 Expression is Up-regulated by Dexamethasone.

Cells cultured on serum coated glass coverslips were treated in the presence of dexamethasone (dex), ascorbate (Asc) or a combination of dex, Asc and β-glycerophosphate (βGP). Untreated cell cultures, i.e. those cultured under standard conditions, were used as a control for ZO-1 expression (A). As previously described, ZO-1 localises to the plasma membrane concentrating at sites of cell to cell contact in untreated cells (A, arrowhead *). A similar distribution was observed for both Asc treated cells and those treated with dex, Asc and βGP (C and D, arrowhead *). Dex treated ROS 17/2.8 cells, however, displayed an increase in ZO-1 expression especially within the cell cytoplasm (B).

Cadherin expression localised at inter-cell boundaries between adjacent cells, and in addition, was detected within the cell cytoplasm (fig. 4.6 B). ZO-1 was localised to a punctate distribution in these cells with ZO-1 immuno-reactivity localised towards areas of cell to cell and cell to matrix contact (punctate structures → fig. 4.6 A). Likewise, α-actinin localised to the cell periphery (fig. 4.5 C, arrowhead *). However, a large cytoplasmic pool of α-actinin was also observed. Vinculin localised towards the apical cell surface in these cells, i.e. the membrane closest to the bone surface, in a focal distribution (fig. 4.6 D, →). The stress fibres detected in figs. 4.5 A and D can be attributed to cross-talk from the TRITC channel where rhodamine phalloidin, F-actin staining, was detected.

These data provide evidence that both the osteoblastic cell line, ROS 17/2.8, and primary osteoblastic cell cultures (RCOBs) express a number of proteins associated with AJ formation. In addition, these studies reveal that osteoblastic cells do not express, at the protein level, the characteristic protein components of the TJ. The following experiments, however, were used to assess TJ marker expression at the mRNA level. Although cells may not express a target protein they may contain the information at the mRNA level, and thus the potential to express a specific protein.

4.3.7 Tight Junction Marker Expression in Osteoblastic cells

4.3.7.1 Expression of an Integral Tight Junction-Associated Protein – Occludin

Using RT-PCR and primers directed against occludin (for primer sequence see methods Chapter 2, table 2.4), the expression of occludin mRNA was detected in

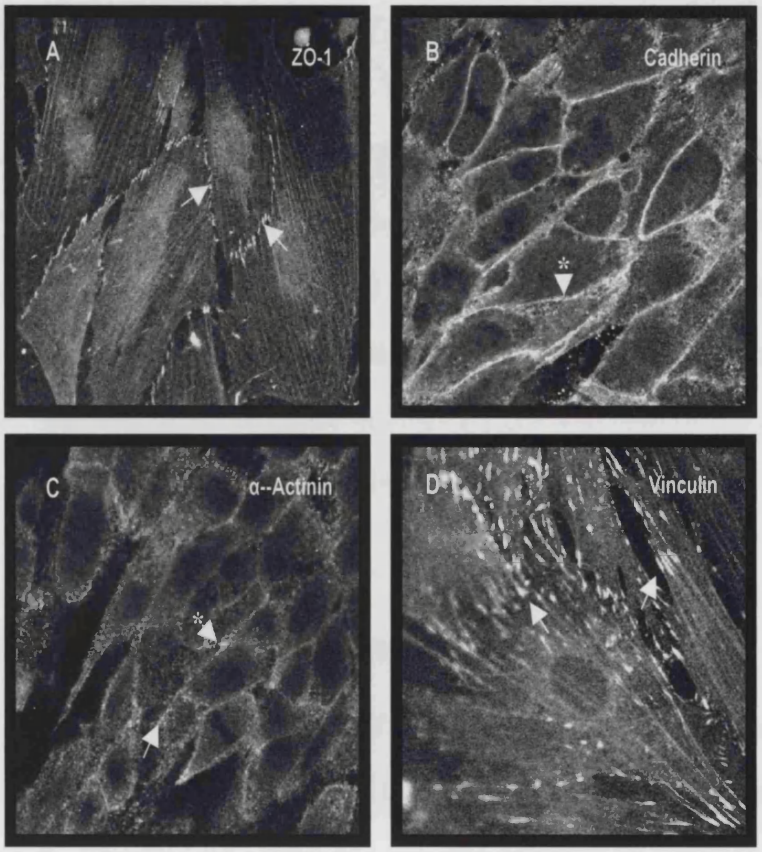

Figure 4.6 Junction Protein Expression and Localisation in Primary Osteoblast-like cells cultured on dentine Slices. ZO-1, as described previously, localised to focal points at sites of cell to cell contact (A, →). Using a pan-cadherin antibody, cadherins were shown to localise to the plasma membrane (B, arrowhead *) with some immuno-reactivity in the cytoplasm. Similarly α-actinin localised both to the cell boundaries of adjacent cells (C, arrowhead *) and to the cytoplasm. Vinculin was localised in a focal distribution towards the apical membrane of the osteoblast (i.e. the side of the cell closest to the bone surface) (D, →), similar to ZO-1 expression.

osteoblastic cells (fig. 4.7 A). Occludin was detected in both ROS 17/2.8 cells and in the mineralising mouse osteoblast cell line MC3T3 (see Chapter 3). Furthermore, the partial cDNA transcripts obtained for osteoblastic occludin appeared to be the same size as those obtained for the rat liver and MDCK controls. Subsequent, cloning and sequence analysis revealed these partial cDNA transcripts to be identical to existing occludin sequences obtained from database searches using BLAST (basic local alignment search tool) (fig. 4.7 B). Although occludin could not be detected using Western blot analysis and immunocytochemistry due to the lack of antibody reactivity in the rat, these findings suggest that osteoblastic cells have the potential to express the TJ associated protein, occludin.

4.3.7.2 Claudin expression in Osteoblastic Cells

As a result of the limited availability of antibodies directed against the claudin family of TJ proteins, the expression of claudins in osteoblastic cells was assessed using RT-PCR. Claudins are a large and growing family of TJ associated proteins with 20 isoforms identified to date. Although these proteins are structurally similar, the level of sequence identity observed between isoforms is limited. Claudins 1 and 2 are the most closely related showing ~ 47 % identity at the amino acid level. In these studies osteoblastic cells were screened for the presence of the two most closely related claudin family members, claudins 1 and 2.

Using degenerate primers directed against claudins 1 and 2 (Chapter 2, table 2.4), claudin 1 and 2 expression was detected at the mRNA level in osteoblastic cells (fig. 4.8 A); ~ 450 bp. Cloning, restriction digestion and sequence analysis revealed that both claudins 1 and 2, are expressed in ROS 17/2.8 and MC3T3 cells.

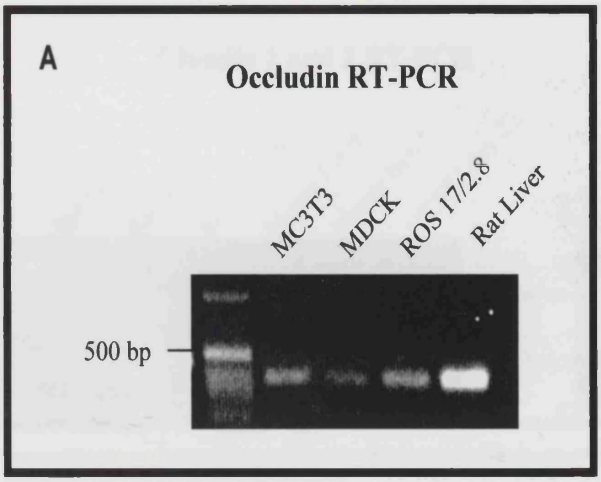

B

```
ROS(98%)     121  actatgaaaccgaactacacgacaggtggcgagtcctgcgatgagctggaggaggactgg 180
Ratliver(100%) 30  cactatgaaaccga-ctacacgacaggtggcgagtcctgcgatgagctggaggaggactgg 89
Occludin     1761 actatgaaaccga-ctacacgacaggtggcgagtcctgcgatgagctggaggaggactgg 1819

             181  ctcagggaatatccacctatcacttcagatcaacagagacaactgtacaagagaaatttt 240
             90   ctcagggaatatccacctatcacttcagatcaacagagacaactgtacaagagaaatttt 149
             1820 ctcagggaatatccacctatcacttcagatcaacagagacaactgtacaagagaaatttt 1879

             241  gatgcaggtttacgggagtataagagtcttactggcagaactcgacgaggtcaacaaaga 300
             150  gatgcaggtttacaggagtataagagt-ttactggcagaactcgacgaggtcaacaaaga 208
             1880 gatgcaggtttacaggagtataagagt-ttactggcagaactcgacgaggtcaacaaaga 1938

             301  gctctctcgtctcgacagagaactggatgactacagagaggagagcgaagagtacatggc 360
             209  gctctctcgtctcgacagagaactggatgactacagagaggagagcgaagagtacatggc 268
             1939 gctctctcgtctcgacagagaactggatgactacagagaggagagcgaagagtacatggc 1998

             361  tgctgctgatgaatataacagactaaagcaagttaagggatctgcagattataaaagcaa 420
             269  tgctgctgatgaatataacagactaaagcaagttaagggatctgcagattataaaagcaa 328
             1999 tgctgctgatgaatataacagactaaagcaagttaagggatctgcagattataaaagcaa 2058

             421  gaagaattactgcaagcagttaaagagccaattatcacacatcaagaggatggtggaag 480
             329  gaagaattactgcaagcagttaaagagcaaattatcacacatcaagaggatggtgggag 387
             2059 gaagaattactgcaagcagttaaagagcaaattatcacacatcaagaggatggtgggag 2117

             481  agactatgacagacggaa 496
             388  --actatgacagacggaa 403
             2118 --actatgacagacggaa 2133
```

Figure 4.7 Occludin mRNA Expression.

RT-PCR analysis reveals that osteoblastic cells express an integral TJ associated protein, occludin, at the mRNA level (A). Cloning and sequence analyses have shown this cDNA transcript to be identical to previously published occludin sequence (B).

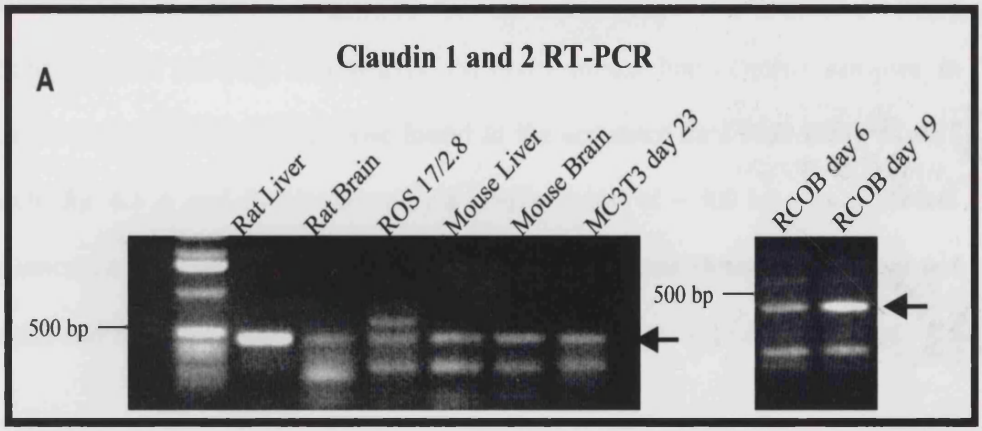

B

```
Rat Cldn 1          70  tgctggggccagcattgtgactgctcaggccatctacgagggactgtggatgtcctgcgt 129
Rat Liver (99%)    225  tgctggggacaacatcgtgactgctcaggccatctacgagggactgtggatgtcctgcgt 284
RCOBs d19 (98%)    228  ---tggggacaacatcgtgactgctcaggccatctacgagggactgtggatgtcctgcgt 284

                   130  ttcgcaaagcaccgggcagatacagtgcaaagtcttcgactccttgctgaatctgaatag 189
                   285  ttcgcaaagcaccgggcagatacagtgcaaagtcttcgactccttgctgaatctgaatag 344
                   285  ttcgcaaagcaccgggcagatacagtgcaaagtcttcgactccttgctgaatctgaatag 344

                   190  tactttgcaggcaaccagagccttgatggtaattggcatcctgctggggctgatcgcaat 249
                   345  tactttgcaggcaaccagagccttgatggtaattggcatcctgctggggctgatcgcaat 404
                   345  tactttgcaggcaaccagagccttgatggtaattggcatcctgctggggctgatcgcaat 404

                   250  ctttgtgtccaccattggcatgaagtgcatgaggtgcttagaagatgatgaagtgcaaaa 309
                   405  ctttgtgtccaccattggcatgaagtgcatgaggtgcttagaagatgatgaagtgcaaaa 464
                   405  ctttgtgtccaccattggcatgaagtgcatgaggtgcttagaagatgatgaagtgcaaaa 464

                   310  gatgtggatggctgtcatcgggggcataatatttgtaatttcaggtctggcgacattagt 369
                   465  gatgtggatggctgtcatcgggggcataatatttgtaatttcaggtctggcgatattagt 524
                   465  gatgtggatggctgtcatcgggggcataatatttgtaatttcaggtctggcgatattagt 524

                   370  ggccacagcatggtatggaaatagaattgttcaagaattctatgaccccatgacccctgt 429
                   525  ggccacagcatggtatggaaatagaattgttcaagaattctatgaccccatgacccctgt 584
                   525  ggccacagcatggtatggaaatagaattgttcaagaattctatgaccccatgacccctgt 584

                   430  caatgccaggtatgaatttggccaggctctctttactggctgggctgctgcctccctctg 489
                   585  caatgccaggtatgaatttggccaggctctctttactggctgggctgctgcctccctctg 644
                   585  caatgccaggtatgaatttggccaggctctctttactggctgggctgctgcctccctctg 644

                   490  cctcctgggaggtg 503
                   645  cctcctgggaggtg 658
                   645  cctcctgggaggtgtcatcctttcctgctcctg 677
```

Figure 4.8 A Claudin 1 and 2 mRNA Expression by Osteoblastic Cells.

RT-PCR analysis revealed that osteoblastic cells express claudins 1 and 2 (A, →). Furthermore, cloning and sequence analysis have shown the sequences obtained for these claudin species to be identical to sequences obtained from liver control samples and to existing database sequences (B).

Furthermore, the claudin sequences identified proved to be identical to those obtained for the rat liver, mouse liver, rat brain, mouse brain control samples, in addition to being identical to those found in the sequence data base using BLAST search (fig. 4.8 A and B). Occasionally a smaller band of ~ 300 bp was observed. Sequence analysis demonstrated that these lower molecular weight bands are not claudin and that they represent nonspecific priming of these degenerate primers.

Although these experiments reveal that osteoblastic cells express a number of claudin family members they do not reflect the complex nature of the TJ. Recent studies have revealed that the tightness of the junctional barrier can be attributed to the specific association of different claudins molecules. Therefore, using RT-PCR, osteoblastic cells were screened for a selected group of claudin family members.

Claudins 3, 4, 5 and 8 have been recently characterised and shown to have a wide tissue distribution; therefore, the ability of osteoblastic cells to express these selected isoforms was assessed using RT-PCR. Claudin 3 mRNA expression was also detected in these cells by RT-PCR (fig. 4.8 B). Sequence analysis showed identity to previously published claudin 3 sequences. These cells, however do not appear to express claudins 4, 5 or 8 (fig. 4.8 C).

These observations indicate that osteoblastic cells cultured *in vitro* have the ability to express a number of proteins implicated in AJ formation and, in addition, express proteins associated with TJs at the mRNA level. These findings strongly suggest that osteoblastic cells have the ability to form and utilise apical junction complexes, possibly in order to achieve directed bone matrix transport. In an attempt to establish the potential ability of these cells to form intercellular junctions

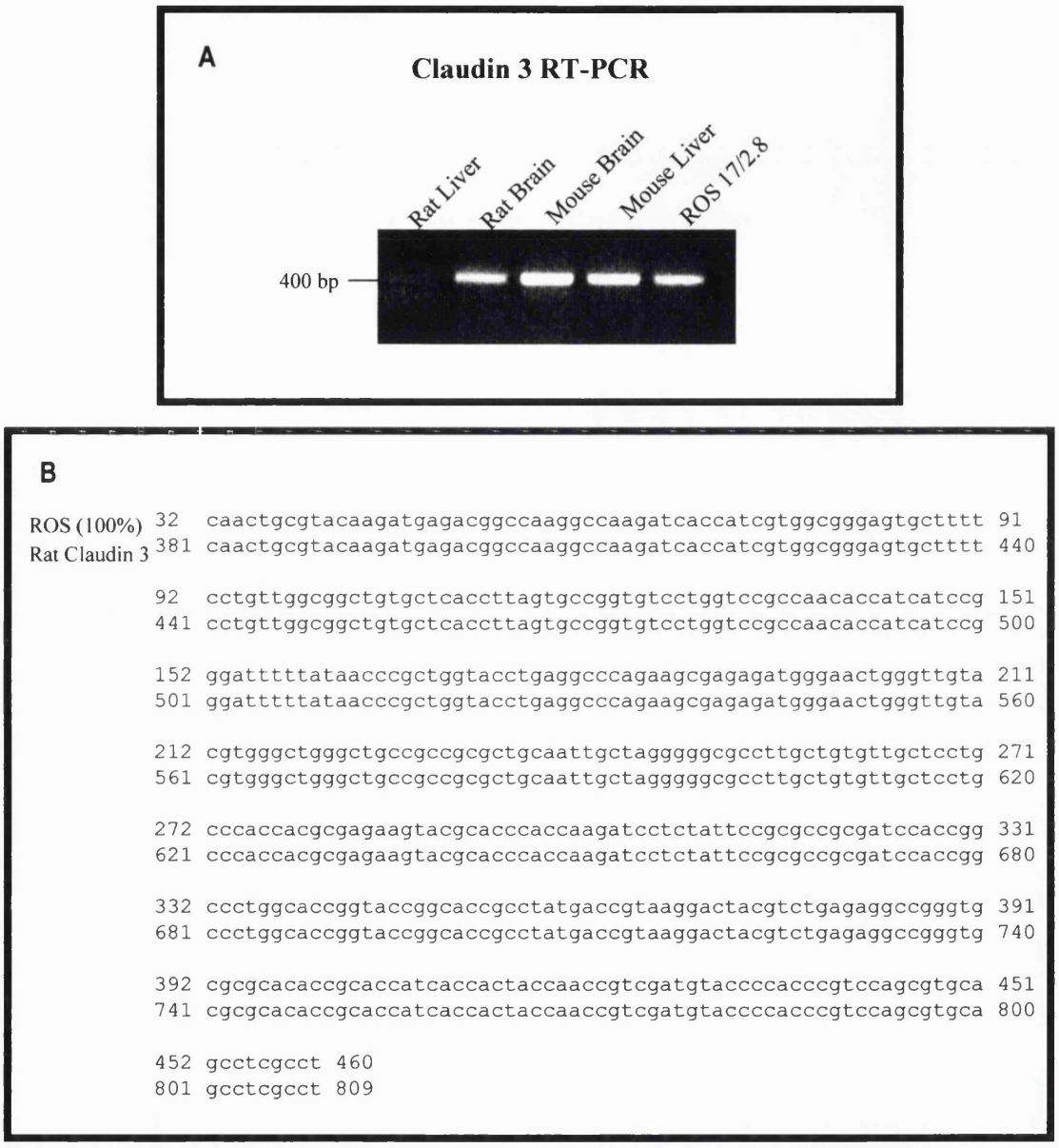

Figure 4.8 B Claudin 3 mRNA Expression by Osteoblastic Cells.

RT-PCR analysis revealed that osteoblastic cells express claudin 3 (A). Furthermore, cloning and sequence analysis has shown the sequences obtained for claudin 3 to be identical to sequences obtained from liver control samples and to existing database sequences (B).

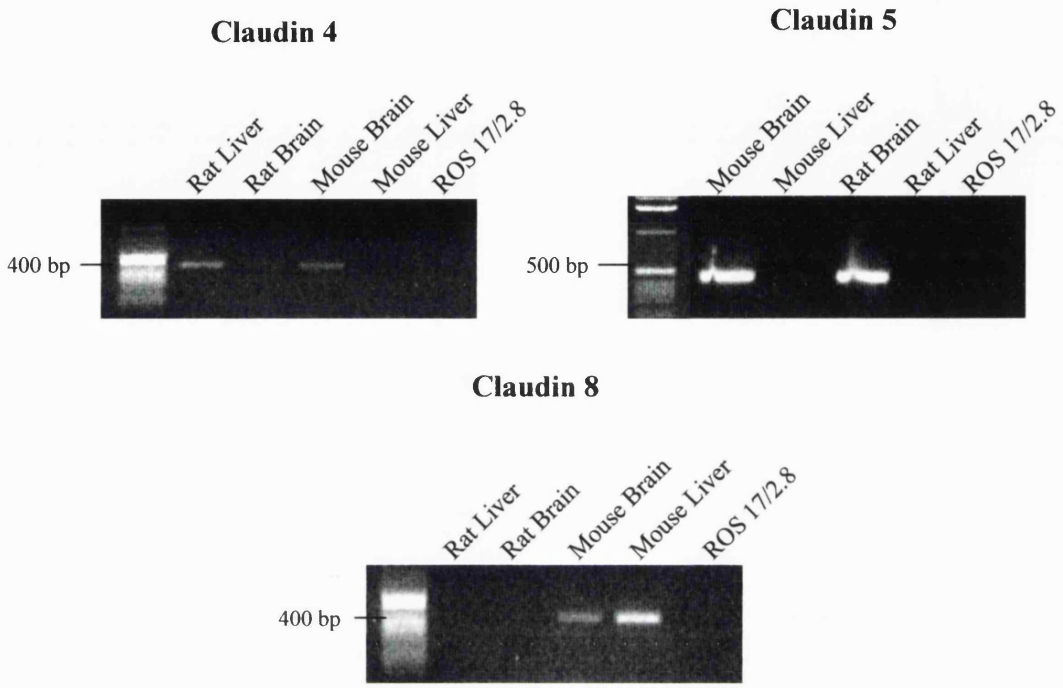

Figure 4.8 C Claudin Expression in Osteoblastic Cells.

RT-PCR analysis revealed that osteoblastic cells do not express claudin 4, 5 or 8.

in vivo the expression of cadherin was determined immunohistochemically on sections of embryonic rat calvaria (fig. 4.9).

4.3.8 *In vivo* Expression of Cadherins

Non-specific alkaline phosphatase and cadherin expression was localised to the cells lining the bone surface on transverse frozen sections of rat calvaria tissue. Specific localisation was observed around the cell periphery, especially at sites of cell to cell contact, indicating the potential of these cells to form intercellular junctional complexes *in vivo*. Unfortunately, localisation of occludin and claudins could not be assessed due to the limited availability and species reactivity of occludin and claudin specific antibodies.

Alkaline phosphatase expression in rat calvaria sections indicated that cells on the trabecular bone surface expressing cadherin had an osteoblastic phenotype (fig. 4.9).

4.4 Discussion

Junction formation in Osteoblast-like Cells

Osteoblasts form intercellular communicating junctions that may be responsible for the co-ordination of these cells into an epithelial type monolayer, enabling them to deposit bone matrix proteins as part of a concerted effort and possibly maximising the efficiency of matrix deposition. In addition, osteoblasts may use junction complex formation to establish and maintain cell polarisation during mineralisation.

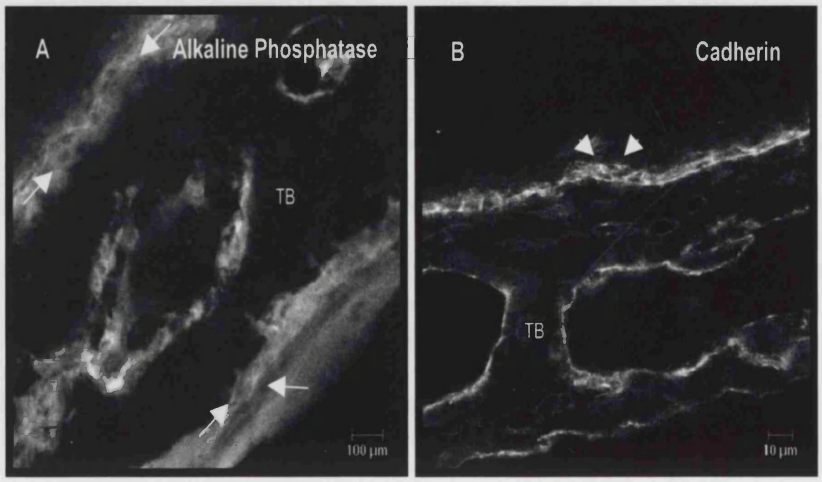

Figure 4.9 Cadherin Expression on Rat Calvaria sections.

Transverse sections of embryonic rat calvaria displayed cadherin immuno-reactivity in cells lining the trabecular bone surface. Specifically, these cells show cadherin expression at sites of cell to cell contact (arrowheads, B). The osteoblast cell phenotype marker alkaline phosphatase was detected in cells lining the bone surface (between arrows, A). TB = trabecular bone.

The data presented provide evidence that osteoblastic cells, such as ROS 17/2.8 and cell populations derived from embryonic rat calvaria, contain the protein components required for AJ formation *in vitro*. Extensive characterisation has revealed that these cells express the following AJ associated proteins: ZO-1, cadherins, α- and β-catenin, α-actinin and vinculin. Furthermore, these proteins were specifically localised towards sites of cell to cell contact in confluent cell cultures indicating the potential of these cells to form junction complexes. In areas of sub-confluence, in addition to a cytoplasmic pool, immuno-reactivity of these proteins was observed in a punctate distribution on the plasma membrane. This possibly reflects the re-distribution of these proteins to points of cell contact prior to the formation of the junction complex. The focal localisation of vinculin under cells and in contact with the matrix suggests that these structures may be focal adhesions.

Although, the presence of tight junction protein markers in osteoblastic could not be detected using immunocytochemistry and Western blot analysis, RT-PCR and sequence analysis revealed that osteoblastic cells have the potential to express occludin, in addition to claudins 1, 2, and 3.

Until recently, occludin was described as being the only integral membrane protein required for TJ formation (Furuse *et al.*, 1996; Furuse *et al.*, 1993). However, the recent development of occludin knockout embryonic stem cells has challenged this view (Saitou *et al.*, 1998). Subsequently, a novel multi-gene family of proteins, the claudins, have been identified and localised to, and implicated in TJ formation (Anderson and Van Itallie, 1999; Furuse *et al.*, 1998a; Furuse *et al.*, 1998b). The ability of these claudin family members to not only localise to the TJ but to actively incorporate into TJ fibrils (Furuse *et al.*, 1998b) has challenged this simplistic view

and consequently led to a re-evaluation of the molecular architecture of the TJ (for review see Tsukita and Furuse, 1999). The ability of osteoblastic cells to express, albeit at the mRNA level, a subset of this integral membrane protein family strongly suggests that these cells, under the appropriate conditions, have the ability to express TJ associated proteins. Moreover, it would therefore seem feasible that osteoblasts have the potential to form TJ complexes.

These studies have focused on characterising the expression of proteins associated with TJ and AJ formation; however, the ability of these cells to form junction complexes has not been investigated at a morphological level in this study. In addition to the extensively characterised GJ communication observed in these cells, osteoblasts were also shown to form AJ (Bhargava *et al.*, 1988; Palumbo *et al.*, 1990). In an attempt to further establish AJ formation and the potential for TJ formation in osteoblasts, we propose to undertake a number of morphological studies using transmission electron microscopy. Having established the potential of osteoblasts to form apical junctional complexes, an entirely new set of questions arises. Are these complexes crucial for osteoblast cell function? Would the inability of osteoblasts to form either AJ/TJ directly or indirectly affect the process of mineralisation? These questions, to varying degrees, have been asked in epithelial cell models. Studies have revealed that apical junctions, in particular TJ, are crucial for epithelial 'barrier' and 'fence' functions. Recent advances using knockout mice have shown AF-6 to be crucial for TJ formation, with AF-6 knockout embryos dying early in development. These knockout mice develop until around embryonic day 9/9.5 when, due to the inability of cells to maintain the cohesive nature of the epithelial monolayer, the epithelium disrupts rendering them non-viable (Citi, 2000; Ikeda *et al.*, 1999).

Cell to Matrix Interactions Influence Cell Polarity

In an attempt to evaluate the optimal conditions required for junction complex formation and hence polarisation in osteoblastic cells, cells were plated onto a variety of substrates and the expression of ZO-1 in these cells examined. Briefly, ZO-1 localises to the plasma membrane in a non-continuous fashion under sub-optimal adhesion conditions, i.e. when the cells are cultured on fibrillar collagen. However, and possibly not surprisingly, ZO-1 in RCOBs cultured on osteopontin localised in a linear fashion towards cell to cell contact sites. This observation possibly re-emphasises the role that osteopontin may play in bone cell attachment and spreading.

In ROS 17/2.8 cells, junction protein expression appears to be dependent upon the substrate onto which these cells were cultured. This suggests that the maintenance and formation of junction complexes depends on interaction with a previously synthesised matrix and the ability of these cells to establish cell to extracellular matrix contact (ECM). It would therefore be interesting to investigate further the mode of cell to matrix adhesion and in particular the potential role of integrins in junction formation and the establishment of cell polarity. Recent investigations have identified a number of integrins in osteoblastic cells, namely, α1, α2, α3, α4, α5, β1 (reviewed by Bennett *et al.*, 2000). There is evidence to suggest that osteoblasts may display different expression patterns of these integrins at different stages of osteoblast development and maturation. β1 is thought to play a major role in osteoblast cell function. Establishing a suitable model to study the role of individual integrins in bone formation has proven to be difficult and null mutations of β1 result in embryonic mortality at a stage of skeletal immaturity (Fassler and Meyer, 1995). In an attempt to overcome these problems, β1 null embryonic stem cells were generated and implanted into mice; cells isolated from the resulting β1

null chimeras showed alterations in their adhesive properties and in extracellular matrix deposition (Brakebusch *et al.*, 1997). In addition, the expression of a dominant negative β1 subunit, targeted to mature osteoblastic cells *in vivo*, has been used to target transgene expression in transgenic mice (Zimmerman *et al.*, 2000). The expression of the dominant negative β1 subunit was controlled by the osteocalcin promoter, which is only expressed in mature osteoblasts and osteocytes. Transgenic animals, with altered integrin function in mature osteoblasts and osteocytes, displayed an osteoporotic phenotype, suggesting a potential role for β1 integrins in bone turnover (Bennett *et al.*, 2000; Zimmerman *et al.*, 2000).

These investigations have revealed that ROS 17/2.8 cells and RCOBs behave differently when cultured on a variety of substrates assessed by the localisation patterns of ZO-1 expression. They suggest that data generated from the analysis and comparison of immortalised cell lines such as ROS 17/2.8 with primary cell culture and *in vivo* osteoblastic cells must be interpreted with caution. Many phenotypic and morphological differences have been identified in transformed cells lines compared to *in vivo* osteoblastic cell function (limitations of ROS 17/2.8 cell cultures have been previously discussed in Chapter 3). Therefore, future studies characterising junction protein expression within osteoblasts should be carried out on RCOB cultures and, in particular, on cells with the ability to form and mineralise nodules *in vitro* (Chapter 3). Such *in vitro* models of mineralisation will present a population of functional osteoblast-like cells and allow junction formation to be investigated and manipulated at various osteoblast differentiation states.

In view of the sequential nature of apical junction complex formation, in particular the suggestion that AJ formation is a pre-requisite for TJ formation (Furuse *et al.*, 1994; Rajasekaran *et al.*, 1996), these data have provided evidence supporting AJ

formation within osteoblast cell monolayers *in vitro*. Therefore, it seems feasible to hypothesise that osteoblastic cells may form tighter intercellular associations during the process of mineralisation.

This idea of sequential junction complex formation is, however, currently under debate. The role of cadherin-mediated AJ formation in epithelial TJ assembly has been examined using calcium switch experiments (Denker and Nigam, 1998). MDCK cell monolayers cultured in the absense of calcium lack cell to cell contact and intercellular junctions. Raising intracellular calcium triggers a series of molecular events that consequently restore the TJ, polarity and transepithelial resistance (Rajasekaran *et al.*, 1996). In contrast to this, Citi and co-workers (1992 and 1994) have demonstrated TJ formation, in the absense of functional AJs, to occur in calcium depleted cell systems. Treatment with kinase inhibitors, such as H-7 or sautrosporine (Citi, 1992; Citi *et al.*, 1994; Denisenko *et al.*, 1994), are required for this to occur. These findings suggest that the mechanisms by which kinase inhibitors promote junctional integrity are cadherin-independent, implying that TJ biogenesis is independent of AJ formation. Studies implicating ZO-1 in the stabilisation of both the AJ and TJ complexes, however, suggest that such a hierarchy exists (Gumbiner, 1987; Howarth and Stevenson, 1995; Itoh *et al.*, 1993). In addition these studies also suggest that PDZ domain (postsynaptic protein-95/discs large/zonula occludens-1, PSD-95/DLG/ZO-1; PDZ) containing proteins, such as ZO-1, may act as 'clustering molecules'. The cellular function of these molecules may be to cluster TJ associated proteins at the plasma membrane, prior to their translocation to the site of intercellular contact, in response to E-cadherin activation (Cereijido *et al.*, 2000).

Observations in freeze fracture EM samples of odontoblasts have demonstrated that they can form AJs and GJs, in addition to TJs, during the process of dentinogenesis (Arana-Chavez and Katchburian, 1997; Calle, 1985) adding credence to the hypothesis that osteoblastic cells may form TJs during the mineralisation process. It is, however, possible that osteoblast-like cells may only express tight junction associated proteins during mineralisation. Of particular interest would be to investigate the ability of osteoblast-like cells to maintain AJ complexes during the process of mineralisation.

Although these studies leave several unanswered questions, this work has provided valuable insight into osteoblast cell function, in particular, the possibility that osteoblastic cells establish and maintain cell polarity through the formation of intercellular junctions. These data suggest that osteoblasts may achieve cell polarity in a similar way to epithelial cells, implicating apical junction formation and cell to matrix interactions as crucial factors in the establishment and maintenance of this cell state. Furthermore, these characterisation studies have set the scene for investigating the mechanisms responsible for the directionality of bone matrix protein secretion. Although osteoblastic bone matrix protein secretion is known to be directional very few studies have focused on characterising the molecular machinery used by these cells to achieve cell polarity or to achieve directional bone matrix protein secretion.

This study has identified key intercellular junction associated proteins that form part of the core molecular mechanisms used by osteoblastic cells to achieve and maintain cell polarity. These results complement the recent findings published by Ilversaro *et al.* (1999) identifying, by means of virus infection, the apical and basolateral membrane domains of osteoblastic cells. These results demonstrate that

osteoblasts are indeed polarised and, thus, have the potential to target newly synthesised bone products specifically towards the site of deposition.

Polarisation and correct targeting of bone matrix proteins towards the specific site of bone deposition is crucial to the bone formation process. Mis-regulated bone formation has been observed in a number of metabolic bone diseases, such as fibrodysplasia of bone, osteopetrosis, osteogenesis imperfecta and Paget's disease. Investigating the process of regulated and vectorial bone matrix protein secretion in disease would provide valuable insight into both normal and pathological osteoblast cell function.

In chapter 5, the identification and characterisation of components of the protein machinery that may be implicated in the directionality of bone matrix protein secretion and thus osteoblast cell function is investigated.

Chapter 5

VESICULAR TRAFFICKING IN OSTEOBLASTS

Chapter 5

VESICULAR TRAFFICKING IN OSTEOBLASTS

5.1 Introduction

Transport between the membrane bound compartments of the secretory pathway is mediated by membrane bound vesicular intermediates. Recent progress has lead to the identification of a number of protein components implicated in vesicle and target membrane fusion events (Sollner *et al.*, 1993b; Trimble *et al.*, 1988), leading to a better understanding of the molecular mechanisms mediating vesicular transport. Ultimately, these studies have led to the definition of the SNARE hypothesis (see Chapter 1 fig. 1.8) (Rothman, 1994; Rothman and Orci, 1992; Sollner *et al.*, 1993a; Sollner *et al.*, 1993b; Sollner and Rothman, 1996) as a possible mechanism for membrane targeting and fusion events. Although a number of studies have challenged this hypothesis, more specifically the stages at which these protein interactions defining vesicle targeting and fusion occur (Nichols *et al.*, 1997; Burgoyne and Morgan, 1998; Clague, 1999; Fasshauer *et al.*, 1997; Shorter and Warren, 1999), the SNARE hypothesis remains a general model for regulated exocytosis.

5.1.1 The SNARE Hypothesis

Briefly, the SNARE hypothesis (Sollner *et al.*, 1993a; Sollner *et al.*, 1993b) proposes specificity of vesicular trafficking to be mediated by a family of membrane bound proteins that localise to the vesicle membrane, v-SNARE (vesicle membrane associated soluble NSF attachment protein receptor), and to the target membrane, t-SNARE (target membrane associated soluble NSF attachment protein receptor).

In addition, this hypothesis emphasises the necessity for specific v-/t-SNARE pairing throughout the transport pathway.

In addition to the integral membrane proteins mediating vesicle tethering and docking events, a number of cytoplasmic proteins have been identified and shown to be crucial for membrane fusion. These fusion proteins NSF, (NEM (N-ethylmaleimide) sensitive fusion protein) and α-SNAP (soluble NSF attachment protein) (McMahon and Sudhof, 1995; Rothman, 1994; Sollner and Rothman, 1996), have been identified in a number of cell types and form part of the conserved core of proteins required for membrane fusion.

5.1.2 Vesicular Transport

Three main steps in vesicular transport have been described: budding, docking and fusion to the target membrane of transport vesicle. Recent studies have identified a highly stable, SDS resistant, VAMP2 (v-SNARE)/syntaxin-1 (t-SNARE)/SNAP25 complex. This core SNARE complex is implicated in vesicle docking/tethering (Fasshauer *et al.*, 1997; Sollner *et al.*, 1993a; Sollner *et al.*, 1993b) and binds α-SNAP and NSF, resulting in the formation of a 20S docking and fusion particle (Rothman, 1994). The precise role of these protein complexes in catalysing membrane fusion remains to be determined; however, existing evidence strongly suggests that the SNARE complex acts as direct catalyst of membrane fusion (Hayashi *et al.*, 1994) (Chen *et al.*, 1999; Weber *et al.*, 2000).

5.2 Aim

Osteoblasts have the ability to direct newly synthesised bone matrix proteins towards the bone surface, specifically to sites of bone formation. The aim of this study was to identify proteins that may play a role in the directionality of bone matrix protein secretion in osteoblasts.

5.3 Specific Objectives

Primarily these studies concentrated on establishing the expression of the general fusion proteins, NSF and SNAP, in osteoblasts. Furthermore, the presence of a SNARE mediated transport pathway was investigated by characterising the expression of possible targeting v-SNAREs, such as VAMP and synaptotagmin, and t-SNAREs, such as syntaxin and SNAP-25, in these cells.

5.4 Specific Methods

5.4.1 Cell Models Used

Both the rat osteosarcoma cell line ROS 17/2.8 and primary osteoblast-like cells derived from embryonic rat calvaria were used as osteoblastic cell models. Primary cells were cultured for 22 days in the presence of β-GP, Asc and dex, under the conditions determined and described in chapter 3, to stimulate nodule formation and mineralisation *in vitro*.

In addition, the neuronal cell line, PC12 phaeochromocytoma, derived from a chromaffin cell tumour was used as a positive control for fusion and SNARE protein expression. Upon treatment with NGF (nerve growth factor), PC12 cells

can be stimulated to differentiate, acquiring some of the characteristics of mature sympathetic neurons.

5.4.2 Neuronal Controls Used for Western Blot Analysis

SNAP/SNARE mediated membrane fusion has been well characterised in the neuronal system. Thus, cell and cell extracts isolated from the neuronal system were used as a comparative control of NSF, α-SNAP and SNARE protein expression. Highly Purified rat synaptic vesicles (5 μg), the crude vesicle containing fraction, lysate pellet fraction 2 (LP2), along with a crude unfractionated brain tissue preparation, (PNS cortex, post nuclear supernatant) were obtained. These fractions were prepared as described by (Huttner *et al.*, 1983). All samples, synaptic vesicle, brain and osteoblastic cell preparations were resuspended in SDS loading buffer and resolved on a 14 % SDS-PAGE gel together with total cell extracts prepared from ROS 17/2.8 cells (~ $1x10^5$ cells were loaded per lane) and days 5 and 19 of primary osteoblast nodule forming and mineralising cell cultures.

5.4.3 RT-PCR – VAMP1 Primers

VAMP1 expression was detected using RT-PCR (methods sections 2.2.6 and 2.2.7) with primers directed against the extreme N-terminal portion of the rat VAMP1 cDNA transcript, VAMP1 5'a, and a second 22 oligomer primer located further downstream, in the region of exon III, VAMP1 3'a (fig. 5.1). The expected size of the VAMP1 PCR product is 256 bp. β-Actin primers were used to assess the quality of the cDNA, with a product size of 592 bp.

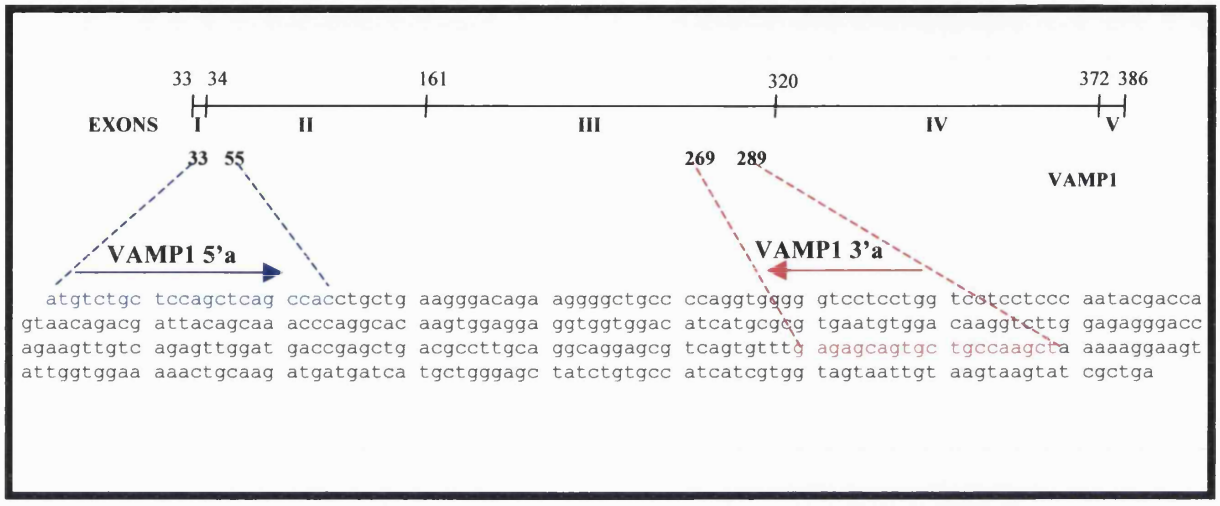

Figure 5.1 Location of VAMP1 Primers on rat VAMP1A cDNA Transcript.

VAMP1 5'a is located at the extreme N-terminal portion of the VAMP1 cDNA transcripts whilst VAMP1 3'a is located further downstream in the region encoding exon III. The expected VAMP1 PCR product size is 256 bp.

5.5 Results

5.5.1 Expression of the General Fusion Machinery Proteins NSF and α-SNAP

The starting point for this study was to determine the presence of the general fusion machinery proteins, α-SNAP and NSF, in osteoblasts. SNAPs and NSF are conserved peripheral membrane proteins that are essential for membrane fusion and are implicated in recycling of SNARE receptors.

A number of SNAP isoforms have been identified to date, α-, β- and γ-SNAP. β-SNAP is believed to have an almost exclusive neuronal tissue distribution, α-SNAP is described as being the ubiquitously expressed SNAP isoform, whilst γ-SNAP is the most distantly related SNAP isoform. Therefore this study determined α-SNAP expression in osteoblastic cells.

5.5.1.1 Western Blot Analysis of α-SNAP and NSF Protein Expression

The presence of NSF and α-SNAP was determined in ROS 17/2.8 and primary osteoblast-like cells taken from days 5 and 19 of nodule forming and mineralising cultures. In addition the neuronal samples (LP2 fraction, PNS cortex, rat purified synaptic vesicles), PC12 cells and NGF-differentiated PC12 cells were used as controls. Using western blot analysis, samples were probed with antibodies directed against NSF and the ubiquitously expressed SNAP isoform, α-SNAP (fig. 5.2).

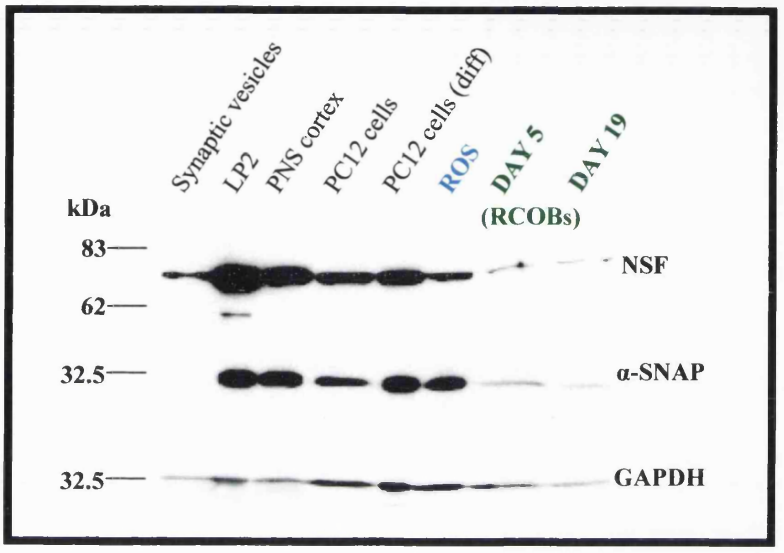

Figure 5.2 Osteoblasts Express the General Fusion Machinery Proteins α-SNAP and NSF. Using western blot analysis, the expression of the general fusion machinery proteins NSF and α-SNAP was determined in neuronal control cells/extracts, the osteoblastic cell line ROS 17/2.8 and in primary osteoblast-like cells (RCOBs) from days 5 and 19 of nodule forming and mineralising cell cultures. NSF and α-SNAP are expressed in both crude brain tissue extracts as well as in PC12 cells. Although α-SNAP expression was not detected on purified rat synaptic vesicles, this vesicle population showed low levels of NSF immuno-reactivity. More importantly, NSF and α-SNAP expression was observed in all the osteoblastic cell populations studied. GAPDH expression was used to assess protein loading.

NSF and α-SNAP both appear to be abundant in the crude brain extracts, PNS cortex and LP2 fractions. In contrast, low levels of NSF expression were detected in purified rat synaptic vesicles; however α-SNAP was not detected. In addition to PC12 cells, the expression of both of these key protein components, α-SNAP and NSF, was observed in osteoblast-like cell cultures. The level of expression observed in these cells, however, appears to be lower than that of the neuronal cell controls. Primary cells from nodule forming and mineralising cell cultures are difficult to harvest due in part to the level of matrix and mineral deposited towards the latter stages of the culture and this may account, in part, for the low levels seen compared to ROS 17/2.8 cells.

5.5.1.2 Immunolocalisation of NSF in Primary Osteoblast-Like Cells

Using confocal laser scanning microscopy and immunocytochemistry, NSF localisation was determined in primary cells taken from day 4 of nodule forming and mineralising cultures. Cells were triple stained with the monoclonal 6E6 antibody, recognising the ATP binding domain of NSF, osteocalcin, a mature osteoblastic phenotype marker, and rhodamine conjugated phalloidin which stains F-actin (fig. 5.3). NSF expression (green) localised to the intracellular organelles associated with the secretory pathway, namely the Golgi and the endoplasmic reticulum (ER). In addition, NSF immuno-reactivity was also detected at the nuclear membrane and at sites of cell-cell/cell-matrix contacts as well as at possible exocytosis sites (indicated by the arrowhead in figure 5.3).

Similarly, osteocalcin expression (blue) localised to the ER and Golgi. Areas of co-localisation of NSF with cortical F-actin are shown in yellow.

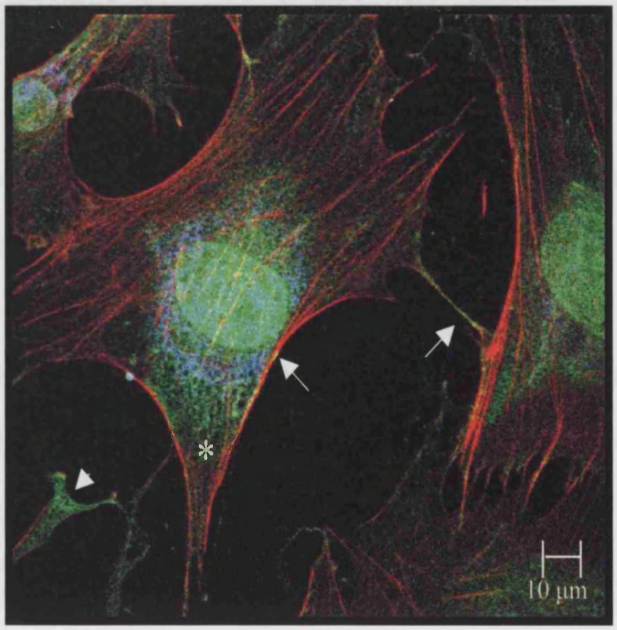

Figure 5.3 NSF Localisation in Primary Osteoblast-Like Cells.

This composite confocal image represents triple immunostaining using specific antibodies directed against NSF (green), osteocalcin (blue) and phalloidin to detect F-actin (red). This was performed on post-proliferative primary osteoblast-like cells taken from day 4 of a nodule forming culture. Osteocalcin, localises to the endoplasmic reticulum and Golgi in these cells. In addition, NSF also localises to intracellular compartments associated with the secretory pathway, Golgi and endoplasmic reticulum (*). Interestingly, NSF immuno-reactivity was also detected at sites of cell to cell, cell to matrix contact (→, areas of co-localisation of NSF with actin are represented in yellow) and at possible exocytosis sites (indicated by the arrowhead).

To investigate further the presence of a SNARE mediated vesicular transport pathway in osteoblast-like cells, cells were screened further for the presence of key SNARE proteins.

5.5.2 v-SNARE Expression in Osteoblasts

A large number of v- and t-SNAREs have been identified to date. These have been grouped into a number of families, of which VAMP and synaptotagmin are two v-SNARE families, and syntaxin is a family of t-SNAREs.

VAMPs (vesicle associated membrane proteins) have been identified and implicated in regulated exocytosis in both neuronal and non-neuronal tissues. Until recently three isoforms of VAMP had been identified, VAMP1 and 2 (Trimble, 1993; Trimble *et al.*, 1988; Trimble *et al.*, 1990) and a third non-neuronal isoform, cellubrevin (Chilcote *et al.*, 1995; Grote *et al.*, 1995; McMahon *et al.*, 1993). In addition to the differential neuronal distribution observed for VAMPs 1 and 2, these proteins have been shown to have a wider tissue distribution (Rossetto *et al.*, 1996). Along with the VAMP family of v-SNAREs, a number of other v-SNAREs have been identified and their role in vesicular trafficking investigated, i.e. the growing family of synaptotagmins, calcium sensitive v-SNAREs.

5.5.2.1 VAMP Expression in Osteoblastic Cells

Although a number of new VAMP isoforms (Advani *et al.*, 1998; Wong *et al.*, 1998b) (Advani *et al.*, 1999; Steegmaier *et al.*, 1999; Zeng *et al.*, 1998) and splice variants (Berglund *et al.*, 1999; Isenmann *et al.*, 1998; Mandic *et al.*, 1997) with varying tissue distributions have been identified, these studies concentrated on the expression of two key VAMP family members, VAMP1 and VAMP2, in osteoblastic cells.

Cellubrevin, implicated in intra-Golgi trafficking (Galli *et al.*, 1994; Link *et al.*, 1993; McMahon *et al.*, 1993) was not investigated since this study investigated events occurring further downstream in the secretory pathway, namely Golgi to plasma membrane trafficking. Using western blotting and immunofluorescence techniques VAMP1 expression was identified in the rat osteoblast cell line ROS 17/2.8.

5.5.2.2 Western Blot Analysis of VAMP1 Expression

Western blot analysis with an antibody directed against the N-terminal portion of the VAMP1 molecule was used to investigate and compare VAMP1 expression in ROS 17/2.8 to that on highly purified rat synaptic vesicles. In addition, the epithelial cell line, MDCK, was used as a negative control (fig. 5.4).

ROS 17/2.8 cells express an isoform of VAMP1 with an apparent molecular weight 2 kDa larger in size than the protein detected on the purified rat synaptic vesicles. VAMP1 expression was not detected in MDCK cells. The differential electrophoretic mobility of VAMP1 expressed in osteoblastic cells may reflect post-translational modifications or an osteoblastic isoform of the VAMP1 v-SNARE. Alternatively this size difference may represent a VAMP1 splice variant, a result of alternative splicing of the VAMP1 cDNA transcript.

5.5.2.3 Immunolocalisation of VAMP1 in ROS 17/2.8 Cells

VAMP1 was localised in osteoblastic cells using indirect immunofluorescence and confocal laser scanning microscopy. ROS 17/2.8 cells and PC12 cells were plated onto glass coverslips, grown to confluence and immunostained for VAMP1 (as described in methods section 2.2.2). A vesicular type cytoplasmic distribution of

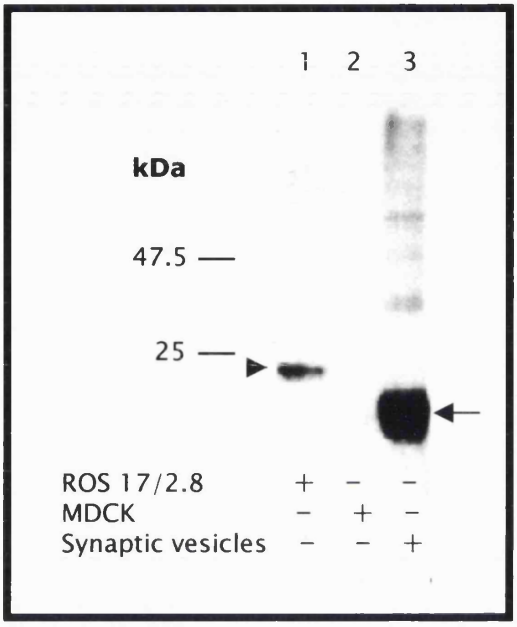

Figure 5.4 ROS 17/2.8 Cells Express an isoform of the v-SNARE, VAMP1.

Using Western blot analysis, VAMP1 was detected in the osteosarcoma cell line ROS 17/2.8 but not in the epithelial cell line MDCK. VAMP1 expressed in ROS 17/2.8 cells (arrowhead) appears to have an apparent molecular weight 2 kDa larger in size than the protein detected on purified rat synaptic vesicles (→).

VAMP1 was observed in undifferentiated PC12 cell populations (fig. 5.5 A, →). Although VAMP1 was detected in a vesicular type distribution within the cytoplasm of ROS 17/2.8 cells, VAMP1 immuno-reactivity showed a perinuclear distribution (fig. 5.5 B, →).

5.5.2.4 Effect of Dexamethasone and Ascorbate Treatment on VAMP1 Expression

Glucocorticoids such as dex stimulate osteoblast cell proliferation and differentiation resulting in an increase in osteogenesis *in vitro*. L-Ascorbate affects bone cell proliferation and is crucial for collagen matrix synthesis *in vitro*. Therefore, treatment of cell cultures with dex and L-Asc was used as a tool to examine whether VAMP1 expression was modulated in osteoblasts under culture conditions promoting osteoblastic cell differentiation.

Cells were treated either with dexamethasone or with L-ascorbate while control cells remained untreated. In addition to VAMP1 expression, the distribution of osteopontin, a non-collagenous bone matrix protein, was observed and the stability of the osteoblastic phenotype monitored histochemically using alkaline phosphatase staining throughout the culture period.

An increase in alkaline phosphatase staining was observed in both Asc and dex treated cultures, compared to untreated cell controls. Although, both Asc and dex treatment showed a stimulatory effect on alkaline phosphatase staining, the intensity of alkaline phosphatase staining was highest in dex treated cell cultures. Despite this increase in alkaline phosphatase staining, no dramatic changes in distribution or amount of VAMP1 were observed in ROS 17/2.8 cells cultured with Asc or dex when compared to control cultures (data not shown).

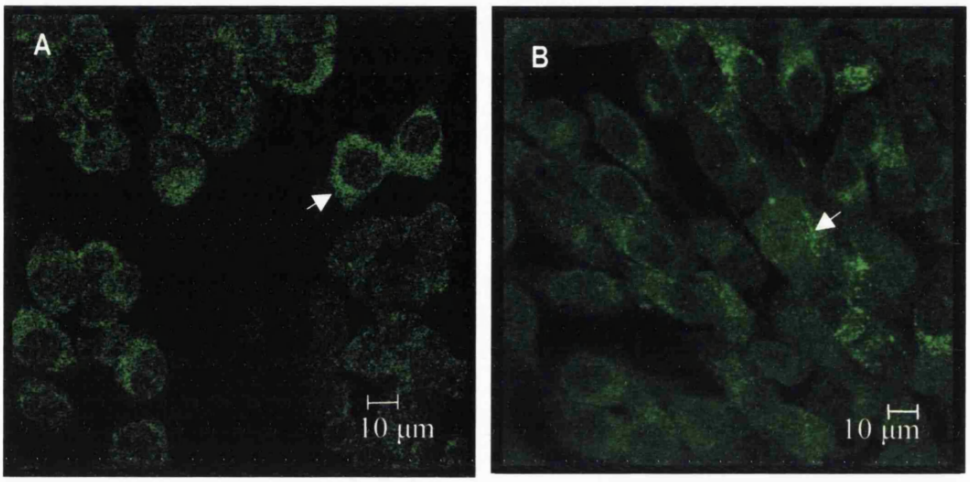

Figure 5.5 VAMP1 Expression In ROS17/2.8 and PC12 Cells.

VAMP1, shown in green, has a cytoplasmic and vesicular type distribution in both PC12 cells (A, →) and in the osteoblast cells line ROS 17/2.8 cells (B). In ROS 17/2.8 cells VAMP1 immuno-reactivity appears to localise to a perinuclear distribution within the cell cytoplasm (B, →).

Results obtained for osteopontin expression revealed osteopontin to have both a perinuclear and cytoplasmic distribution in ROS 17/2.8 cells, which remains largely unaffected by Asc treatment. In some experiments, osteopontin expression appears to be elevated in dex treated cultures although, this was not rigorously investigated (data not shown).

5.5.2.5 VAMP1 Expression in Nodule Forming Cell Cultures

VAMP1 protein expression was determined in primary osteoblastic cells taken from day 16 of nodule forming and mineralising cell cultures. The intracellular localisation of VAMP1 was investigated in condensing nodules and compared to the localisation of the Golgi marker GM130. Triple staining was carried out using rhodamine conjugated phalloidin (red, F-actin), antibodies directed against the N-terminus of VAMP1 (green) as well as the Golgi marker, GM130 (blue). VAMP1 was shown to be expressed in the cells forming the nodule (fig. 5.6 A) and in the cells of the monolayer (fig. 5.6 B); however, VAMP1 staining was more intense in cells forming the nodule (fig. 5.6 A). Lateral views of the nodule, taken in the ZX plane (fig. 5.6 A), confirm that these cells organise themselves into multi-layers forming the three dimensional nodule structure, similar to those determined ultrastructurally by Aubin and co-workers, 1988. Higher magnification of the cells forming the monolayer reveals VAMP1 expression to be vesicular, localising to the cytoplasm (fig. 5.6 B), comparable to the VAMP1 distribution observed in ROS 17/2.8 cells (fig. 5.5).

Figure 5.6 VAMP1 Localisation in Nodule Forming Cultures.

Primary osteoblastic cells from day 16 of a nodule forming culture were stained for the presence of VAMP1. Triple staining using rhodamine conjugated phalloidin (red), VAMP1 (green) and the Golgi marker, GM130 (blue) indicated that VAMP1 was expressed in all the cells (A); moreover, VAMP1 expression is concentrated in cells forming the nodule structure (x16 view). Higher magnification (x63) demonstrated VAMP1 expression to be cytoplasmic and most intense in cells localising towards the nodule (A). The lateral view (ZX) illustrates that cells on top of the nodule have higher VAMP1 expression levels. In addition, VAMP1 was observed in cells forming the monolayer (B) and localised to the cell cytoplasm in vesicular-like structures. There was no evidence suggesting co-localisation of VAMP1 with the Golgi marker, GM130, in these cells.

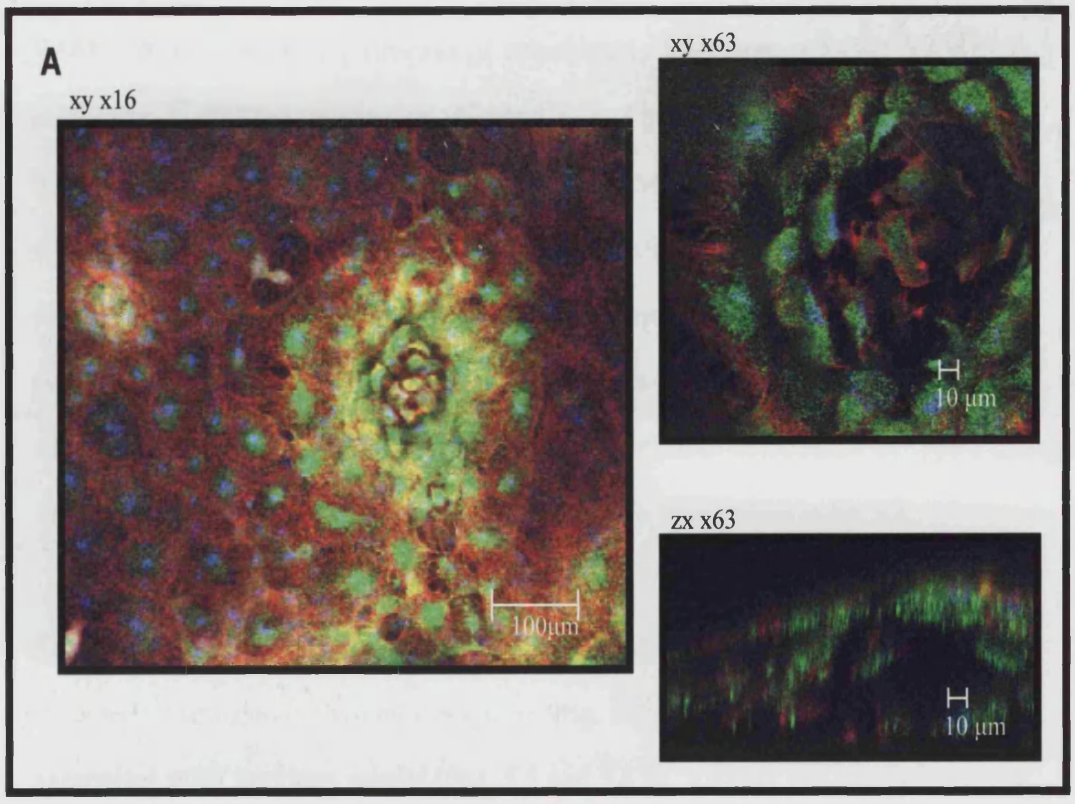
A
xy x16
100µm
xy x63
10 µm
zx x63
10 µm

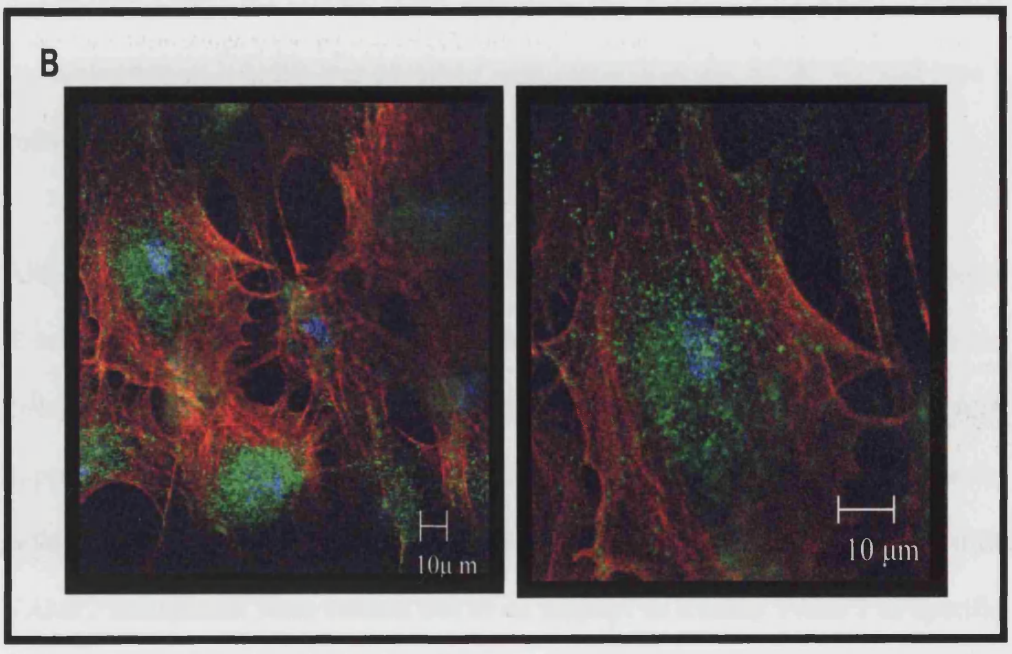
B
10µ m
10 µm

5.5.2.6 Co-localisation of VAMP1 with Transported Matrix Proteins

VAMP1 protein expression in osteoblast-like cells indicates a possible role for VAMP1 in the secretory pathways of osteoblasts. However, whether VAMP1 is implicated in directed matrix protein secretion has not been determined. Therefore, in an attempt to elucidate the specific role for VAMP1 during bone matrix protein secretion, dual labelling of ROS 17/2.8 cells with VAMP1 and the transported matrix proteins osteocalcin (fig. 5.7 A) and type I collagen (fig. 5.7 B) was performed. VAMP1 is shown in green whilst both osteocalcin and type I collagen are shown in blue. Areas of apparent co-localisation of osteocalcin or type I collagen and VAMP1 is indicated by arrows and appears pale blue/white in fig. 5.7.

Typically, osteocalcin localises to the ER and Golgi whilst type I collagen is found dispersed throughout the cell cytoplasm (fig. 5.7 A and B, shown in blue). In agreement with previous results (figs. 5.5 and 5.6 B), VAMP1 has a vesicular type distribution within the osteoblast cell cytoplasm (fig. 5.7 A and fig. 5.7 B). Limited co-localisation of VAMP1 was observed with osteocalcin (fig. 5.7 A, →), and type I collagen (fig. 5.7 B, →) in these cells.

Although the specific intracellular localisation of VAMP1 has not yet been determined, we hypothesise that the vesicular structures observed in osteoblastic cells could represent biosynthetic transport intermediates, a hypothesis which is supported by the observation that VAMP1 expression increases in the osteoblastic cells forming nodule structures, fig. 5.6 A and B. Further investigations into VAMP1 localisation were carried out in an attempt to localise VAMP1 to specific subcellular compartments of the secretory pathway (discussed in detail in Chapter 6).

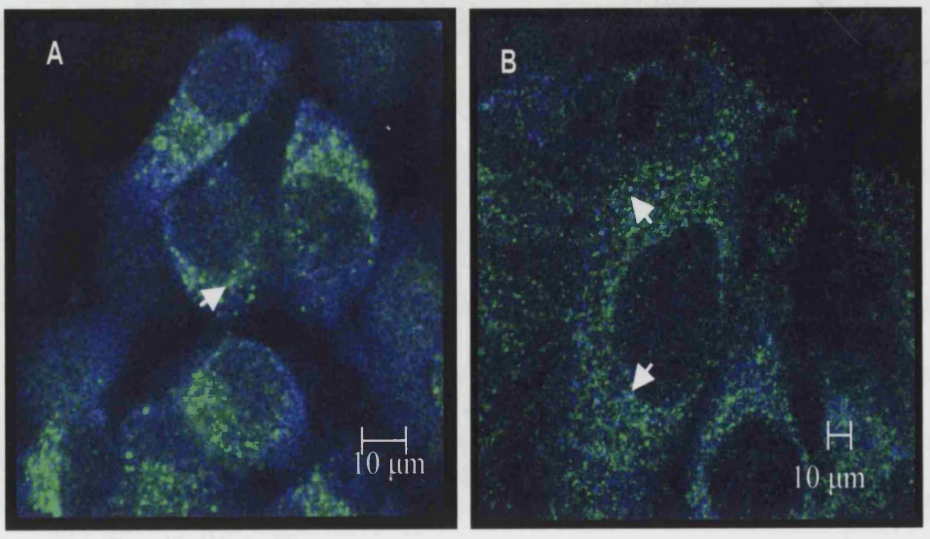

Figure 5.7 VAMP1 Co-localistion with Osteocalcin and Type I Collagen.

Using dual labelling techniques, VAMP1 co-localisation with transported bone matrix proteins, osteocalcin and type I collagen, was determined in ROS 17/2.8 cells. FITC labelled VAMP1 (green) has a vesicular distribution throughout the cell cytoplasm (figs. A and B) whilst osteocalcin (A, blue) localises to the ER and Golgi and type I collagen staining is dispersed throughout the cytoplasm (B, blue).

These *in vitro* studies outline v-SNARE protein expression in osteoblastic cells, though they may not represent osteoblastic cell behaviour and SNARE protein expression *in vivo*. Therefore to determine VAMP1 expression *in vivo*, immunohistochemistry was performed on cryostat sections of rat calvaria.

5.5.2.7 VAMP1 Expression in Embryonic Rat Calvaria

Transverse frozen sections of day 21 embryonic rat calvaria were collected at 7 μm intervals and individual bone cells identified immunohistochemically. Osteoclasts were identified using the F11 antibody directed against the rat β_3 integrin, which recognises the vitronectin receptor ($\alpha_v\beta_3$) expressed on the osteoclast cell surface. Similarly osteoblasts were identified using the mature osteoblast phenotype marker osteocalcin. VAMP1 expression was determined as described previously in methods section 2.2.4. Osteoclasts were identified as large cells situated on the trabecular bone (TB) surface (fig. 5.8), whereas osteoblasts were identified as cuboidal cells lining the bone surface. Osteocalcin expression was also detected at lower levels within the osteocyte lacunae (fig. 5.8). VAMP1 was observed towards the bone surface in these rat calvarial sections (fig. 5.8) and higher magnification (x63) revealed VAMP1 immuno-reactivity in cells lining the trabecular bone surface, though not all osteocalcin positive osteoblasts appeared to express VAMP1 equally. Immuno-reactivity was also detected in the skin and hair follicles; this is due to a known contamination of the polyclonal VAMP1 antibody preparation with antibodies recognising keratin.

Figure 5.8 VAMP1 is Localised to the Trabecular Bone Surface in Rat Calvaria.

Transverse sections were collected at 7 μm intervals from either embryonic day 21 or day 3 rat calvaria. Osteoclasts cells were identified, using the F11 antibody directed against the rat β_3 integrin, as large rounded cells on the trabecular bone surface (TB). Likewise, osteoblasts were identified as cuboidal cells lining the bone surface using the osteoblast phenotype marker osteocalcin. In addition, osteocalcin immuno-reactivity was also detected at lower levels within the osteocyte lacunae embedded within the trabecular bone (arrowhead). VAMP1 expression was localised to the bone surface and at higher magnification and appears to be present in a subpopulation of cells lining the bone surface (→). VAMP1 immuno-reactivity was also detected in the skin, in particular localised to the hair follicles, which is due to a known contamination of the polyclonal VAMP1 antibody with antibodies recognising keratin. TB = trabecular bone, OB = Osteoblast, OC=Osteoclast.

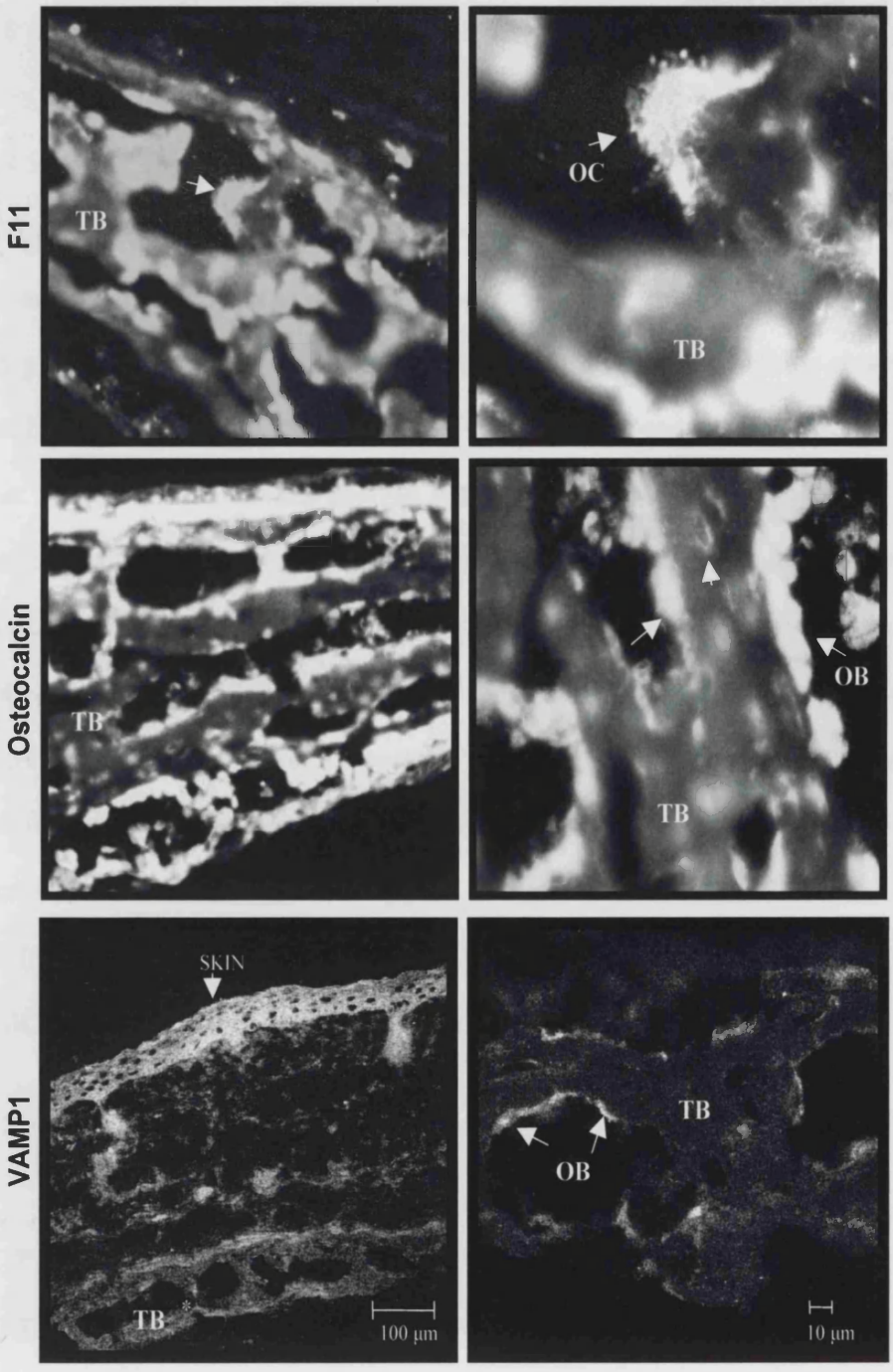
F11
TB
OC
TB
Osteocalcin
TB
OB
TB
VAMP1
SKIN
TB
100 µm
TB
OB
10 µm

5.5.2.8 VAMP1 mRNA Expression

VAMP1 mRNA expression was determined in the rat osteosarcoma cell line ROS 17/2.8 cells using RT-PCR (methods section 2.2.6 and 2.2.7) and VAMP1 specific primers, VAMP1 5'a and VAMP1 3'a (fig. 5.1). Rat brain cDNA prepared from day 3 Sprague Dawley rat pups was used as a positive control for VAMP1 expression, whilst β-actin primers were used to assess the quality of the cDNA. Representative PCR products, resolved by agarose gel electrophoresis, revealed the cDNA products obtained for ROS cell VAMP1 to be the same size as those obtained for rat brain, ~250 bp (fig. 5.9). Similarly, VAMP1 PCR products obtained for rat cardiac fibroblasts, rat calvaria derived osteoblasts and MC3T3 cells were of the expected size. Occasionally, a larger band of ~800 bp was observed. Sequence analysis demonstrated that these higher molecular weight bands represented non-specific priming of degenerate primers; these bands were identifed as collagen. Furthermore, VAMP1 was expressed throughout nodule formation and mineralisation in primary osteoblast cell cultures (RCOBs) at days 4, 7, 12 and 17. Dexamethasone treatment did not appear to have any effect on VAMP1 mRNA levels (not shown). Likewise, VAMP1 mRNA was detected in the osteoblast cell line MC3T3-E1 throughout nodule formation and mineralisation, at days 0, 6, 12, 15, 20 and 25.

5.5.3 v-SNARE and t-SNARE Expression in Osteoblastic Cells

SNAREs specific for neurotransmitter release have been identified and localised to two distinct cellular compartments of the synaptic vesicle and the pre-synaptic plasma membrane. VAMP and synaptotagmin, a calcium sensitive v-SNARE, localise to the small synaptic vesicle (SSV) whilst syntaxin and SNAP-25 localise to the pre-synaptic plasma membrane regulating neurotransmitter release.

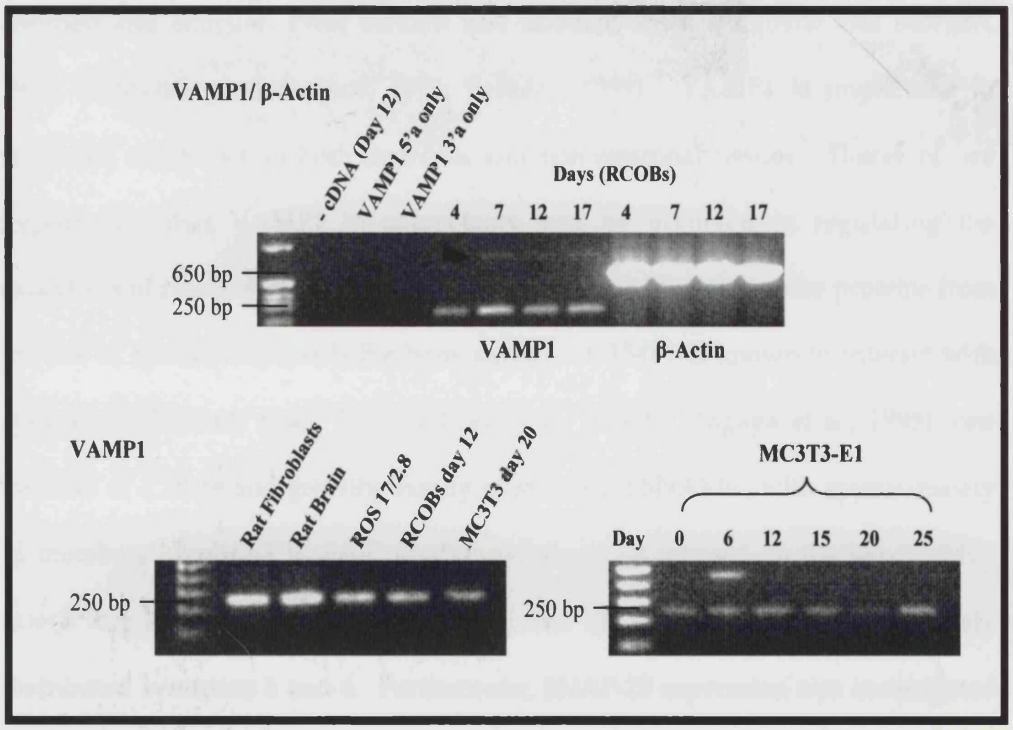

Figure 5.9 VAMP1 mRNA Expression in Osteoblast-like Cell Cultures – As Determined by RT-PCR Analysis. Representative VAMP1 PCR amplification products obtained using cDNA derived from days 4, 7, 12 and 17 of primary nodule forming cultures (RCOBs) resolved by agarose gel electrophoresis revealed VAMP1 mRNA to be expressed throughout nodule formation and mineralisation. All samples including the rat brain control samples expressed a band of around 250 bp, corresponding to VAMP1. Similarly, VAMP1 expression determined in the osteoblast cell lines ROS 17/2.8 and MC3T3-E1 revealed VAMP1 products of the expected size. In addition and similar to RCOBs, MC3T3-E1 cells express VAMP1 at the mRNA level throughout nodule formation and mineralisation. The cDNA quality was checked using β-actin PCR amplification. Occasionally a larger band of ~800 bp was observed. Sequence analysis demonstrated that these higher molecular weight bands represented non-specific priming of VAMP1 degenerate primers and were identified as collagen.

Further to establishing VAMP1 expression in osteoblastic cells, the presence of other possible interacting v- and t-SNAREs was investigated, with particular emphasis on the protein components constituting the conserved fusion machinery (Bennett and Scheller, 1993; Bennett and Scheller, 1994; Burgoyne and Morgan, 1998; McMahon and Sudhof, 1995; Pelham, 1999). VAMP1 is implicated in regulated exocytosis in both neuronal and non-neuronal tissues. Therefore, we hypothesise that VAMP1 in osteoblasts may be involved in regulating the exocytosis of newly synthesised bone matrix proteins, directing these proteins from the site of synthesis towards the bone surface. VAMP1 is known to interact with syntaxin 1 (Bennett *et al.*, 1992; Sollner *et al.*, 1993b) (Tagaya *et al.*, 1995), one member of a large and growing family of syntaxin t-SNAREs, with approximately 16 members identified to date. Initial investigations focused on the key VAMP1 interacting syntaxin, syntaxin 1 (HPC1), and on the expression of the widely distributed syntaxins 4 and 6. Furthermore, SNAP-25 expression was investigated in ROS 17/2.8 cells and in primary osteoblast-like cells from days 5 and 19 of nodule forming cell culture.

The synaptotagmins are a large family of v-SNARES of which approximately 13 have been identified to date, synaptotagmins I-XII and synaptotagmin B/K. Each member of this family has a unique tissue specific distribution and a number of synaptotagmins have been implicated in calcium sensitive regulated exocytosis. Therefore, the expression of a number of key synaptotagmin family members was investigated in osteoblast-like cells. The expression of the neuronal isoform synaptotagmin I and the closely related synaptotagmin II (~75 % identity at the amino acid level) (Geppert *et al.*, 1991) as well as the expression of synaptotagmin IV, a ubiquitously expressed general v-SNARE, was assessed in osteoblast-like cells and neuronal cell controls.

5.5.3.1 Western Blot Analysis of SNARE expression in Osteoblasts

Syntaxin and SNAP-25 Expression in Osteoblast-like Cells

Western blotting confirmed the presence of syntaxin 1 (using the HPC1 antibody) in the neuronal PC12 cell controls; however, we were unable to detect syntaxin 1 expression in osteoblastic cells (fig. 5.10).

Antibodies directed against the more widely distributed syntaxins 4 and 6 revealed syntaxin 6 to be expressed in the neuronal controls, PC12 cells and rat synaptic vesicles; furthermore, syntaxin 6 expression was observed in osteoblastic cells. In contrast, neither neuronal cells nor osteoblastic cell expressed syntaxin 4. Similarly, the expression of SNAP-25 was determined in ROS 17/2.8 cells and primary osteoblast-like cell from days 5 and 19 of nodule forming culture (fig. 5.10). SNAP-25 expression was observed in both the PC12 cell controls and on purified rat synaptic vesicles; however, SNAP-25 expression was not detected in osteoblastic cell cultures (fig. 5.10).

Synaptotagmin Expression in Osteoblasts

The expression of the neuronal isoform synaptotagmin I, the closely related synaptotagmin II and the general v-SNARE synaptotagmin IV was assessed in osteoblast-like cells and in neuronal controls (fig. 5.11). As expected, neuronal cells expressed both synaptotagmins I and II. Synaptotagmins are sensitive to cleavage by proteolysis; therefore, the presence of a 47.5 kDa cleavage product in these samples was not surprising.

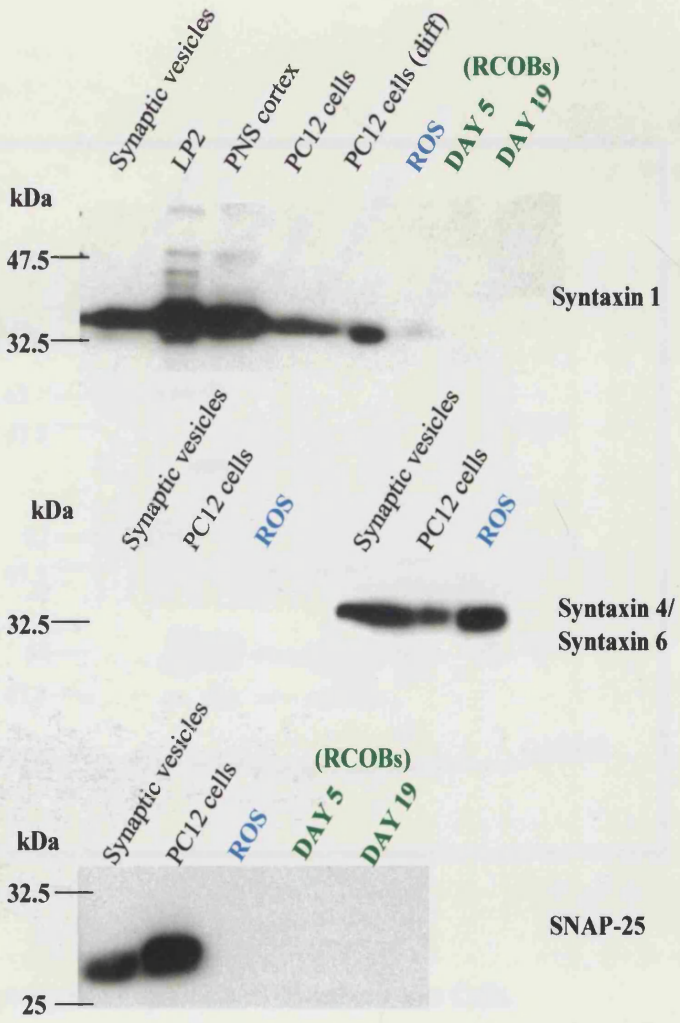

Figure 5.10 Syntaxin and SNAP-25 Expression in Osteoblastic cells.

Syntaxin 1 (HPC1) and SNAP-25 protein expression appears to be abundant in the neuronal control samples; however, these proteins were not detected in osteoblasts. Osteoblastic cell populations, ROS 17/2.8 and RCOBs, express the Golgi t-SNARE, syntaxin 6. Syntaxin 4 expression was not detected in either neuronal or osteoblastic cells.

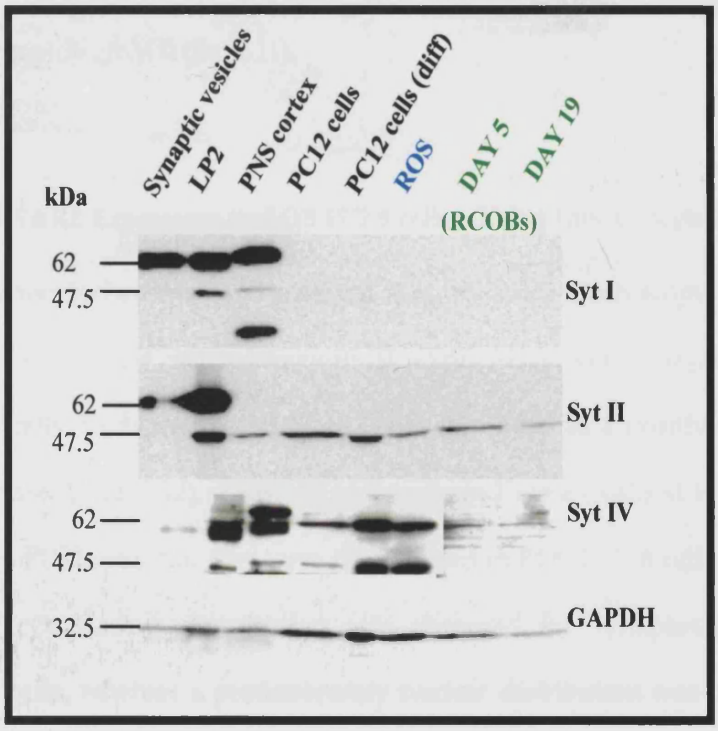

Figure 5.11 Synaptotagmin Expression in Osteoblast-like Cells.

Using neuronal cells and cell extracts as controls, synaptotagmin expression was determined in osteoblastic cells. Although synaptotagmin I was not expressed in osteoblasts, its expression was confirmed in neuronal controls. Interestingly, a band of around 47 kDa was observed for synaptotagmin II in both PC12 and osteoblastic cells. Furthermore, the general v-SNARE synaptotagmin IV was identified in osteoblasts. GAPDH was used to assess protein loading.

Although we were unable to detect the presence of the neuronal isoform synaptotagmin I, the expression of synaptotagmin IV was detected in osteoblastic cells. Interestingly, osteoblastic cells also appeared to express the calcium sensitive v-SNARE synaptotagmin II (fig. 5.11).

5.5.3.2 v-/t-SNARE Expression in ROS 17/2.8 cells – Using Immunocytochemistry

Using immunocytochemistry and confocal laser scanning microscopy, syntaxin 1 (HPC1), SNAP-25 and synaptotagmin II expression were characterised in ROS 17/2.8 cells; undifferentiated PC12 cells were used as a positive control of protein expression (fig. 5.12). SNAP-25 and syntaxin 1 were localised to the plasma membrane in PC12 cells, but they were not detected in ROS 17/2.8 cells. However, a vesicular cytoplasmic distribution was observed for synaptotagmin II in ROS 17/2.8 cells, whereas a predominately nuclear distribution was observed in PC12 cells. Furthermore, synaptotagmin II was found localised in primary osteoblastic cells forming the nodule structure and had a similar distribution in these cells as VAMP1.

Synaptotagmin II Expression in Primary Nodule Forming Cell Cultures

As synaptotagmin protein, detected by western blotting and immunocytochemistry, was expressed in the osteoblast cell line ROS 17/2.8, synaptotagmin II protein expression was examined in nodule forming cells taken from day 16 of nodule forming and mineralising cell cultures. Similar to VAMP1 expression, the level of synaptotagmin II expression observed was highest in cells forming the nodule; moreover, at higher magnification synaptotagmin II was observed to be expressed not only in the multilayered cells but also in cells forming the supporting monolayer (fig. 5.13).

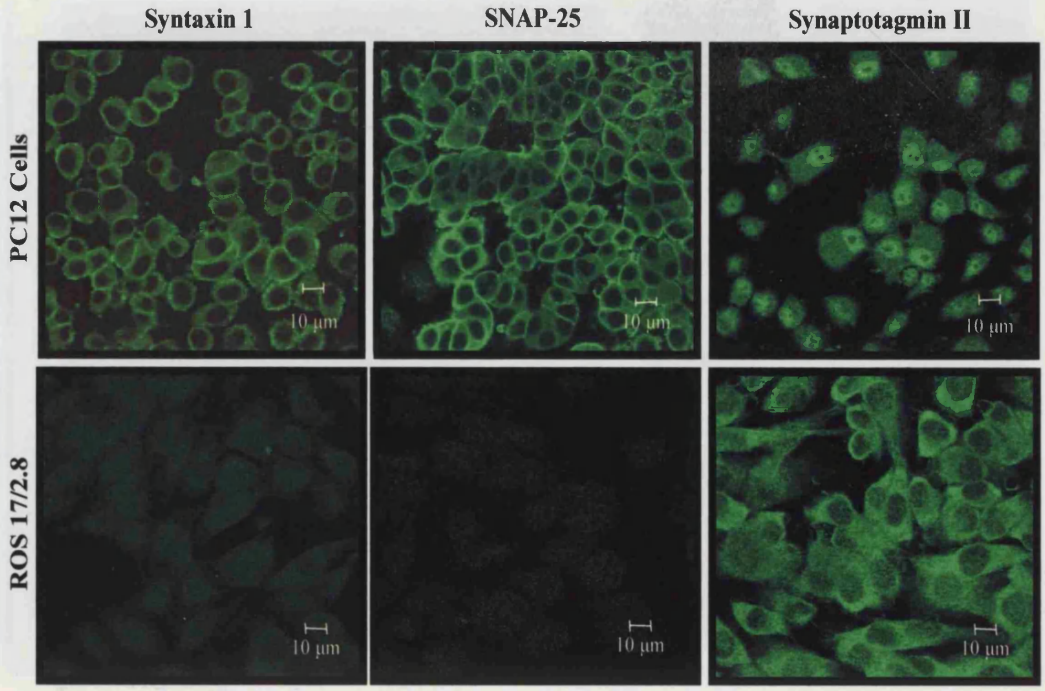

Figure 5.12 Syntaxin 1, SNAP-25 and Synaptotagmin II Expression in PC12 and ROS 17/2.8 cells. Both SNAP-25 and syntaxin 1 localised to the plasma membrane in PC12 cells. However, SNAP-25 and syntaxin 1 protein expression were not detected in ROS 17/2.8 cells. In contrast to the mainly nuclear distribution observed for synaptotagmin II in PC12 cells, ROS 17/2.8 cells contain a large cytoplasmic pool of this protein which was distributed throughout the cell in a vesicular-like manner.

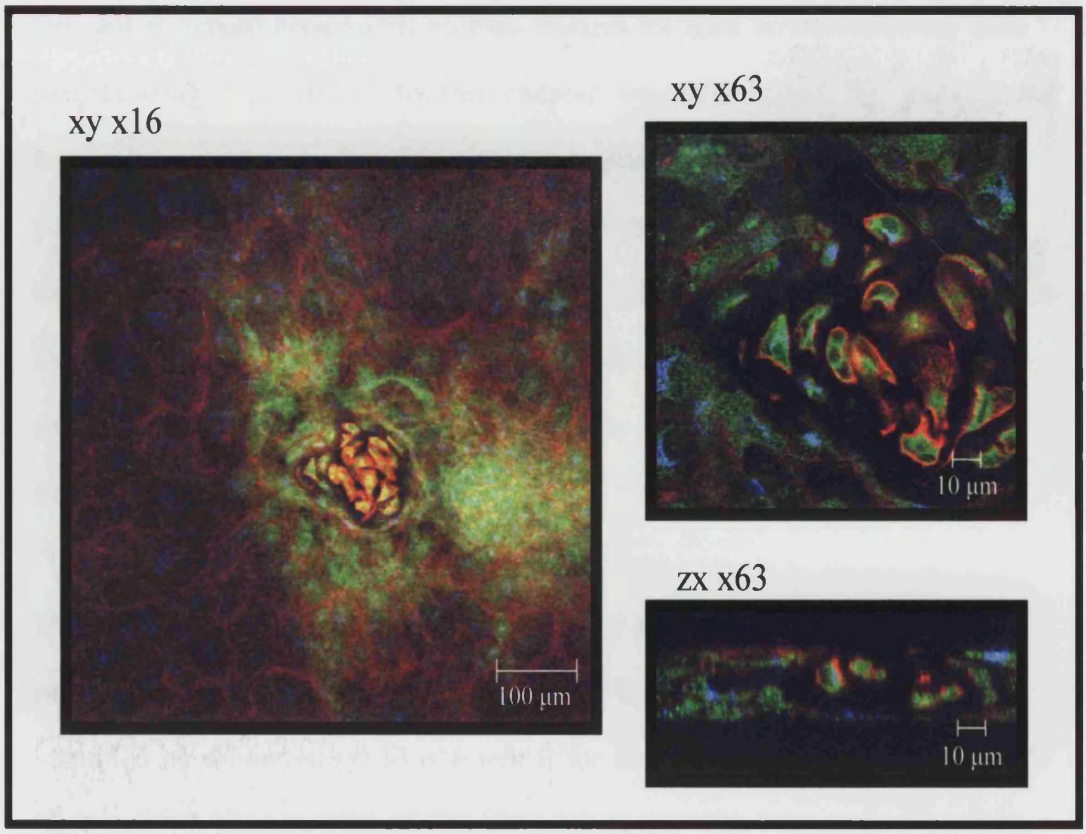

Figure 5.13 Synaptotagmin II Expression in Primary Osteoblastic Nodule Forming Cell Cultures. Triple staining using synaptotagmin II (green), GM130 (blue) and F-actin (red), revealed synaptotagmin II to be highly expressed in cells forming the nodule; however, synaptotagmin II was also expressed in cells forming the supporting monolayer. Although synaptotagmin II expression was observed in the multilayered cells of the nodule, higher magnification (ZX x63) indicated that there was no apparent co-localisation of synaptotagmin II with the Golgi marker GM130.

5.6 Discussion

Osteoblasts deposit bone matrix proteins towards the bone surface and away from neighbouring capillaries. In this chapter we investigated the molecular mechanisms mediating directed bone matrix protein secretion. Osteoblasts are polarised cells with their apical and basolateral membranes (Ilvesaro *et al.*, 1999) segregated by the presence of apical junction complexes (results Chapter 4). Herein we investigated a number of protein components, implicated in both regulated and constitutive secretion pathways in other cells, which may be responsible for vectorial transport within osteoblasts.

The presence of the general fusion machinery proteins, α-SNAP and NSF, in osteoblasts is not surprising, particularly since they have been characterised and identified as conserved proteins essential for membrane fusion (Burgoyne and Morgan, 1998; Morgan, 1995; Pfeffer, 1996; Schekman, 1998; Whiteheart *et al.*, 1992; Woodman, 1997). Although the stage at which these proteins act is currently debated, undoubtedly they are key components of a vesicle mediated transport pathway (Burgoyne and Morgan, 1998; Klenchin and Martin, 2000; Nichols *et al.*, 1997).

Transport and membrane fusion events have been well characterised and described in the neuronal cell system, where specificity of membrane fusion and the regulation of exocytotic events are crucial for neurotransmitter release and signal transduction (Bennett and Scheller, 1993; Bennett and Scheller, 1994; Schiavo and Stenbeck, 1998; Sollner *et al.*, 1993a). It is for these reasons that the neuronal system was used as a positive control for these studies.

A number of protein components have been identified and implicated in SNARE mediated transport pathways (Rothman, 1994; Sollner *et al.*, 1993a). In this study we investigated the presence of key v-/t- SNAREs, implicated in the late steps of the secretory pathway, that is Golgi to plasma membrane trafficking. In particular, this study focused on the expression of VAMP1, although recent studies have identified a plethora of other VAMP isoforms and splice variants (discussed in detail in Chapter 6). Both VAMP1 and VAMP2 are implicated in a late step of the secretory pathway. VAMP2 protein expression was, however, not detected in osteoblastic cells. The widely distributed non-neuronal isoform, cellubrevin, was not investigated, as it is mainly involved in intra-Golgi trafficking.

The data presented reveal VAMP1 to be expressed in the osteoblast cell lines, ROS 17/2.8 and MC3T3-E1, in addition to being expressed in primary osteoblast-like cells derived from day 21 embryonic rat calvaria. Furthermore, Western blot analysis revealed the VAMP1 isoform expressed in osteoblasts to have an apparent molecular weight 2 kDa larger in size than the neuronal isoform detected on purified rat synaptic vesicles. Further investigations into this molecular weight difference are presented in chapter 6. Recently, a growing number of VAMP1 splice variants have been identified and localised to specific membrane bound compartments of the secretory pathway, suggesting that the highly variable C-terminal portion of this protein is responsible for specific targeting and possibly for the localisation of the protein (Berglund *et al.*, 1999; Isenmann *et al.*, 1998; Mandic *et al.*, 1997). In an attempt to establish a specific intracellular localisation of VAMP1 within osteoblasts, and hence a possible functional role, sequence analysis of this osteoblastic VAMP1 protein was carried out (Chapter 6).

Although a functional role for VAMP1 in osteoblasts has not yet been determined, osteoblastic cells clearly express some of the key protein components required for a SNARE mediated transport pathway.

Co-localisation studies of VAMP1 with a number of transported bone matrix proteins, such as osteocalcin, osteopontin and type I collagen were performed. These data revealed limited co-localisation of VAMP1 with both collagen and osteocalcin, although the specific subcellular distribution of VAMP1 remains unclear. Further studies, possibly using cyclohexamide treatment prior to co-localisation studies, may determine whether or not VAMP1 is associated with bone matrix transport in osteoblasts. Furthermore, the use of immuno-electron microscopy may enable us to identify the specific vesicular type structures that VAMP1 localises to within these cells.

A number of functional studies using an *in vitro* model of mineralisation (Chapter 3) could be used to assess VAMP1 function within the osteoblast. VAMPs characteristically contain specific neurotoxin cleavage sites; therefore, cleavage of this protein with these toxins should render the protein inactive. The effect of inactivation of VAMP1 on mineralisation could be assessed using primary nodule forming and mineralising cell cultures. The initial problem presented would be to ensure the incorporation of the neurotoxins into cells, particularly at the late stages of culture. To overcome this problem, one of several approaches could be taken: the neurotoxin could be cloned, overexpressed and the plasmid transfected into the mineralising cell line MC3T3-E1. Alternatively, toxin could be delivered using microinjection techniques. Subsequently, the effect of VAMP1 inactivity on matrix and mineral deposition could be assessed *in vitro*.

VAMP1 expression on sections of rat calvaria revealed VAMP1 to localise to the trabecular bone surface, more specifically in plump cells lining the bone surface; this indicated that osteoblasts express VAMP1 *in vivo*. Recent investigations, have shown bone to be highly innervated (Serre *et al.*, 1999); this could potentially cause difficulty in microscopic interpretation. However, the isolation, and immunocytochemical analysis, of osteoblastic cells has revealed that these cells do indeed express VAMP1, indicating that the VAMP1 expression observed was in osteoblasts. VAMP1 immuno-reactivity was also detected at high levels in the surrounding skin and hair follicles, which is probably due to a known contamination of the VAMP1 polyclonal antibody preparation with antibodies to keratin.

The presence of other possible interacting v- and t-SNAREs was also investigated. Particular emphasis was placed on investigating the expression of protein components constituting the conserved fusion machinery (Bennett and Scheller, 1993; Bennett and Scheller, 1994; Burgoyne and Morgan, 1998; McMahon and Sudhof, 1995; Pelham, 1999). VAMP1 is known to interact with syntaxin 1, one member of a large and growing family of syntaxin t-SNAREs. Due to the size and diversity of this family of SNARE proteins, and limited antibody availability, initial investigations focused on the expression of syntaxin 1, the key VAMP1 interacting t-SNARE, and on the expression of the widely distributed syntaxin isoforms, syntaxin 4 and 6.

These studies demonstrated that osteoblastic cells express the Golgi SNARE, syntaxin 6. Interestingly, osteoblastic cells do not express syntaxin 1 indicating that there are other VAMP1 specific t-SNAREs in osteoblasts. Syntaxin 4, a VAMP2 interacting protein expressed in a variety of tissues, which is localised to the plasma

membrane (Fujita *et al.*, 1998), was not detected in either osteoblastic cells or in the neuronal cell control samples. Due to the lack of a positive control for the commercial syntaxin 4 antibody, these results have to be interpreted with some caution. Although, these studies have provided an insight into t-SNARE expression in osteoblastic cells, future experiments would have to be performed to identify VAMP1 interacting proteins within osteobastic cells. Osteoblastic VAMP1 DNA could be inserted into a GST-fusion vector. Following over-expression in *E.coli*, the purified GST-fusion protein could be used to isolate VAMP-1 interacting proteins from ROS 17/2.8 or primary osteoblast cell culture extracts.

Further investigations have revealed that osteoblastic cells may also contain a calcium regulated exocytotic pathway. In particular, we have identified the expression of the general v-SNARE, synaptotagmin IV, and the calcium regulated, synaptotagmin II, in osteoblastic cells. Immunocytochemical analysis revealved synaptotagmin II expression to be concentrated in cells forming the nodule structure.

Although these results indicate that osteoblastic cells express a subset of the proteins components required for a vesicle mediated, regulated exocytosis pathway, further investigations must be undertaken to identify the full complement of proteins involved. Furthermore, functional experiments would determine the implications of a SNARE mediated transport pathway on osteoblast cell function.

5.7 Summary

- Osteoblastic cells express the general fusion machinery proteins, NSF and α-SNAP.
- Western blot analysis revealed that osteoblastic cells express an isoform of the general v-SNARE, VAMP1, implicated in regulated exocytosis in a number of neuronal and non-neuronal cells.
- In *in vitro* models of mineralisation, VAMP1 is concentrated in cells forming the nodule.
- *In vivo*, VAMP1 localises to plump osteoblastic cells lining the trabecular bone surface.
- Limited co-localisation of VAMP1 was observed in ROS 17/2.8 cells with the transported bone matrix proteins osteocalcin and type I collagen.
- Osteoblasts express the widely distributed Golgi t-SNARE, syntaxin 6, the general v-SNARE, synaptotagmin IV, and the calcium sensitive v-SNARE, synaptotagmin II.

We hypothesise that the protein components identified, NSF and α-SNAP, VAMP1 and synaptotagmin II may form part of the exocytotic machinery which may be responsible for directed bone matrix protein secretion by the osteoblast.

Chapter 6

SEQUENCE ANALYSIS AND LOCALISATION OF VAMP1 IN OSTEOBLASTS

Chapter 6

SEQUENCE ANALYSIS AND LOCALISATION OF VAMP1 IN OSTEOBLASTS

6.1 Introduction

VAMP1 (vesicle associated membrane protein 1) is a 13 kDa protein (Trimble, 1993; Trimble *et al.*, 1988; Trimble *et al.*, 1990) implicated in neuroexocytosis (Schiavo and Stenbeck, 1998; Sollner *et al.*, 1993a; Sollner and Rothman, 1996; Taubenblatt *et al.*, 1999; Tsui and Banfield, 2000). Although VAMP1 was initially identified and localised in neuronal tissues recent investigations have shown VAMP1 to have a wider tissue distribution (Mandic *et al.*, 1997; Rossetto *et al.*, 1996). Furthermore, novel VAMP isoforms, VAMP 4, 5, 7 (toxin insensitive VAMP, TI-VAMP), and VAMP8 (endobrevin) (Coco *et al.*, 1999; Prekeris *et al.*, 1999; Steegmaier *et al.*, 1999; Wong *et al.*, 1998b; Zeng *et al.*, 1998), have been identified in non-neuronal tissues. In addition, a number of VAMP1 splice variants have been identified indicating neurone independent roles of VAMP in vesicle targeting (Berglund *et al.*, 1999; Isenmann *et al.*, 1998; Mandic *et al.*, 1997).

6.1.1 Structure of VAMP1

Characterisation of humanVAMP1 (hVAMP1) revealed that the VAMP1 cDNA transcript is encoded by 5 exons, each of which contain the specific information required for the 4 structural domains of the protein. Trimble and co-workers (1988) describe VAMP1 as a predominately cytoplasmic protein (the cytoplasmic domain is encoded by exons I-IV), containing a short intra-vesicular C-terminal portion (encoded by exon V) (Trimble, 1993; Trimble *et al.*, 1988). The structural domains of

VAMP1 are defined as an amino terminal region (divergent between isotypes), a proline rich domain, a highly conserved central region (containing the specific sites cleaved by neurotoxins), a single transmembrane spanning domain and a short carboxyl terminal segment (Chapter 1, fig. 1.10).

Although the specific locations of intron/exon boundaries have been identified for the hVAMP1 cDNA transcript, the location of these sites in rVAMP1 remains unknown. Therefore, in an attempt to localise VAMP gene specific primers on the rVAMP1 coding region a comparison was made with the hVAMP1, coding region (353 bp). rVAMP1 shows approximately 93 % homology to the hVAMP1 cDNA coding sequence. Similar to hVAMP1 exons were located at the following sites on the rVAMP1 coding region; exon I, is encoded by base pairs 33-34, exon II, 34-161, exon III, 161-320, exon IV, 320-372, exon V, 372-386 (Chapter 1, fig. 1.11).

At the onset of this study, three isoforms of VAMP had been identified, VAMP 1 and 2, which were believed to be mainly neuronally specific, and a third isoform with an non-neuronal tissue distribution, cellubrevin. Recent investigations have demonstrated that in addition to cellubrevin, VAMP1 and VAMP2 have a wider tissue distribution than previously anticipated (Rossetto *et al.*, 1996). In addition to their differential expression in brain, (Elferink *et al.*, 1989; Trimble *et al.*, 1990), VAMP1 and VAMP2 are present in a number of rat tissues (see Chapter 1, Table 1.5) (Rossetto *et al.*, 1996). The presence of such v-SNAREs in non-neuronal tissues emphasises their potential role in constitutive exocytosis and further strengthens the argument that the molecular machinery mediating regulated exocytosis is, at least in part, conserved (Bennett and Scheller, 1993; Burgoyne and Morgan, 1998). Moreover, and perhaps more importantly, these findings suggest that non-neuronal secretory cells may also have the potential to regulate exocytotic events with the

same stringency as observed in the neuronal system and imply VAMP mediated exocytosis to be universal.

6.1.2 VAMP1 Splice Variants

In addition to the identification of a number of novel VAMP isoforms (Advani *et al.*, 1998; Advani *et al.*, 1999; Coco *et al.*, 1999; Steegmaier *et al.*, 1999; Wong *et al.*, 1998b; Zeng *et al.*, 1998), a growing number of VAMP1 splice variants have been identified (Berglund *et al.*, 1999; Isenmann *et al.*, 1998; Mandic *et al.*, 1997). As products of alternative splicing between exons IV and V, these proteins characteristically contain altered C-terminal residues. Recent data by Isenmann and co-workers (1998) have suggested these different C-terminal residues target these proteins to specific subcellular compartments of the secretory pathway.

6.1.2.1 Sequence Analysis and Localisation of VAMP1 Splice Variants

Sequence analysis revealed the rat neuronal VAMP1 isoform, rVAMP1A, has a C-terminal sequence, YIFT (Elferink *et al.*, 1989). Consequent localisation studies have demonstrated exclusive localisation of VAMP1A to synaptic vesicles. In contrast, hVAMP1B, the first splice variant of human VAMP1A to be identified (Isenmann *et al.*, 1998), contains positively charged C-terminal residues, RRD, which have been implicated in targeting of hVAMP1B to mitochondria, demonstrated by transfection studies in human endothelial cells (Isenmann *et al.*, 1998). In addition to being expressed in human endothelial cells, the hVAMP1B splice variant has also been identified in human fibroblasts and neutrophils (Isenmann *et al.*, 1998).

In 1997 Mandic and co-workers identified a rat isoform of the VAMP1B splice variant, rVAMP1B. Similarly, rVAMP1B contains a positively charged C-terminal residue sequence SKYR. Furthermore, it has been suggested that rVAMP1B may also be targeted to mitochondria, although specific co-localisation of rVAMP1B to mitochondria has not yet been determined (Mandic *et al.*, 1997) (fig. 6.1).

In addition to the splice variants described above (fig. 6.1), Berglund and co-workers (1999) have further investigated the highly variable C-terminal portion of VAMP1, identifying four more splice variants of this v-SNARE, VAMP1C to F. As with VAMP1B, sequence variation occurred at the extreme C-terminal portion of the VAMP1 cDNA transcript as a direct result of alternative splicing between exon IV and V, with exons I-IV remaining conserved. Moreover, these studies showed that VAMP1C to F splice variants were widely expressed throughout the brain, and in kidney, peripheral blood mononuclear cells, eosinophils and neutrophils (Berglund *et al.*, 1999).

6.2 Aim

In attempt to understand better the possible role of VAMP1 in osteoblasts, VAMP1 expression, and more specifically VAMP1 intracellular localisation, was determined in osteoblastic cells.

6.3 Specific Objectives

In an attempt to investigate the 2 kDa molecular weight difference of osteoblastic VAMP1, the cDNA transcript was amplified and sequenced. Furthermore the

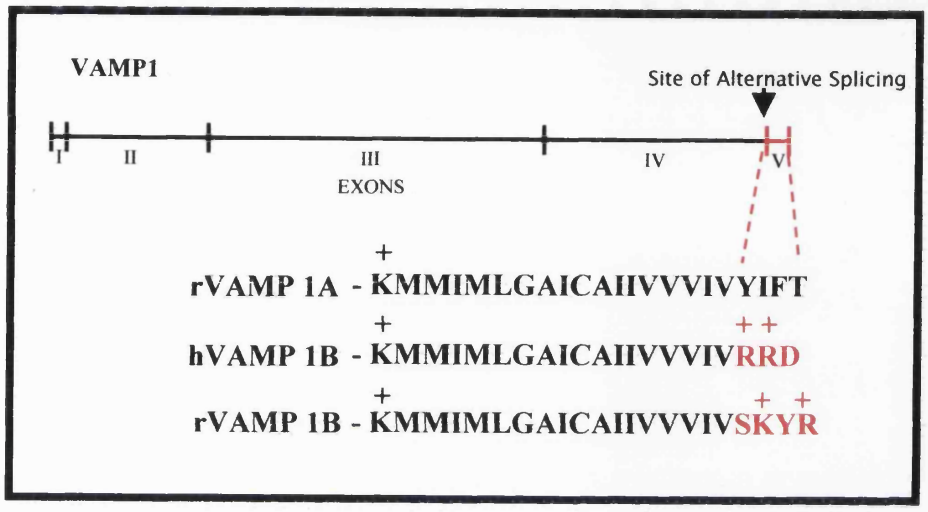

Figure 6.1 VAMP1 Splice Variants.

VAMP1 splice variants result from alternative splicing between exons IV and V, creating an altered carboxyl terminal amino acid residue sequence. Human and rat splice variants, hVAMP1B and rVAMP1B have been identified. hVAMP1B contains a positively charged C-terminal residue sequence, RRD, and is targeted to mitochondria. Similarly, rVAMP1B contains the positively charged sequence SKYR.

specific localisation of VAMP1 was investigated using indirect immunofluorescence in studies designed to assess co-localisation of VAMP1 protein expression to specific membrane bound compartments.

6.4 Specific Methods

6.4.1 PCR Amplification and Cloning of VAMP1

Using PCR methods and degenerate primers directed against the extreme N-terminal portion of the VAMP1A coding region (VAMP1 5'a) and against the C-terminal region 250-273 bp, VAMP1 3'a (Chapter 2, table 2.5), VAMP1 cDNA was amplified in osteoblastic cells. Amplified PCR products were resolved on an agarose gel and representative VAMP1 products purified and cloned into the TA cloning vector pGEM-T (2.2.9, 2.2.10). Recombinant plasmids were identified in *E.coli* transformed cells using X-gal/IPTG (blue/white) selection (2.2.11.3) and VAMP1 containing plasmids identified by digestion with the restriction endonucleases Apa I and Nde I (2.2.12.1). The resulting recombinant plasmids were sequenced using the dye terminator kit and an ABI Prism (2.2.14).

6.4.1.1 Amplification of the C-terminal Portion of VAMP1 – 3' RACE

As discussed above, a number of VAMP1 splice variants have been identified, all of which exhibited sequence divergence at their extreme C-terminal ends. Therefore, using sequential PCR and a combination of gene specific and anchor primers (table 6.1), 3' RACE reaction (rapid amplification of cDNA ends, Chapter 2, fig. 2.2) was performed (methods section 2.2.8) and used to amplify the extreme C-terminal portion of VAMP1. To investigate the possibility that osteoblastic cells may also be

expressing a VAMP1 splice variant the resulting PCR products were cloned and sequenced. Specific localisation of the gene specific primers VAMP1 5'a and VAM 3' RACE in relation to the VAMP1 coding region are described in fig. 6.2. VAMP1 5'a is located at the extreme N-terminal portion of the VAMP1 cDNA coding region, whilst VAM 3' RACE is located further downstream in the region encoded by exon III.

6.5 Results

6.5.1 VAMP1 Expression in Osteoblast-Like Cells

Western blot analysis demonstrated an isoform of the targeting v-SNARE, VAMP1, is expressed in osteoblastic cells (see Chapter 5). This VAMP1 isoform appeared to be 2 kDa larger in size than the neuronal isoform expressed on purified rat synaptic vesicles (Fig. 5.4). Several reasons for this difference in molecular weight have been previously discussed (Chapter 5); the size difference observed may be due to either post-translational modifications or it may reflect a novel osteoblast specific VAMP1 isoform. However, in view of recent publications, it seems more likely that this size difference reflects a novel VAMP1 splice variant. Therefore, in attempt to determine the nature of VAMP1 expressed by osteoblasts, sequence analysis was performed on cloned VAMP1 5'a and 3'a PCR products in addition to VAMP1 3' RACE reaction products.

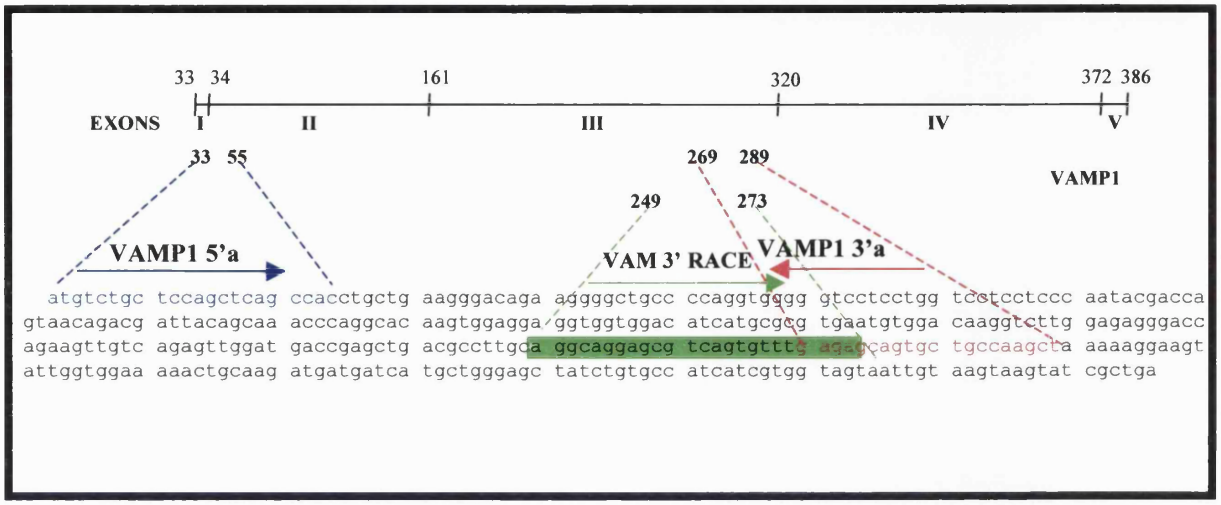

Figure 6.2 Localisation of the Gene Specific Primers VAMP1 5'a , VAMP1 3'a and VAM 3' RACE on the Rat VAMP1 cDNA Transcript. VAMP1 5'a is a 22-mer oligonucleotide located at the extreme N-terminal portion of the VAMP1 coding region, in the region encoding exon I and exon II (shown in blue). VAMP1 3'a is a 20-mer oligonucleotide located further downstream of VAMP1 5'a, between the 269 and 289 bp portion in the region of exon III (shown in red). The expected size of the VAMP1 5'a and 3'a PCR products is 256 bp. Similar to VAMP1 3'a, VAM 3' RACE is located downstream of the VAMP1 5'a primer between 250 to 273 bp, (shown in green), in the region of exon III, with a short 5 bp region of overlap between VAMP1 3'a and VAM3' RACE.

6.5.2 Investigating the 2 kDa Molecular weight Difference

The differential electrophoretic mobility of VAMP1 expressed by osteoblastic cells was investigated using sequence analysis. Initially, primers directed against the full length rat VAMP1A transcript along with PCR were used to determine the site, if any, of sequence variation. Sequence analysis revealed the N-terminal 80 % of rat VAMP1 expressed in osteoblasts to be identical to that of the neuronal VAMP1 cDNA transcript; however, the absence of the remaining C-terminal 20 % suggested that sequence divergence, would occur at the C-terminus. In an attempt to investigate further C-terminal sequence divergence, and to obtain the complete osteoblastic VAMP1 cDNA sequence, classical 3′ RACE was performed.

6.5.2.1 Amplification of 3′ End of VAMP1

3′ RACE reaction was used to amplify the extreme C-terminal portion of VAMP1 expressed in the osteoblastic cell line ROS 17/2.8 and rat brain, with rat brain samples being used as a control for VAMP1 expression. RACE reaction was performed as described in Chapter 2, section 2.2.8. RACE reaction products were resolved using agarose gel electophoresis and are shown in fig. 6.3.

Total RNA was isolated from both ROS 17/2.8 cells and rat brain extract (fig. 6.3 A) and reverse transcribed, with the resulting single stranded cDNA product being used as a template for the synthesis of the double stranded VAMP1 5′a and R_o cDNA product. The presence of a smear housing a number of 'gene specific' bands was detected between 200 – 900 bp for both rat brain and ROS 17/2.8 samples (fig. 6.3 B). Using nested PCR with a second set of gene specific primers, VAM3′ RACE and the internal anchor primer R_I, this double stranded cDNA product was subjected to a second round of amplification (fig. 6.3 C). This second round of

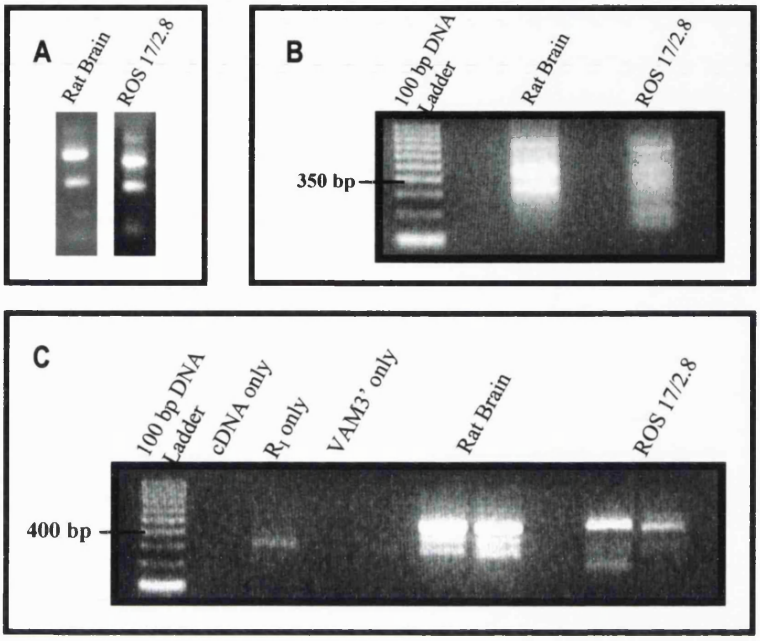

Figure 6.3 3′ RACE Reaction Products.

Total RNA was isolated from both ROS 17/2.8 cells and rat brain extract (A) and reverse transcribed, the resulting single stranded cDNA was used as a template for the synthesis of the double stranded VAMP1 5′a and R_o cDNA product (B). PCR products obtained from first round PCR amplification using VAMP1 5′a and the external anchor primer R_o were diluted and used as the starting material for the subsequent second round PCR amplification. Second round amplification was performed using the gene specific primer VAM 3′ RACE and the internal anchor primer R_I. The VAMP1, second round amplification products from ROS 17/2.8 and rat brain samples were resolved by agarose gel electrophoresis (C).

amplification led to the identification of three bands in rat brain, with approximate sizes of 250 bp, 350 bp and 400 bp. Similarly, multiple bands were identified in the ROS 17/2.8 RACE reaction product, ~200 bp and 450 bp. These bands were purified and cloned into pGEM-T expression vectors and transformed into competent *E. coli* JM109 cells. Subsequent sequence analysis of the rat brain 400 bp RACE products and ROS 17/2.8, 200 bp and 450 bp RACE products led to the identification of two possible VAMP1 splice variants in osteoblastic cells, VAMP1-OB_1 and VAMP1-OB_T.

VAMP1-OB_1 appeared to be the product of alternative splicing between exons IV and V, resulting in an elongated C-terminal portion of 17 amino acids long. This 17 amino acid C-terminal extension could account for a 1.5 kDa size difference in the protein detected using Western blot analysis. Hypothesising that this elongated VAMP1 sequence identified in ROS 17/2.8 cells could be an osteoblast specific isoform, it is referred to as VAMP1-OB_1. Furthermore, a second splice variant, VAMP1-OB_T, was detected in these cells. VAMP1-OB_T resulted from alternative splicing between exons III and IV and reflects a possible truncated VAMP1 cDNA transcript, without the characteristic VAMP1 transmembrane spanning domain. The sequences obtained were translated into protein sequence and the open reading frames encoding the VAMP1 C-terminal portions are shown in fig. 6.4.

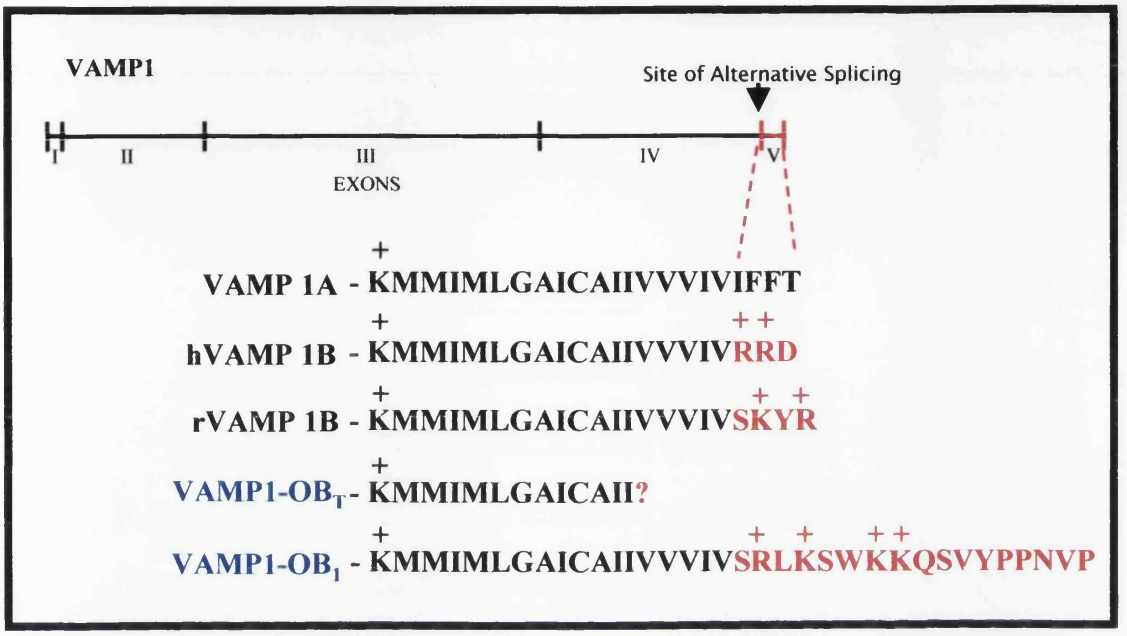

Figure 6.4 Osteoblastic VAMP1 Splice Variants.

Two splice variants with sequence divergence occurring at the C-terminus have been identified in osteoblastic cell preparations. VAMP1-OB$_T$ represents a truncated isoform of the VAMP1 cDNA transcript with alternative splicing occurring between exons III and IV, resulting in a VAMP1 transcript without the transmembrane spanning domain. In line with previously reported VAMP1 splice variants, VAMP1-OB$_1$ is a result of alternative splicing between exons IV and V, resulting in altered C-terminal residues. Notably, VAMP1-OB$_1$ contained an elongated C-terminal portion consisting of 17 amino acids, which could account for a 1.5 kDa difference in molecular weight observed by Western Blot analysis (see Chapter 5, fig. 5.4).

6.5.3 Validation of Osteoblastic VAMP1 Splice Variants

In order to rule out the possibility that the sequences obtained for these splice variants were an artefact of either the 3′ RACE reaction or the cloning procedure, primers were designed directed against the C-terminal portion of these sequences and these C-terminal portions amplified using PCR. In addition, primers were designed against a number of rat VAMP1 splice variants and the neuronal VAMP1A isoform (table 6.1). Using PCR, the expression of VAMP1 isoforms was determined on ROS 17/2.8 cells, primary osteoblast-like cells (RCOBs) and the mouse cell line, MC3T3-E1.

PCR analysis using the general N-terminal VAMP1 primer, VAMP1 5′a, and primers directed against the known VAMP1 splice variant, VAMP1B, in addition to those directed against the elongated C-terminal portion of rat VAMP1-OB demonstrated that osteoblastic cells express rVAMP1B, the mitochondria targeted splice variant. However, the previously defined rVAMP1-OB_1 and rVAMP1-OB_T splice variants were not detected, suggesting these products to be artefacts of the RT-PCR and cloning procedures. Furthermore, using rat brain as a positive control for VAMP1 expression, the inability of osteoblastic cells to express the neuronal VAMP1A isoform was established.

6.5.3.1 Identification of VAMP1 Splice Variants Using RT-PCR

Using the general N-terminal VAMP1 5′ primer, VAMP1 5′a, and the relevant 3′ primer, either VAMP1-OB, VAMP1B or neuronal VAMP1A (using VAMP1 3′a primer), PCR was performed to assess VAMP1 splice variant expression in osteoblastic cells and rat brain tissue (fig. 6.5).

VAMP1 Splice Variants	PRIMER SEQUENCE (5'-3')	T_m
VAMP1 5'a	ATGTCTGCTCCMGCTCAGCCAC	74 °C
VAMP1 3'a	AGCTTGGCAGCACTKSTYTC	64 °C
VAMP1B.	CAGTGCCTCAGCGATACTTACTTA	70 °C
$VAMP1B_{nt}$	CTCCATCAAGGAACATCCTTG	62 °C
$VAMP1\text{-}OB_T$	AAGTTCTCACCTGGCTCTTTCC	66 °C
VAMP1-OB	CAGAGTCTAGTGGAGACCTTC	64 °C

Table 6.1 VAMP1 Splice Variant Primer Sequences.

PCR was carried out using the general N-terminal VAMP1 5' primer and primers directed against the VAMP1B splice variant. In addition, primers were designed against the C-terminal portion of the elongated splice variant identified in ROS 17/2.8 cells. An estimate of primer melting temperature (T_m) was calculated as $T_m \cong 4\ (G+C) + 2\ (A+T)$.

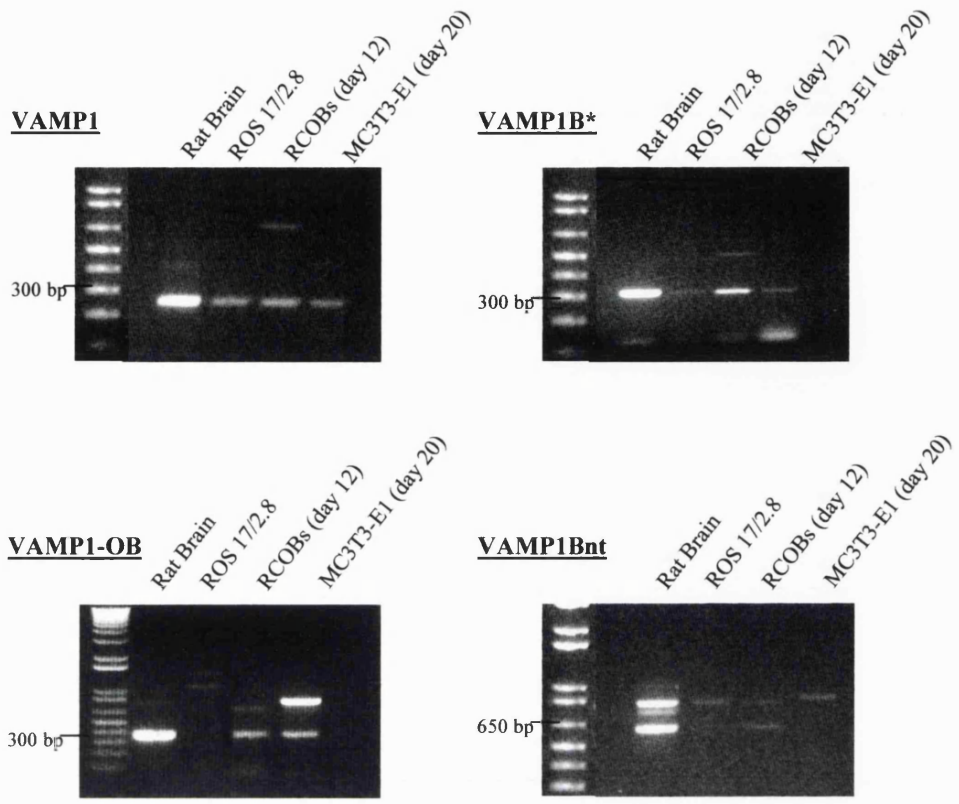

Figure 6.5 PCR Analysis of VAMP1 Splice Variant Expression in Osteoblastic Cells. Osteoblastic cells, ROS 17/2.8, RCOBs (day 12) and MC3T3-E1 (day 23) were assessed for the expression of the VAMP1 splice variant rVAMP1B using primers directed against both the coding region, VAMP1B*, and the non-translated region, $VAMP1B_{nt}$. In addition the expression of the previously identified osteoblastic VAMP1 splice variant $VAMP1\text{-}OB_1$ was determined. VAMP1 expression using the general VAMP1 primers VAMP1 5'a and VAMP1 3'a and rat brain cDNA were used as positive controls. The expected PCR product sizes and those obtained, by comparison with 1 kB DNA plus ladders resolved on a agarose gel are shown in table 6.2.

PCR products resolved using gel electrophoresis revealed a number of VAMP1 products of expected size, and those observed are shown in table 6.2.

Multiple bands were identified using gel electrophoresis (fig. 6.5). Therefore, in an attempt to identify VAMP1 specific bands, PCR products were resolved by agarose gel electrophoresis and subsequently, transferred to Nylon membrane for Southern Blot analysis (fig. 6.6). VAMP1 specific bands were purified and cloned into pGEM-T expression vectors. Following transformation and plasmid purification these clones were sequenced.

6.5.4 Sequence Analysis of VAMP1 Splice Variants Identified in Osteoblasts

Sequence analysis of these amplified PCR products revealed that osteoblastic cells express two VAMP1 splice variants, rVAMP1B and VAMP1-OB (fig. 6.7), the latter a potentially osteoblast specific splice variant containing a positively charged C-terminal residue sequence, RQD. VAMP1-OB was expressed in both the rat osteosarcoma cell line, ROS 17/2.8 and in primary osteoblast-like cells, RCOBs. In addition, sequence analysis revealed two populations of VAMP1 to exist in rat brain, VAMP1A and the mitochondria targeted VAMP1B splice variant.

6.5.5 VAMP1 Localisation in Osteoblastic Cells

Following the identification and localisation of VAMP1 to vesicular type structures within osteoblast-like cells (see Chapter 5, figs. 5.5, 5.6 and 5.7), we hypothesised that these structures are biosynthetic vesicular intermediates that may be responsible for mediating directional protein secretion within these cells. Therefore, to investigate the role of VAMP1 in the secretory pathway of osteoblasts

Primer Combination	Expected Product Size (bp)	Obtained PCR Product Size (bp)			
		Rat Brain	ROS 17/2.8	RCOBs (day 19)	MC3T3 (day 23)
VAMP1 5'a VAMP1-OB	497 bp	350 bp 500 bp	1100 bp	350 bp 700 bp	350 bp 700 bp
VAMP1 5'a VAMP1-OB_T	570 bp	500 bp 600 bp 800 bp	-?	500 bp 600 bp	600 bp
VAMP1 5'a VAMP1B.	360 bp	350 bp	350 bp?	350 bp 800 bp	350 bp
VAMP1 5'a $VAMP1B_{nt}$	542 bp	500 bp 550 bp 650 bp	-?	500 bp 650 bp	-?
VAMP1 5'a VAMP1 3'a (VAMP1A)	256 bp	250 bp	250 bp	250 bp	250 bp

Table 6.2 Analysis of VAMP1 Splice Variants using RT-PCR .

The above table describes both the expected product size and the obtained PCR product sizes estimated by gel electrophoresis and comparison with 1 kB DNA plus ladder (Gibco, Life Technologies, UK).

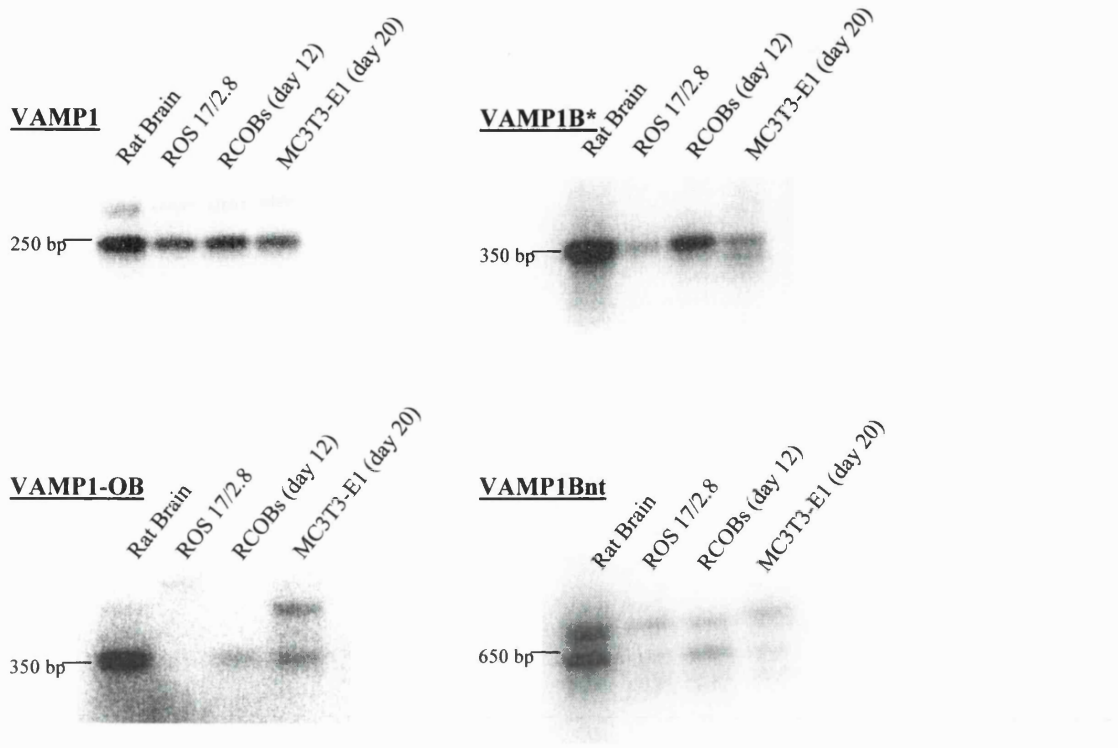

Figure 6.6 Osteoblastic VAMP1 Splice Variants Identified using RT-PCR and Southern Blot Analysis. Osteoblastic cells were screened for the presence of the VAMP1 splice variant, rVAMP1B; using primers directed against both the coding region, VAMP1B*, and the non-translated region, $VAMP1B_{nt}$. In addition the expression of the previously identified osteoblastic VAMP1 splice variants $VAMP1\text{-}OB_1$ was determined. VAMP1 expression using the general VAMP1 primers VAMP1 5'a and VAMP1 3'a and rat brain cDNA were used as positive controls. PCR products were resolved using agarose gel electrophoresis and VAMP1 specific bands identified using Southern Blot analysis and a VAMP1 specific probe generated from VAMP1 5'a and 3'a PCR products.

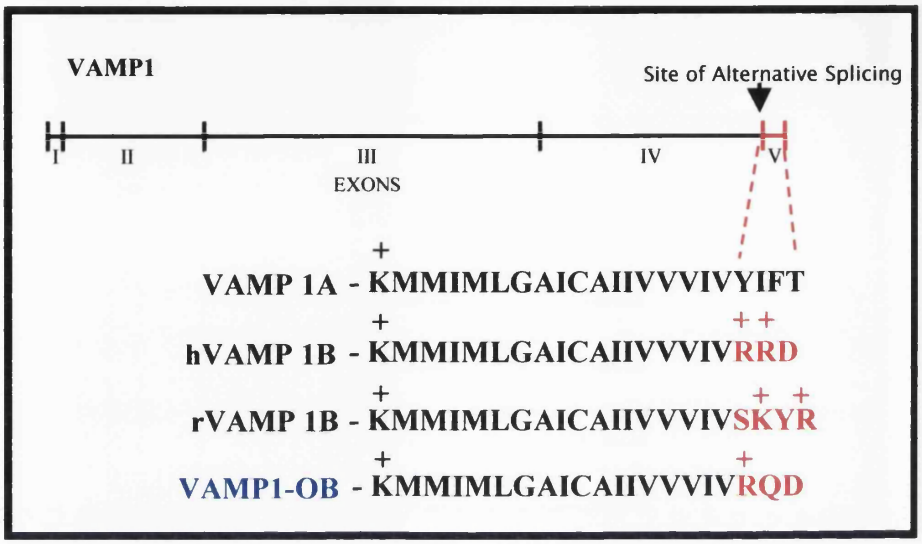

Figure 6.7 VAMP1-OB and rVAMP1B Expression in Osteoblasts.

Sequence analysis revealed that osteoblastic cells express two splice variants of the v-SNARE VAMP1, rVAMP1B and a potentially osteoblast specific splice variant VAMP1-OB. These splice variants result from alternative splicing between exons IV and V, giving rise to altered C-terminal residues.

an attempt was made to localise VAMP1 expression to specific membrane compartments.

In particular, the identification of the positively charged rVAMP1B splice variant in osteoblasts led to the investigation of VAMP1 co-localisation with mitochondria, performed using the mitochondria dye MitoTracker GREEN in ROS 17/2.8 cells. Furthermore, the localisation of VAMP1 to the acidic compartments, such as the lysosomes, was determined using LysoTracker RED (fig. 6.8).

VAMP1 was shown to have a vesicular type distribution in ROS 17/2.8 cells (fig. 6.8 B). In some cells VAMP1 distribution appears to be located in a perinuclear position (fig. 6.8 B, →); this differed from the cytoplasmic distribution seen in PC12 cells (fig. 6.8 A). In areas of confluent cells lysosomes (red), localised to the cytoplasm in a polarised manner (fig. 6.8 C), but VAMP1 had only limited co-localisation with these acidic compartments observed, yellow (fig. 6.8 C, →). Similarly, limited co-localisation of VAMP1 (red) with the mitochondria (green) was observed (fig. 6.8 D). Previous studies (Chapter 5) have demonstrated limited co-localisation of VAMP1 with transported matrix proteins type I collagen and osteocalcin (figs. 6.8 E and F). There was no co-localisation of VAMP1 with either the Golgi marker GM130 (see Chapter 5) or the ER within osteoblasts (Golgi and ER localisation in osteoblastic cells is shown in fig. 6.8 E, F). Therefore, the specific localisation of VAMP1 in osteoblasts remains largely undefined, as does the specific function of VAMP1 in these cells.

Figure 6.8 VAMP1 Co-localisation in Osteoblastic Cells.

VAMP1 has a vesicular type distribution in osteoblastic cells, distributed in a perinuclear fashion in a sub-set of these ROS 17/2.8 cells (B, →) as opposed to the predominately cytoplasmic distribution observed in undifferentiated PC12 cells (A). Limited co-localisation of VAMP1 (green) was observed with the lysosomes (red, C, with areas of co-localisation shown in yellow, →). Similarly, limited co-localisation of VAMP1 (red) was observed with the mitochondria (green, D with co-localisation shown in yellow, →). We have previously demonstrated areas of co-localisation of VAMP1 (green) with osteocalcin and type I collagen (blue), (E and F, with co-localisation shown in pale blue/white, →). Localisation of both the Golgi and ER in these cells, in addition to previous co-localisation experiments (Chapter 5), has demonstrated no apparent localisation of VAMP1 to these intracellular compartments. (Figures 6.8 A and B, E and F are identical to previously shown images in figs. 5.5 and 5.7 respectively).

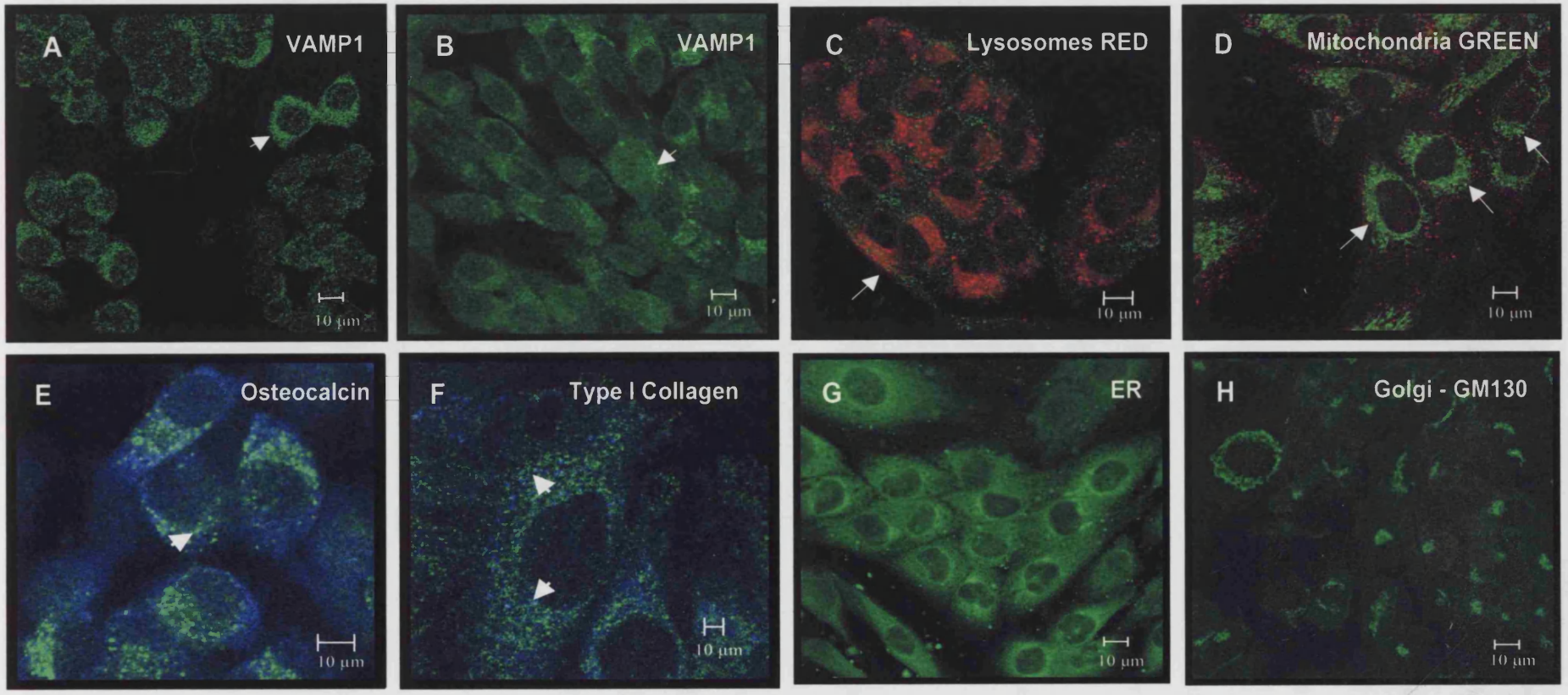
A
VAMP1
10 µm
B
VAMP1
10 µm
C
Lysosomes RED
10 µm
D
Mitochondria GREEN
10 µm
E
Osteocalcin
10 µm
F
Type I Collagen
10 µm
G
ER
10 µm
H
Golgi - GM130
10 µm

6.6 Discussion

Sequence analysis has revealed that osteoblasts express two splice variants of the v-SNARE VAMP1, rVAMP1B and VAMP1-OB. Similar to previously identified splice variants of neuronal VAMP1A (Berglund *et al.*, 1999; Isenmann *et al.*, 1998; Mandic *et al.*, 1997), these splice variants are products of alternative splicing between exons IV and V on the VAMP1 cDNA transcript and have altered carboxyl terminal residues, with the remaining N-terminal portion of the protein being highly conserved. Although immunocytochemistry has revealed VAMP1 localisation in osteoblastic cells to be vesicular, the specific localisation and potential function of VAMP1 in osteoblasts has not yet been determined. We hypothesise that these cytoplasmic vesicular structures could represent vesicular transport intermediates and may be responsible for the intracellular transport of newly synthesised bone matrix proteins.

The apparent up-regulation of VAMP1, in nodule forming cells of terminally differentiated primary cell cultures, suggests that rVAMP1B and VAMP1-OB may be implicated in the process of matrix deposition. Northern blot analysis, on samples harvested during nodule formation and mineralisation, would provide quantitative means of assessing VAMP1 expression in osteoblastic cells at various differentiation states and, in addition, provide insight into its potential role in the directional process of bone matrix deposition.

In an attempt to identify a potential functional role for VAMP1 in osteoblastic cells, a number of co-localisation experiments were performed. Initial investigations revealed limited co-localisation of VAMP1 with the transported matrix proteins osteocalcin and type I collagen.

Both rVAMP1B and VAMP1-OB contain positively charged C-terminal residues; therefore, the possibility that these proteins were localising to other sub-cellular compartments was investigated. Isenmann and co-workers (1998) have previously reported localisation of the positively charged hVAMP1B splice variant to the mitochondria. Using the mitochondria marker, Mito-Tracker GREEN, in addition to the lysosome marker, Lyso-Tracker RED, limited co-localisation of VAMP1 was observed with these compartments (fig. 6.8). Further investigations revealed no apparent co-localisation with either the Golgi or the endoplasmic reticulum. Although no conclusions with regard to VAMP1 function can be made from these observations, immunocytochemistry indicates a potential role for VAMP1 in the secretory pathway of osteoblastic cells (Chapter 5, figs. 5.5 and 5.6).

In an attempt to establish the precise role of VAMP1 in osteoblastic cells, we propose to undertake a number of functional studies. Using the *in vitro* model of nodule formation and mineralisation, established in chapter 3, we will attempt to inactivate VAMP1 through specific cleavage with neurotoxin and assess the effect that VAMP1 inactivation has on osteoblast cell function.

We have identified a previously unreported VAMP1 splice variant, VAMP1-OB, in osteoblasts, and we propose to determine whether or not this protein is an osteoblast specific VAMP1 isoform. By generating radioactively labelled probes directed against the specific VAMP1-OB C-terminal portion, using Northern blot analysis on multiple tissue blots, the specific distribution of VAMP1-OB can be assessed in a variety of rat tissues. The results reported in this chapter demonstrate the expression of the v-SNARE VAMP1 in osteoblastic cells; however, we have not yet accounted for the 2 kDa molecular weight difference displayed by Western blot analysis (Chapter 5, fig.5.4). In view of the evidence obtained from sequence

analysis, it would seem feasible to assume that this size difference is due to post-translational modifications that would remain undetected by sequence analysis.

Through these studies, identifying and characterising VAMP1 expression in osteoblastic cells, we propose to direct future investigations towards establishing a functional role for VAMP1 in osteoblasts, testing our hypothesis that VAMP1 is implicated in the directionality of bone matrix protein secretion. We propose that studies using immuno-electron microscopy may enable us to identify the vesicular structures that VAMP1 localises to, thus enabling us to investigate further the role of VAMP1 in osteoblast cell function. In addition, treatment with cycloheximide and glycoslyation inhibitors together with pulse chase experiments would provide a tool for identifying VAMP1 co-localisation with transported bone matrix proteins and identify whether glycosylation changes are the cause of size variation in VAMP1.

Analysis of VAMP1 amino acid sequence has revealed a potential N-glycosylation site, asparagine(Asn)-threonine(Thr)-threonine(Thr)-serine(Ser), located within the N-terminal region of the molecule, amino acids 27 to 30. However, the presence of the consensus tripeptide, Asn-Xaa-Ser, is not sufficient to conclude that the asparagine residue is glycosylated. Characteristically, N-glycosylation occurs in the endoplasmic reticulum. The VAMP1 protein sequence does not contain a typical N-terminal leader sequence, which is necessary for translocation into the endoplasmic reticulum. Recently, Kim and co-workers (1999) identified, using a series of point mutations and deletions, an endoplasmic reticulum targeting signal within VAMP2. These findings identify the targeting signal as the 16 residues amino-terminal to the hydrophobic transmembrane spanning domain. These

residues are believed to form an amphipathic helix containing four conserved lysine residues. Although these findings support the hypothesis that VAMP is initially targeted to the endoplasmic reticulum, prior to being sorted and directed to their final destinations within the secretory pathway, potential N-terminal modifications, such as N-glycosylation, seem unlikely. C-terminal anchorage to the membrane would exclude the N-terminal portion and the identified N-glycosylation site from the lumen of the endoplasmic reticulum, thus, preventing glycosylation. In addition to the N-glycosylation site described above, VAMP1 contains one potential protein kinase C phosphorylation site, two casein kinase II phosphorylation sites and three N-myristolyation sites. It would therefore seem reasonable to assume that the differential electrophoretic mobility of osteoblastic VAMP1 may potentially be due to differences in phosphorylation.

Chapter 7

CONCLUDING REMARKS AND FUTURE AIMS

Chapter 7

CONCLUDING REMARKS AND FUTURE AIMS

7.1 Summary

7.1.1 Intercellular Communication Between Osteoblasts

- Osteoblasts express a number of protein components associated with the adherens junction: ZO-1, cadherins, α and β-catenins, α-actinin and vinculin.
- In addition, osteoblastic cells express, at the mRNA level, integral membrane proteins associated with tight junction formation: occludin, claudins 1, 2 and 3.

7.1.2 Vesicular Trafficking in Osteoblasts

- Osteoblastic cells express the general fusion machinery proteins, α-SNAP and NSF.
- Osteoblastic cells express an isoform of the v-SNARE, VAMP1, with an apparent molecular weight 2 kDa larger in size than the VAMP1 protein expressed on purified rat synaptic vesicles.
- Sequence analysis revealed that osteoblasts express two splice variants of the v-SNARE VAMP1, rVAMP1B and VAMP1-OB.
- VAMP1 localises to a vesicular cytoplasmic distribution in osteoblastic cells, with limited co-localisation of VAMP1 observed with the transported proteins type I collagen and osteocalcin.
- VAMP1 expression concentrated in cells forming the nodule structure in mineralialising cell cultures, *in vitro*.

- Furthermore, osteoblasts express a calcium regulated v-SNARE, synaptotagmin II, and the general v-SNARE synaptotagmin IV. In addition, osteoblastic cells express the Golgi t-SNARE, syntaxin 6.

7.2 Intercellular Communication Between Osteoblasts

The directional nature of bone matrix protein secretion suggests that osteoblasts have the ability to define their membrane domains. Recent investigations, demonstrating differential targeting of haemagglutanin (HA) and vesicular stomatis virus glycoprotein G (VSV-G) to specific membranes, have defined the apical and basolateral domains within the osteoblast and, hence, polarisation within these cells (Ilvesaro *et al.*, 1999).

Chapter 4, provides evidence to support the hypothesis that osteoblasts use a molecular machinery similar to epithelial cells to achieve and maintain cell polarisation. Furthermore, these results indicate that cell to cell interaction within an osteoblast cell monolayer is potentially mediated through the formation of apical junctional complexes, in addition to the previously characterised GJ channels (Bhargava *et al.*, 1988; Doty, 1981; Palumbo *et al.*, 1990; Schirrmacher *et al.*, 1992; Steinberg *et al.*, 1994; Yamaguchi *et al.*, 1995; Ziambaras *et al.*, 1998). Specifically, osteoblasts express a number of protein components associated with AJ formation, implying that the stability and adhesive nature of the osteoblast monolayer is mediated by the homotypic association of calcium dependent glycoproteins. Recent evidence has implicated cadherin expression and subsequent cell to cell interactions in osteoblast cell differentiation (Cheng *et al.*, 1998). In addition, morphological studies have identified the presence of these adherens-like junctional

complexes between osteoblastic cells (Bhargava *et al.*, 1988; Palumbo *et al.*, 1990; Stanka, 1975).

In view of the sequential nature of apical junction formation, taken with the identification of specific TJ protein mRNA products within osteoblastic cell populations, it would seem reasonable to assume that osteoblastic cells have the potential to form TJ complexes. The observation, using freeze fracture techniques, that odontoblasts form TJs in addition to AJs and GJs during the process of dentinogenesis adds credence to this assumption (Arana-Chavez and Katchburian, 1997; Calle, 1985). Therefore, we hypothesise that osteoblastic cells may express TJ-associated proteins and form TJ complexes during the process of mineralisation. The molecular structure of these TJs on osteoblastic cells, however, has not yet been fully investigated. Our studies have identified, at the mRNA level, the expression of a subset of TJ-associated proteins, occludin, claudin 1, 2 and 3 in osteoblasts, with the partial cDNA transcripts of occludin, claudin 1, 2 and 3 identified being identical to their sequence counterparts isolated from rat liver, MDCK cells and those reported in sequence databases. Future studies evaluating differential expression of junction proteins, in conjunction with careful morphological analysis at different stages during *in vitro* nodule formation and mineralisation, should enable us to determine the ability of these cells to form TJ complexes.

Having established the potential of osteoblasts to form apical junctional complexes, the question of whether or not these complexes are crucial to osteoblast cell function remains. Would the inability of these cells to form either TJ or AJ adversely affect the process of mineralisation? Evidence from studies using TJ-protein knockout mice suggests TJ complexes to be crucial for the stability of the epithelial cell monolayer with AF-6 knockouts being lethal.

Therefore, it seems likely, that if osteoblasts could be rendered unable to express junctional protein complexes that the process of mineralisation would be impeded. Calcium depletion experiments could be established in short-term osteoblast cultures *in vitro*, in an attempt to address these questions. Bearing in mind the sequential formation of apical junctional complexes, it would seem feasible that disruption of the AJs would consequently lead to an inhibition of potential TJ formation. Calcium depletion, through the addition of 5 mM EGTA, would exert a direct effect on the calcium dependent cadherin molecules, thus preventing AJ formation in these cultures. A second, and possibly more specific approach, would involve the use of antisense oligonucleotides. Theoretically, the antisense oligonucleotide hybridises to the corresponding mRNA forming a complex that subsequently blocks translation of the target protein. Alternatively, this hybridisation can lead to RNase H activation and cleavage of the mRNA. Antisense oligonucleotides directed against specific TJ or AJ protein components could be introduced into long-term (22 day) primary osteoblast-like nodule forming and mineralising cultures. Antisense agents act as specific inhibitors of gene expression when introduced into cell cultures; however, the potential limitations of specificity, uptake and stability would have to be assessed to render this approach viable.

If apical junctional complex mediated cell polarisation is indeed required for directed bone matrix protein secretion then these experiments, knocking out TJ/AJ-associated protein expression and recruitment to plasma membrane, would result in the inability of these cells to deposit matrix or to mineralise *in vitro*, which could be assessed experimentally.

Other observations in this thesis have implicated cell to matrix interactions in the specific localisation of junction protein components and possibly cell polarisation.

Specifically, differential localisation of the AJ/TJ associated protein ZO-1 was observed in osteoblastic cells cultured on different ECM proteins. Of particular interest is the localisation of ZO-1 to focal-like contacts when cultured on dentine slices (Chapter 4, fig. 4.4). These observations suggest that in the absence of apical junction complex formation, the recruitment and localisation of junction complex associated proteins to the plasma membrane of adjacent cells is limited to cell to matrix and potential cell to cell contact sites. These observations uncover a number of unanswered questions. Does ZO-1 utilise its protein-protein interaction capacity to recruit vinculin or other focal contact associated proteins to the AJ plaque or does this protein have a junction complex independent function? These results indicate that the formation and, possibly, the maintenance of intercellular junctional complexes to be dependent on ECM interactions and on previously synthesised matrix. Could this be a possible mechanism by which osteoblasts regulate AJ and potential TJ formation?

Recent characterisation of cell to matrix interactions have revealed that osteoblasts, like other cell types, mediated these cell to matrix interactions through the heterodimeric association of cell surface glycoproteins, integrins. Specific characterisation of integrin expression has led to the identification of α1, α2, α3, α4, α5 and β1 on osteoblastic cells (reviewed by Bennett *et al.*, 2000, in press). There is evidence to suggest that osteoblasts may display different expression patterns of these integrins at different stages of osteoblast development and maturation. β1 is thought to play a major role in osteoblast cell function. Establishing a suitable model to study the role of individual integrins in bone formation has proven to be difficult, null mutations of β1 resulting in embryonic mortality at a stage of skeletal immaturity (Fassler and Meyer, 1995). In an attempt to overcome these problems, β1 null embryonic stem cells were generated and implanted into mice. On

examination, cells isolated from the resulting β1 null chimeras showed alterations in their adhesive properties and in extracellular matrix deposition (Brakebusch *et al.*, 1997). In addition, the expression of a dominant negative β1 subunit, targeted to mature osteoblastic cells *in vivo*, has been used to target transgene expression in transgenic mice (Zimmerman *et al.*, 2000). The expression of the dominant negative β1 subunit was controlled by the osteocalcin promoter, which is only expressed in mature osteoblasts and osteocytes. Transgenic animals, with altered integrin function in mature osteoblasts and osteocytes, displayed an osteoporotic phenotype, suggesting, a potential role for β1 integrins in bone turnover (Bennett *et al.*, 2000; Zimmerman *et al.*, 2000). It, thus, seems likely that cell to cell and cell to matrix interactions may work in concert to optimise matrix deposition in osteoblastic cells.

Our studies characterising junction associated protein expression in osteoblastic cells have established the possible mechanisms by which these cells achieve and maintain a polarised state. Subsequent studies therefore focused on identifying protein components of the molecular machinery responsible for polarised bone matrix protein secretion in these cells.

7.3 Vesicular Trafficking in Osteoblasts

Early observations in osteoblastic cells identified the presence of the v-SNARE, VAMP1 (vesicle associated membrane protein 1). VAMP1 has been implicated in regulated exocytosis in a number of neuronal and non-neuronal tissues; therefore, we hypothesised that VAMP1 may be a candidate protein implicated in bone matrix protein secretion.

Through sequence analysis we identified the presence of two VAMP1 splice variants in osteoblastic cell populations: the previously reported rVAMP1B splice variant (Isenmann *et al.*, 1998) and an uncharacterised VAMP1-OB splice variant. Both of these splice variants are products of alternative splicing between exons IV and V and have altered C-terminal portions (Berglund *et al.*, 1999; Isenmann *et al.*, 1998; Mandic *et al.*, 1997) compared to neuronal VAMP1A (Trimble *et al.*, 1988). In addition, both of these VAMP1 splice variants exhibit sequence identity to VAMP1A in their N-terminal portion with sequence divergence restricted to the terminal residues of the C-terminus. VAMP1 has been localised to a vesicular type cytoplasmic distribution within osteoblastic cells, a distribution that may be representative of biosynthetic vesicular transport intermediates. The hypothesis that VAMP1 associates with biosynthetic vesicular intermediates was supported by the observation that VAMP1 expression is concentrated in the cells forming the nodule structures, possibly indicating an up-regulation of the expression of this protein during *in vitro* nodule formation and mineralisation.

In an attempt to assess a possible functional role for VAMP1 in osteoblastic cells, VAMP1 co-localisation with transported matrix proteins such as osteocalcin and type I collagen was assessed. These experiments demonstrated limited co-localisation of VAMP1 with these proteins; however, we were unable to determine a potential functional role for this protein using these methods alone. Further co-localisation experiments with specific membrane bound compartments revealed no apparent co-localisation of VAMP1 with either the Golgi marker GM130 or a marker specific for the endoplasmic reticulum. Limited co-localisation of VAMP1 was observed with mitochondria and lysosomes. No conclusive results with regard to VAMP1 function in osteoblasts can be made from these limited observations.

Therefore, we propose to undertake the following investigations in an attempt to determine the functional role of VAMP1 in osteoblastic cells.

We will attempt to establish the specific localisation of VAMP1 in osteoblastic cells, focusing, in particular, on the vesicular type structures identified, using immunocytochemistry and confocal laser scanning microscopy and immuno-electron microscopy. Furthermore, using the *in vitro* model of nodule formation and mineralisation (described in Chapter 3) as a cellular model of osteoblastic function, we will attempt to inactivate VAMP1 through specific cleavage with neurotoxins and assess the affect that VAMP1 has on mineralisation and thus on osteoblast cell function. An alternative approach would involve the use of VAMP1 specific antisense probes, described in section 7.2.

The identification of VAMP1-OB expression in osteoblastic cells is of particular interest. Could VAMP1-OB represent an osteoblast specific v-SNARE? In an attempt to address this question we propose to determine VAMP1-OB tissue distribution. By generating probes directed against the specific C-terminal portion of VAMP1-OB, using Northern blot analysis on multiple tissue blots the extent of VAMP1-OB expression in rat tissues could be determined. Although we have identified the expression of the VAMP1 splice variants rVAMP1B and VAMP1-OB in osteoblastic cells, we have yet to account for the differential electrophoretic mobility of the VAMP1 protein. We hypothesise that this 2 kDa size difference could be due to post-translational modifications, such as variation in carbohydrate attachment, that would remain undetected by sequence analysis. Analysis of the VAMP1 protein sequence has revealed the presence of a potential N-glycosylation site; however, the N-terminal location of this site suggests N-glycosylation of VAMP1 to be unlikely (discussed in detail in Chapter 6, section 6.6). Three

potential phosphorylation sites have been identified in VAMP1, suggesting that variation in phosphorylation may be responsible for the differential electrophoretic mobility of osteoblastic VAMP1.

Additional observations have revealed that, although VAMP1 appears to be up-regulated in and concentrated to cells forming the nodule structure, VAMP1 mRNA levels appear largely unaffected during nodule formation and mineralisation. To quantitatively assess differential VAMP1 expression during nodule formation and mineralisation it would be valuable to assess VAMP1 expression at different stages of primary osteoblastic cell culture using Northern Blot analysis.

Limited studies have identified a number of v-SNARE interacting proteins in osteoblastic cells. It is clear from these results that osteoblasts fail to express syntaxin 1, the general VAMP1 interacting t-SNARE. However, these studies have revealed osteoblastic cells to express the Golgi t-SNARE, syntaxin 6. In an attempt to characterise and identify more fully possible VAMP1-interacting proteins, VAMP1-OB DNA obtained from 3' RACE reaction could be inserted into a GST-fusion vector. Following over-expression in *E.coli* the purified GST-fusion protein could be used to isolate VAMP1- interacting proteins from ROS 17/2.8 cell or primary osteoblast-like cell extracts. Recently, the yeast two-hybrid system has been used to identify potential VAMP interacting proteins. Although a novel VAMP associated protein of 33 kDa has been identified (VAP33) (Skehel *et al.*, 2000) and implicated in the delivery of components to the synaptic terminals (Skehel *et al.*, 2000), no VAMP1 interacting t-SNAREs have been identified using this assay. This may be due in part to the complex nature of the interactions responsible for SNARE complex formation. SNARE proteins interact through the formation of

α-helical coiled-coils, which are based on the presence of repeated heptad motifs within their sequence (Chapman *et al.*, 1994; Harbury, 1998; Terrian and White, 1997). SNAP-25 contributes two helical segments while VAMP and syntaxin each contribute one (Chapman *et al.*, 1994; Montal, 1999). This coiled-coil structure has been implicated in the tethering of target membranes, facilitating the formation of the SNARE complex (Clague, 1999). In addition, this coiled-coil structure contributes to the stability of the fusion core complex. Poirier and co-workers (1998) have described the SNARE complex as a parallel four-stranded α-helical bundle (Poirier *et al.*, 1998). This increase in the helical content, associated with SNARE complex formation, indicates that major conformational changes occur during SNARE complex assembly (Fasshauer *et al.*, 1999; Fasshauer *et al.*, 1997; Fiebig *et al.*, 1999). Therefore, it seems reasonable to assume that the components of this fusion complex only interact with each other once they have adopted the correct conformation, which is difficult to achieve in the yeast two-hybrid system.

Having established potential components of the constitutive exocytotic pathway in osteoblastic cells, the question of a calcium modulated exocytotic pathway was addressed. Interestingly, we identified the presence of the general v-SNARE, synaptotagmin IV and the calcium sensitive v-SNARE synaptotagmin II. Although these v-SNAREs have yet to be characterised fully, *in vitro* analysis has located synaptotagmin II to the cells forming the nodule structures in primary osteoblastic cells, in a similar manner to VAMP1 distribution in these cells.

The identification, in osteoblasts, of the general fusion machinery proteins NSF and α-SNAP, in addition to the presence of rVAMP1B, VAMP1-OB and synaptotagmin, strongly suggests that bone matrix deposition may be achieved through a SNARE mediated mechanism of membrane targeting and fusion. In addition to a

constitutive mechanisms of regulated bone matrix protein secretion it would seem likely that these cells also possess a calcium regulated mechanism of secretion.

7.4 Implications for Disease

Through these studies we have gained valuable insight into osteoblast cell function. Comprehending the molecular mechanisms utilised by osteoblastic cells to achieve directionality of bone matrix proteins will not only lead to a better understanding of osteoblast cell function but will subsequently allow us to evaluate possible therapeutic targets in disease states which result from mis-targeted or mis-regulated bone formation processes. Therefore, careful identification and characterisation of vectorial transport in osteoblasts may lead to a fuller understanding of the molecular switch responsible for bone matrix deposition, potentially leading to means of *in vivo* regulation of osteoblast cell function.

List of Published Abstracts

Oral Presentation

Prele, C., Horton, M. A. and Stenbeck, G. (1999). Unraveling the secretory pathways in osteoblasts. Journal of Bone and Miner. Res. *14* (6), 1031.

Published Abstracts

Prele, C., Horton, M. A. and Stenbeck, G. (1998). Molecular mechanisms of vectoral transport in osteoblasts. Bone *22* (3), 17S.

Prele, C., Horton, M. A. and Stenbeck, G. (1999) Identification of a novel v-SNARE isoform in osteoblasts. Calcif Tissue Int *64*, S55.

Chapter 8

REFERENCES

References

Aberle, H., Schwartz, H., and Kemler, R. (1996). Cadherin-catenin complex: protein interactions and their implications for cadherin function. J Cell Biochem *61*, 514-23.

Advani, R. J., Bae, H. R., Bock, J. B., Chao, D. S., Doung, Y. C., Prekeris, R., Yoo, J. S., and Scheller, R. H. (1998). Seven novel mammalian SNARE proteins localize to distinct membrane compartments. J Biol Chem *273*, 10317-24.

Advani, R. J., Yang, B., Prekeris, R., Lee, K. C., Klumperman, J., and Scheller, R. H. (1999). VAMP-7 mediates vesicular transport from endosomes to lysosomes. J Cell Biol *146*, 765-76.

Anderson, J. M., and Van Itallie, C. M. (1995). Tight junctions and the molecular basis for regulation of paracellular permeability. Am J Physiol *269*, G467-75.

Anderson, J. M., and Van Itallie, C. M. (1999). Tight junctions: closing in on the seal. Curr Biol *9*, R922-4.

Arana-Chavez, V. E., and Katchburian, E. (1997). Development of tight junctions between odontoblasts in early dentinogenesis as revealved by freeze fracture. The Anat Rec *248*, 332-338.

Aubin, J. E., Turksen, K., and Heersche, J. N. M. (1993). Osteoblast Cell Lineage. Academic press Inc.

Babich, M., and Foti, L. R. (1994). E-cadherins identified in osteoblastic cells: effects of parathyroid hormone and extracellular calcium on localization. Life Sci *54*, L201-8.

Balch, W. E., Dunphy, W. G., Braell, W. A., and Rothman, J. E. (1984). Reconstitution of the transport of protein between successive compartments of the Golgi measured by the coupled incorporation of N-acetylglucosamine. Cell *39*, 405-16.

Balda, M. S., and Anderson, J. M. (1993). Two classes of tight junctions are revealed by ZO-1 isoforms. Am J Physiol *264*, C918-24.

Balda, M. S., and Matter, K. (1998). Tight junctions. J Cell Sci *111*, 541-547.

Bark, I. C. (1993). Structure of the chicken gene for SNAP-25 reveals duplicated exon encoding distinct isoforms of the protein. J Mol Biol *233*, 67-76.

Bark, I. C., and Wilson, M. C. (1994). Human cDNA clones encoding two different isoforms of the nerve terminal protein SNAP-25. Gene *139*, 291-2.

Baron, R. E. (1996). Anatomy and Ultrastructure of Bone. In Primer on Metabolic Bone Diseases and Disorders of Mineral Metabolism, ed. Favus, M. J., Lippincott-Raven, Vol. pp. 3-10

Beatch, M., Jesaitis, L. A., Gallin, W. J., Goodenough, D. A., and Stevenson, B. R. (1996). The tight junction protein ZO-2 contains three PDZ (PSD-95/Discs-Large/ZO-1) domains and an alternatively spliced region. J Biol Chem *271*, 25723-6.

Beck, R. G., Sullivan, E. C., Moran, E., and Zerler, B. (1998). Relationship between alkaline phosphatase levels, osteopontin expression, and mineralization in differentiating MC3T3-E1 osteoblasts. J Cell Biochem *68*, 269-280.

Bellows, C. G., and Aubin, J. E. (1989). Determination of numbers of osteoprogenitors present in isolated fetal rat calvaria cells in vitro. Dev Biol *133*, 8-13.

Bellows, C. G., Aubin, J. E., and Heersche, J. N. (1987). Physiological concentrations of glucocorticoids stimulate formation of bone nodules from isolated rat calvaria cells in vitro. Endocrinology *121*, 1985-92.

Bellows, C. G., Aubin, J. E., Heersche, J. N., and Antosz, M. E. (1986). Mineralized bone nodules formed in vitro from enzymatically released rat calvaria cell populations. Calcif Tissue Int *38*, 143-54.

Bellows, C. G., Aubin, J. E., and Heersche, J. N. M. (1991). Initiation and progression of mineralization of bone nodules formed in vitro: the role of alkaline phosphatase and organic phosphate. Bone and Mineral *14*, 27-40.

Bellows, C. G., Heersche, J. N., and Aubin, J. E. (1990). Determination of the capacity for proliferation and differentiation of osteoprogenitor cells in the presence and absence of dexamethasone. Dev Biol *140*, 132-8.

Bellows, C. G., Reimers, S. M., and Heersche, J. N. (1999). Expression of mRNAs for type-I collagen, bone sialoprotein, osteocalcin, and osteopontin at different stages of osteoblastic differentiation and their regulation by 1,25 dihydroxyvitamin D3. Cell Tissue Res *297*, 249-59.

Bennett, J. H., Moffatt, S., Horton, M. (2000) Cell Adhesion Molecules in Human Osteoblasts: Structure and Function. Histol. Histopath. (in press).

Bennett, M. K., Calakos, N., and Scheller, R. H. (1992). Syntaxin: a synaptic protein implicated in docking of synaptic vesicles at presynaptic active zones. Science *257*, 255-9.

Bennett, M. K., Garcia-Arraras, J. E., Elferink, L. A., Peterson, K., Fleming, A. M., Hazuka, C. D., and Scheller, R. H. (1993). The syntaxin family of vesicular transport receptors. Cell *74*, 863-73.

Bennett, M. K., and Scheller, R. H. (1993). The molecular machinery for secretion is conserved from yeast to neurons. Proc. Natl. Acad. Sci. *90*, 2559-2563.

Bennett, M. K., and Scheller, R. H. (1994). A molecular description of synaptic vesicle membrane trafficking. Annu Rev Biochem *63*, 63-100.

Beresford, J. N., Bennett, J. H., Devlin, C., Leboy, P. S., and Owen, M. E. (1992). Evidence for an inverse relationship between the differentiation of adipocytic and osteogenic cells in rat marrow stromal cell cultures. J Cell Sci *102*, 341-51.

Berglund, L., Hoffmann, H. J., Dahl, R., and Petersen, T. E. (1999). VAMP-1 has a highly variable C-terminus generated by alternative splicing. Biochem Biophys Res Commun *264*, 777-80.

Bhargava, U., Bar-Lev, M., Bellows, C. G., and Aubin, J. E. (1988). Ultrastructural analysis of bone nodules formed in vitro by isolated fetal rat calvaria cells. Bone *9*, 155-63.

Birchmeier, W., Weidner, K. M., and Behrens, J. (1993). Molecular mechanisms leading to loss of differentiation and gain of invasiveness in epithelial cells. J Cell Sci Suppl *17*, 159-64.

Blasi, J., Chapman, E. R., Link, E., Binz, T., Yamasaki, S., De Camilli, P., Sudhof, T. C., Niemann, H., and Jahn, R. (1993a). Botulinum neurotoxin A selectively cleaves the synaptic protein SNAP-25. Nature *365*, 160-163.

Blasi, J., Chapman, E. R., Yamasaki, S., Binz, T., Niemann, H., and Jahn, R. (1993b). Botulinum neurotoxin C1 blocks neurotransmitter release by means of cleaving HPC-1/syntaxin. Embo J *12*, 4821-8.

Bock, J. B., Klumperman, J., Davanger, S., and Scheller, R. H. (1997). Syntaxin 6 functions in trans-Golgi network vesicle trafficking. Mol Biol Cell *8*, 1261-71.

Bock, J. B., Lin, R. C., and Scheller, R. H. (1996). A new syntaxin family member implicated in targeting of intracellular transport vesicles. J Biol Chem *271*, 17961-5.

Boskey, A. L. (1992). Mineral-matrix interactions in bone and cartilage. Clin Orthop 244-74.

Boskey, A. L. (1998). Biomineralization: conflicts, challenges, and opportunities. J Cell Biochem Suppl *31*, 83-91.

Boskey, A. L., Boyan, B. D., Doty, S. B., Feliciano, A., Greer, K., Weiland, D., Swain, L. D., and Schwartz, Z. (1992a). Studies of matrix vesicle-induced mineralization in a gelatin gel. Bone Miner *17*, 257-62.

Boskey, A. L., Camacho, N. P., Mendelsohn, R., Doty, S. B., and Binderman, I. (1992b). FT-IR microscopic mappings of early mineralization in chick limb bud mesenchymal cell cultures. Calcif Tissue Int *51*, 443-8.

Boskey, A. L., Stiner, D., Doty, S. B., Binderman, I., and Leboy, P. (1992c). Studies of mineralization in tissue culture: optimal conditions for cartilage calcification. Bone Miner *16*, 11-36.

Brakebusch, C., Hirsch, E., Potocnik, A., Fassler, R. (1997). Genetic analysis of beta1 integrin function: confirmed, new and revised roles for a crucial family of cell adhesion molecules. J Cell Sci *110*, 2895-904.

Brimhall, B. B., Sikorski, K. A., Torday, J., Shahsafaei, A., Haley, K. J., and Sunday, M. E. (1999). Syntaxin 1A is transiently expressed in fetal lung mesenchymal cells: potential developmental roles. Am J Physiol *277*, L401-11.

Brose, N., Petrenko, A. G., Sudhof, T. C., and Jahn, R. (1992). Synaptotagmin: a calcium sensor on the synaptic vesicle surface. Science *256*, 1021-5.

Bruzzone, R., White, T. W., and Goodenough, D. A. (1996a). The cellular internet: on-line with connexins. BioEssays *18*, 709-718.

Bruzzone, R., White, T. W., and Paul, D. L. (1996b). Connections with connexins: the molecular basis of direct intercellular signaling. Eur J Biochem *238*, 1-27.

Burgoyne, R. D., and Morgan, A. (1998). Analysis of regulated exocytosis in adrenal chromaffin cells: insights into NSF/SNAP/SNARE function. Bioessays *20*, 328-35.

Burridge, K., Fath, K., Kelly, T., Nuckolls, G., and Turner, C. (1988). Focal adhesions: transmembrane junctions between the extracellular matrix and the cytoskeleton. Annu Rev Cell Biol *4*, 487-525.

Butler, W. T. (1995). Dentin matrix proteins and dentinogenesis. Connect Tissue Res *33*, 59-65.

Butler, W. T., Ritchie, H. H., and Bronckers, A. L. (1997). Extracellular matrix proteins of dentine. Ciba Found Symp *205*, 107-15.

Calle, A. (1985). Intercellular junctions between human odontoblasts. Acta Anat. *122*, 138-144.

Cereijido, M., Shoshani, L., Contreras, R. G. (2000). Molecular physiology and pathophysiology of tight junctions. I. Biogenesis of tight junctions and epithelial polarity. Am J Physiol Gastrointest Liver Physiol *279*, G477-82.

Chambers, R. C., and Laurent, G. J. (1997). Collagens. In The Lung, ed. Crystal, R. G. and West, J. B., Lippincott-Raven, Philadelphia. Vol. pp. 709-727

Chapman, E. R., An, S., Barton, N., and Jahn, R. (1994). SNAP-25, a t-SNARE which binds to both syntaxin and synaptobrevin via domains that may form coiled coils. J Biol Chem *269*, 27427-32.

Chapman, E. R., Hanson, P. I., An, S., and Jahn, R. (1995). Ca2+ regulates the interaction between synaptotagmin and syntaxin 1. J Biol Chem *270*, 23667-71.

Chavrier, P., and Goud, B. (1999). The role of ARF and Rab GTPases in membrane transport. Curr Opin Cell Biol *11*, 466-75.

Chen, Y. A., Scales, S. J., Patel, S. M., Doung, Y. C., and Scheller, R. H. (1999). SNARE complex formation is triggered by Ca2+ and drives membrane fusion. Cell *97*, 165-74.

Cheng, S., Lecanda, F., Davidson, M. K., Warlow, P. M., Zhang, S., Zhang, L., Suzuki, S., St. John, T., and Civitelli, R. (1998). Human osteoblasts express a repertoire of cadherins, which are critical for BMP-2-induced osteogenic differentiation. J Bone Miner Res *13*, 633-644.

Chilcote, T. J., Galli, T., Mundigl, O., Edelmann, L., McPherson, P. S., Takei, K., and De Camilli, P. (1995). Cellubrevin and synaptobrevins: similar subcellular localization and biochemical properties in PC12 cells. J Cell Biol *129*, 219-31.

Chomczynski, P., and Sacchi, N. (1987). Single-step method of RNA isolation by acid guanidinium thiocyanate-phenol-chloroform extraction. Anal Biochem *162*, 156-9.

Chung, C. H., Golub, E. E., Forbes, E., Tokuoka, T., and Shapiro, I. M. (1992). Mechanism of action of beta-glycerophosphate on bone cell mineralization. Calcif Tissue Int *51*, 305-11.

Citi, S. (2000). Introduction: opening up tight junctions. Semin Cell Dev Biol *11*, 277-9.

Citi, S. (1992). Protein kinase inhibitors prevent junction dissociation induced by low extracellular calcium in MDCK epithelial cells. J Cell Biol *117*, 169-78.

Citi, S., and Cordenonsi, M. (1998). Tight junction proteins. Biochim Biophys Acta *1448*, 1-11.

Citi, S., Sabanay, H., Jakes, R., Geiger, B., and Kendrick-Jones, J. (1988). Cingulin, a new peripheral component of tight junctions. Nature *333*, 272-6.

Citi, S., Volberg, T., Bershadsky, A. D., Denisenko, N. and Geiger, B. (1994). Cytoskeletal involvement in the modulation of cell-cell junctions by the protein kinase inhibitor H-7. J Cell Sci *107*, 683-92.

Clague, M. J. (1999). Membrane transport: Take your fusion partners. Curr Biol *9*, R258-60.

Coco, S., Raposo, G., Martinez, S., Fontaine, J. J., Takamori, S., Zahraoui, A., Jahn, R., Matteoli, M., Louvard, D., and Galli, T. (1999). Subcellular localization of tetanus neurotoxin-insensitive vesicle-associated membrane protein (VAMP)/VAMP7 in neuronal cells: evidence for a novel membrane compartment. J Neurosci *19*, 9803-12.

Cordenonsi, M., D'Atri, F., Hammar, E., Parry, D. A., Kendrick-Jones, J., Shore, D., and Citi, S. (1999). Cingulin contains globular and coiled-coil domains and interacts with ZO-1, ZO-2, ZO-3, and myosin. J Cell Biol *147*, 1569-82.

Cowles, E. A., DeRome, M. E., Pastizzo, G., Brailey, L. L., and Gronowicz, G. A. (1998). Mineralization and the expression of matrix proteins during in vivo bone development. Calcif Tissue Int *62*, 74-82.

Craig, S. W., and Pardo, J. V. (1979). alpha-Actinin localization in the junctional complex of intestinal epithelial cells. J Cell Biol *80*, 203-10.

Darchen, F., and Goud, B. (2000). Multiple aspects of Rab protein action in the secretory pathway: focus on Rab3 and Rab6. Biochimie *82*, 375-84.

Dascher, C., Matteson, J., and Balch, W. E. (1994). Syntaxin 5 regulates endoplasmic reticulum to Golgi transport. J Biol Chem *269*, 29363-6.

Delany, A. M., Dong, Y., and Canalis, E. (1994). Mechanisms of glucocorticoid action in bone cells. J Cell Biochem *56*, 295-302.

Denisenko, N., Burighel, P. and Citi, S. (1994). Different effects of protein kinase inhibitors on the localization of junctional proteins at cell-cell contact sites. J Cell Sci *107*, 969-81.

Denker, B. M. and Nigam, S. K. (1998). Molecular structure and assembly of the tight junction. Am J Physiol *274*, F1-9.

Donahue, H. J., Li, Z., Zhou, Z., and Yellowley, C. E. (2000). Differentiation of human fetal osteoblastic cells and gap junctional intercellular communication. Am J Physiol Cell Physiol *278*, C315-22.

Doty, S. B. (1981). Morphological evidence of gap junctions between bone cells. Calcif Tissue Int *33*, 509-12.

Drenckhahn, D., and Franz, H. (1986). Identification of actin-, alpha-actinin-, and vinculin-containing plaques at the lateral membrane of epithelial cells. J Cell Biol *102*, 1843-52.

Ducy, P., Desbois, C., Boyce, B., Pinero, G., Story, B., Dunstan, C., Smith, E., Bonadio, J., Goldstein, S., Gundberg, C., Bradley, A., and Karsenty, G. (1996). Increased bone formation in osteocalcin-deficient mice. Nature *382*, 448-52.

Duncan, R. R., Shipston, M. J., and Chow, R. H. (2000). Double C2 protein. A review. Biochimie *82*, 421-6.

Eakle, K. A., Bernstein, M., and Emr, S. D. (1988). Characterization of a component of the yeast secretion machinery: identification of the SEC18 gene product. Mol Cell Biol *8*, 4098-109.

Ebnet, K., Schulz, C. U., Meyer Zu Brickwedde, M. K., Pendl, G. G., and Vestweber, D. (2000). Junctional Adhesion Molecule (JAM) interacts with the PDZ domain containing proteins AF-6 and ZO-1. J Biol Chem

Einhorn, T. A. (1996). The Bone Organ System: Form and Function. In Osteoporosis, ed. Marcus, R., Feldman, D. and Kelsey, J., Academic Press, Inc., Vol. pp. 3-22

Elferink, L. A., Trimble, W. S., and Scheller, R. H. (1989). Two vesicle-associated membrane protein genes are differentially expressed in the rat central nervous system. J Biol Chem *264*, 11061-4.

Erlebacher, A., Filvaroff, E. H., Ye, J. Q., and Derynck, R. (1998). Osteoblastic responses to TGF-beta during bone remodeling. Mol Biol Cell *9*, 1903-18.

Fasshauer, D., Antonin, W., Margittai, M., Pabst, S. and Jahn, R. (1999). Mixed and non-cognate SNARE complexes. Characterization of assembly and biophysical properties. J Biol Chem *274*, 15440-6.

Fasshauer, D., Otto, H., Eliason, W. K., Jahn, R., and Brunger, A. T. (1997). Structural changes are associated with soluble N-ethylmaleimide-sensitive fusion protein attachment protein receptor complex formation. J Biol Chem *272*, 28036-28041.

Fassler, R. and Meyer, M. (1995). Consequences of lack of beta 1 integrin gene expression in mice. Genes Dev *15*, 1896-908.

Fedde, K. N., Blair, L., Silverstein, J., Coburn, S. P., Ryan, L. M., Weinstein, R. S., Waymire, K., Narisawa, S., Millan, J. L., MacGregor, G. R., and Whyte, M. P. (1999). Alkaline phosphatase knock-out mice recapitulate the metabolic and skeletal defects of infantile hypophosphatasia. J Bone Miner Res *14*, 2015-26.

Ferrari, S. L., Traianedes, K., Thorne, M., Lafage-Proust, M. H., Genever, P., Cecchini, M. G., Behar, V., Bisello, A., Chorev, M., Rosenblatt, M., and Suva, L. J. (2000). A role for N-cadherin in the development of the differentiated osteoblastic phenotype. J Bone Miner Res *15*, 198-208.

Fiebig, K. M., Rice, L. M., Pollock, E. and Brunger, A. T. (1999). Folding intermediates of SNARE complex assembly. Nat Struct Biol *6*, 117-23.

Franceschi, R. T., Iyer, B. S., and Cui, Y. (1994). Effects of ascorbic acid on collagen matrix formation and osteoblast differentiation in murine MC3T3-E1 cells. J Bone Miner Res *9*, 843-54.

Franke, W. W., Cowin, P., Schmelz, M., and Kapprell, H. P. (1987). The desmosomal plaque and the cytoskeleton. Ciba Found Symp *125*, 26-48.

Fries, E., and Rothman, J. E. (1980). Transport of vesicular stomatitis virus glycoprotein in a cell-free extract. Proc Natl Acad Sci U S A 77, 3870-4.

Fujita, H., Tuma, P. L., Finnegan, C. M., Locco, L., and Hubbard, A. L. (1998). Endogenous syntaxins 2, 3 and 4 exhibit distinct but overlapping patterns of expression at the hepatocyte plasma membrane. Biochem J *329*, 527-38.

Furuse, M., Fujimoto, K., Sato, N., Hirase, T., and Tsukita, S. (1996). Overexpression of occludin, a tight junction-associated integral membrane protein, induces the formation of intracellular multilamellar bodies bearing tight junction-like structures. J Cell Sci *109*, 429-35.

Furuse, M., Fujita, K., Hiiragi, T., Fujimoto, K., and Tsukita, S. (1998a). Claudin-1 and -2: novel integral membrane proteins localizing at tight junctions with no sequence similarity to occludin. J Cell Biol *141*, 1539-50.

Furuse, M., Itoh, M., Hirase, T., Nagafuchi, A., Yonemura, S., Tsukita, S., and Tsukita, S. (1994). Direct association of occludin with ZO-1 and its possible involvement of the localization of occludin at tight junctions. The Journal of Cell Biology *127*, 1617-1626.

Furuse, M., Sasaki, H., Fujimoto, K., and Tsukita, S. (1998b). A single gene product, claudin-1 or 2, reconstitutes tight junction strands and recruits occludin in fibroblasts. J Cell Biol *143*, 391-401.

Furuse, M., Tetsuaki, H., Itoh, M., Nagafuchi, A., Yonemura, S., Tsukita, S., and Tsukita, S. (1993). Occludin: a novel integral membrane protein localizing at tight junctions. J Cell Biol *123*, 1777-1788.

Galli, T., Chilcote, T., Mundigl, O., Binz, T., Niemann, H., and De Camilli, P. (1994). Tetanus toxin-mediated cleavage of cellubrevin impairs exocytosis of transferrin receptor-containing vesicles in CHO cells. J Cell Biol *125*, 1015-24.

Geiger, B., Volberg, T., Ginsberg, D., Bitzur, S., Sabanay, I., and Hynes, R. O. (1990). Broad spectrum pan-cadherin antibodies, reactive with the C-terminal 24 ammino acid residues of N-cadherin. Journal of Cell Science *97*, 607-614.

Geiger, B., Volk, T., Volberg, T., and Bendori, R. (1987). Molecular interactions in adherens-type contacts. J Cell Sci Suppl *8*, 251-72.

Geppert, M., Archer, B. T. d., and Sudhof, T. C. (1991). Synaptotagmin II. A novel differentially distributed form of synaptotagmin. J Biol Chem *266*, 13548-52.

Grigoriadis, A. E., Heersche, J. N. M., and Aubin, J. E. (1988). Differenciation of muscle, fat, cartilage and bone from progenitor cells present in bone-derived clonal cell population: effect of dexamethasone. J Cell Biol *106*, 2139-2151.

Gronowicz, G., and Raisz, L. G. (1996). Bone Formation Assays. In Principles of Bone Biology, ed. Bilezikian, J. P., Raisz, L. G. and Rodan, G. A., Academic Press, Vol. pp. 1253-1265

Grote, E., Hao, J. C., Bennett, M. K., and Kelly, R. B. (1995). A targeting signal in VAMP regulating transport to synaptic vesicles. Cell *81*, 581-9.

Gumbiner, B. (1987). Structure, biochemistry, and assembly of epithelial tight junctions. Am J Physiol *253*, C749-58.

Gumbiner, B., Lowenkopf, T., and Apatira, D. (1991). Identification of a 160-kDa polypeptide that binds to the tight junction protein ZO-1. Proc Natl Acad Sci U S A *88*, 3460-4.

Harada, S., Matsumoto, T., and Ogata, E. (1991). Role of ascorbic acid in the regulation of proliferation in osteoblast- like MC3T3-E1 cells. J Bone Miner Res *6*, 903-8.

Harbury, P. A. (1998). Springs and zippers: coiled coils in SNARE-mediated membrane fusion. Structure *6*, 1487-91.

Haskins, J., Gu, L., Wittchen, E. S., Hibbard, J., and Stevenson, B. R. (1998). ZO-3, a novel member of the MAGUK protein family found at the tight junction, interacts with ZO-1 and occludin. J Cell Biol *141*, 199-208.

Hatsuzawa, K., Hirose, H., Tani, K., Yamamoto, A., Scheller, R. H., and Tagaya, M. (2000). Syntaxin 18, a SNAP receptor that functions in the endoplasmic reticulum, intermediate compartment, and cis-Golgi vesicle trafficking. J Biol Chem *275*, 13713-20.

Hay, E., Lemonnier, J., Modrowski, D., Lomri, A., Lasmoles, F., and Marie, P. J. (2000). N- and E-cadherin mediate early human calvaria osteoblast differentiation promoted by bone morphogenetic protein-2. J Cell Physiol *183*, 117-28.

Hayashi, T., McMahon, H., Yamasaki, S., Binz, T., Hata, Y., Sudhof, T. C., and Niemann, H. (1994). Synaptic vesicle membrane fusion complex: action of clostridial neurotoxins on assembly. Embo J *13*, 5051-61.

Hayashi, T., Yamasaki, S., Nauenburg, S., Binz, T., and Niemann, H. (1995). Disassembly of the reconstituted synaptic vesicle membrane fusion complex in vitro. Embo J *14*, 2317-25.

Hazzard, J., Sudhof, T. C., and Rizo, J. (1999). NMR analysis of the structure of synaptobrevin and of its interaction with syntaxin. J Biomol NMR *14*, 203-7.

Herrenknecht, K. (1996). Cadherins. In Molecular Biology of Cell Adhesion Molecules, ed. Horton, M. A., John Wiley and Sons, Vol. pp. 45-70

Herrenknecht, K., Ozawa, M., Eckerskorn, C., Lottspeich, F., Lenter, M., and Kemler, R. (1991). The uvomorulin-anchorage protein alpha catenin is a vinculin homologue. Proc Natl Acad Sci U S A *88*, 9156-60.

Hirase, T., Staddon, J. M., Saitou, M., Ando-Akatsuka, Y., Itoh, M., Furuse, M., Fujimoto, K., Tsukita, S., and Rubin, L. L. (1997). Occludin as a possible determinant of tight junction permeability in endothelial cells. J Cell Sci *110*, 1603-13.

Hirling, H., Steiner, P., Chaperon, C., Marsault, R., Regazzi, R., and Catsicas, S. (2000). Syntaxin 13 is a developmentally regulated SNARE involved in neurite outgrowth and endosomal trafficking. Eur J Neurosci *12*, 1913-23.

Hodel, A. (1998). Snap-25. Int J Biochem Cell Biol *30*, 1069-73.

Hohl, T. M., Parlati, F., Wimmer, C., Rothman, J. E., Sollner, T. H., and Engelhardt, H. (1998). Arrangement of subunits in 20 S particles consisting of NSF, SNAPs, and SNARE complexes. Mol Cell 2, 539-48.

Howarth, A. G. and Stevenson, B. R. (1995). Molecular environment of ZO-1 in epithelial and non-epithelial cells. Cell Motil Cytoskeleton *31*, 323-32.

Hughes, F. J., and Aubin, J. E. (1998). Culture of Cells of the Osteoblast Lineage. In Methods in Bone Biology, ed. Arnett, T. R. and Henderson, B., Chapman & Hall, Vol. pp.

Hunter, G. K., Hauschka, P. V., Poole, A. R., Rosenberg, L. C., and Goldberg, H. A. (1996). Nucleation and inhibition of hydroxyapatite formation by mineralized tissue proteins. Biochem J *317*, 59-64.

Huttner, W. B. (1993). Snappy exocytoxins. Nature *365*, 104-105.

Huttner, W. B., Schiebler, W., Greengard, P., and De Camilli, P. (1983). Synapsin I (protein I), a nerve terminal-specific phosphoprotein. III. Its association with synaptic vesicles studied in a highly purified synaptic vesicle preparation. J Cell Biol *96*, 1374-88.

Ibaraki, K., Horikawa, H. P., Morita, T., Mori, H., Sakimura, K., Mishina, M., Saisu, H., and Abe, T. (1995). Identification of four different forms of syntaxin 3. Biochem Biophys Res Commun *211*, 997-1005.

Ikeda, W., Nakanishi, H., Miyoshi, J., Mandai, K., Ishizaki, H., Tanaka, M., Togawa, A., Takahashi, K., Nishioka, H., Yoshida, H., Mizoguchi, A., Nishikawa, S., and Takai, Y. (1999). Afadin: A key molecule essential for structural organization of cell-cell junctions of polarized epithelia during embryogenesis. J Cell Biol *146*, 1117-32.

Ilvesaro, J., Metsikko, K., Vaananen, K., and Tuukkanen, J. (1999). Polarity of osteoblasts and osteoblast-like UMR-108 cells. J Bone Miner Res *14*, 1338-44.

Isenmann, S., Khew-Goodall, Y., Gamble, J., Vadas, M., and Wattenberg, B. W. (1998). A splice-isoform of vesicle-associated membrane protein-1 (VAMP-1) contains a mitochondrial targeting signal. Mol Biol Cell *9*, 1649-60.

Itoh, M., Furuse, M., Morita, K., Kubota, K., Saitou, M., and Tsukita, S. (1999a). Direct binding of three tight junction-associated MAGUKs, ZO-1, ZO-2, and ZO-3, with the COOH termini of claudins. J Cell Biol *147*, 1351-63.

Itoh, M., Morita, K., and Tsukita, S. (1999b). Characterization of ZO-2 as a MAGUK family member associated with tight as well as adherens junctions with a binding affinity to occludin and alpha catenin. J Biol Chem *274*, 5981-6.

Itoh, M., Nagafuchi, A., Moroi, S., and Tsukita, S. (1997). Involvement of ZO-1 in cadherin-based cell adhesion through its direct binding to α catenin and actin filaments. J Cell Biol *138*, 181-192.

Itoh, M., Nagafuchi, A., Yonemura, S., Kitani-Yasuda, T., and Tsukita, S. (1993). The 220-kD protein colocalizing with cadherins in non-epithelial cells is identical to ZO-1, a tight junction-associated protein in epithelial cells: cDNA cloning and immunoelectron microscopy. J Cell Biol *121*, 491-502.

Itoh, M., Yonemura, S., Nagafuchi, A., Tsukita, S., and Tsukita, S. (1991). A 220-kD undercoat-constitutive protein: Its specific localization at cadherin-based cell-cell adhesion sites. J Cell Biol *115*, 1449-1462.

Jahn, R., and Sudhof, T. C. (1999). Membrane fusion and exocytosis. Annu Rev Biochem *68*, 863-911.

Jesaitis, L. A., and Goodenough, D. A. (1994). Molecular characterization and tissue distribution of ZO-2, a tight junction protein homologous to ZO-1 and the Drosophila discs-large tumor suppressor protein. J Cell Biol *124*, 949-61.

Johnson, T. F., Morris, D. C., and Anderson, H. C. (1989). Matrix vesicles and calcification of rachitic rat osteoid. J Exp Pathol *4*, 123-32.

Katahira, J., Sugiyama, H., Inoue, N., Horiguchi, Y., Matsuda, M., and Sugimoto, N. (1997). Clostridium perfringens enterotoxin utilizes two structurally related membrane proteins as functional receptors in vivo. J Biol Chem 272, 26652-8.

Keon, B. H., Schafer, S., Kuhn, C., Grund, C., and Franke, W. W. (1996). Symplekin, a novel type of tight junction plaque protein. J Cell Biol *134*, 1003-18.

Kim, P. K., Hollerbach, C., Trimble, W. S., Leber, B. and Andrews, D. W. (1999). Identification of the endoplasmic reticulum targeting signal in vesicle-associated membrane proteins. J Biol Chem *274*, 36876-82.

Kirsch, T., Nah, H., Shapiro, I. M., and Pacifici, M. (1997). Regulated production of mineralization-competent matrix vesicles in hypertrophic chondrocytes. J Cell Biol *137*, 1149-1160.

Klenchin, V. A., and Martin, T. F. (2000). Priming in exocytosis: Attaining fusion-competence after vesicle docking. Biochimie *82*, 399-407.

Koval, M., Geist, S. T., Westphale, E. M., Kemendy, A. E., Civitelli, R., Beyer, E. C., and Steinberg, T. H. (1995). Transfected connexin45 alters gap junction permeability in cells expressing endogenous connexin43. J Cell Biol *130*, 987-95.

Koval, M., Harley, J. E., Hick, E., and Steinberg, T. H. (1997). Connexin46 is retained as monomers in a trans-Golgi compartment of osteoblastic cells. J Cell Biol *137*, 847-57.

Kumar, N. M. (1999). Molecular biology of the interactions between connexins. Novartis Found Symp *219*, 6-16.

Kwon, O. J., Gainer, H., Wray, S., and Chin, H. (1996). Identification of a novel protein containing two C2 domains selectively expressed in the rat brain and kidney. FEBS Lett *378*, 135-9.

Lecanda, F., Towler, D. A., Ziambaras, K., Cheng, S., Koval, M., Steinberg, T. H., and Civitelli, R. (1998). Gap junctional communication modulates gene expression in osteoblastic cells. Molecular Biology of the Cell *9*, 2249-2258.

Lewis, J. E., Wahl III, J. K., Sass, K. M., Jensen, P. J., Johnson, K. R., and Wheelock, M. J. (1997). Cross-talk between adherens junctions and desmosomes depends on plakoglobin. J Cell Biol *136*, 919-934.

Lian, J. B., Stein, G. S., Canalis, E., Robey, P. G., and Boskey, A. L. (1999). Bone Formation: Osteoblast Lineage Cells, Growth factors, Matrix proteins and the minerlization process. In Primer on the Metabolic Bone Diseases and Disorders of mineral metabolism, ed. Favus, M. J., Lippincott Williams & Wilkins, pp. 14 - 29.

Lian, J. B., Stein, G. S., Stein, J. L., and van Wijnen, A. J. (1998). Osteocalcin gene promoter: unlocking the secrets for regulation of osteoblast growth and differentiation. J Cell Biochem Suppl *31*, 62-72.

Link, E., McMahon, H., Fischer von Mollard, G., Yamasaki, S., Niemann, H., Sudhof, T. C., and Jahn, R. (1993). Cleavage of cellubrevin by tetanus toxin does not affect fusion of early endosomes. J Biol Chem *268*, 18423-6.

Luegmayr, E., Glantschnig, H., Varga, F., and Klaushofer, K. (2000). The organization of adherens junctions in mouse osteoblast-like cells (MC3T3-E1) and their modulation by triiodothyronine and 1,25-dihydroxyvitamin D3. Histochem Cell Biol *113*, 467-78.

Malaval, L., Modrowski, D., Gupta, A. K., and Aubin, J. E. (1994). Cellular expression of bone-related proteins during in vitro osteogenesis in rat bone marrow stromal cell cultures. J Cell Physiol *158*, 555-572.

Mandai, K., Nakanishi, H., Satoh, A., Obaishi, H., Wada, M., Nishioka, H., Itoh, M., Mizoguchi, A., Aoki, T., Fujimoto, T., Matsuda, Y., Tsukita, S., and Takai, Y. (1997). Afadin: A novel actin filament-binding protein with one PDZ domain localized at cadherin-based cell-to-cell adherens junction. J Cell Biol *139*, 517-28.

Mandic, R., Trimble, W. S., and Lowe, A. W. (1997). Tissue-specific alternative RNA splicing of rat vesicle-associated membrane protein-1 (VAMP-1). Gene *199*, 173-9.

Mandon, B., Nielsen, S., Kishore, B. K., and Knepper, M. A. (1997). Expression of syntaxins in rat kidney. Am J Physiol *273*, F718-30.

Marsh, M. E., Munne, A. M., Vogel, J. J., Cui, Y., and Franceschi, R. T. (1995). Mineralization of bone-like extracellular matrix in the absence of functional osteoblasts. J Bone Miner Res *10*, 1635-43.

Martin-Martin, B., Nabokina, S. M., Lazo, P. A., and Mollinedo, F. (1999). Co-expression of several human syntaxin genes in neutrophils and differentiating HL-60 cells: variant isoforms and detection of syntaxin 1. J Leukoc Biol *65*, 397-406.

Martin-Padura, I., Lostaglio, S., Schneemann, M., Williams, L., Romano, M., Fruscella, P., Panzeri, C., Stoppacciaro, A., Ruco, L., Villa, A., Simmons, D., and Dejana, E. (1998). Junctional adhesion molecule, a novel member of the immunoglobulin superfamily that distributes at intercellular junctions and modulates monocyte transmigration. J Cell Biol *142*, 117-27.

Martinez, I., Chakrabarti, S., Hellevik, T., Morehead, J., Fowler, K., and Andrews, N. W. (2000). Synaptotagmin VII regulates Ca(2+)-dependent exocytosis of lysosomes in fibroblasts. J Cell Biol *148*, 1141-49.

McMahon, H. T., and Sudhof, T. C. (1995). Synaptic core complex of synaptobrevin, syntaxin, and SNAP25 forms high affinity alpha-SNAP binding site. J Biol Chem *270*, 2213-7.

McMahon, H. T., Ushkaryov, Y. A., Edelmann, L., Link, E., Binz, T., Niemann, H., Jahn, R., and Sudhof, T. C. (1993). Cellubrevin is a ubiquitous tetanus-toxin substrate homologous to a putative synaptic vesicle fusion protein. Nature *364*, 346-9.

Merzdorf, C. S., and Goodenough, D. A. (1997). Localization of a novel 210 kDa protein in Xenopus tight junctions. J Cell Sci *110*, 1005-12.

Mitic, L. L., and Anderson, J. M. (1998). Molecular architecture of tight junctions. Annu Rev Physiol *60*, 121-42.

Mitic, L. L., Schneeberger, E. E., Fanning, A. S., and Anderson, J. M. (1999). Connexin-occludin chimeras containing the ZO-binding domain of occludin localize at MDCK tight junctions and NRK cell contacts. J Cell Biol *146*, 683-93.

Mitic, L. L., Van Itallie, C. M., and Anderson, J. M. (2000). Molecular physiology and pathophysiology of tight junctions I. Tight junction structure and function: lessons from mutant animals and proteins. Am J Physiol Gastrointest Liver Physiol *279*, G250-4.

Montal, M. (1999). Electrostatic attraction at the core of membrane fusion. FEBS Lett *447*, 129-30.

Montecucco, C., Papini, E., and Schiavo, G. (1996). Bacterial protein toxins and cell vesicle trafficking. Experientia *52*, 1026-1032.

Morgan, A. (1995). Exocytosis. Essays Biochem *30*, 77-95.

Morita, K., Furuse, M., Fujimoto, K., and Tsukita, S. (1999a). Claudin multigene family encoding four-transmembrane domain protein components of tight junction strands. Proc Natl Acad Sci U S A *96*, 511-6.

Morita, K., Sasaki, H., Fujimoto, K., Furuse, M., and Tsukita, S. (1999b). Claudin-11/OSP-based tight junctions of myelin sheaths in brain and Sertoli cells in testis. J Cell Biol *145*, 579-88.

Morita, K., Sasaki, H., Furuse, M., and Tsukita, S. (1999c). Endothelial claudin: claudin-5/TMVCF constitutes tight junction strands in endothelial cells. J Cell Biol *147*, 185-94.

Mundy, G. R., Boyce, B., Hughes, D., Wright, K., Bonewald, L., Dallas, S., Harris, S., Ghosh-Choudhury, N., Chen, D., Dunstan, C., and *et al.* (1995). The effects of cytokines and growth factors on osteoblastic cells. Bone *17*, 71S-75S.

Muresan, Z., Paul, D. L., and Goodenough, D. A. (2000). Occludin 1B, a variant of the tight junction protein occludin. Mol Biol Cell *11*, 627-34.

Nagata, T., Bellows, C. G., Kasugai, S., Butler, W. T., and Sodek, J. (1991). Biosynthesis of bone proteins [SPP-1 (secreted phosphoprotein-1, osteopontin), BSP (bone sialoprotein) and SPARC (osteonectin)] in association with mineralized-tissue formation by fetal-rat calvarial cells in culture. Biochem J *274*, 513-20.

Nakamura, N., Yamamoto, A., Wada, Y., and Futai, M. (2000). Syntaxin 7 mediates endocytic trafficking to late endosomes. J Biol Chem *275*, 6523-9.

Nefussi, J. R., Brami, G., Modrowski, D., Oboeuf, M., and Forest, N. (1997). Sequential expression of bone matrix proteins during rat calvaria osteoblast differentiation and bone nodule formation in vitro. J Histochem Cytochem *45*, 493-503.

Newton, A. C. (1995). Protein kinase C. Seeing two domains. Curr Biol *5*, 973-6.

Nichols, B. J., Ungermann, C., Pelham, H. R., Wickner, W. T., and Haas, A. (1997). Homotypic vacuolar fusion mediated by t- and v-SNAREs. Nature *387*, 199-202.

Nicholson, B. J., Weber, P. A., Cao, F., Chang, H., Lampe, P., and Goldberg, G. (2000). The molecular basis of selective permeability of connexins is complex and includes both size and charge. Braz J Med Biol Res *33*, 369-78.

Noda, M., Yoon, K., Prince, C. W., Butler, W. T., and Rodan, G. A. (1988). Transcriptional regulation of osteopontin production in rat osteosarcoma cells by type beta transforming growth factor. J Biol Chem *263*, 13916-21.

Nollet, F., Kools, P., and van Roy, F. (2000). Phylogenetic analysis of the cadherin superfamily allows identification of six major subfamilies besides several solitary members. J Mol Biol *299*, 551-72.

Nose, A., Nagafuchi, A., and Takeichi, M. (1987). Isolation of placental cadherin cDNA: identification of a novel gene family of cell-cell adhesion molecules. Embo J *6*, 3655-61.

Oda, H., Uemura, T., Shiomi, K., Nagafuchi, A., Tsukita, S., and Takeichi, M. (1993). Identification of a Drosophila homologue of alpha-catenin and its association with the armadillo protein. J Cell Biol *121*, 1133-40.

Okazaki, M., Takeshita, S., Kawai, S., Kikuno, R., Tsujimura, A., Kudo, A., and Amann, E. (1994). Molecular cloning and characterization of OB-cadherin, a new member of cadherin family expressed in osteoblasts. J Biol Chem *269*, 12092-8.

Orsulic, S., and Peifer, M. (1996). An in vivo structure-function study of armadillo, the beta-catenin homologue, reveals both separate and overlapping regions of the protein required for cell adhesion and for wingless signaling. J Cell Biol *134*, 1283-300.

Osborne, S. L., Herreros, J., Bastiaens, P. I., and Schiavo, G. (1999). Calcium-dependent oligomerization of synaptotagmins I and II. Synaptotagmins I and II are localized on the same synaptic vesicle and heterodimerize in the presence of calcium. J Biol Chem *274*, 59-66.

Otto, F., Thornell, A. P., Crompton, T., Denzel, A., Gilmour, K. C., Rosewell, I. R., Stamp, G. W., Beddington, R. S., Mundlos, S., Olsen, B. R., Selby, P. B. and Owen, M. J. (1997). Cbfa1, a candidate gene for cleidocranial dysplasia syndrome, is essential for osteoblast differentiation and bone development. Cell *89*, 765-71.

Owen, M. (1988). Marrow stromal stem cells. J Cell Sci Suppl *10*, 63-76.

Owen, M., and Friedenstein, A. J. (1988). Stromal stem cells: marrow-derived osteogenic precursors. Ciba Found Symp *136*, 42-60.

Owen, T. A., Aronow, M., Shalhoub, V., Barone, L. M., Wilming, L., Tassinari, M. S., Kennedy, M. B., Pockwinse, S., Lian, J. B., and Stein, G. S. (1990). Progressive development of the rat osteoblast phenotype in vitro: reciprocal relationships in expression of genes associated with osteoblast proliferation and differentiation during formation of the bone extracellular matrix. J Cell Physiol *143*, 420-30.

Oyler, G. A., Higgins, G. A., Hart, R. A., Battenberg, E., Billingsley, M., Bloom, F. E. and Wilson, M. C. (1989). The identification of a novel synaptosomal-associated protein, SNAP-25, differentially expressed by neuronal subpopulations. J Cell Biol *109*, 3039-52.

Palumbo, C., Palazzini, S., and Marotti, G. (1990). Morphological study of intercellular junctions during osteocyte differentiation. Bone *11*, 401-406.

Peacock, R. E., Keen, T. J., and Inglehearn, C. F. (1997). Analysis of a human gene homologous to rat ventral prostate.1 protein. Genomics *46*, 443-9.

Pelham, H. R. (1999). SNAREs and the secretory pathway-lessons from yeast. Exp Cell Res *247*, 1-8.

Perin, M. S., Brose, N., Jahn, R., and Sudhof, T. C. (1991a). Domain structure of synaptotagmin (p65). J Biol Chem *266*, 623-9.

Perin, M. S., Johnston, P. A., Ozcelik, T., Jahn, R., Francke, U., and Sudhof, T. C. (1991b). Structural and functional conservation of synaptotagmin (p65) in Drosophila and humans. J Biol Chem *266*, 615-22.

Pfeffer, S. R. (1996). Transport vesicle docking: SNAREs and associates. Annu. Rev. Cell. Dev. Biol. *12*, 441-461.

Poirier, M. A., Xiao, W., Macosko, J. C., Chan, C., Shin, Y. K. and Bennett, M. K. (1998). The synaptic SNARE complex is a parallel four-stranded helical bundle. Nat Struct Biol *5*, 765-9.

Prekeris, R., Yang, B., Oorschot, V., Klumperman, J., and Scheller, R. H. (1999). Differential roles of syntaxin 7 and syntaxin 8 in endosomal trafficking. Mol Biol Cell *10*, 3891-908.

Quarles, L. D., Yohay, D. A., Lever, L. W., Caton, R., and Wenstrup, R. J. (1992). Distinct proliferative and differentiated stages of murine MC3T3-E1 cells in culture: an in vitro model of osteoblast development. J Bone Miner Res *7*, 683-92.

Quinones, B., Riento, K., Olkkonen, V. M., Hardy, S., and Bennett, M. K. (1999). Syntaxin 2 splice variants exhibit differential expression patterns, biochemical properties and subcellular localizations. J Cell Sci *112*, 4291-304.

Rajasekaran, A. K., Hojo, M., Hulma, T., and Rodriguez-Boulan, E. (1996). Catenins and zonula occludens-1 form a complex during early stages in the assembly of tight junctions. J Cell Biol *132*, 451-463.

Ralston, E., Beushausen, S., and Ploug, T. (1994). Expression of the synaptic vesicle proteins VAMPs/synaptobrevins 1 and 2 in non-neural tissues. J Biol Chem *269*, 15403-6.

Ravichandran, V., Chawla, A., and Roche, P. A. (1996). Identification of a novel syntaxin- and synaptobrevin/VAMP-binding protein, SNAP-23, expressed in non-neuronal tissues. J Biol Chem *271*, 13300-3.

Ravichandran, V., and Roche, P. A. (1997). Cloning and identification of human syntaxin 5 as a synaptobrevin/VAMP binding protein. J Mol Neurosci *8*, 159-61.

Reddi, A. H. (1995). Bone morphogenetic proteins, bone marrow stromal cells, and mesenchymal stem cells. Maureen Owen revisited. Clin Orthop 115-9.

Roach, H. I. (1994). Why does the bone matrix contain non-collagenous proteins? The possible roles of osteocalcin, osteonectin, osteopontin and bone sialoprotein in bone mineralisation and resorption. Cell Biology International *18*, 617-628.

Rodan, G. A. (1992). Introduction to bone biology. Bone *13*, S3-S9.

Rodan, G. A. and Harada, S. (1997). The missing bone. Cell *89*, 677-80.

Rossetto, O., Gorza, L., Schiavo, G., Schiavo, N., Scheller, R. H., and Montecucco, C. (1996). VAMP/synaptobrevin isoforms 1 and 2 are widely and differentially expressed in nonneuronal tissues. J Cell Biol *132*, 167-79.

Rossi, G., Salminen, A., Rice, L. M., Brunger, A. T., and Brennwald, P. (1997). Analysis of a yeast SNARE complex reveals remarkable similarity to the neuronal SNARE complex and a novel function for the C terminus of the SNAP-25 homolog, Sec9. J Biol Chem 272, 16610-7.

Rothman, J. E. (1994). Mechanisms of intracellular protein transport. Nature *372*, 55-63.

Rothman, J. E., and Orci, L. (1992). Molecular dissection of the secretory pathway. Nature *355*, 409-15.

Rowe, T., Dascher, C., Bannykh, S., Plutner, H., and Balch, W. E. (1998). Role of vesicle-associated syntaxin 5 in the assembly of pre-Golgi intermediates. Science *279*, 696-700.

Rudiger, M. (1998). Vinculin and α-catenin: shared and unique functions in adherens junctions. BioEssays *20*, 733-740.

Saitou, M., Fujimoto, K., Doi, Y., Itoh, M., Fujimoto, T., Furuse, M., Takano, H., Noda, T., and Tsukita, S. (1998). Occludin-deficient embryonic stem cells can differentiate into polarized epithelial cells bearing tight junctions. J Cell Biol *141*, 397-408.

Schekman, R. (1998). Membrane fusion. Ready...aim...fire!. Nature *396*, 514-5.

Schiavo, G., Benfenati, F., Poulain, B., Rossetto, O., Polverino de Laureto, P., DasGupta, B. R., and Montecucco, C. (1992). Tetanus and botulinum-B neurotoxins block neurotransmitter release by proteolytic cleavage of synaptobrevin. Nature *359*, 832-5.

Schiavo, G., Malizio, C., Trimble, W. S., Polverino de Laureto, P., Milan, G., Sugiyama, H., Johnson, E. A., and Montecucco, C. (1994). Botulinum G neurotoxin cleaves VAMP/synaptobrevin at a single Ala-Ala peptide bond. J Biol Chem *269*, 20213-6.

Schiavo, G., Matteoli, M., and Montecucco, C. (2000). Neurotoxins affecting neuroexocytosis. Physiol Rev *80*, 717-66.

Schiavo, G., Osborne, S. L., and Sgouros, J. G. (1998). Synaptotagmins: more isoforms than functions? Biochem Biophys Res Commun *248*, 1-8.

Schiavo, G., Santucci, A., Dasgupta, B. R., Mehta, P. P., Jontes, J., Benfenati, F., Wilson, M. C., and Montecucco, C. (1993a). Botulinum neurotoxins serotypes A and E cleave SNAP-25 at distinct COOH-terminal peptide bonds. FEBS Lett *335*, 99-103.

Schiavo, G., Shone, C. C., Bennett, M. K., Scheller, R. H., and Montecucco, C. (1995). Botulinum neurotoxin type C cleaves a single Lys-Ala bond within the carboxyl-terminal region of syntaxins. J Biol Chem *270*, 10566-70.

Schiavo, G., Shone, C. C., Rossetto, O., Alexander, F. C., and Montecucco, C. (1993b). Botulinum neurotoxin serotype F is a zinc endopeptidase specific for VAMP/synaptobrevin. J Biol Chem *268*, 11516-9.

Schiavo, G., and Stenbeck, G. (1998). Molecular analysis of neurotransmitter release. Essays Biochem *33*, 29-41.

Schirrmacher, K., Schmitz, I., Winterhager, E., Traub, O., Brummer, F., Jones, D., and Bingman, D. (1992). Characterization of gap junctions between osteoblast-like cells in culture. Calcif Tissue Int *51*, 285-290.

Serre, C. M., Farlay, D., Delmas, P. D., and Chenu, C. (1999). Evidence for a dense and intimate innervation of the bone tissue, including glutamate-containing fibers. Bone *25*, 623-9.

Shorter, J., and Warren, G. (1999). A role for the vesicle tethering protein, p115, in the post-mitotic stacking of reassembling Golgi cisternae in a cell-free system. J Cell Biol *146*, 57-70.

Simonsen, A., Bremnes, B., Ronning, E., Aasland, R., and Stenmark, H. (1998). Syntaxin-16, a putative Golgi t-SNARE. Eur J Cell Biol *75*, 223-31.

Skehel, P. A., Fabian-Fine, R. and Kandel, E. R. (2000). Mouse VAP33 is associated with the endoplasmic reticulum and microtubules. Proc Natl Acad Sci U S A *97*, 1101-6.

Sollner, T., Bennett, M. K., Whiteheart, S. W., Scheller, R. H., and Rothman, J. E. (1993a). A protein assembly-disassembly pathway in vitro that may correspond to sequential steps of synaptic vesicle docking, activation, and fusion. Cell *75*, 409-18.

Sollner, T., Whiteheart, S. W., Brunner, M., Erdjument-Bromage, H., Geromanos, S., Tempest, P., and Rothman, J. E. (1993b). SNAP receptors implicated in vesicle targeting and fusion. Nature *362*, 318-324.

Sollner, T. H., and Rothman, J. E. (1996). Molecular machinery mediated by vesicle budding, docking and fusion. Experientia *52*, 1021-1025.

Stanka, P. (1975). Occurrence of cell junctions and microfilaments in osteoblasts. Cell Tissue Res *159*, 413-22.

Steegmaier, M., Klumperman, J., Foletti, D. L., Yoo, J. S., and Scheller, R. H. (1999). Vesicle-associated membrane protein 4 is implicated in trans-Golgi network vesicle trafficking. Mol Biol Cell *10*, 1957-72.

Steegmaier, M., Oorschot, V., Klumperman, J., and Scheller, R. H. (2000). Syntaxin 17 Is Abundant in Steroidogenic Cells and Implicated in Smooth Endoplasmic Reticulum Membrane Dynamics. Mol Biol Cell *11*, 2719-2731.

Steegmaier, M., Yang, B., Yoo, J. S., Huang, B., Shen, M., Yu, S., Luo, Y., and Scheller, R. H. (1998). Three novel proteins of the syntaxin/SNAP-25 family. J Biol Chem *273*, 34171-9.

Steel, G. J., Laude, A. J., Boojawan, A., Harvey, D. J., and Morgan, A. (1999). Biochemical analysis of the Saccharomyces cerevisiae SEC18 gene product: implications for the molecular mechanism of membrane fusion. Biochemistry *38*, 7764-72.

Steinberg, T. H., Civitelli, R., Geist, S. T., Robertson, A. J., Hick, E., Veenstra, R. D., Wang, H. Z., Warlow, P. M., Westphale, E. M., Laing, J. G., and *et al.* (1994). Connexin43 and connexin45 form gap junctions with different molecular permeabilities in osteoblastic cells. Embo J *13*, 744-50.

Stenbeck, G. (1998). Soluble NSF-attachment proteins. Int J Biochem Cell Biol *30*, 573-577.

Stevenson, B. R., Siliciano, J. D., Mooseker, M. K., and Goodenough, D. A. (1986). Identification of ZO-1: a high molecular weight polpeptide associated with the tight junction (zonula occludins) in variety of epithelia. J Cell Biol *103*, 755-766.

Sudhof, T. C., and Rizo, J. (1996). Synaptotagmins: C2-domain proteins that regulate membrane traffic. Neuron *17*, 379-88.

Sudo, H., Kodama, H. A., Amagai, Y., Yamamoto, S., and Kasai, S. (1983). In vitro differentiation and calcification in a new clonal osteogenic cell line derived from newborn mouse calvaria. J Cell Biol *96*, 191-8.

Sugita, S., and Sudhof, T. C. (2000). Specificity of Ca2+-dependent protein interactions mediated by the C2A domains of synaptotagmins. Biochemistry *39*, 2940-9.

Sumitani, S., Ramlal, T., Liu, Z., and Klip, A. (1995). Expression of syntaxin 4 in rat skeletal muscle and rat skeletal muscle cells in culture. Biochem Biophys Res Commun *213*, 462-8.

Sutton, R. B., Davletov, B. A., Berghuis, A. M., Sudhof, T. C., and Sprang, S. R. (1995). Structure of the first C2 domain of synaptotagmin I: a novel Ca2+/phospholipid-binding fold. Cell *80*, 929-38.

Suzuki, S. T. (1996). Structural and functional diversity of cadherin superfamily: Are new members of the cadherin superfamily involved in signal transduction pathway? J Cell Biochem *61*, 531-542.

Tagaya, M., Toyonaga, S., Takahashi, M., Yamamoto, A., Fujiwara, T., Akagawa, K., Moriyama, Y., and Mizushima, S. (1995). Syntaxin 1 (HPC-1) is associated with chromaffin granules. J Biol Chem *270*, 15930-3.

Tang, B. L., Low, D. Y., and Hong, W. (1998a). Syntaxin 11: a member of the syntaxin family without a carboxyl terminal transmembrane domain. Biochem Biophys Res Commun *245*, 627-32.

Tang, B. L., Low, D. Y., Lee, S. S., Tan, A. E., and Hong, W. (1998b). Molecular cloning and localization of human syntaxin 16, a member of the syntaxin family of SNARE proteins. Biochem Biophys Res Commun *242*, 673-9.

Tang, B. L., Low, D. Y., Tan, A. E., and Hong, W. (1998c). Syntaxin 10: a member of the syntaxin family localized to the trans-Golgi network. Biochem Biophys Res Commun *242*, 345-50.

Tang, B. L., Tan, A. E., Lim, L. K., Lee, S. S., Low, D. Y., and Hong, W. (1998d). Syntaxin 12, a member of the syntaxin family localized to the endosome. J Biol Chem *273*, 6944-50.

Taubenblatt, P., Dedieu, J. C., Gulik-Krzywicki, T., and Morel, N. (1999). VAMP (synaptobrevin) is present in the plasma membrane of nerve terminals. J Cell Sci *112*, 3559-67.

Terrian, D. M., and White, M. K. (1997). Phylogenetic analysis of membrane trafficking proteins: a family reunion and secondary structure predictions. Eur J Cell Biol *73*, 198-204.

Trimble, W. S. (1993). Analysis of the structure and expression of the VAMP family of synaptic vesicle proteins. J Physiol Paris *87*, 107-15.

Trimble, W. S., Cowan, D. M., and Scheller, R. H. (1988). VAMP-1: a synaptic vesicle-associated integral membrane protein. Proc Natl Acad Sci U S A *85*, 4538-42.

Trimble, W. S., Gray, T. S., Elferink, L. A., Wilson, M. C., and Scheller, R. H. (1990). Distinct patterns of expression of two VAMP genes within the rat brain. J Neurosci *10*, 1380-7.

Tsui, M. M., and Banfield, D. K. (2000). Yeast Golgi SNARE interactions are promiscuous. J Cell Sci *113*, 145-52.

Tsukita, S. (1989). Isolation of cell-to-cell adherens junctions from rat liver. J Cell Biol *108*, 31-41.

Tsukita, S., and Furuse, M. (1999). Occludin and claudins in tight-junction strands: leading or supporting players? Trends Cell Biol *9*, 268-73.

Turksen, K., and Aubin, J. E. (1991). Positive and negative immunoselection for enrichment of two classes of osteoprogenitor cells. J Cell Biol *114*, 373-384.

Valdez, A. C., Cabaniols, J. P., Brown, M. J., and Roche, P. A. (1999). Syntaxin 11 is associated with SNAP-23 on late endosomes and the trans-Golgi network. J Cell Sci *112*, 845-54.

Van Itallie, C. M., and Anderson, J. M. (1997). Occludin confers adhesiveness when expressed in fibroblasts. J Cell Sci *110*, 1113-21.

Vogel, K., and Roche, P. A. (1999). SNAP-23 and SNAP-25 are palmitoylated in vivo. Biochem Biophys Res Commun *258*, 407-10.

Wada, Y., Kataoka, H., Yokose, S., Ishizuya, T., Miyazono, K., Gao, Y. H., Shibasaki, Y., and Yamaguchi, A. (1998). Changes in osteoblast phenotype during differentiation of enzymatically isolated rat calvaria cells. Bone *22*, 479-85.

Wang, H., Frelin, L., and Pevsner, J. (1997). Human syntaxin 7: a Pep12p/Vps6p homologue implicated in vesicle trafficking to lysosomes. Gene *199*, 39-48.

Wang, Y., Sugita, S., and Sudhof, T. C. (2000). The RIM/NIM family of neuronal C2 domain proteins. Interactions with Rab3 and a new class of Src homology 3 domain proteins. J Biol Chem *275*, 20033-44.

Weber, T., Parlati, F., McNew, J. A., Johnston, R. J., Westermann, B., Sollner, T. H., and Rothman, J. E. (2000). SNAREpins are functionally resistant to disruption by NSF and alphaSNAP. J Cell Biol *149*, 1063-72.

Weiss, E. E., Kroemker, M., Rudiger, A. H., Jockusch, B. M., and Rudiger, M. (1998). Vinculin is part of the cadherin-catenin junctional complex: complex formation between alpha-catenin and vinculin. J Cell Biol *141*, 755-64.

Whiteheart, S. W., Brunner, M., Wilson, D. W., Wiedmann, M., and Rothman, J. E. (1992). Soluble N-ethylmaleimide-sensitive fusion attachment proteins (SNAPs) bind to a multi-SNAP receptor complex in Golgi membranes. J Biol Chem *267*, 12239-43.

Whiteheart, S. W., Griff, I. C., Brunner, M., Clary, D. O., Mayer, T., Buhrow, S. A., and Rothman, J. E. (1993). SNAP family of NSF attachment proteins includes a brain-specific isoform. Nature *362*, 353-5.

Williams, R. L., and Katan, M. (1996). Structural views of phosphoinositide-specific phospholipase C: signalling the way ahead. Structure *4*, 1387-94.

Willott, E., Balda, M. S., Fanning, A. S., Jameson, B., Van Itallie, C., and Anderson, J. M. (1993). The tight junction protein ZO-1 is homologous to the Drosophila discs-large tumor suppressor protein of septate junctions. Proc Natl Acad Sci U S A *90*, 7834-8.

Wilson, D. W., Wilcox, C. A., Flynn, G. C., Chen, E., Kuang, W. J., Henzel, W. J., Block, M. R., Ullrich, A., and Rothman, J. E. (1989). A fusion protein required for vesicle-mediated transport in both mammalian cells and yeast. Nature *339*, 355-9.

Wittchen, E. S., Haskins, J., and Stevenson, B. R. (1999). Protein interactions at the tight junction. Actin has multiple binding partners, and zo-1 forms independent complexes with zo-2 and zo-3. J Biol Chem *274*, 35179-85.

Wong, P. P., Daneman, N., Volchuk, A., Lassam, N., Wilson, M. C., Klip, A., and Trimble, W. S. (1997). Tissue distribution of SNAP-23 and its subcellular localization in 3T3-L1 cells. Biochem Biophys Res Commun *230*, 64-8.

Wong, S. H., Xu, Y., Zhang, T., and Hong, W. (1998a). Syntaxin 7, a novel syntaxin member associated with the early endosomal compartment. J Biol Chem *273*, 375-80.

Wong, S. H., Zhang, T., Xu, Y., Subramaniam, V. N., Griffiths, G., and Hong, W. (1998b). Endobrevin, a novel synaptobrevin/VAMP-like protein preferentially associated with the early endosome. Mol Biol Cell *9*, 1549-63.

Woodman, P. (1998). Vesicle transport: more work for the Rabs? Curr Biol *8*, R199-201.

Woodman, P. G. (1997). The roles of NSF, SNAPs and SNAREs during membrane fusion. Biochim Biophys Acta *1357*, 155-72.

Wuthier, R. E. (1986). Mechanisms of matrix vesicle-mediated mineralization. In Cell mediated calcification and matrix vesicles, ed. Ali, S. Y., Elsevier Science Publishers B. V., Vol. pp. 47-55

Wymann, M. P., and Pirola, L. (1998). Structure and function of phosphoinositide 3-kinases. Biochim Biophys Acta *1436*, 127-50.

Xiao, G., Cui, Y., Ducy, P., Karsenty, G., and Francheschi, R. T. (1997). Ascorbic acid-dependent activation of the osteocalcin promoter in MC3T3-E1 preosteoblasts: requirements for collagen matrix synthesis and the presence of an intact OSE2 sequence. Mol Endocrinol *11*, 1103-1113.

Yamaguchi, A., and Kahn, A. J. (1991). Clonal osteogenic cell lines express myogenic and adipocytic developmental potential. Calcif Tissue Int *49*, 221-5.

Yamaguchi, D. T., Huang, J. T., and Ma, D. (1995). Regulation of gap junction intercellular communication by pH in MC3T3- E1 osteoblastic cells. J Bone Miner Res *10*, 1891-9.

Yamamoto, T., Harada, N., Kano, K., Taya, S., Canaani, E., Matsuura, Y., Mizoguchi, A., Ide, C., and Kaibuchi, K. (1997). The Ras target AF-6 interacts with ZO-1 and serves as a peripheral component of tight junctions in epithelial cells. J Cell Biol *139*, 785-95.

Yamamoto, T., Harada, N., Kawano, Y., Taya, S., and Kaibuchi, K. (1999). In vivo interaction of AF-6 with activated Ras and ZO-1. Biochem Biophys Res Commun *259*, 103-7.

Yap, A. S., Brieher, W. M., and Gumbiner, B. M. (1997). Molecular and functional analysis of cadherin-based adherens junctions. Annu Rev Cell Dev Biol *13*, 119-46.

Yonemura, S., Itoh, M., Nagafuchi, A., and Tsukita, S. (1995). Cell-to-cell adherens junction formation and actin filament organization: similarities and differences between non-polarized fibroblasts and polarized epithelial cells. J Cell Sci *108*, 127-42.

Zeng, Q., Subramaniam, V. N., Wong, S. H., Tang, B. L., Parton, R. G., Rea, S., James, D. E., and Hong, W. (1998). A novel synaptobrevin/VAMP homologous protein (VAMP5) is increased during in vitro myogenesis and present in the plasma membrane. Mol Biol Cell *9*, 2423-37.

Zhang, X., Rizo, J., and Sudhof, T. C. (1998). Mechanism of phospholipid binding by the C2A-domain of synaptotagmin I. Biochemistry *37*, 12395-403.

Zhao, N., Hashida, H., Takahashi, N. and Sakaki, Y. (1994). Cloning and sequence analysis of the human SNAP25 cDNA. Gene *145*, 313-4.

Zhou, H. Y., Takita, H., Fujisawa, R., Mizuno, M., and Kuboki, Y. (1995). Stimulation by bone sialoprotein of calcification in osteoblast-like MC3T3-E1 cells. Calcif Tissue Int *56*, 403-7.

Ziambaras, K., Lecanda, F., Steinberg, T. H., and Civitilli, R. (1998). Cyclic strech enhances gap junctional communication between osteoblastic cells. J Bone Miner Res *13*, 218-228.

Zimmerman, D., Jin, F., Leboy, P., Hardy, S. and Damsky, C. (2000). Impaired bone formation in transgenic mice resulting from altered integrin function in osteoblasts. Dev Biol *220*, 2-15